NTNU
Norwegian University of
Science and Technology

Field Development Study of an Offshore Gas Asset in Tanzania using Reservoir and Surface Network Simulations

Case Study: Block 2 Offshore Tanzania

Nyorobi Busanda Kiyuga

Petroleum Engineering
Submission date: July 2016
Supervisor: Milan Stanko, IPT
Co-supervisor: Richard Rwechungura, IPT
Ambrose Itika, University of Dar es Salaam
Ghati Mwita, Statoil Tanzania

Norwegian University of Science and Technology
Department of Petroleum Engineering and Applied Geophysics

Disclaimer

I declare that this report is my own work and that all sources of information used in this report have been fully acknowledged

Abstract

A Block 2 gas field offshore Tanzania is still under development. Statoil Tanzania is the operator, and has confirmed a development concept of subsea production systems tied to an offshore liquefied natural gas (LNG) facility, and suggested the initial production strategy from three reservoirs which are Zafarani, Lavani Main and Lavani Deep. However, further studies can be made to find the optimal production strategy.

This thesis focused on performing more field development studies for the Block 2 through integration of reservoir and surface network models. The study was not limited to Statoil proposed strategy; Tangawizi reservoir was also included in the study. Since the field was new, most of the data were sensitive and have not yet been disclosed. Therefore, the study was done using few published data, petroleum engineering calculations, correlations and reasonable assumptions.

The reservoir model was created in MBAL by assuming that reservoir is a Tank. PROSPER was used to model the wells and the surface networks were modelled in GAP. GAP was used as the platform to integrate the reservoir, well and surface networks models and performing network solving as well as prediction runs. The production strategies were made by considering 1 LNG train capacity of 5 MTPA, and then extended to 2 LNG trains capacity of 10 MTPA in total. A simple economic model was included to evaluate the economic viability of the field.

Two most attractive production strategies were obtained and named as Optional Strategy One and Optional Strategy Two. For 1 LNG train capacity, the production plateau rate was estimated to 635.6 MMscf/day which doubled when 2 LNG trains capacity was considered. During prediction runs, the Optional Strategy One was almost similar to the Statoil proposed production strategy except for the initial production plateau length from Zafarani. Optional Strategy One provided the field plateau length 31 years. Optional Strategy Two provided the plateau length of 30 years with production from Tangawizi, Lavani Main and Deep. On exploring different techniques to prolong the plateau, producing Zafarani reservoir after natural production plateau of Optional Strategy Two appeared to be the best solution with added cumulative NPV of 5.55%. Optional Strategy One confirmed best rate of return (0.31). When 2 LNG trains had to

be considered, production from all four reservoirs gave 21 years of production plateau length.

Flow assurance evaluation on the main transportation pipeline using HYSYS, indicated presences of low liquid loading to the maximum of 0.0256 fraction of liquid holdup. Also, the formation of Type II hydrate was detected. A study on how to inhibit formed hydrates was then done by injection of inhibitors, typically Methanol (MeOH) and Triethylene glycol (TEG).

Acknowledgement

Firstly, I would like to express my deep gratitude to my thesis supervisor Professor Milan Stanko, he encouraged me to do this topic and he was always there to guide and to show support to meet the objectives. He always inspired me with a sentence “work hard”.

Besides, I humbly acknowledge my co supervisors; Professor Richard Rwechungura and Dr Ambrose Itika, without their valuable assistance this project would not have been completed.

My appreciation extends to Dr. Enock Masanja, Mr. Godwin Nsemwa, Mr. Dismas Kalitenge, Miss Witnes Kihega and Miss Frida Andalu for their inspirations and constructive suggestions on my work.

I would also like to thank Statoil, Norwegian University of Science and Technology (NTNU) and University of Dar es Salaam (UDSM) for their financial support and provision of all necessary facilities required for my work.

Unique gratitude goes to my lovely mother, Miss Mary Mhango, my friends and relatives for their moral support throughout my project and life in general. You are all appreciated

Above all, to the Great Almighty, has been faithful to me, I appreciate his countless love.

Table of Contents

List of Figure

List of Tables

Nomenclature

ΔP_{choke}	Pressure drop across the choke
ΔP_t	Total pressure drop
B_g	Formation volume factor of gas
B_{gi}	Initial formation volume factor of gas
B_w	Formation volume factor of water
B_{wi}	Initial formation volume factor of water
C_{FL}	Flowline Coefficient
C_{PL}	Pipeline Coefficient
C_T	Tubing Coefficient
C_{Tnew}	New tubing Coefficient
$C_{Tpresent}$	Present tubing Coefficient
C_p	Specific heat capacity at constant pressure
G_i	Initial gas in place
G_p	Cumulative produced gas
G_{pu}	Ultimate cumulative produce gas
M_{air}	Air molecular weight, lbm/lbm mol;
M_g	Gas molecular weight, lbm/lbm mol;
M_i	Molecular weight of component i in gas mixture
M_w	Molecular weight
M_{wi}	Molecular weight of an individual component
P_{in}	Pressure at the inlet of the pipe
P_{out}	Pressure at the outlet of the pipe
P_{wf}	Flowing bottomhole pressure
S_g	Gas saturation
S_o	Oil saturation
S_w	Water saturation
S_{wi}	Irreducible water saturation
T_R	Temperature at reservoir conditions
T_c	Critical temperature
T_{pc}	Pseudo critical temperature
T_{pr}	Pseudo reduced temperature

T_r	Pseudo reduce temperature
T_{sc}	Temperature at standard conditions
T_{sc}	Temperature at standard conditions
V_R	Gas volume at reservoir conditions
V_{sc}	Gas volume at standard conditions
W_e	Water influx
W_i	Injected water
W_p	Produced water
Z_R	Gas deviation factor at reservoir conditions
Z_i	Initial gas deviation factor
Z_{sc}	Gas deviation factor at standard conditions
c_f	Fluid compressibility
c_t	Total compressibility
c_w	Water compressibility
$m(p_R)$	Pseudo reduced reservoir pressure function
$m(p_{wf})$	Pseudo reduced bottomhole pressure function
q_{gsc}	Gas rate at standard conditions
p_R	Pressure at reservoir conditions
p_R	Pressure at reservoir conditions
p_c	Critical pressure
n	Number of moles of gas
p_i	Initial pressure
p_o	Reference pressure
p_{pc}	Pseudo critical pressure
p_{pr}	Pseudo reduced pressure
p_{sc}	Pressure at standard conditions
y_i	Mole fraction of component i
R	Universal gas constant
T	Absolute temperature
V	Volume
Z	Dimensionless quantity (z-factor) or gas deviation factor
n	Number of pound moles of gas
p	Pressure

p_r	Pseudo reduce pressure
p_{sc}	Pressure at standard conditions
f_f	Fanning friction factor
y_i	Mole fraction of an individual component
D	Pipe diameter
G	Gas volume
L	Pipe length
U	Overall Heat transfer Coefficient
Z	Gas deviation factor
k	Permeability
m	Mass
n	Number of moles
r	Radius
y	Reduced-density parameter

Greek

γ_g	Gas specific gravity, unit less;
μ_g	Gas viscosity
ρ_g	Gas density
ρ_{air}	Air density
π	Pie
ϕ	Porosity
ϕ_e	Effective porosity

Abbreviations

AOF	Absolute Open Flow potential
atm	Atmosphere
BG	British Gas
BWRS	Benedict-Webb-Rubin-Starling
CAPEX	Capital Expenditures
CF	Cash Flow
CMG	Computer Modelling Group
CNG	Compressed Natural Gas
CNG	Compressed natural gas
cP	Centipoise
Delta _P	Pressure drop
dp	Pressure drop at the choke defined in GAP
Drillex	Drilling Expenditures
DST	Drill Stem Test
EOS	Equation of State
Eq.	Equation
FPSO	Floating, Production Storage
GTL	Gas to liquids
HC	Hydrocarbon
HC	Hydrocarbons
HSE	Health Safety and Environment
HTC	Heat transfer Coefficient
IGIP	initial gas in place
IGIP	Initial Gas in Place
IRR	Internal Rate of Return
JV	Joint Venture
KC	Kozeny-Carman model
LD	Lavani Deep
LM	Lavani Main
LNG	liquefied natural gas
LNG	Liquefied Natural Gas

LPG	Liquefied Petroleum Gas
mD	millidarcies
mD	Millidarcies
MEG	Mono Ethylene Glycol
MeOH	Methanol
MMscf	Million standard cubic feet
MTPA	Metric tonnes per annum
NGH	Gas to hydrate
NPV	Net Present Value
NTNU	Norwegian University of Science and Technology
OPEX	Operating Expenditures
PNG	pipeline natural gas
PR	Peng-Robinson
PVT	Pressure Volume and Temperature
R.F	Recovery Factor
scf	standard cubic feet
SPAR	Seagoing Platform for Acoustic Research
SRK	Soave-Redlich-Kwong
STP	Standard Temperature and Pressure
Tcf	Trillion cubic feet
TEG	Triethylene glycol
TGP	Tanzania Gas Project
TLP	Tension Leg Platforms
TPDC	Tanzania Petroleum Development Corporation
TRR	Total Recoverable Reserves
U.S	United State
UDSM	University of Dar es Salaam
USD	United State Dollar
VBA	Visual Basic for Applications

Units and Conversion Factors

In petroleum industry, several units may be used, and these units may vary from one country to another. This study used both oil field units (psi, ft^3, °*R* and lbm) and SI units (bar, m^3, °C and kg).

Appropriate conversion factors are used to change from one unit system to another. Comprehensive discussion of units and conversion tables (conversion factors from oil field units to SI units) can be found in Appendix A of monograph a book of (Whiston & Brule, 2000).

Chapter 1: Introduction

1.1 Introduction and Background

Hydrocarbon exploration activities in Tanzania have been under way since 1952. Various multinational petroleum companies have been involving activities. So far, there is no oil discovered; only significant natural gas discoveries both onshore and offshore have been made. Total of six onshore discoveries have been made at Songo Songo, Mnazi Bay, Mkuranga, Kiliwani, Ntorya and Mamba Kofi with other deep sea natural gas discoveries in Block 1, 2, 3 and 4 (TPDC, 2014). All the discoveries sum up to 57.27 Tcf initial gas in Place (IGIP) discovered in Tanzania (Muhongo, 2016).

Currently, only two onshore natural gas discoveries (Songo Songo and Mnazi Bay) have been commercially exploited. The huge discovery in deep sea of the county has led to planning of an onshore Joint Venture (JV) Liquefied Natural Gas (LNG) project. An onshore JV is between the operator of Block 1, 3 and 4 (BG Group) and the operator of Block 2 (Statoil Tanzania) (Holm, 2015).

In this thesis, the study focused on Tanzania Gas Project (TGP); the project is located at Block 2 offshore Tanzania (Figure 1). The Block 2 is operated by Statoil Tanzania on behalf of TPDC with the working interest of 65%, the remaining interest of 35% is held by ExxonMobil Exploration and Production Tanzania Limited (Statoil, 2016). The study aimed at performing reservoir simulations in combination with surface network simulations to come up with the optimal field developments plan of the field.

Gas field development planning involves multiple disciplines including geologist, reservoir engineer and production engineer to bring out a field development plan process which is technically feasible as well as economically viable. For efficient development and operation of a natural gas reservoir, it is important to understand the reservoir characteristics and the well performance. In performing economic analysis of the field, it is important to predict the future recovery of the reservoir and the producing wells of the field for further development and expenditures (Ahmed & Mckinney, 2005).

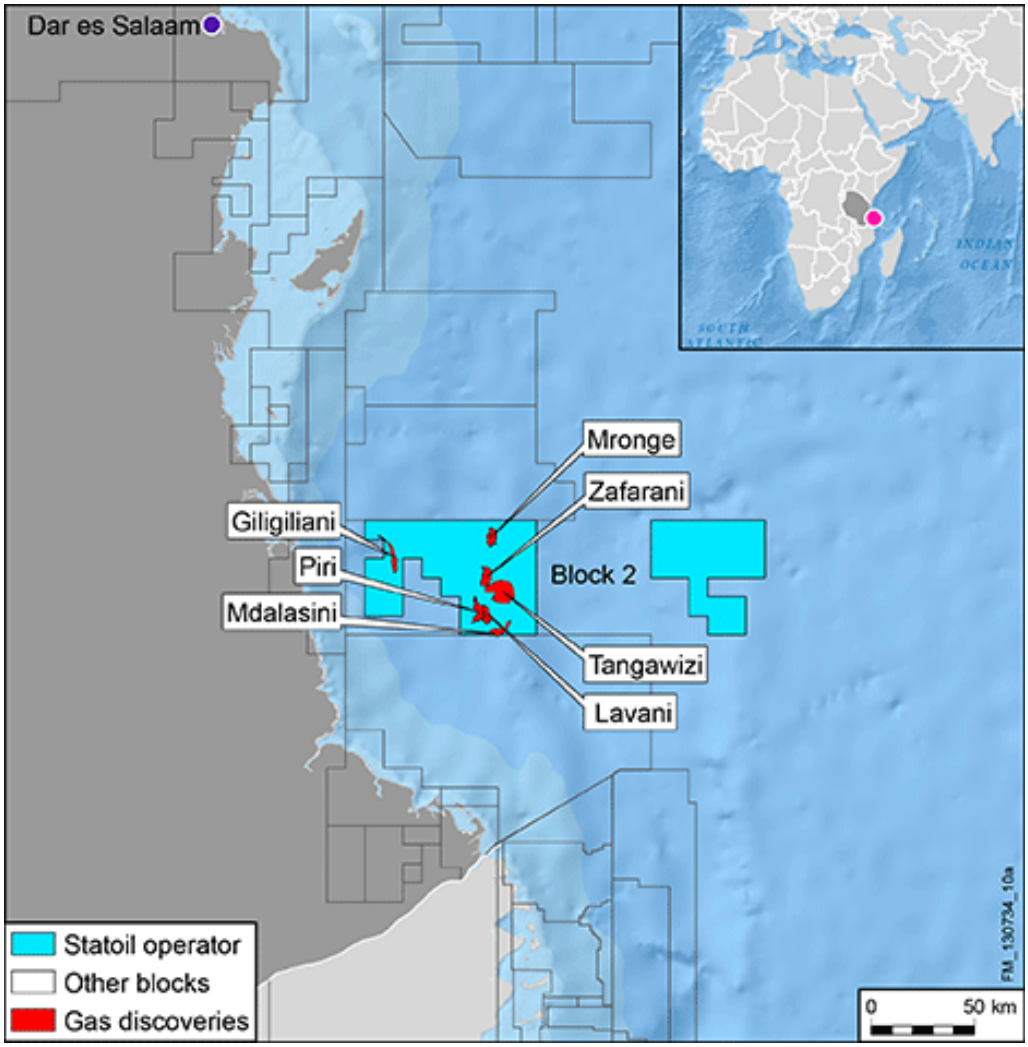

Figure 1-Gas Reservoirs discoveries in Block 2 (Statoil, 2016)

The gas field development study of Block 2 is still under development. In (Holm, 2015), it has been said that the subsea concept which is subsea tie back to onshore LNG plant will be implemented, this concept resembles the subsea concept previous made in Ormen Lange and Snøhvit in the North Sea. Moreover, the production strategy which involved production of three reservoirs (Zafarani, Lavani Main and Lavani Deep) was proposed.

(Kiyuga, 2016), performed field development study in simple Excel model using few published data, reasonable engineering calculations and assumptions. The study was limited to the Statoil proposed strategy which yielded the production plateau length of 31.35 years with the production plateau rate of 480.28 MMscf/day.

In this context, the study was extended by performing development study on multiple options including the Statoil proposed production strategy. Only four reservoirs were considered for the studies which are Zafarani, Lavani Main, Lavani Deep and Tangawizi. The reservoir models were constructed on MBAL, the well model was performed using PROSPER and the surface network model was constructed in GAP. GAP was then used as the platform to integrate the reservoir, well and surface networks and performing prediction runs.

1.2 Objectives

1.2.1 Main objective

To perform field development studies on an offshore Tanzania gas asset using reservoir and surface network simulations

1.2.2 Specific objectives

a. To develop numerical models of the reservoirs and production system that resemble Block 2 using data available in the public domain
b. To determine the production profile of the field using the production system and strategy proposed by Statoil
c. To suggest other production strategies, determine the production profiles and compare with the strategy mentioned in (a) to obtain optimal production strategy
d. To investigate production system options to prolong the plateau.
e. To evaluate potential field flow assurance issues such as hydrate formations and slugging during the life of the asset

Chapter 2: Literature Review

2.0 Natural Gas Reservoirs

Reservoirs are referred as porous and permeable subsurface rock at elevated temperature and pressure (Whiston & Brule, 2000). The reservoirs that initially contain free gas are termed as gas reservoirs. Depending on gas compositions, existing temperature and pressure, the mixture in gas reservoirs can be "dry", "wet" or "condensate". Gas reservoirs may be volumetric (having no water influx) or may have water influx from a contiguous water-bearing source (Ahmed & Mckinney, 2005).

Natural gas reservoirs are composed of low molecular weight alkanes (methane through Butane) and non-hydrocarbons such as carbon dioxide, nitrogen and hydrogen sulphides. The typical compositions are shown on Table 1.

Table 1-Typical natural gas compositions (Demirbas, 2010)

Component	Typical analysis (volume %)	Range (volume %)
Methane	94.9	87.0–96.0
Ethane	2.50	1.8–5.1
Propane	0.20	0.1–1.5
Isobutene	0.03	0.01–0.3
n-Butane	0.03	0.01–0.3
Isopentane	0.01	Trace to 0.14
n-Pentane	0.01	Trace to 0.14
Hexane	0.01	Trace to 0.06
Nitrogen	1.60	1.3–5.6
Carbon dioxide	0.70	0.1–1.0
Oxygen	0.02	0.01–0.1
Hydrogen	Trace	Trace to 0.02

The classification of whether the natural gas reservoir is dry, wet or condensate, two approaches can be used as described by (Curtis H. Whiston, 2000), (1) "by location of reservoir temperature with respect to the critical temperature and cricondentherm and (2) by the location of the first stage separator temperature and pressure with respect to

phase diagram of the reservoir fluid". Figure 2, illustrates the reservoir fluids in a phase diagram and location of dry gas reservoir.

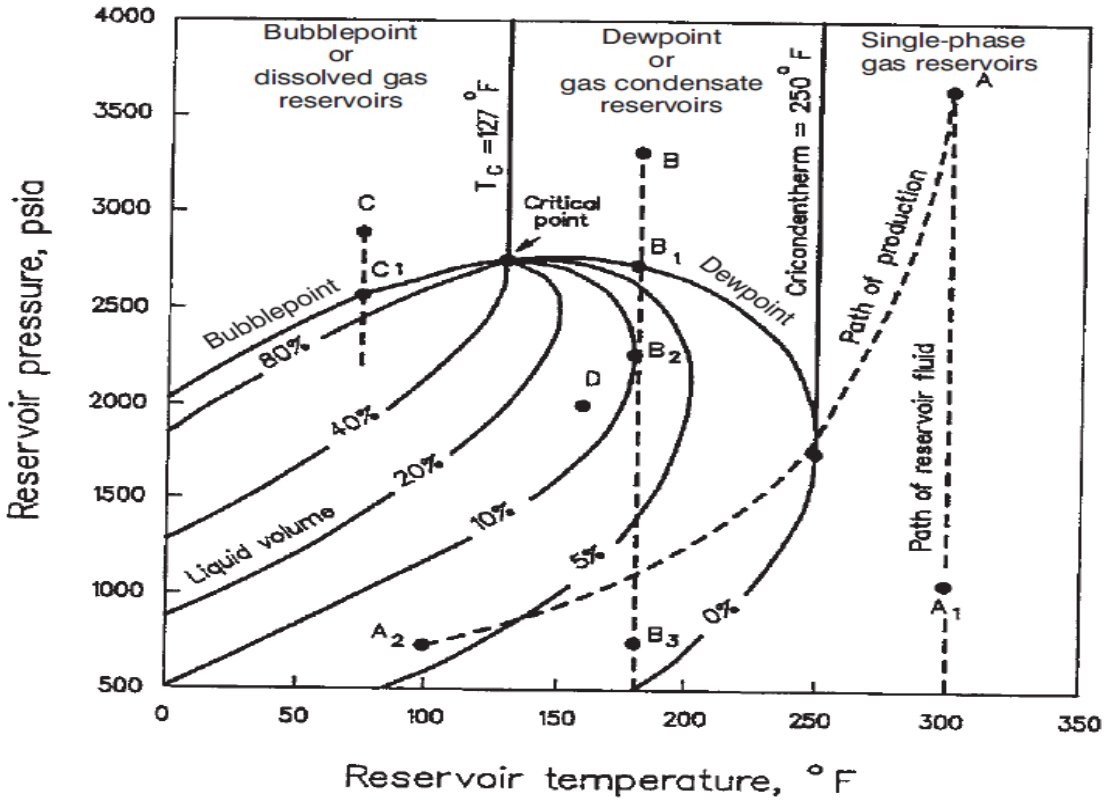

Figure 2- $p - T$ diagram illustrating reservoir fluids (Whiston & Brule, 2000)

Arbitrary, the reservoir with average reservoir temperature below the critical temperature is considered reservoir oil, and the reservoir with average reservoir temperature above the critical temperature (T_C) is considered reservoir gas.

2.1 Natural Gas Reservoir Properties

Reservoir properties include reservoir rock properties and reservoir fluid properties. These properties are accurately determined by laboratory analysis, the procedure which requires enough data. However, in lack of laboratory data, correlations are viable alternative to estimate the reservoir properties. The gas reservoir properties calculations and correlations are discussed below.

2.1.1 Gas Volumetric Properties

The properties of the natural gas mixture depend on the composition, temperature and pressures conditions. This section, briefly describes the natural gas volumetric properties and how they can be calculated or correlated.

2.1.1.1 Gas Molecular Weight (M_g)

Since natural gas is the mixture of different molecules of various sizes and molecular weight, therefore, the observed molecular weight for gas mixture with n components is called molar average molecular weight (John & Wattenbarger, 1996). This molar average molecular weight is determined by Kays mixing rule as shown by the following expression

$$M_g = \sum_{i=1}^{n} y_i M_i \qquad 2.1$$

Where y_i= mole fraction of component i in a gas mixture, fraction and M_i=molecular weight of component i in gas mixture, lbm/lbm-mol.

2.1.1.2 Gas Specific Gravity (γ_g)

At the same temperature and pressure, the gas specific gravity is defined as the ratio of densities of the gas (ρ_g) and dry air (ρ_{air}) as shown Eq. 2. 2. At standard conditions (p=14.7 psia and T=60°F) both a dry air and gas are modelled using ideal gas law (John & Wattenbarger, 1996). Eq. 2. 2 can then be expressed in terms of average molecular weights of gas and dry air (such M_g and M_{air}) (Eq. 2. 3).

$$\gamma_g = \frac{\rho_g}{\rho_{air}} \qquad 2.2$$

$$\gamma_g = \frac{M_g}{M_{air}} \qquad 2.3$$

2.1.2 PVT Properties

2.1.2.1 Gas Formation Volume Factor (B_g)

The gas formation volume factor provides the relationship between the gas volumes at reservoir conditions and the volume of produced gas at standard condition as shown on Eq. 2. 4.

$$B_g = \frac{V_R}{V_{sc}} = \frac{p_{sc} Z_R T_R}{T_{sc} Z_{sc} p_R} \qquad 2.4$$

Whereby, parameters with subscript R are expressed at reservoir conditions, and those with subscript sc are expressed at standard conditions. Applying the standard conditions values for customary units (p_{sc}=14.7 psia, T_{sc}=520 °R and Z=1) to Eq. 2. 5, the B_g is reduced to

$$B_g = 0.02827 \frac{Z_R T_R}{p_R} \text{ ft}^3/\text{scf} \qquad 2.5$$

2.1.2.2 Gas Viscosity

The typical viscosity ranges for most of the gas system vary from 0.02 to 0.03 cP at both for all pressure conditions, and the absolute value viscosity does not greatly from gas to gas system (reservoirs) (Whiston, 2002). Different reliable correlations have been developed to estimate gas viscosities such as Dempsey, Lucas and Lee Gonzalez with an accuracy of about ±3% for most applications; the most PVT laboratories use Lee Gonzalez gas viscosity correlation (Whiston & Brule, 2000).

Description of Lee Gonzalez correlation is shown below:

$$\mu_g = A_1 \, x10^{-4} \exp(A_2 {\rho_g}^{A_3}) \qquad 2.6$$

Where,

$$A_1 = \frac{(9.379 + 0.01607 M_g) T^{1.5}}{209.2 + 19.26 M_g + T} \qquad 2.7$$

$$A_2 = 3.448 + (\frac{986.4}{T}) + 0.01009M_g \quad 2.8$$

$$A_3 = 2.447 - 0.2224A_2 \quad 2.9$$

Whereby, μ_g is expressed in cP, ρ_g in g/cm^3 and T in ^{o}R

The accuracy of this correlation is from 0.02 to 0.04 for gas specific gravity less than 1.0 and with errors up to 0.2 for gas condensates with specific gravity greater than 1.5.

2.1.2.3 Z-factor

Z-factor is defined as the ratio of the actual volume of one mole of real gas mixture to the volume of one mole of an ideal gas. The Z-factor expresses the deviation of real gas from ideal gas behaviour.

Generally, Z-factor to predict the gas behaviour is presented by Standing and Katz Z-factor chart (Figure 3). However, some authors have empirically generated equations which fit to the original Standing-Katz chart. Hall and Yarborough present an accurate empirical expression of the Standing- Katz chart using Carnahan-Starling hard-sphere EOS (Eq. 2. 10).

$$Z = \alpha \frac{p_{pr}}{y} \quad 2.10$$

Whereby,

$\alpha = 0.06125texp[-1.2(1-t)^2]$, $t = {}^1/_{T_{pr}}$,

y is the reduced-density parameter which is solved as;

$$f(y) = 0 = -\alpha p_{pr} + \frac{y + y^2 + y^3 - y^4}{(1-y)^3} - (14.76t - 9.76t^2 + 4.58t^3)y^2 + (90.7t - 242.2t^2 + 42.4t^3)y^{2.18+2.82t} \quad 2.11$$

Derivative of Eq. 2. 11 yields Eq. 2. 12

$$\frac{df(y)}{dy} = \frac{y + 4y + 4y^2 + 4y^3 - y^4}{(1-y)^4} - (29.52t - 19.52t^2 + 9.16t^3)y + (2.18 + 2.82t)(90.7t - 242.2t^2 + 42.4t^3)y^{2.18+2.82t} \quad 2.12$$

The expression is solved by Newton-Raphson procedure with initial seed of $y = 0.001$, the convergence to obtain a solution is always between 3 to 10 iterations (Whiston & Brule, 2000).

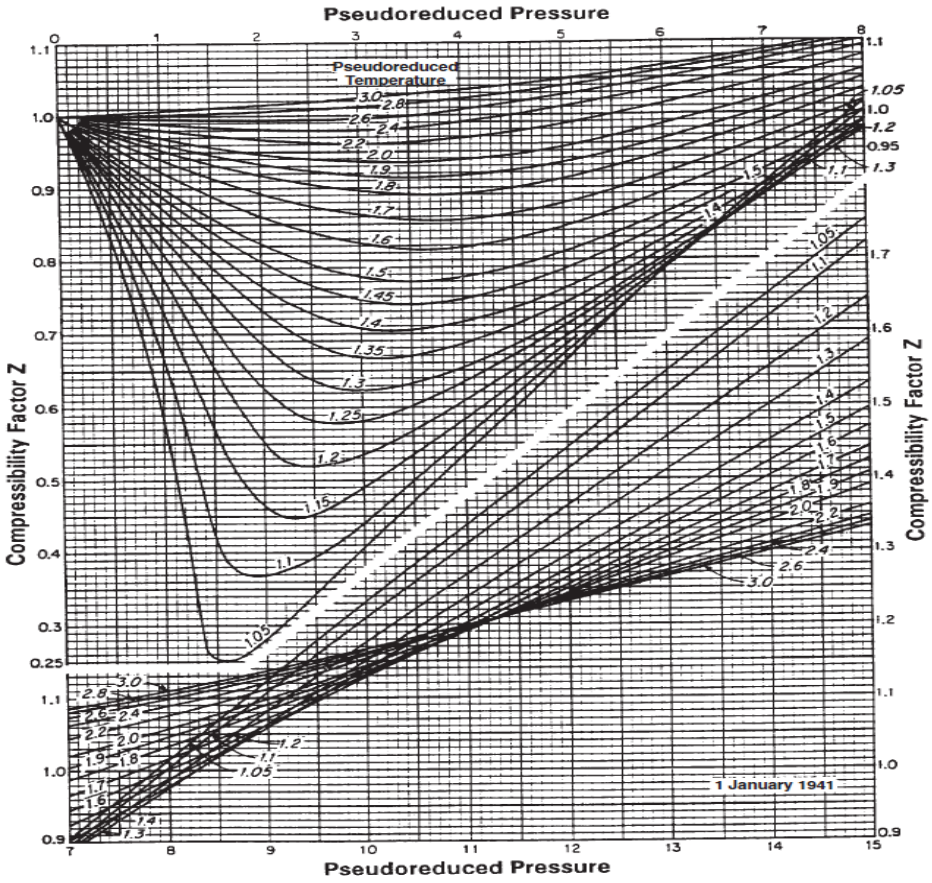

Figure 3-Standing-Katz Z-factor chart (Whiston & Brule, 2000)

2.1.2.4 Gas Pseudocritical Properties

In multicomponent systems, pressure and temperature are usually normalized to pseudo reduced pressure and temperature. The use of normalized parameters makes the gas properties to be similar even if the composition is changed. The pseudo reduced pressure (p_r) and pseudo reduced temperature (T_r) are expressed as $p_r = p/p_c$ and $T_r = T/T_c$ respectively. Where p_c and T_c are critical pressure and temperature respectively. T_c and p_c are valid for most pure components, the same relation can be

used for gas mixture when mixture of pseudo properties (T_{pc} and p_{pc}) are used (Whiston & Brule, 2000).

Sutton developed correlation to estimate pseudocritical pressures and temperature from gas specific gravity. The regression analysis from raw data for the specific gravity ranges from 0.57 to 1.68 generated Eq. 2. 13 and Eq. 2. 14 (Craft, et al., 1991).

$$T_{pc\mathrm{HC}} = 169.2 + 349.5\gamma_{g\mathrm{HC}} - 74.0\,\gamma_{g\mathrm{HC}}^2 \qquad 2.13$$

$$P_{pc\mathrm{HC}} = 756.8 - 131\gamma_{g\mathrm{HC}} - 3.6\gamma_{g\mathrm{HC}}^2 \qquad 2.14$$

2.1.3 Reservoir Rock and Fluid Properties

Understanding of the reservoir rock properties is important for field development study; this help to estimate performance of the reservoir and to have fully understanding and control of the production process. These properties are estimated in laboratory or by use of empirical functions. The following sections describe the most. The laboratory investigation of these properties can be found in (Amyx, et al., 1960) and (Zolotukhin & Ursin, 2000).

2.1.3.1 Porosity

Porosity describes rock's fluid storage capacity. The laboratory porosity measurement methods include; full-diameter core analysis, grain-volume measurements based on Boyle's law, bulk-volume measurements, pore-volume measurement and fluid-summation method. Porosity can also be estimated from well log, although this method is not very accurate. The rock porosity can either be reported as total or effective porosity, petroleum engineer is interested in effective porosity as it describes the porosity of interconnected pores.

(Zolotukhin & Ursin, 2000) Described several idealised porosity model which have been developed to approximate porous rock media and varied characteristics as listed below

a) Idealised porous medium represented by a system of parallel cylindrical pores (pipes). This model may be used in some situations where fluid flow is modelled under simplified conditions. Estimated porosity is 0.785 or 78.5%.

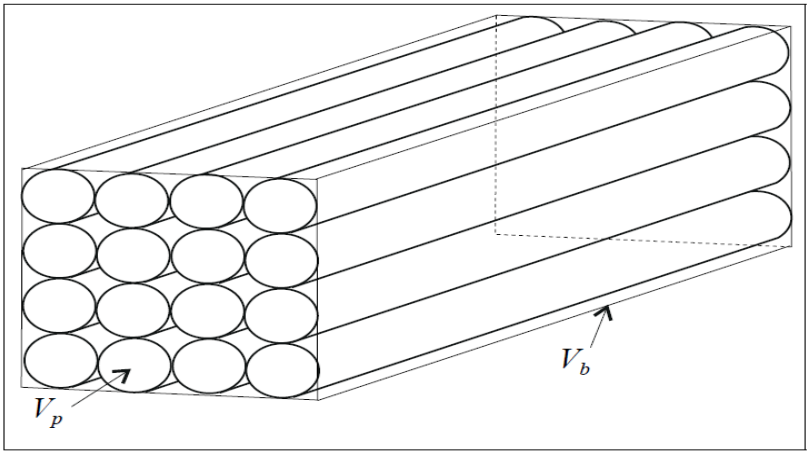

Figure 4-Idealised porous medium of parallel cylindrical pores (pipes) (Zolotukhin & Ursin, 2000).

b) Idealised porous medium represented by a regular system of cubic-packed spheres. Estimated porosity is 0.476 or 47.6%

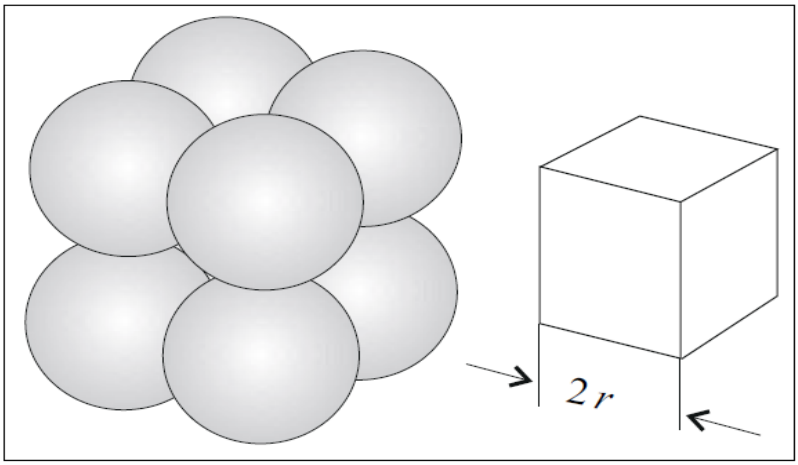

Figure 5-Idealised porous of regular system of cubic-packed spheres (Zolotukhin & Ursin, 2000)

c) Idealised porous medium represented by a regular system of orthorhombic-packed spheres. Estimated porosity is 0.395 or 39.5%

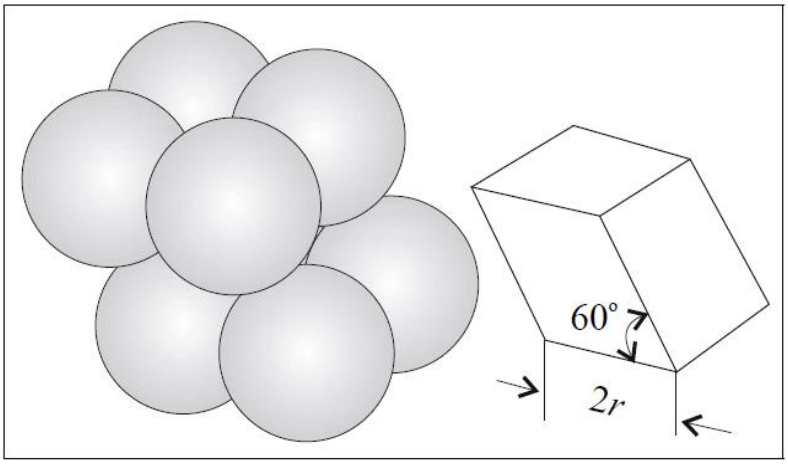

Figure 6-Idealised porous medium of regular system of orthorhombic-packed spheres (Zolotukhin & Ursin, 2000)

d) Idealised porous medium represented by regular system of rhombohedral-packed spheres. Estimated porosity is 0.26 or 26.0%

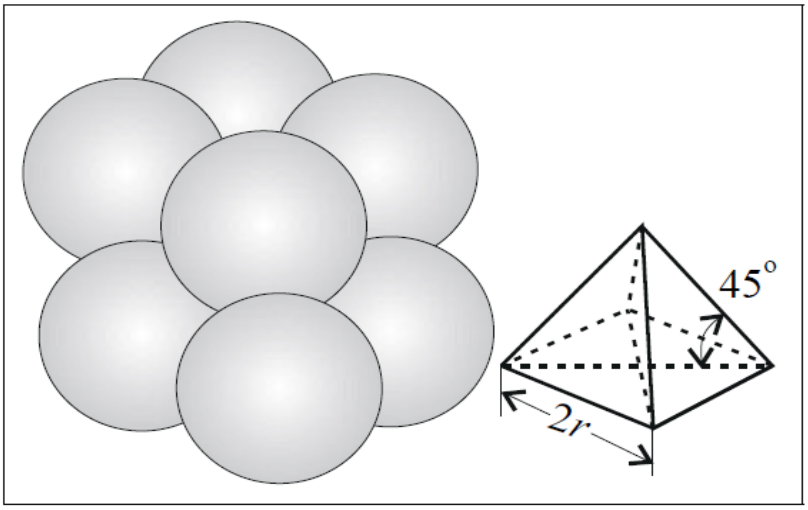

Figure 7-Idealised porous medium of regular system of rhombohedral-packed spheres (Zolotukhin & Ursin, 2000)

e) Idealised porous medium represented by an irregular system of spheres with different radii. This model serves as "mental image" for complex porous structure of rocks.

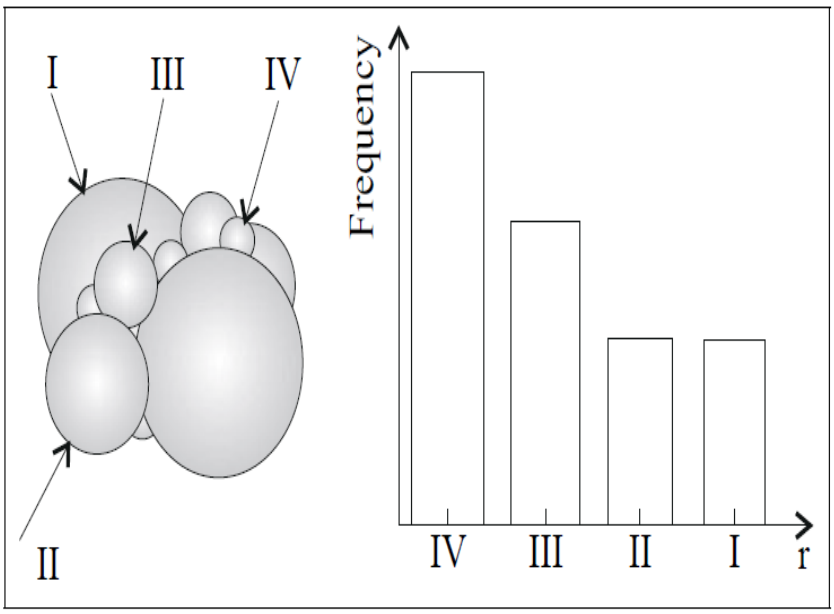

Figure 8-Idealised porous medium represented of irregular system of spheres with different radii (Zolotukhin & Ursin, 2000)

2.1.3.2 Permeability

Reservoir permeability describes the rock's capacity to transport fluids through its interconnected pores. Henry Darcy in 1856 performed the experiment for linear and horizontal flow incompressible fluid with constant elevation which resulted to the relationship shown in equation**.** Darcy's law is the common method used in laboratories to obtain permeability of the rock. This is an empirical observation of flow conditions to obtain permeability.

$$q = -\frac{k}{\mu} A \frac{\Delta p}{\Delta l} \qquad 2.15$$

Where Δp=difference in manometer levels, i.e. hydrostatic height difference, atm; A=cross-sectional area of the filter, cm^2; k=proportionality coefficient (permeability), Darcy; Δl=thickness of the filter in the flow direction, cm and μ=fluid viscosity, cP. These units are in Darcy units.

2.1.3.3 Permeability- Porosity Relationship

The most widely accepted model for porosity-permeability relationship is Kozeny-Carman model (KC) based on the concept of capillary tube model (Costa, 2006). However, no single function exists for permeability as this property is related to the porous rock properties such as grain shapes and sizes. From continued interest of finding permeability-porosity relationship, laboratory measurements of permeability and porosity provides the correlation between porosity and permeability for different rock types.

From core data of many consolidated sandstone and carbonate reservoirs, the logarithmic permeability-porosity relationship is linear (Nelson, 1994). The logarithmic-linear form particularly used for sandstones formation is given by Eq. 2. 16, C and D are constants which are very approximate and equal to 7 (PetroWiki, 2015).

$$\log_{10} k \;=\; C \log_{10} \phi_e + D \qquad 2.16$$

Where k=permeability, mD and ϕ_e=rock effective porosity, fraction.

2.1.3.4 Relative Permeability

The concept of Darcy's law is applicable for single fluid flow in the rock. In petroleum reservoirs, however, the rocks are saturated with two or more fluids. Therefore, it is necessary to restate the Darcy's law by introducing the concept of effective permeability to describe the simultaneous flow of more than one fluid (Amyx, et al., 1960).

$$q_i \;=\; -\frac{k_{ie}}{\mu_i} A \frac{\Delta p_i}{\Delta l} \qquad 2.17$$

The subscript i denoted the fluid phase and k_{ie} is the effective permeability; $k_{ie} = k$ for 100% saturation. All parameters are in Darcy units.

The relationship of effective permeability and absolute permeability (100% saturation with a single fluid) of a porous system relation defines relative permeability (k_{ri}) of the rock.

Symbolically, the relative permeability is expressed as

$$k_{ri} = \frac{k_{ie}}{k} \qquad 2.18$$

The relative permeability can be investigated by performing laboratory experiments under considerable simplified example that; relative permeabilities are the function of fluid saturations only (Zolotukhin & Ursin, 2000). In the presence of two co-existing phases, the typical relative permeability curves can be represented as shown in Figure 9.

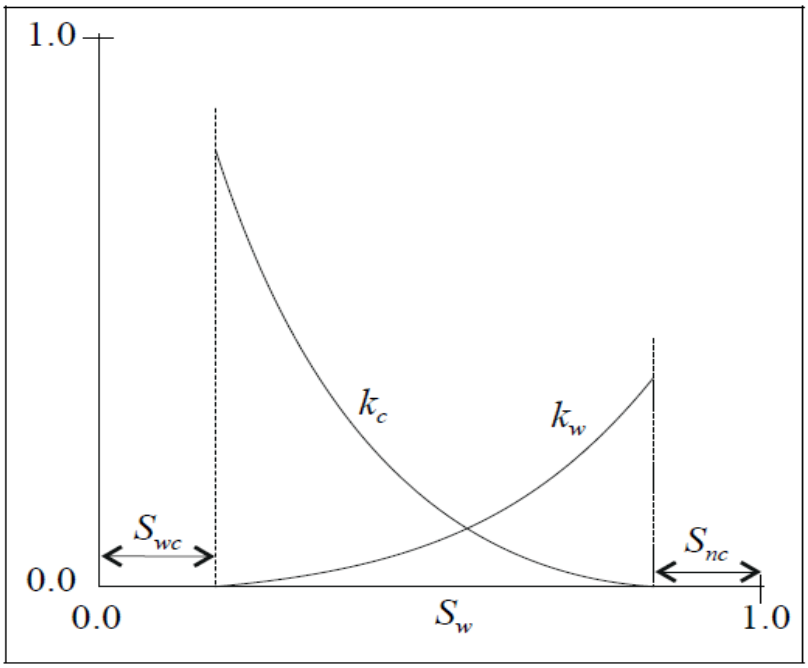

Figure 9-Relative permeability characteristics for a two-phase flow, where S_w is the wetting phase and S_n is the non-wetting phase (Zolotukhin & Ursin, 2000)

The relative permeability of two phases can also be correlated from Corey function. This model assumes the wetting and non-wetting phase-relative permeabilities to be independent of the saturations of the other phases and requires only a single suite of gas / oil-relative permeability data.

The gas-water system correlations are as shown in Eq.2. 19 and Eq.2. 20.

$$k_{rg} = k_{rgcw}\left[\frac{s_g - s_{gc}}{1 - s_{gc} - s_{wi}}\right]^{n_g} \qquad 2.19$$

$$k_{rw} = k_{rwgc}\left[\frac{S_w - S_{wi}}{1 - S_{wi}}\right]^{n_w} \quad 2.20$$

Where k_{rg}=relative permeability of gas, k_{rw}=water relative permeability respectively, n_g = Corey exponents for gas, n_w= Corey exponents for water, subscript gc defines the critical conditions, S_w=Water saturation, S_{wi}=Irreducible water saturation and S_g= gas saturation

,

The models above can be used for wider range of rock and wettability characteristics, and the end points of gas-liquid relative permeability curves while still retaining the shape of the curves. All the relative permeabilities and saturations are unit less.

2.1.3.5 Fluid Saturations

The rock pore spaces are completely saturated with fluids. Therefore, saturation is the measure of fluids volume present in the pore spaces of the rock. There are three fluid types existing in the reservoir which are oil, gas and water. This is not always the case, as some reservoirs consist of water and gas or oil and gas. The summation of fluid saturations in the porous medium is unity (Eq. 2. 21).

$$S_o + S_g + S_w = 1 \quad 2.21$$

Eq. 2. 21, applies when the reservoir consists of oil, gas and water. For gas reservoir the fluid saturation is presented by Eq.2. 22.

$$S_g + S_w = 1 \quad 2.22$$

Fluid saturation is estimated by and some laboratory experiments such as Dean-Stark experiment for measuring initial fluid saturations, however some scholars have correlated the case as described in section 2.1.3.6.

2.1.3.6 Porosity-Water Saturation Relationship

The relationship of porosity and irreducible water saturation has been described by number of authors. The more general relationship is given by Eq. 2. 23. The Q value

ranges from 0.8 to 1.3 with many reservoirs close to 1.0 (Michael, et al., June 7-10 2006).

$$Porosity^{Q}\ x\ Irreducible\ water\ saturation\ = Constant \qquad 2.\ 23$$

The ranges of constant for different rock properties are given below:

- Sandstones 0.02-0.10
- Intergranular Carbonates 0.01-0.06
- Vuggy Carbonates 0.005-0.06

(Buckles, 1965) Proposed the hyperbolic relationship of porosity and connate water saturation (Eq. 2. 24), the relationship is a unique solution to the more general equation (Eq. 2. 23)

$$Porosity\ x\ Irreduciable\ water\ saturation\ = Constant \qquad 2.\ 24$$

Eq. 2. 24 can be linearized to yield Eq. 2. 25.

$$\log_{10}\ Irreduciable\ water\ saturation = \log_{10} Constant - \log_{10} Porosity \qquad 2.\ 25$$

2.1.3.7 Compressibility

Compressibility of a substance expresses the relation of substance's change in volume as the pressure change under isothermal condition (Eq. 2. 26). The units are in reciprocal of pressure units.

$$c = -\frac{1}{v}\left(\frac{dv}{dp}\right)_T \qquad 2.\ 26$$

For any compressible fluid, the isothermal compressibility is described by the following expression

$$c = \frac{1}{p} - \frac{1}{Z}\left(\frac{dZ}{dp}\right)_T \qquad 2.\ 27$$

2.2 Equation of State (EOS)

An equation which describes the relationship of volume of the gas, pressure and temperature is referred as EOS (John & Wattenbarger, 1996). Equation of state formulation is used for phase equilibrium and property calculations, and it provides consistency and smoothness of gas compositions and properties near a critical point (Coats, 1980). This section describes a list of the most useful EOS in petroleum industry.

2.2.1 Ideal Gas Equation

The ideal gas equation (Eq. 2. 28) is the simplest EOS; it was empirically developed by combining two laws which are Boyle's law and Charles' law. Boyle's law states that; for a given mass of a gas at constant temperature, the pressure-volume product, pV, is constant, and Charles' law states that; for a given mass of a gas at constant pressure, the volume/temperature ratio, V/T, is constant. The equation is applicable at low pressure

$$pV = nRT \qquad 2.\ 28$$

Where p=pressure, psia; V=volume, ft^3; n=number of pound moles of gas; R=universal gas constant=10.732 psia-ft^3/^{o}R-lbm-mol; and T=absolute temperature, ^{o}R.

2.2.2 Real Gas Law

Real gas law is the modified ideal gas equation. A correction factor, Z-factor is included. The Z-factor accounts for non-ideal gas behaviour, at ideal pressure and temperature Z=1.0. The real gas law holds at relatively high pressure and low temperature, its expression is as shown in Eq. 2. 29.

$$pV = ZnRT \qquad 2.\ 29$$

Where Z= dimensionless quantity (Z-factor) or gas deviation factor

Somewhat better gas law and of historical interest can be presented by Van der Waals Eq.2. 30. This equation approximately account for long range forces and the volume occupied by molecules.

$$\left(p + \frac{n^2 a}{v^2}\right)(v - nb) = ZnRT \qquad 2.30$$

Where a and b are Van der Waals constants, and v is the molar volume.

The real fluids EOS that are widely used and do work reasonably near dew point and for both liquids and gases are Soave-Redlich-Kwong (SRK), Peng-Robinson (PR), and Benedict-Webb-Rubin-Starling (BWRS). SRK, PR along with Van der Waals are *cubic* equation of state as the polynomial expansion results yield the cubic density term being the highest order term. BWRS adds fifth & sixth power and exponential density terms. The cubic equations of state are limited to low densities (Modisette, 2000).

The general equation governing the cubic equation of states is given as

$$\left(p = \frac{RT}{v - b} + \frac{RT}{v^2 + Av + B}\right) \qquad 2.31$$

For Van der Waal equation, both A and B are zero (Eq.2. 30)

For the SRK equation of state, B becomes zero and $A = b$. a and b are given by

$$a = \frac{0.42748 R^2 T_c^2}{p_c}[1 + (0.48 + 1.574\omega - 0.176\omega^2)(1 - T_r^{0.5})]^2 \qquad 2.32$$

$$b = \frac{0.08664 R T_c}{p_c} \qquad 2.33$$

In the PR equation of state $A = 2b$ and $B = -b^2$. a and b are given by

$$a = \frac{0.45724 R^2 T_c^2}{p_c}[1 + (0.37464 + 1.54226\omega - 0.26992\omega^2)(1 - T_r^{0.5})]^2 \qquad 2.34$$

$$b = \frac{0.07780 R T_c}{p_c} \qquad 2.35$$

Where w= Pitzer acentric factor; T_r= reduced temperature and the subscript c refers to critical conditions. All parameters are in field units

The SRK and PR equation of states can further be derived by substituting the respective numerical expressions of a and b. Also, these equations can be expressed in terms of density with $v = M/\rho$.

2.3 Gas Field Development Concept

During field development plan processes, it is important to identify development concepts, in a technical feasible manner and in the best economic performance manner. The main objective is to maximize the revenue of the given investment. Conveniently, all possible concepts are identified, resulting in a field development plan matrix which is comprised of decision variables such as type of exploited hydrocarbon, hub concept, and well type and transport options (Rodriguez-Sanchez*, et al., 2012). Table 2 shows three examples of field development plan matrix.

Table 2-Field development plan matrix (Rodriguez-Sanchez*, et al., 2012)

Hydrocarbon	**Hub**	**Well**	**Transport**
Oil	Semi-Submersible	Vertical	Tanker
Oil & Gas	Fixed Platform	Directional	Pipe
Gas	TLP	Horizontal	
	FPSO	Multi-Lateral	
	SPAR		

The technical part is crucial in defining the objectives and strategies of the project. t Technical screening processes has to be done combined with economical evaluation to discards the concepts with no value while accepting the concepts which have value to come up with the best case concept.

2.3.1 Hub

There are basically two categories of offshore structures: these structures are either fixed or moved from place to place (floating) systems. Fixed platforms involve of Jacket Structure, Gravity based, Compliant Structures and Guyed towers while floating systems involve of Floating Production, Storage and Offloading (FPSO), Semi-submersible platforms, SPAR platforms and Tension Leg Platforms (TLPs). Platform categories and

their applicability water depth are shown in Figure 10. In selecting of the development concept, detailed evaluations of the pros and cons of the concepts should be considered. The critical issues of selection of the mentioned concepts are detailed discussed in (Abbott, et al., 1995).

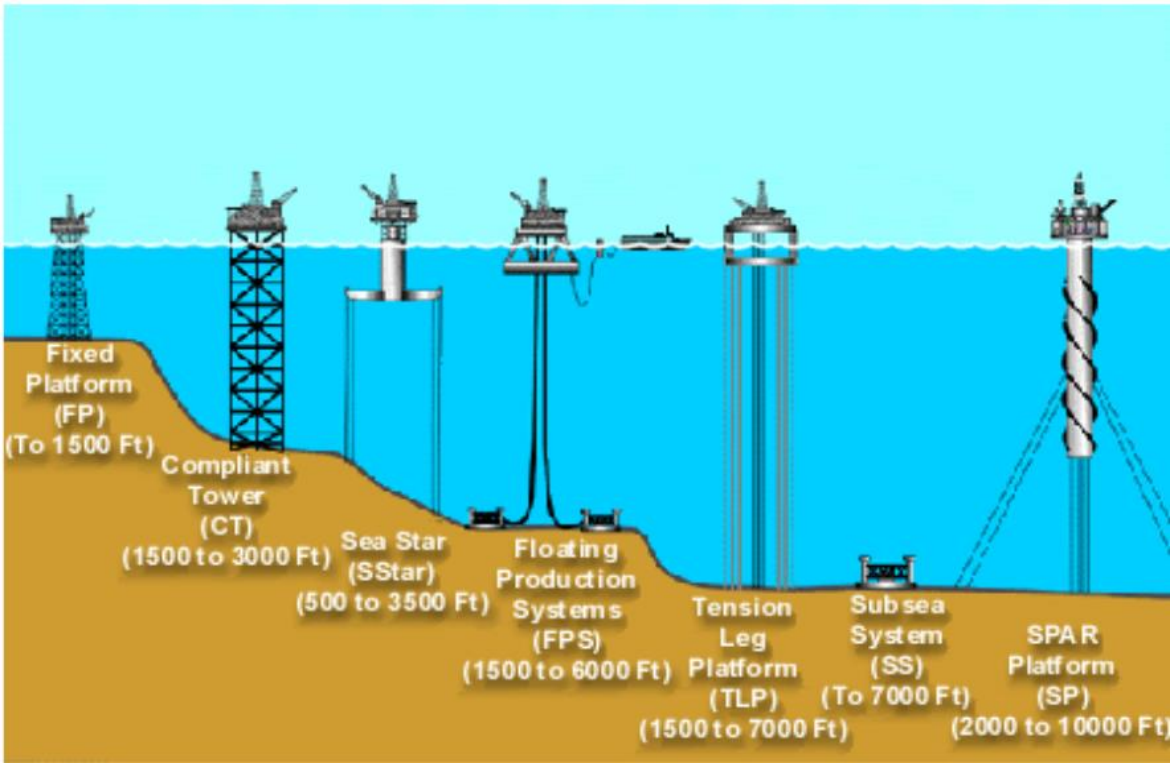

Figure 10-Offshore structures with their water depths (Diego Vannucci, 2011)

Subsea tie back techniques are sometimes developed for deepsea water fields, the development does not require platform at the field itself (Abbott, et al., 1995). The field development architecture may involve manifold, individual well or Daisy chained well tied back to the production facility. These subsea tie back architectures are as illustrated in Figure 11.

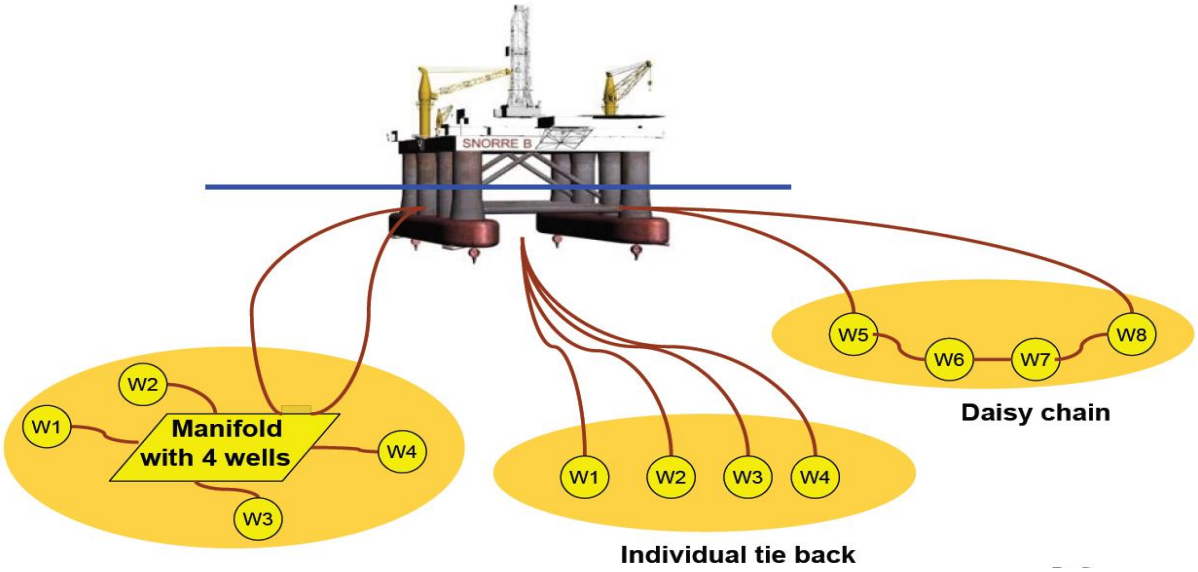

Figure 11- Subsea tie back field development architectures (Hallset, 2009)

2.3.2 Wells Configurations

Once the well has been drilled must be completed. The process involves a number of stages such as well casing completion and installation of the wellhead. These actions are taken to convert the borehole into an operational system for controlling recovery. (National Petroleum Council (America), 2011). Once the casing is installed, the *tubing* which runs up the extracted hydrocarbons to the surface is inserted inside the casing. The production casing is typically 2 to 11 inches (Devold, 2013). Figure 12 illustrates example of downhole well development. The figure shows the number and sizes of casing strings that might be needed for a deepwater Gulf of Mexico well (National Petroleum Council (America), 2011).

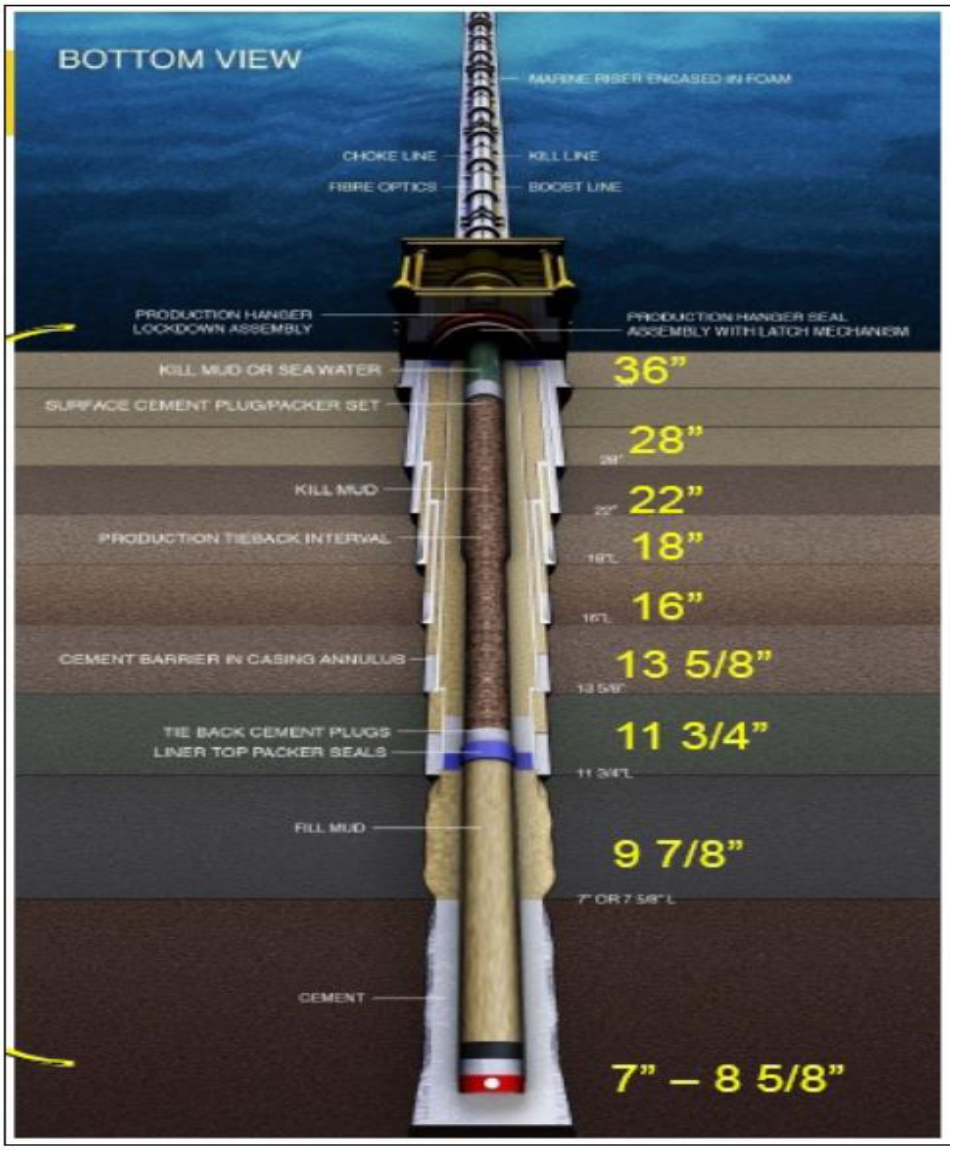

Figure 12- Downhole well development (National Petroleum Council (America), 2011)

The tubing size is usually determined by carrying out sensitivity analysis using nodal analysis (detailed discussion in section 2.6.6) to ensure optimum tubing size which meats the requirement of the well during entire production life (Renpu, 2011). The tubing performance relationship is as shown in Figure 13. From this figure the following observations are seen. (Note: these results shown below are for a particular case, fluids, formation, depth, etc. They might not be applicable as a general rule).

- Tubing has the highest lifting efficiency when $Q_L > Q_A$, 114.3-mm (4 ½ in.)
- Tubing is more economic when $Q_A > Q_L > Q_B$, 73-mm (2 7/8 in.) and
- Tubing is most appropriate when $Q_L > Q_C$, 60.3-mm (2 3/8 in.)

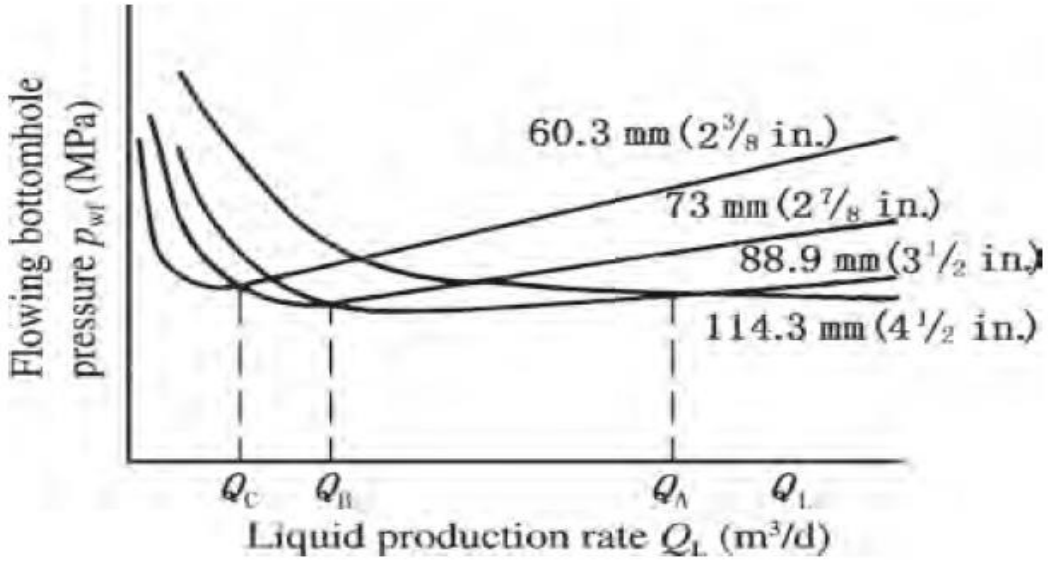

Figure 13-Tubing size effect on lifting capability (Renpu, 2011)

In the offshore gas field, the subsea wells constructions can be done in two ways (Figure 14). The wells can be made in satellite way, whereby vertical wells are drilled above the area of interests; these wells are then connected to the manifold. In the second way, the wells are a clustered on templates (cluster manifold) and then the cluster manifold is joined to the main manifold. The Clustered wells are usually deviated or inclined to reach different parts of the reservoir. In terms of cost, vertical wells are cheaper than deviated wells.

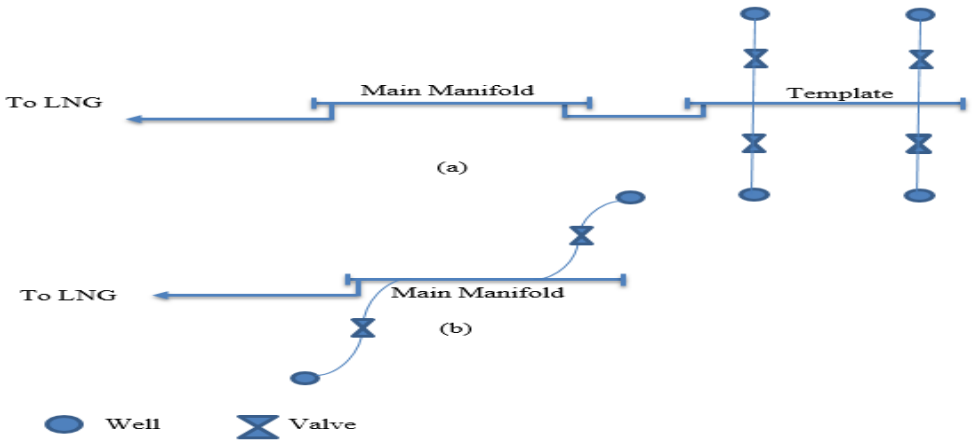

Figure 14-(a) Configuration of well in a template/cluster (b) Configuration of satellite wells

2.3.3 Transportation of Natural Gas

Natural gas transportation consists of complex pipeline transportation system consisting of interstate and to some extent intrastate pipelines. Methods for natural gas transportation include pipeline (PNG), liquefied natural gas (LNG) compressed natural gas (CNG), gas to hydrate (NGH) and gas to liquids (GTL) (Javanmardi, et al., 2007).

Commonly used transportation infrastructures are PNG where the natural gas is transported in gaseous state, and LNG where natural gas (merely methane) is liquefied and transported in special tankers. NGH and CNG should be used at cost less than LNG and when the PNG is not possible.

PNG is undisputed because it remains the safest and most viable means of getting the gas from the point of production to the market (Adewumi, 1997). However, LNG is nowadays becoming potential compared to traditional PNG, other potential options such as CNG and micro LNG may be opted (Dale, 2013). Figure 15 illustrates feasible natural gas transportation technologies in terms of gas volume and distance to market in Norway.

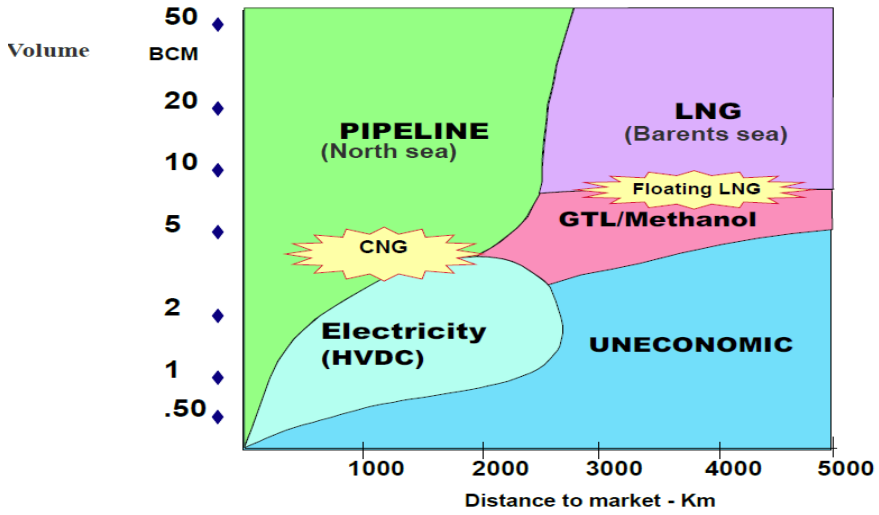

Figure 15- Natural gas transportation technologies (Dale, 2013).

2.4 Block 2 Natural Gas Field Offshore Tanzania

2.4.1 Ownership

In 2007 Statoil signed a production sharing agreement (PSA) for Block 2 with Tanzania Petroleum Corporation (TPDC). As the operator of this block, Statoil Tanzania AS has 65% working interest with ExxonMobil Exploration and Production Limited as a partner with 35% interest. The Block 2 covers an area of approximately 5,500 square kilometres and lies in water depths between 1 500 to 3 000 metres (Statoil, 2016).

2.4.2 Exploration Activities and Discoveries

Exploration program started in year 2012, and up to date total of eight (8) successful discoveries have been made out of thirteen (13) wells that have been drilled. These discoveries include Zafarini-1, Lavani-1, Lavani-2, Tangawizi-1, Giligiliani-1, Mronge-1, Piri-1 and Mdalasini-1 (Maden, 2015). The combined discoveries have proved around 22 Tcf IGIP (Statoil, 2016).

2.4.3 Discoveries Characterizations

The discoveries are characterized by water depths ranging from 2 200 m to 2600 m combined with a seabed consisting of deep water, large scale canyons, channel and steep inclination towards the shore. The large scale canyons are smooth with steep inclination (+4 to +5 degrees) due to water depths and the steep escarpment near the shore is between 20-30 degrees. The sea water surface temperature may be approximated to 30 ℃, while that in deep water is +3 to +4 ℃. The reservoir fluids are very dry (merely methane) (Holm, 2015). The large scale seabed topography is as illustrated in Figure 16.

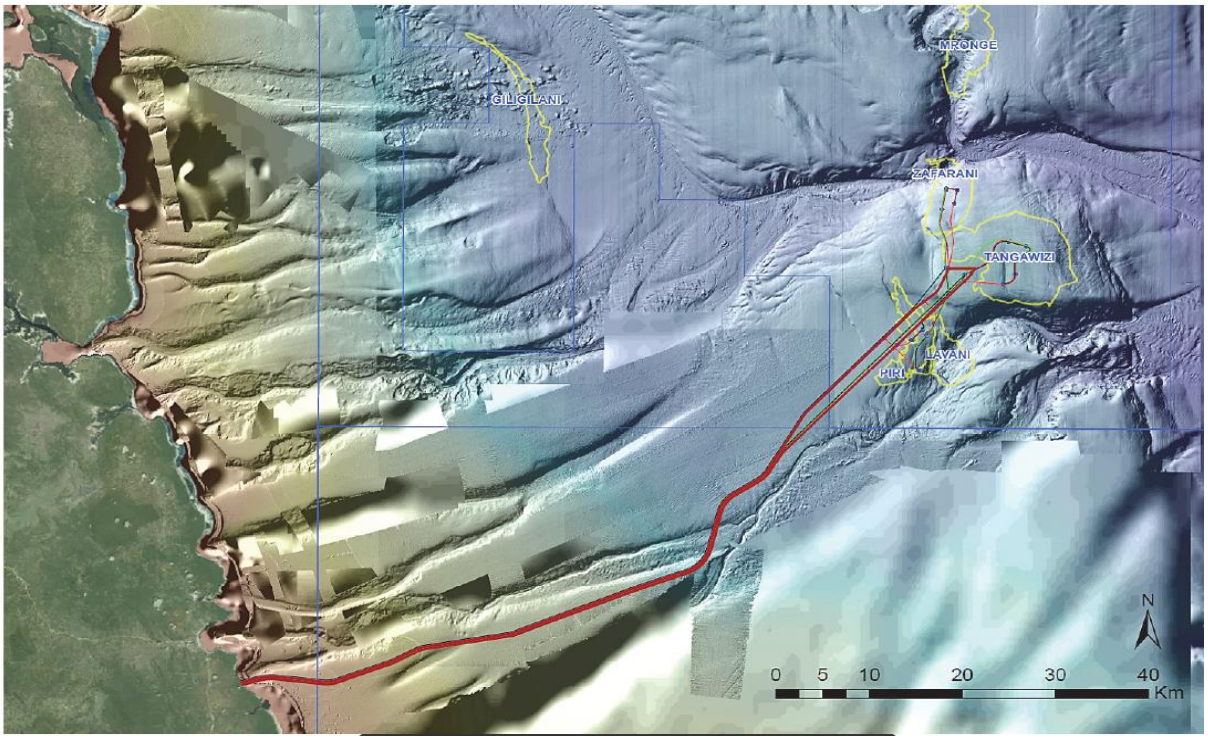

Figure 16-Seabed topography of Tanzania Gas Project (Holm, 2015)

2.4.4 Discoveries Locations and Geology

Zafarani-1 and Piri-1 have been made in Lower Cretaceous sandstones (Statoil , 2014). Zafarani-1 encountered 120 metres of excellent quality reservoir with high porosity and high permeability (Statoil, 2013). The Lavani-1 which is 16 kilometres south of Zafarani-1 discovery, encountered 95 metres of excellent quality reservoir sandstone with high porosity and high permeability (Statoil, 2012). The Lavani-2 well is deeper and located about 5 kilometres southeast of the Lavani-1 discovery well and 20 kilometres south of the Zafarani-1 discovery well. (Statoil, 2013). The Tangawizi –1 was drilled by Ocean Rig Poseidon drilling rig 10 kilometres from Zafarani and Lavani and was made in sandstones of tertiary age (Statoil, 2013). Mdalasini-1 was made in tertiary and cretaceous sandstone at the southernmost edge of the Block 2 (Maden, 2015). The Mronge-1 was drilled by the Drillship Discoverer Americas, and it is located 20 kilometres north of the Zafarani discovery (Statoil, 2013). Giligiliani-1 was made in upper Cretaceous sandstones at the western part of Block 2 (Statoil, 2014).

2.4.5 DST at Block 2

The good reservoir quality and connectivity was confirmed after the DST test operation on Zafarani-2. The well was flowed at maximum of 66 MMscf/day which was constrained by equipment rate capacity. The obtained production rate of the well is estimated to be higher than the rate obtained during the test (Michelsen, 2014).

2.4.5 Development Concept

According to (Holm, 2015), the selected development concept for Block 2 in Tanzania is the Subsea to Beach concept, whereby the subsea production system tied back to an onshore LNG plant, and the transportation is done via multiphase pipeline. The subsea layout is as shown in Figure 17.

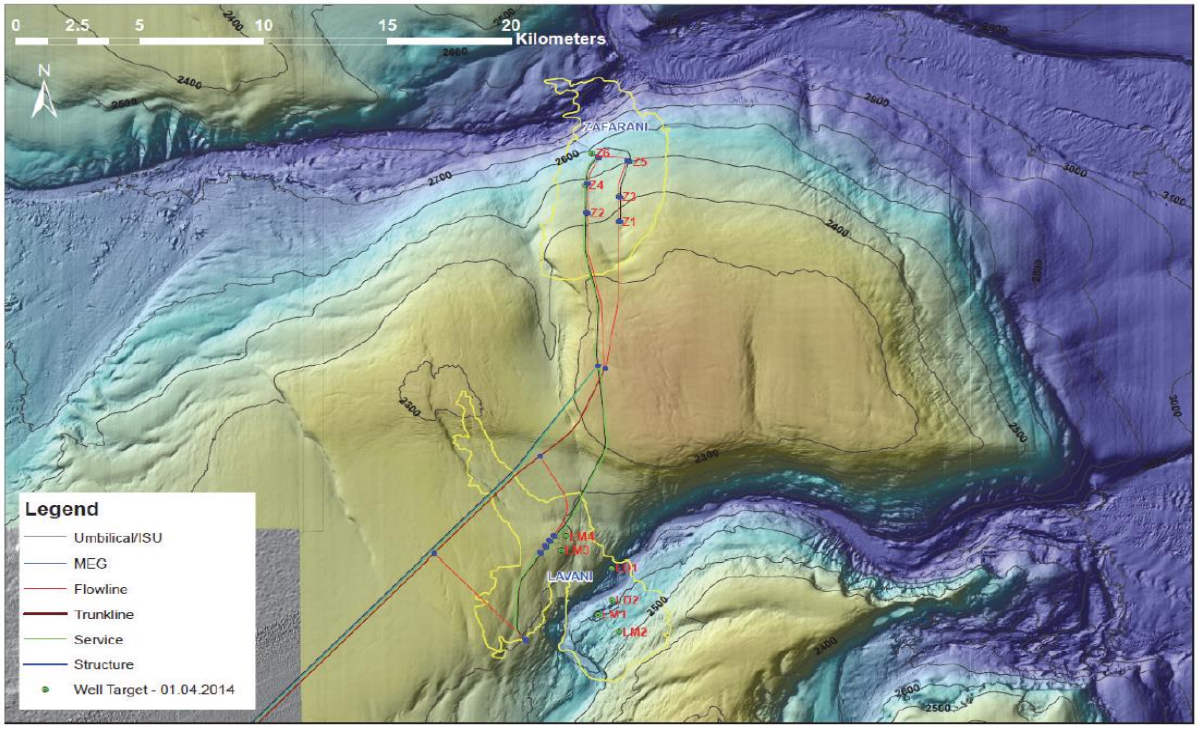

Figure 17-Subsea Layout (Holm, 2015)

2.5 Gas Reservoir Modelling

Gas reservoir can be modelled into three different methods which are, material balance method, and decline curve analysis and reservoir simulation. The methods can be used independently or in combination to provide more confidence in the results obtained, for example, reservoir simulation can be used in with decline curve analysis.

2.5.1 Material Balance Equation (MBE)

The gas material balance can be applied to estimate the initial gas in place (IGIP), predicting gas recovery and identifying drive mechanism of the reservoir. Material balance equation follows a statement of conservation of mass that; the mass of hydrocarbons (HC) initially in place is equal to sum of the mass produced and the mass still remaining in the reservoir (Zolotukhin & Ursin, 2000).

Modeling of gas production using MBE can be done in various forms, depending on reservoir conditions and driving mechanisms associated to the gas reservoir of interest. Such forms includes, gas material balance by considering water drive, gas reservoirs with abnormally high-pressure, and low permeability gas reservoirs.

When the dry gas reservoir is considered volumetric, the reservoir is considered a tank with no external energy support, such as absence of water influx. If connect water expansion and rock compressibility are also negligible; the gas expansion will be the only driving mechanism for gas production (John & Wattenbarger, 1996). The tank model assumption is limited to some reservoir properties such as low permeability and compartmentalization. However, this model can be used when there is little reservoir data and when reservoir uncertainties are large (Baker Hughes, 2010). The gas MBE for volumetric gas reservoir is shown by Eq. 2. 36.

$$GB_{gi} = \left(G - G_p\right)B_g \qquad 2.36$$

Eq. 2. 36 can be redefined to Eq. 2. 37, when $B_g = (constant)\frac{z}{p}$ and $B_{gi} = (constant)\frac{Z_i}{P_i}$, from real gas equation of state are applied. Eq. 2. 37 gives straight line relationship with negative slope when $\frac{p}{z}$ is plotted against G_P.

$$\frac{p}{Z} = \frac{p_i}{Z_i}(1 - \frac{G_P}{G}) \qquad 2.37$$

or equivalently:

$$\frac{p}{Z} = \frac{p_i}{Z_i}(1 - R.F)$$

Where by, $R.F$ signifies the gas recovery factor as the function of cumulative gas produced (G_P).

When the gas reservoir is subjected to water influx from nearby aquifer, encroaching water is taken into account. The gas pore volume at initial conditions will be equal to the gas pore volume at later conditions plus the pore volume change due to water influx (ΔV_p).

$$GB_{gi} = \big(G - G_p\big)B_g + \Delta V_p \qquad 2.38$$

ΔV_p is affected with both water influx and amount of water produced as:

$$\Delta V_p = W_e - W_p B_w \qquad 2.39$$

Combination of Eq.2. 38 and Eq. 2. 39 yield the general gas MBE with external pressure support from aquifer (Eq. 2. 40).

$$GB_{gi} = \big(G - G_p\big)B_g + W_e - W_p B_w \qquad 2.40$$

For high pressure gas reservoirs, the cumulative effective compressibility (c_e) is counted in MBE. The c_e accounts for pore and water compressibility, gas solubility and total water associated with gas reservoir volume (Fetkovich, et al., 1998).

The form of such MBE is

$$\frac{p}{Z}(1-c_e(p_i - p)) = \frac{p_i}{Z_i}(1 - \frac{G_P}{G}) \qquad 2.41$$

Whereby c_e is defined as

$$c_e = \frac{c_{tw}(p) + c_f(p) + M[c_{tw}(p) + c_f(p)]}{1-S_{wi}} \qquad 2.42$$

c_{tw} and c_f are total water and formation compressibility terms.

M, quantifies the ratio of the sum of interbedded non-pay volume, and the limited aquifer contribution to pressure support to the net pay volume.

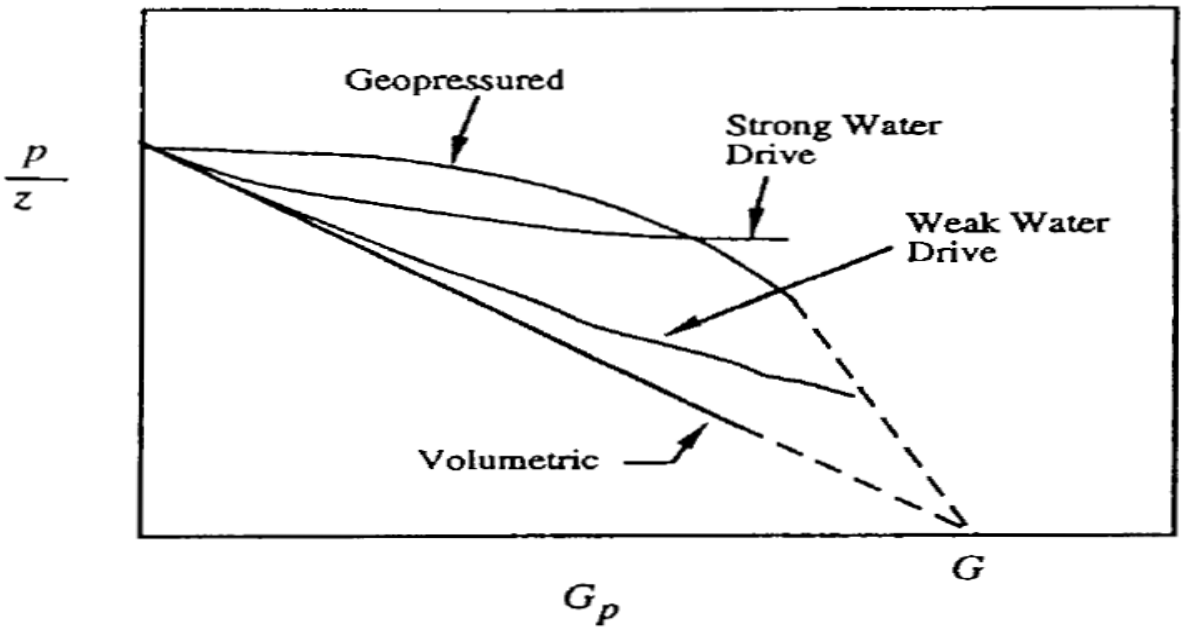

Figure 18-Exhibition of $\frac{p}{z}$ against G_p line trends for various drive mechanisms (John & Wattenbarger, 1996)

2.5.2 Decline Curve Analysis

Decline curve analysis is used in forecasting gas and oil production, and is applied on matured fields. There are three types of production decline curves which are exponential, hyperbolic and harmonic. The mathematical development of these curves was given by (ARPS, 1944).

Based on (ARPS, 1944), the conventional empirical rate/time decline equation is given by

$$q(t) = \frac{q_i}{(1 + bD_i t)^{1/b}} \qquad 2.43$$

These curves can be used to analyse and extrapolate decline curves from actual production history. The b-value can be selected from any desired number from $0 \leq b \leq 1$. For b=0, the type of decline is exponential, for $0 < b < 1$ the type of decline is hyperbolic and for b=1 the type of decline behaves harmonically (Gentry, 1972).

2.5.3 Reservoir Simulation

The valuable aspect of reservoir simulation modeling is to determine reservoir performance and performing production forecasting. There are two approaches to perform reservoir simulations, namely; analytical approach and numerical approach.

It is impossible to obtain analytical solution for many reservoir problems; rather numerical (finite-difference) approach is mostly employed as the alternative to numerical approach. The finite different approach is usually called reservoir simulation. Reservoir simulator data are taken from available information such as well logs, core analysis, geological descriptions, pressure data and production data (John & Wattenbarger, 1996). The good thing with reservoir simulation is the capability of dealing with complex reservoir characteristics.

The following simple example for one dimensional (1 D) demonstrates the finite difference of the diffusivity equation.

$$\frac{\partial^2 p}{\partial^2 x} = \frac{\phi\mu}{0.00633k}\frac{\partial p}{\partial t} \qquad 2.44$$

The numerical approximation is done by using Taylor series analysis, and the discretized form is given in the following form:

$$\frac{p_{i-1}^{n+1} - 2p_i^{n+1} + p_{i+1}^{n+1}}{\Delta t} = \frac{\phi\mu}{0.00633k}\frac{p_i^{n+1} - p_i^n}{\Delta t} \qquad 2.45$$

Superscript n and $n+1$ indicate the "old" and "new" time levels respectively.

Eq. 2. 45 is an *implicit* finite-difference equation because it has more than one unknown (p_{i-1}^{n+1}, p_i^{n+1} and p_{i+1}^{n+1}). The Eq. 2. 45 would have been solved *explicitly* with one unknown (p_i^{n+1}) by discretizing the left side of the equation at n time level. The explicit finite difference equation is of no practical use because e it is unstable for practical time steps (John & Wattenbarger, 1996).

2.6 Production Performance Optimization

The entire production system in petroleum engineering involves analysis of reservoir potential, well performance and flowline capacity. The reservoir models are detailed

explained in section 2.4. The well is the component which links the surface facilities and the reservoir. Analysing of the well performance affects the entire operational system (reservoir, flowline and the processing facility).

2.6.1 Well Performance

Determination of the well performance depends on two performance relationships, the first being the inflow relationship performance (IPR) and the second is the vertical lift performance (VLP). The IPR gives the relationship between fluid flowrate towards the wellbore and the drawdown (reservoir-wellbore pressure difference) as shown on Figure 19. The VLP describes the ability of the reservoir fluids to pass through tubing as shown on Figure 20 (Bikoro, 2005). The ability of the reservoir to deliver into the bottom of the well must be combined with the vertical lift performance (Economides, et al., 1994); the two phenomenon are closely related because the end condition of IPR is the initial condition of VLP.

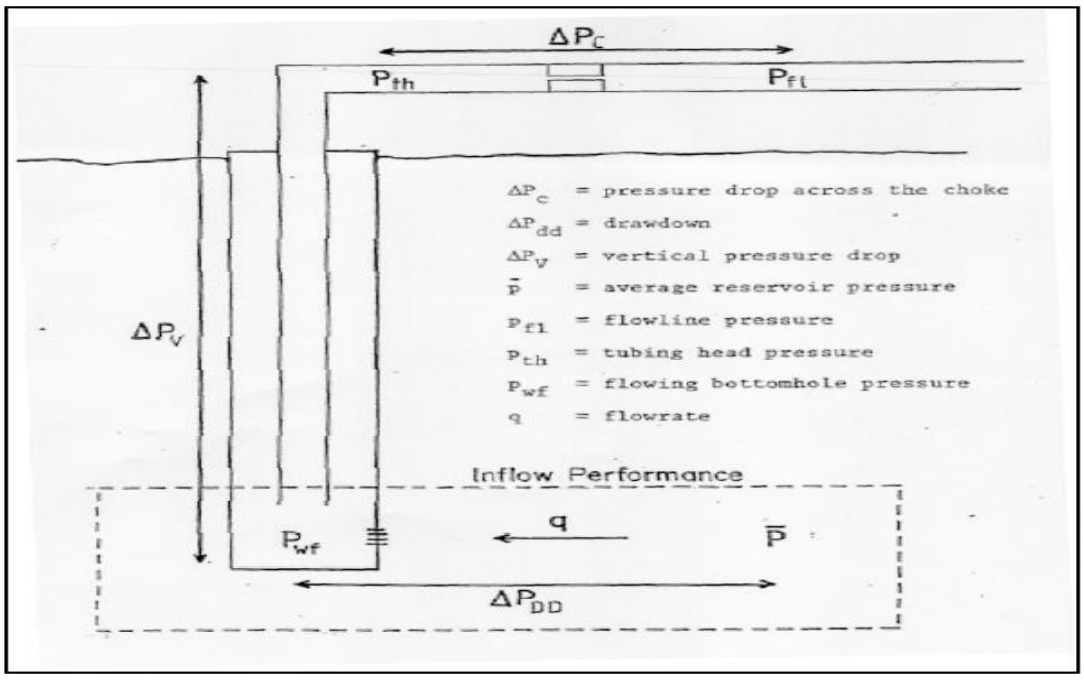

Figure 19- Schematic illustration of Inflow Performance Relationship (Bikoro, 2005)

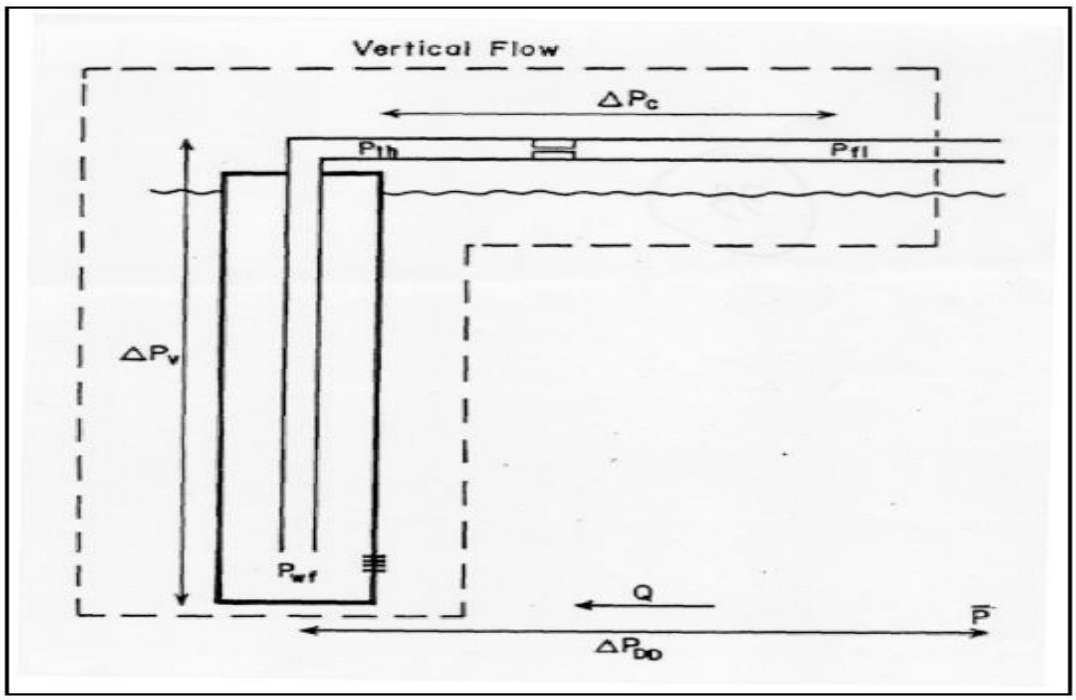

Figure 20- Schematic illustration of Vertical Lift Performance (Bikoro, 2005)

Gas well performance is determined based on its flow capacity, the flow capacity entails the relationship between the inflow gas rate and the sand face pressure or flowing bottom-hole pressure.

2.6.2 Gas Flow in Porous Media

The flow of fluid in the reservoir rocks are classed according to fluid type, reservoir geometry and flow conditions. The fluid types are classified as incompressible, slightly compressible or compressible. According to flow system time dependences, three conditions are classed as steady state, transient and late transient or pseudo steady state. In case of reservoir geometry, two geometries which are linear and radial are of practical interest (Craft, et al., 1991). However, in this context, the radial flow geometry is the most interested geometry for calculations.

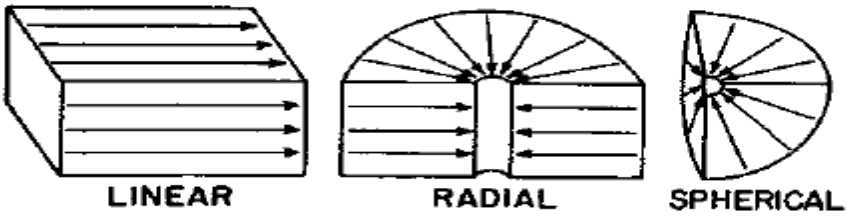

Figure 21- Common flow Regimes (Craft, et al., 1991)

The flow of fluid in the reservoir rocks is described by diffusivity equation. Discussion of the diffusivity equation in this context is limited to compressible fluid (gas), as the flowing gas in the reservoir rock.

The diffusivity equation developed from combination of material balance equation (continuity equation), Darcy's equation and Equation of State (EOS) typically a real gas law. For compressible fluid, the equation comes in various forms of pressure and time variables (Craft, et al., 1991). The pressure and time variables are pseudopressure and time and pressure squared and time variables.

The basic radial differential form for single phase flow is given as:

In terms of pressure-squared and time function

$$\frac{1}{r}\frac{\partial}{\partial r}\left(r\frac{\partial p^2}{\partial r}\right)=\frac{\phi\mu c_t}{k}\frac{\partial p^2}{\partial t} \qquad 2.46$$

In terms of pseudopressure and time function

$$\frac{1}{r}\frac{\partial}{\partial r}\left(r\frac{\partial m(p)}{\partial r}\right)=\frac{\phi\mu c_t}{k}\frac{\partial m(p)}{\partial t} \qquad 2.47$$

2.6.2.1 Pseudopressure against Pressure-squared Functions

In 1966, Russel and Goodrich, and Al-Hussainy, Ramey and Crawford simultaneously developed reliable analytical solutions of Eq. 2. 46 and Eq. 2. 47 respectively (Dake, 1983). The pressure squared formulation by Russel and Goodrich can be a reasonable approximation on solving the diffusivity equation. However, the assumptions (μ_g and Z are constant) used are limiting and can lead to large error in high rate wells with large variations in the flowing pressure (Economides, et al., 1994). The better linearized solution to the basic diffusivity equation done using real gas pseudo-pressure function ($m(p)$) was developed by Al-Hussainy and Ramey. The real gas pseudopressure function can be used for any flowing pressure ranges since is properly adjusted for the viscosity and the gas deviation factor.

$m(p)$ for real gas is defined as,

$$m(p) = 2\int_{p_o}^{p} \frac{p}{\mu Z} dp \qquad 2.48$$

Arbitrary, p_o is the reference pressure which is always set to zero.

It is more comfortable to deal with pressure squared formulation than dealing with pseudopressure formulation (integral transformation). Therefore, (Dake, 1983) presented how pseudopressure function can be examined in the easiest way. The method describes how a table of $m(p)$ values can be numerically generated as the function of actual pressure. The parameters in the integrand of Eq. 2. 48 can be obtained from PVT analysis of gas at reservoir temperature or, by knowing gas gravity, standard correlations of μ_g and Z at reservoir temperature. A graph of $m(p)$ versus p gives almost linear relationship for hi pressures in excess of 2 800 psia. The relationship can be used for entire life of the reservoir.

2.6.2.2 Stabilized Solutions to the Diffusivity Equation

For practical use, the diffusivity equation is solved when the flow is stabilized (steady state and pseudo steady state). The steady state flow occurs when the gas rate has the same value at all radii because the pressure change with respect to time at any location of the reservoir is zero. The pseudo steady state is achieved when the flow is boundary dominated; no flow at the outer boundary and the rate is constant (Ikoku, 1984). The steady state is never achieved at natural production; unless pressure is supported, for example during injection processes.

In order to solve the differential diffusivity equation, it is necessary to specify the boundary conditions near wellbore and the external boundaries of the reservoir. The near wellbore conditions are the same for both steady state and pseudo steady state flow, thus, the radius (r) is equal to the wellbore radius (r_w) and the pressure is equal to the bottom hole flowing pressure (p_{wf}). The outer (external) boundaries are different for steady state and pseudo steady state. Steady state outer boundary is $p_e = p_R(r = 0.6r_e)$ and the pseudo steady state outer boundary is $p_e = p_R(r = 0.472r_e)$.

The solutions of diffusivity equation as the subject of gas rate at standard conditions are presented below:

Steady state equation in pressure squared function (Eq. 2. 49) and pseudopressure function (Eq. 2. 50).

$$q_{gsc} = \frac{0.703\ kh(p_R^2 - p_{wf}^2)}{T_R \mu z(\ln(\frac{r_e}{r_w}) - \frac{1}{2} + s)} \quad 2.49$$

$$q_{gsc} = \frac{0.703\ kh(m(p_R) - m(p_{wf}))}{T_R(\ln(\frac{r_e}{r_w}) - \frac{1}{2} + s)} \quad 2.50$$

Pseudosteady state equation in pressure squared function (Eq. 2. 51) and pseudopressure function (Eq.2. 52).

$$q_{gsc} = \frac{0.703\ kh(p_R^2 - p_{wf}^2)}{T_R \mu z(\ln(\frac{r_e}{r_w}) - \frac{3}{4} + s)} \quad 2.51$$

$$q_{gsc} = \frac{0.703\ kh(m(p_R) - m(p_{wf}))}{T_R(\ln(\frac{r_e}{r_w}) - \frac{3}{4} + s)} \quad 2.52$$

Where k= permeability, mD; h=net-pay thickness, ft.; p=pressure, psia; T=temperature, $°R$; μ =viscosity, cP an Z= Z-factor, unitless.

2.6.3 Gas Well Deliverability

In order to obtain the productivity capacity of a gas well, different deliverability tests are undertaken. The common well productivity indicator is called Absolute Open Flow (AOF) potential (AOF refers to the maximum flow rate the well could deliver against zero sandface pressure). Such tests are also applicable in generating the Inflow Performance Relationship (IPR) (IPR describes relationship between the well flow rate and the flowing bottomhole pressure of the well) of the well.

The most common gas-well deliverability tests discussed in separate articles are; flow after flow tests, isochronal modified isochronal test and single point. The flow after flow test is primarily limited to long time required for stabilization in low permeability reservoirs. Consequently, isochronal and modified isochronal tests were developed for short time tests (Johnston, et al., 1991).

The linear and non-linear relationships of the reservoir gas rate-pressure behaviour for the well are described in section 2.6.3.1 and 2.6.3.2 respectively.

2.6.3.1 The Linear Gas Rate-Pressure Behaviour (backpressure equation)

Rawlins and Shellhardt in 1936 developed the classic backpressure equation (Eq.2. 53) after interpreting hundred multi-rate gas well tests. The backpressure equation gives a straight line trend on log-log plot of rate versus delta pressure squared ($p_R^2 - p_{wf}^2$), whereby n equals the reciprocal of the backpressure straight line (Golan & Whitson, 1991).

$$q_{gsc} = C_R(p_R^2 - p_{wf}^2)^n \qquad 2.53$$

n values range from 0.5 to 1. When $n = 1$, the backpressure equation assumes Darcy flow for n less than one non-Darcy flow is evident in the reservoir (Economides, et al., 1994). The backpressure coefficient (C_R) accounts for the rock and fluid properties, transient effects and flow geometry. Its value is not constant unless for stabilized flow (pseudo steady state) exists (Golan & Whitson, 1991).

Eq.2. 41 can be written in pseudo pressure functions as shown by Eq.2. 54.

$$q_{gsc} = C_R(m(p_R) - m(p_{wf}))^n \qquad 2.54$$

The analytical expression for C_R when $n = 1$, and the flow is in pseudosteady state are given by Eq. 2. 55 in pressure squared function and Eq. 2. 56 in pseudopressure function.

$$C_R = \frac{0.703kh}{T_R\mu z(\ln(\frac{r_e}{r_w}) - \frac{3}{4} + s)} \qquad 2.55$$

$$C_R = \frac{0.703kh}{T_R(\ln(\frac{r_e}{r_w}) - \frac{3}{4} + s)} \qquad 2.56$$

2.6.3.2 The Non-linear Gas Rate-Pressure Behaviour (Forchheimer equation)

The Darcy's law breaks down for high velocity flow, and several models and experimental background to modify the Darcy's flow in order to account for high velocity flow are discussed by Muskat in 1937. The more accepted model was proposed by Forchheimer in 1901 as presented in Eq. 2. 57 (Golan & Whitson, 1991).

The more exact deliverability relationship for stabilized gas flow is as shown in Eq.2. 58. This relationship is the solution of the differential equation for gas flow in porous media using the Forchheimer equation. (Economides, et al., 1994).

$$p_R^2 - p_{wf}^2 = Aq + Bq^2 \qquad 2.57$$

The term A stands for Darcy coefficient and B stands non-Darcy coefficient

$$q_{gsc} = \frac{0.703kh(p_R^2 - p_{wf}^2)}{T_R\mu z(\ln(\frac{r_e}{r_w}) - \frac{3}{4} + s + Dq_{gsc})} \qquad 2.58$$

The term Dq is referred to as the turbulence skin effect. The term D is the function of turbulence factor β which have been correlated in terms of rock properties, permeability and porosity (John & Wattenbarger, 1996). The term D is expressed as

$$D = \frac{2.715\ x10^{-12}\ \ \beta kMp_{sc}(p_R^2 - p_{wf}^2)}{h\mu p_{wf} r_w T_{sc}} \qquad 2.59$$

The β correlation is given by

$$\beta = 1.88\ x10^{10}k^{-1.47}\phi^{-0.53} \qquad 2.60$$

When rearranging Eq.2. 58 in the form of equation Eq. 2. 57 and performing correct algebra, the analytical expressions of coefficients A and B can be determined as presented in Eq.2. 61 and Eq. 2. 62 correspondingly

$$A = \frac{1424\mu z T_R\left(p_R^2 - p_{wf}^2\right)}{kh}\left(\ln\left(\frac{r_e}{r_w}\right) - \frac{3}{4} + s\right) \qquad 2.61$$

$$B = \frac{1424\mu z T_R D}{kh} \qquad 2.62$$

It is possible to approximate the Forchheimer quadratic equation to reservoir backpressure equation, by assuming the non-Darcy coefficient equals to zero.

2.6.4 Flow in a Well, Gathering Lines and Pipelines

The entire gas production system comprises of reservoir, wells, flow lines and pipelines. Prediction of pressure drops doesn't stop on the reservoir as discussed in section 2.6.2, nonetheless, the whole entire system pressure drops prediction must be performed to obtain well's ability to deliver the gas to the main transportation pipeline. It is also important to predict the temperature profile in a pipeline. This discussion proceeds in the following subsections of this section. Note: all the equations under this sections are in field units.

2.6.4.1 Gas Flow in Conduits

Conduit stands for tubing, flowlines or pipelines. For single phase flow in a pipe, the pressure drop over a distance L is governed by mechanical energy balance equation (Eq.2. 63)

$$\frac{dp}{\rho}+\frac{udu}{2g_c}+\frac{g}{g_c}dz+\frac{2f_f u^2 dL}{g_c D}+dW_s=0 \qquad 2.\,63$$

The overall pressure drop is a function of potential energy (Δp_{PE}), kinetic energy (Δp_{KE}) and frictional contributions (Δp_F). When there is no shaft work device for instance, pump compressor or turbine in the pipeline; (dW_s) becomes zero (Economides, et al., 1994).

The (Δp_{PE}) account for the pressure change due to the hydrostatic head

$$\Delta p_{PE}=\frac{g}{g_c}dz \qquad 2.\,64$$

The (Δp_{KE}) accounts for the pressure drop resulting from velocity of the fluid between two positions.

$$\Delta p_{KE} = \frac{udu}{2g_c} \quad 2.65$$

The (Δp_F) is the pressure drop due to friction and is given by Fanning equation

$$(\Delta p_F) = \frac{2f_f u^2 dL}{g_c D} \quad 2.66$$

Where, f_f is the Fanning friction factor, for laminar flow is simply expressed as the function of Reynolds number (N_{Re}) (Eq. 2. 67), whereas for turbulent flow f_f may depend on both N_{Re} and the relative pipe roughness (ϵ) (2. 68).

$$f_f = \frac{16}{N_{Re}} \quad 2.67$$

$$\epsilon = \frac{k}{D} \quad 2.68$$

Whereby k=length of the protrusions on the pipe wall

Commonly, f_f is obtained from Moody friction factor chart which was generated from the implicit Colebrook-white equation (Eq.2. 69), explicitly the equation with similar accuracy to the Colebrook-White equation was developed by Chen in 1979, and this is Chen equation (2. 70) (Economides, et al., 1994).

$$\frac{1}{\sqrt{f_f}} = -4log\left(\frac{\epsilon}{3.7065} + \frac{1.2613}{N_{Re}\sqrt{f_f}}\right) \quad 2.69$$

$$\frac{1}{\sqrt{f_f}} = -4log\left\{\frac{\epsilon}{3.7065} - \frac{5.0452}{N_{Re}} log\left[\frac{\epsilon^{1.1098}}{2.8257} + \left(\frac{7.149}{N_{Re}}\right)^{0.8981}\right]\right\} \quad 2.70$$

For compressible fluid (Gas), the compressibility of the fluid must be considered when solving Eq. 2. 63, as the fluid density and fluid velocity vary along the pipe, the average compressibility (Z_{av}) estimated as the function of average temperature (T_{av}) is used.

By using the average values of Z and T in Eq. 2. 63 with $dW_s = 0$, the equation can be integrated to yield

$$p_{in}^2 = e^s p_{out}^2 + \frac{32 f_f}{\pi^2 D^5 g_c \sin\theta}\left(\frac{Z_{av} T_{av} q_g p_{sc}}{T_{sc}}\right)^2 (e^s - 1) \qquad 2.71$$

The $\sin\theta$ term accounts for the pipe deviation from vertical and the e^s term accounts for elevation, where s is defined as

$$s = \frac{-(2)(28.97)\gamma_g(\frac{g}{g_c})\sin\theta\, L}{Z_{av} T_{av} R} \qquad 2.72$$

Eq. 2. 71 relates the inlet pressure and outlet pressure for non-horizontal flow of gas and can be rearranged to

$$q_g = \left[\frac{T_{sc}}{Z_{av} T_{av} p_{sc}}\left(\frac{\pi^2 D^5 g_c \sin\theta}{32 f_f}\right)^{0.5} \frac{e^{s/2}}{(e^s - 1)^{0.5}}\right] (\frac{P_{in}^2}{e^s} - P_{out}^2)^{0.5} \qquad 2.73$$

Eq. 2. 73 represents the *tubing equation* and its general form is simply

$$q_g = C_T(\frac{P_{in}^2}{e^s} - P_{out}^2)^{0.5} \qquad 2.74$$

For tubing is convenient to define $p_{in} = p_{wf}$ and $p_{out} = p_{wh}$

Where C_T is the tubing coefficient expressed as

$$C_T = \frac{T_{sc}}{Z_{av} T_{av} p_{sc}}\left(\frac{\pi^2 D^5 g_c \sin\theta}{32 f_f}\right)^{0.5} \frac{e^{s/2}}{(e^s - 1)^{0.5}} \qquad 2.75$$

When the tubing is vertical, $\sin\theta$ will be one.

For the case of horizontal flow, $\sin\theta$ and e^s terms are both zero, Eq. 2. 63 can be integrated to yield

$$p_{in}^2 - p_{out}^2 = \frac{1854.08\,\gamma_g f_f\, Z_{av} T_{av}}{\pi^2 D^5 g_c R}\left(\frac{q_g p_{sc}}{T_{sc}}\right)^2 L \qquad 2.76$$

Again, Eq.2. 76 can be rearranged to

$$q_g = \left[\frac{T_{sc}}{p_{sc}}\left(\frac{\pi^2 D^5 g_c R}{1854.08\,\gamma_g f_f\, Z_{av} T_{av} L}\right)^{0.5}\right](p_{in}^2 - p_{out}^2)^{0.5} \qquad 2.77$$

Eq. 2. 77 represents the *gathering lines and pipelines*; its general form is simply

$$q_g = C_{PL}(p_{in}^2 - p_{out}^2)^{0.5} \qquad 2.78$$

For gathering line and pipeline is convenient to define $p_{in} = p_{up}$ and $p_{out} = p_{dwn}$

Where C_{PL} is the pipeline coefficient expressed as

$$C_{PL} = \frac{T_{sc}}{p_{sc}}\left(\frac{\pi^2 D^5 g_c R}{1854.08\,\gamma_g f_f\, Z_{av} T_{av} L}\right)^{0.5} \qquad 2.79$$

(Fetkovich, 1975), gave the relation of C_T or C_{PL} against the flow string diameter, the new coefficients can be changed by defining the new diameter of the flow string as given in Eq.2. 80.

$$\frac{C_{Tnew}}{C_{Tpresent}} = \frac{D^{2.612}new}{D^{2.612}present} \qquad 2.80$$

2.6.4.2 Gas Flow in Chokes

During gas production from reservoir, it is necessary to install the wellhead choke. The wellhead choke provides the well head choke is put as the restriction the production rate. The rate is restricted due to number of factors including the prevention of coning and sand production, satisfying production limits and surfaces equipment rate and pressure constraints (Economides, et al., 1994).

2.6.4.3 Subsea Gathering Systems and Networks

a) Manifolds

Subsea manifolds/ templates act as subsea production gathering system where the dry completion well on the main field feeds. The main functions of subsea manifolds include commingling all the production wells and isolation of individual well and diverting it to the test separator if any. The manifold/Template structure is as shown in Figure 22.

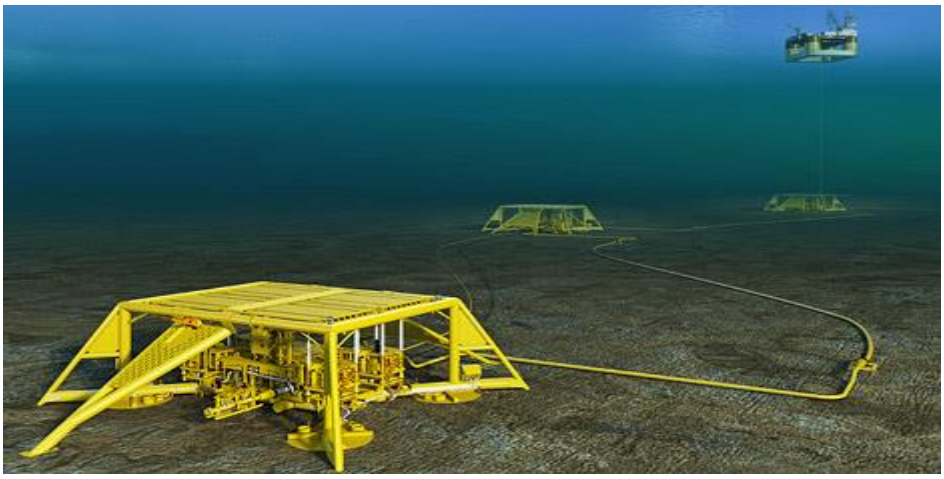

Figure 22-Example of subsea template Courtesy Statoil

b) Common Kind of Gathering Networks

There are two common kind of gathering as illustrated by (Szilas, 1975). These gathering are depicted in Figure 23. In the first gathering system, all the flowlines are joined at a common point (junction) (Figure 23, left). In the second gathering system, individual wells are joined at common pipeline (Figure 23, right).

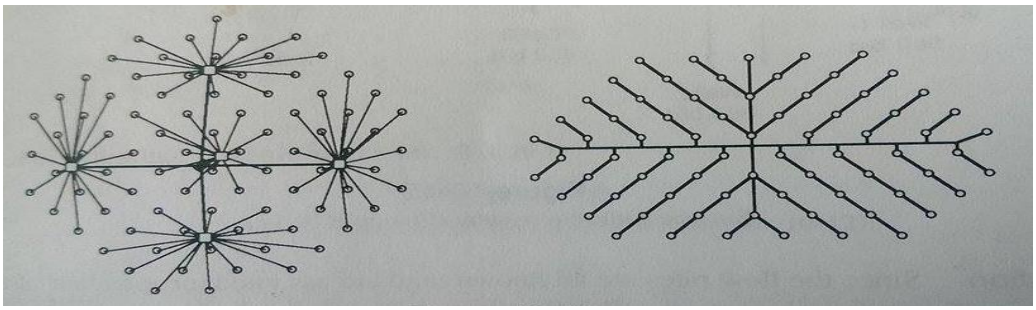

Figure 23- Two common Gathering networks (Szilas, 1975)

When individual flowlines are commingled at a common junction the pressure at the common point will be equal for all flow lines (Figure 23, left). The flowing tubing pressure (ptf_i) of an individual well i can be related to the common junction pressure (p_{junc}) as shown in Eq.2. 81. In the system where individual wells are connected at a common junction (Figure 23, right), the pipeline flow rate is the sum of the upstream well flow rates. The individual wellhead pressures are the calculated by starting at the junction and working upstream (Economides, et al., 1994).

$$ptf_i = p_{junc} + \Delta p_{Li} + \Delta p_{Ci} + \Delta p_{fi} \qquad 2.81$$

Where Δp_{Li}=pressure drop through flowline, Δp_{Ci}=pressure drop through choke (if present), Δp_{fi}=pressure drop through fittings.

2.6.4.4 Temperature in a Pipeline

In gas lines, cooling of gas is done by two mechanisms which are heat losses and gas expansions. Heat losses take into account energy balance of the pipeline system. Therefore, accurate predictions of heat loss and temperature profile in gas production pipeline are essential for designing and evaluation of pipeline operations (Guo, et al., 2006). When gas cools through expansion, temperature drops below the surrounding temperature. This influence is due to Joule Thompson effect.

The relationship between the temperature of flowing fluid (inside the pipe) and surrounding temperature (sea temperature) is presented by a general Eq.2. 82. Figure 24 illustrates the temperature loss inside the pipeline.

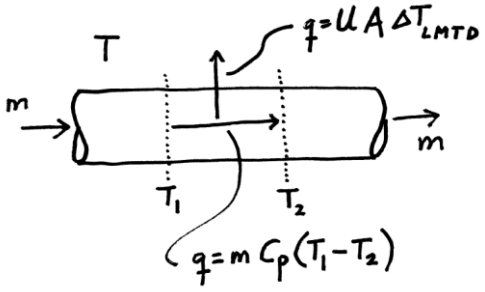

Figure 24: Heat transfer in a pipeline (Guðmundsson, 2011)

$$T_2 = T + (T_1 - T)\exp(\frac{-U\pi D}{mC_p}L) \qquad 2.82$$

Where T_2=final fluid temperature, T_1 =initial fluid temperature, L=pipe length, U=overall heat transfer, C_p=Specific heat at constant pressure, T=surrounding temperature and D= pipe diameter.

The heat transfer Coefficient depends on the type of pipe used, According to (Guðmundsson, 2011), U value ranges are given as: for insulated pipeline on seafloor 1<U (W/m^2. K) <2 and for non-insulated pipeline on seafloor 15<U (W/m^2.K) <25.

2.6.5 Flow Control and Monitoring

2.6.5.1 X-Tree

The production well does not only include a vertical conduit from the wellhead back to a formation. Usually the wellhead has an equipment (production Christmas tree) mounted to regulate and monitor the extraction of hydrocarbon. The Christmas tree is composed of master gate valve, a pressure gauge, a wing valve, a swab valve, check valves and a choke as shown in (Figure 25).

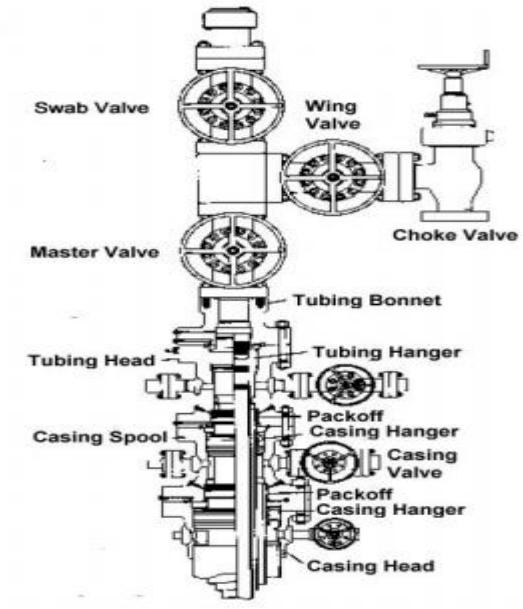

Figure 25-A Christmas tree (Devold, 2013)

Functions of these components as explained by (Devold, 2013) are as follows:

- Master gate valve provides full opening so that the specialized toll may be run through it.

- Pressure gauge is the minimum instrumentation above the master gate valve,
- Wing valve is used when shutting in the well so that the tubing pressure can be easily read.
- Swab valve is used to gain access to the well during wireline operations, intervention and other workover procedures
- Check valve closes when there is back flow.
- Choke valve (Discussed in section 2.6.4.2).

2.6.5.2 Separation

The purpose of the horizontal production separators is to split the well stream flow into desirable fractions as it may contain crude oil, gas, condensates water and other contaminants.

In petroleum industry, the classic production separator in terms of design and type is a gravity separator. When the well flow is fed into gravity separator, the retention time of five minutes is taken to allow segregation of the well flow components. Often, the pressure is reduced in stages to allow control of volatile components (Devold, 2013). Figure 26 illustrates example of gravity separator.

Figure 26-Horizontal gravity separator (Devold, 2013)

2.6.6 Flow Equilibrium Analysis

Flow equilibrium analysis can be referred as nodal analysis. As a comprehensive, yet simple tool for calculating and displaying flowing pressure as the function of production rate and various design parameters such as tubing size, gas lift rate and separation

pressure (Hein, 1987). This kind of system analysis is done by analysing the entire production system as a single unit (Hossain, 2008). The entire production system includes all components-beginning with the static reservoir pressure, ending with the separator, and including inflow performance, as well as flow across the completion, up the tubing string (including any downhole restrictions and safety valves), across the surface choke (if applicable), through horizontal flowlines, and into the separation facilities (Brown & Lea, 1985). The models discussed in chapter 2.63 and 2.64 are applicable for hydraulic calculations in nodal analysis. The possible pressure losses n in the production system are depicted in Figure 27.

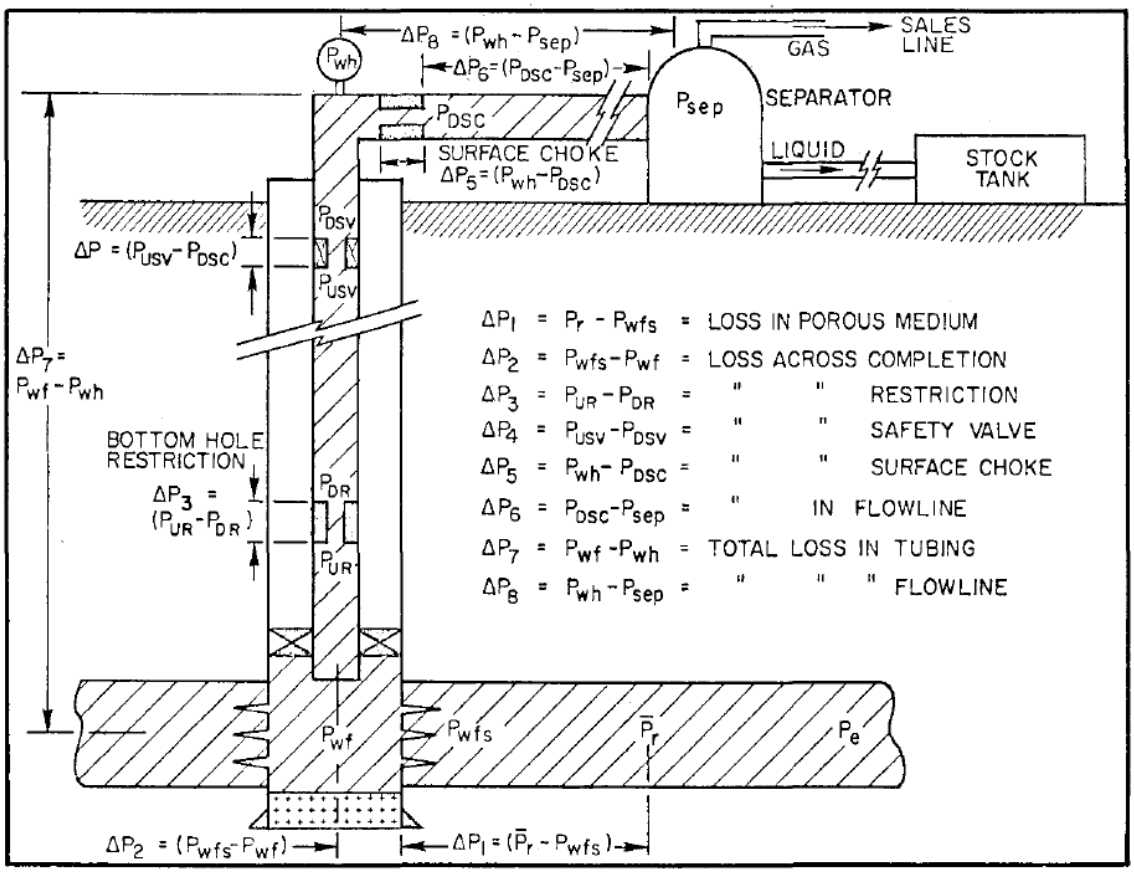

Figure 27-Possible pressure losses in complete production system (Brown & Lea, 1985)

In order to perform hydraulic calculations, the reference node which is the delimeter between two halves of the pipeline should be specified. The nodes of the production system are as shown in Figure 28. Other two nodes which are upstream node (source) and downstream node (sink) should also be specified, consequently, the nodal analysis can be done by performing concurrent calculations from the source to the reference

node and the counter-current calculations from the sink node to the reference node as illustrated in Figure 29 .

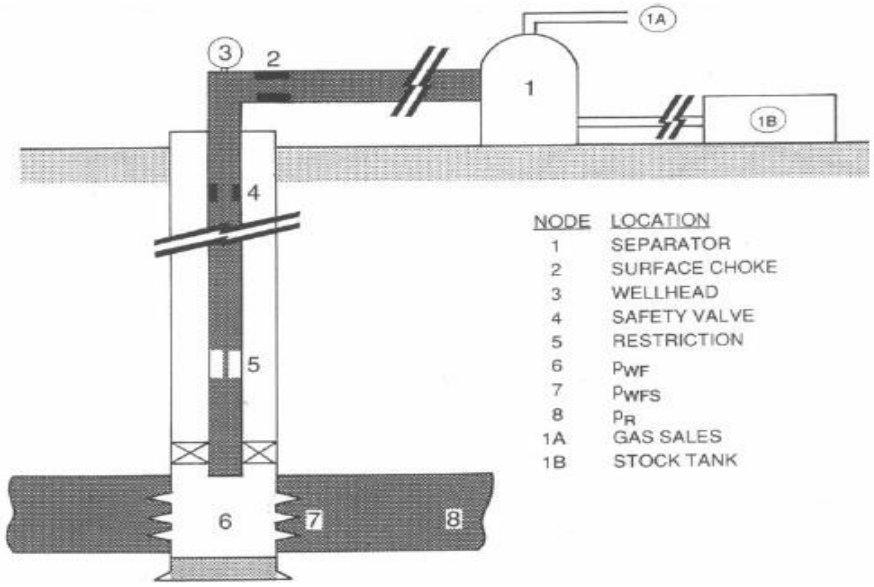

Figure 28-Production system nodes (Hossain, 2008)

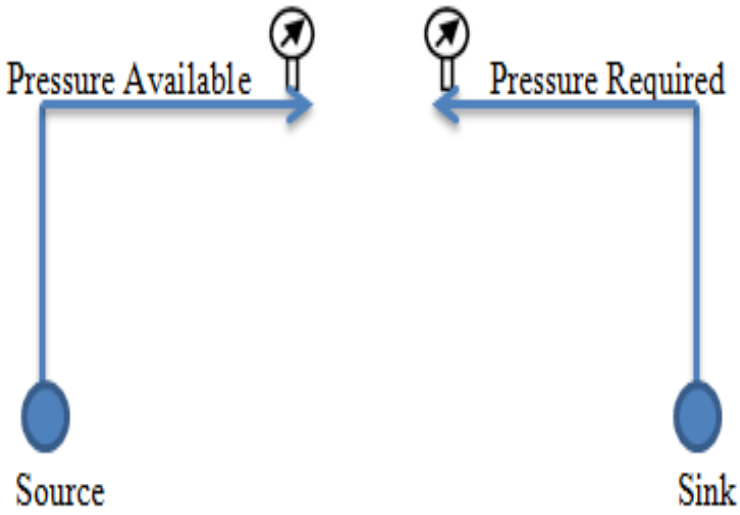

Figure 29- Schematic view of the flow equilibrium calculation

These hydraulic calculations of the two flow strings; the inflow section and the outflow section will generate available and demand/required curve respectively. The intersection of the two curves depicts the total system solution. The available curve and required curve are presented in Figure 30.

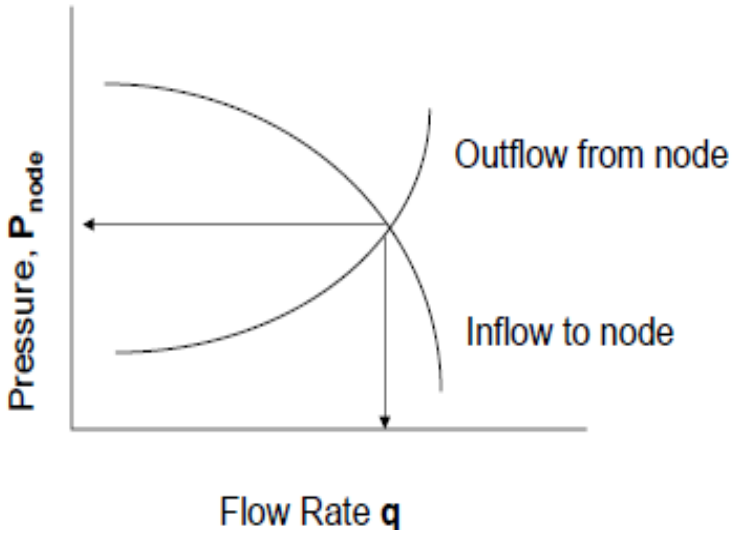

Figure 30- Available and required curves during equilibrium analysis (Hossain, 2008)

2.7 Production Scheduling

Production scheduling refers to the process of how the offtake of gas from reservoir is going to be with respect to time. The process involves many sensitivity analyses of the field production rate as the function of reservoirs deriving mechanisms. This is an important part of field development, since it creates the gas production profile which has to be calculated to estimate the income due to hydrocarbon sales. Therefore, production profile is vital factor during economic evaluation of the field (Rodriguez-Sanchez*, et al., 2012). The schematic production patterns of the gas illustrated in Figure 31 was presented by (A. Rojey, 1997). The figure shows the three production stages, the first stages being the build-up stage whereby the production increases gradually with the increase of drilled wells, the second stage is the period of stabilized production called production plateau, and the last stage is the decline stage whereby the production decreases as more gas is withdrawn from the reservoir.

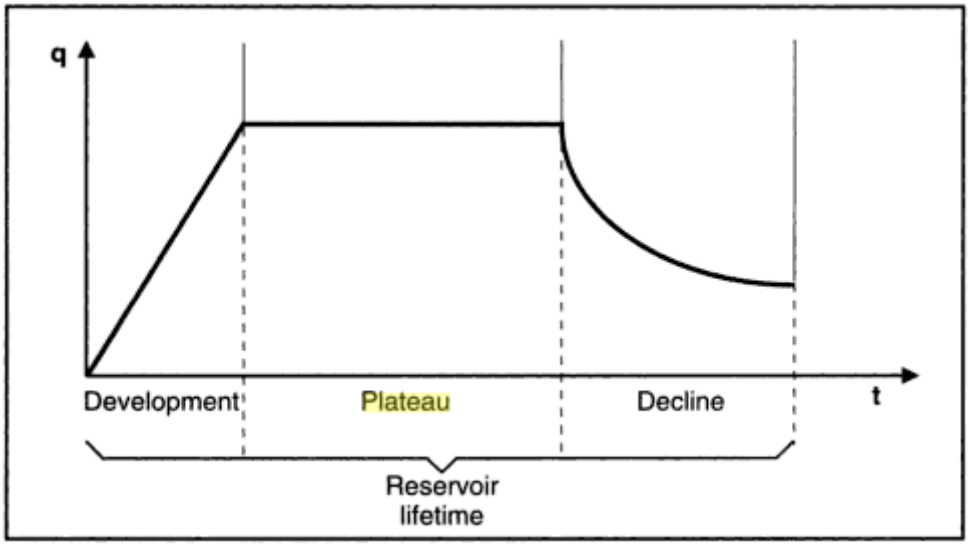

Figure 31- Schematic production patterns of the gas reservoir (A. Rojey, 1997)

For the gas reservoir, production scheduling is mainly governed with production plateau rate (height) and the production plateau length whereby the question of how much gas will be produced and for how long gas should be produced is fully addressed. The answer to this question depends on the sales contract between a buyer and producer, and sometimes the production is constrained with production facilities such as flow lines, pipelines and separator.

2.7.1 Gas Reservoir Offtake Modes

The offtake of the gas from the gas reservoirs could be done in two modes; these modes are called Mode A and Mode B. The Mode A is usually run in a constant rate-pressure declines mode and applied for the stand alone filed where the production of gas has to be done from the beginning of production (no existing infrastructure). The Mode B is run in a constant pressure-rate decline mode and usually operated on a satellite field using an existing infrastructure (Stanko & Golan, 2015), (Stanko, 2016). The modes are illustrated in Figure 32. The general implicit assumption for Mode A has been that an optimized production schedule would result in an optimized economic return (Padget & Tuer, 1980).

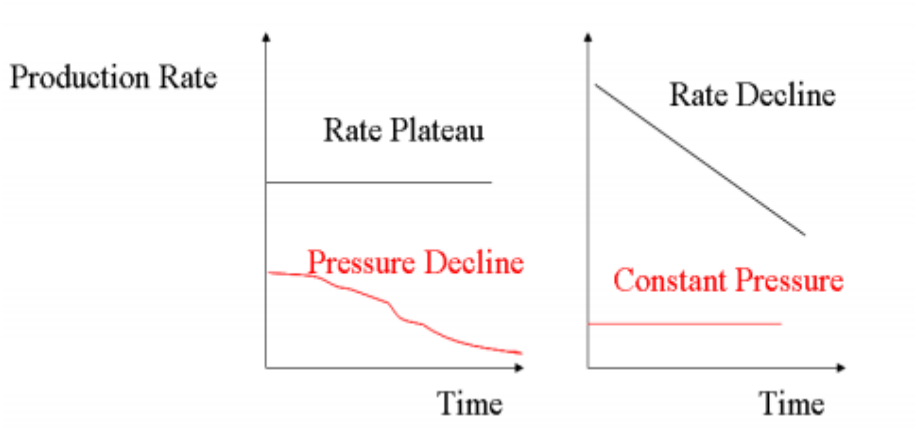

Figure 32-Reservoir offtake modes (Stanko & Golan, 2015),

2.7.2 Estimation of Production Plateau rate

As the rule of thumb, the first step estimation of the production plate rate might be done on the total recoverable reserves from the reservoir (Stanko, 2016). The rule of thumb formula is defined as

$$Annual\ offtake = (0.035 - 0.05)TRR \qquad 2.83$$

Whereby TRR stands for Total Recoverable Reserves or the ultimate cumulative gas production (Gp_u) defined as

$$Gp_u = R.FxIGIP \qquad 2.84$$

Whereby $R.F$=ultimate recovery factor and $IGIP$ is the initial gas in place

2.7.3 Prolonging the Production Plateau

After the natural production of the plateau period, it is possible to perform some modification for the production system. Prolonging the plateau will provide value to the gas field by increasing recovery, and hence, increasing the revenue of the field from added production. Techniques measures to prolong the plateau highlighted by (Golan & Stanko, 2015) during the field development course at NTNU are pressure maintenance, productive and efficient well completion, stimulation, increasing number of wells and boosting of the flow. All the techniques increase the available pressure in the equilibrium analysis (more discussion of flow equilibrium analysis are given in section 2.6.4).

2.7.3.1 Pressure Maintenance

After the dry gas reservoir has been depleted, pressure maintenance could be done with carbon dioxide injection, this method has not yet been recognized and has not been practiced economically (Chawarwan Khana, 2013).

2.7.3.2 Productive and Efficient Well Completion

Productive and efficient well completion can be done in two ways which are horizontal well completion or by enlarging the tubing diameter (Golan & Milan, 2015). These techniques ensure significant productivity and ultimate recovery, and should be decided during development stages before installation is done.

Horizontal wells have proven effectiveness by creating unique production environments for many different formations (Smith & Lyinda, 2015). In order to effectively deplete tight gas reservoirs and attain high flow rates, horizontal wells provide an attractive alternative over vertical wells, since tight gas reservoirs would require number of vertical wells drilled at close spacing to efficiently drain the reservoir (Ahmed & Mckinney, 2005).

To calculate gas flow rate for horizontal well, Joshi in 1991 introduced the concept of effective wellbore radius ($r_w^{\backslash}$) given by:

$$r_w^{\backslash} = \frac{r_{eh}(\frac{L}{2})}{a\left[1+\sqrt{1-\left(\frac{L}{2a}\right)^2}\right]\left[\frac{h}{2r_w}\right]^{\frac{h}{L}}} \qquad 2.85$$

With

$$a = \frac{L}{2}\left[0.5+\sqrt{0.5-\left(\frac{2r_{eh}}{L}\right)^4}\right]^{0.5} \qquad 2.86$$

And

$$r_{eh} = \sqrt{\frac{43560A}{\pi}} \qquad 2.87$$

Where L = length of the horizontal well, ft.; h = thickness, ft.; r_w= wellbore radius, ft.; r_{eh} = horizontal well drainage radius, ft.; a = half the major axis of the drainage ellipse, ft. and A = drainage area of the horizontal well, acres.

When completion is done by increasing the tubing size (diameter), the tubing coefficient (C_T) in Eq. 2. 74 changes, and consequently enhance the well production.

2.7.3.3 Well Stimulation

Like in productive and efficient well completion, well stimulation must be decided during development studies. Well stimulation involves fracturing or acidizing technique. This technique is of little benefit in undamaged well.

According to (Economides, et al., 1994), the most common acids used are hydrochloric acid (HCl) and mixture of hydrochloric and hydrofluoric acids (HF/HCl). Acid selection, type and strength for sandstone or carbonates are based primarily on field experience with particular formation. The standers treatment consisted of 15 wt% HCl for carbonates, for sandstones a 3 wt% HF, 12% HCl mixture precede by 15% HCl preflush.

Predominantly, as a general case, stimulation had great influence on changing the C_R in the back pressure equation, therefore enhances well production.

2.7.3.4 Increasing Number of Wells

Provided that the amount of gas drained from the reservoir to the surface is the same, drilling more wells creates paths to the surface, hence, increases the plateau length. (Golan & Milan, 2015) described the concept that more wells with less rate per well provides higher available pressure at the wellhead, then provides less pressure loss in the reservoir and in the tubing per well. Therefore, the wells operate in parallel mode whereby the total rate is equal to the summation of individual's well rate (Eq.2. 88), and the total pressure drop and pressure drops of the individual wells are equal (Eq.2. 89)

$$q_{Total} = \sum_{i=1}^{n} q_i \qquad 2.88$$

$$\Delta p_{Total} = \Delta p_1 = \Delta p_2 \ldots\ldots\ldots\ldots\ldots\ldots = \Delta p_n \qquad 2.89$$

The concept of parallel wells is other way around true for series arrangement, for example in ESP stages in series.

2.7.3.5 Boosting of the Flow

Installation of wellhead compressor is another solution to boost the flow for the purpose of extending the plateau length after the natural production of the gas reservoir. The wellhead compressor creates pressure drop through reduction of the pressure at the production well thus, influencing reservoir gas expansion and hence the gas flow to the production well (A. Muggeridge, 2013)

Other measures can be used which are necessary for reducing required pressure; these include reducing of separator pressure and increasing the size of flow line.

2.9 Fluid Flow Assurance

It is vital to address flow assurance problem during gas production. This is important as flow assurance problems may lead to drastic effect on production plateau, as well as damaging of production infrastructures. Addressing flow assurance in well tubing, flowlines and pipelines will ensure successful, economical production and transportation of the natural gas (Irmann-Jacobsen, 2012).

In natural gas production, some of the flow assurance problems which can be addressed are slugging, formation of hydrates, liquid loading, erosion and corrosion.

2.9.1 Gas Hydrates

This section will address the hydrate formations and possible mitigation measures which might be done to avoid hydrate formations. It is very important to address this because; hydrate formation may be very rapid process which may eventually lead to pipeline blockage.

2.9.1.1 Hydrate Formations

Hydrate forms when the natural gas is in contact with liquid water at low temperature and high pressure. At 20 °C and 100 bara, small hydrocarbon molecules (typically methane and ethane) tend to stabilize water molecules (Guðmundsson, 2011). The stabilized hydrate structure is illustrated in Figure 33.

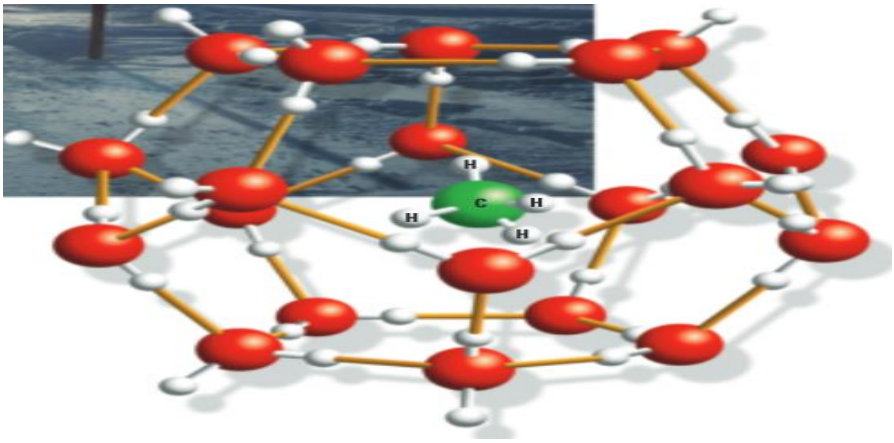

Figure 33-Stabilized hydrate structure (Schulumberger , 2010)

Two common gas hydrate structures are Type I and Type II, with the third structure recently reported which is Type H. Type I are formed with simple molecules like methane, ethane and hydrogen sulphide while Type II are formed by larger molecules like propane, and butane when combine with water to form diamond lattice structure (Covington, et al., 1999).

2.9.1.2 Inhibiting Hydrate Formation

Common hydrate controlling strategies are hydraulic methods (depressurisation), heat control methods (insulation, heat tracing), chemical methods (monoethylene glycol (MEG), methanol (MeOH), kinetic inhibitors) and water removal (subsea processing).

When using hydraulic or heat control methods, successful depressurization means that the manifold pressure should fall below the formation hydrate pressure at ambient seabed temperature. Thermal insulation enables the flowing temperatures in the subsea system to remain above the critical hydrate temperatures (Davalath, et al., 2004).

Chemical inhibitors (alcohols and glycols) act as anti-freezing agent to supress the hydrate formation temperature, hence prevents the formation of hydrate. The mechanisms of this is clearly illustrated in Figure 34, showing how MEG supresses the hydrate formation temperature.

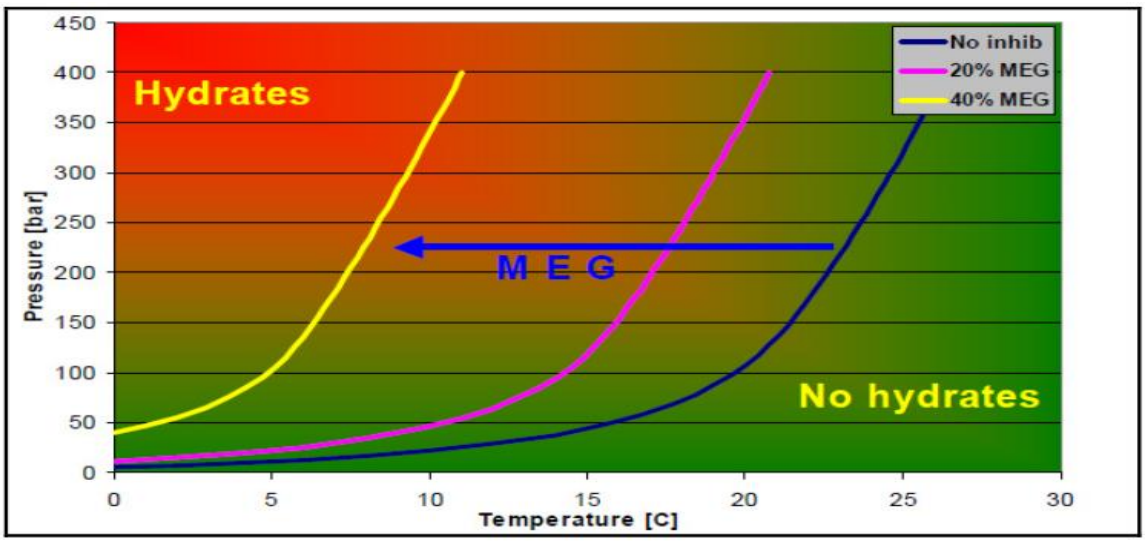

Figure 34- Hydrate phase diagram (Bokin, et al., 2010)

2.9.2 Multiphase Flow

The knowledge of multiphase flow in pipes is very important to the success of the facilities operation. In the petroleum industry, most engineering applications make use of flow pattern, liquid holdup and pressure gradient in the design and processes of surface facilities (Ehizoyanyan, et al., 2015).

2.9.2.1 Flow Regimes

Flow patterns prediction is an important aspect of modelling evaporation and condensation (Thome, 2004). Flow patterns transition depends on topography fluid properties, pipe size, flow rates and corresponding pressure drop (Ehizoyanyan, et al., 2015). The flow patterns are normally experienced in vertical, inclined and horizontal components of the gas production systems. Depending on the gas –liquid velocity and gas –liquid ratio, (Multiphase Technology, Inc, 2015) described the following observed flow regimes.

- Dispersed bubble flow is observed at high velocity and low gas/liquid ratio
- Smooth or wavy stratified flow is observed for low flow rates of liquid and gas
- Rolling waves of liquids are formed for intermediate liquid velocities which eventually increase to the point of forming plug and slug flow.
- Annular flow is expected for very high gas velocities

Figure 35 depicts the flow patterns in horizontal and vertical components of the production system.

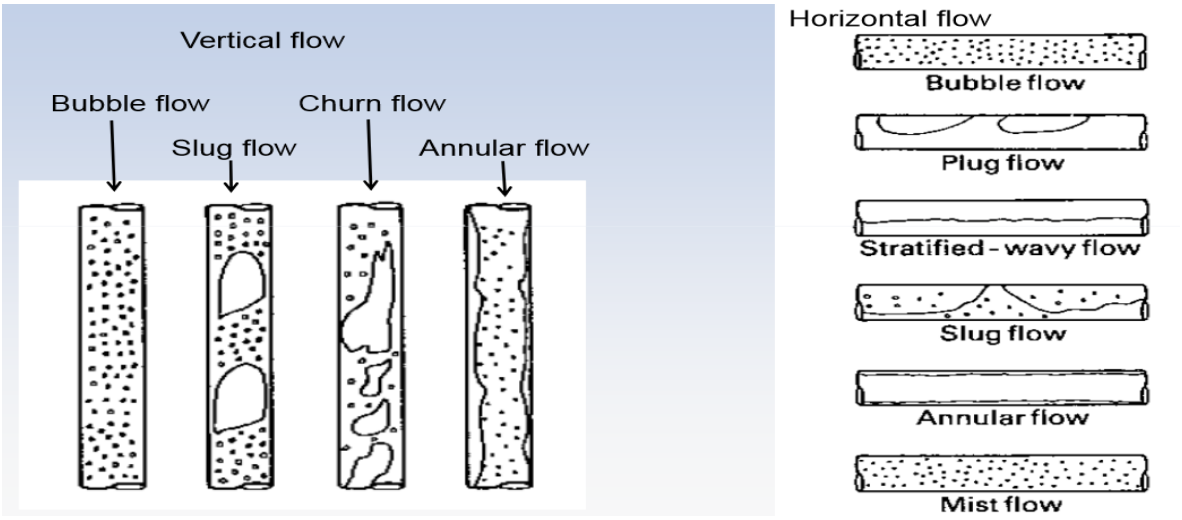

Figure 35-Flow patterns in horizontal and vertical components (Stopford, 2011)

2.9.2.2 Liquid Holdup

Another most important parameter in estimating the pressure drop in inclined or vertical flow is liquid holdup. It is defined as the fraction of in-situ volume which is liquid in gas/liquid multiphase flow (Hagedorn & Brown, 1965).

Liquid holdup (H_L) is calculated as

$$H_L = \frac{A_L}{A} \qquad 2.90$$

Where A_L= cross sectional area of the occupied by liquid and A= is the total cross sectional area of the pipe.

Sometimes may be expressed in terms of gas phase (H_g) as

$$H_g = \frac{A_g}{A} \qquad 2.91$$

Where A_g= cross sectional area of the occupied by gas and A= is the total cross sectional area of the pipe.

For the complete pipe occupied by two phases Eq. 2. 92 is valid

$$H_g = 1 - H_L \qquad 2.92$$

Liquid holdup is influenced by multiphase flow dynamics and mass transfer between two moving phases (gas and liquid). For the case of flow dynamics, when gas and liquid are flowing along the pipeline, slippage will occur as the consequence of gas travelling at faster velocity than liquid. In low points of the pipelines liquid accumulation occurs since liquid is heavier than gas. Evaporation of fluids and condensation of gases are essential circumstances to describe holdup due to mass transfer between two moving phases.

2.9.2.3 Pressure Drop Correlations

Correlations used to calculate pressure drop in gas-liquid phase flow originates from the mechanical energy balance given by Eq.2. 63. The most widely used multiphase pressure drop correlations for vertical components have been developed by (Hagedorn & Brown, 1965), (Duns & Ros, 1963), and (Aziz & Govier, 1972). The method to calculate liquid holdup and pressure gradient in inclined pipe was proposed by Brill & Beggs and Mukherjee & Brill and While Barnea. The detailed descriptions of the above correlations can be found in (Beggs & Brills, 1973), (Mukherjee & Brill, 1985) and (Barnea, 1987).

At the moment, brief on the correlation is highlighted as described in (Bai & Qiang, 2005)

- Duns and Ros correlation was developed based on extensive experimental research of oil and air mixture. This correlation is for vertical two phase flow in wells
- Hagedorn and Brown correlations was developed based on an experimental study of pressure gradients in small diameter vertical conduits.
- Aziz and Govier correlation was developed flowing the study of pressure drop in wells producing oil and gas.
- Beggs and Brill correlation was developed following a study of two phase flow in horizontal and inclined pipe based on upon a flow regime map. It was then revised and enhanced by (1) considering an extra flow regime of froth which assumes no-slip holdup and (2) changing the friction factor from standard

smooth pipe model, to utilise a single phase friction factor based on average fluid velocity.

- Mukherjee and Brill correlation was developed following a study of pressure drop in two-phase inclined flow. The correlation was verified with Prudhoe Bay and North Sea data.

2.9.3 Erosion

Erosion is mainly caused by sand production. Severe erosion problems may occur in screens, chokes and fitting. Sand production is unavoidable; therefore wells are completed with measures such as gravel pack and sand screen to prevent sand production as shown in Figure 36.

Figure 36-Gravel pack and sand screen to prevent sand production (Statoil, 2013)

2.9.4 Corrosion

Corrosion of steel is the electrochemical process which depends on the partial pressure of the component, pH, temperature and concentration of corrosion products (Bokin, et al., 2010). This is the common pipeline problem associated with presences of water and corrosive materials such as carbon dioxide (CO_2) and hydrogen sulphide (H_2S). Corrosion problem can be avoided by controlling the variables that govern corrosion occurrence, for example, removal of sour gases.

2.10 Brief explanation on Reservoir and Surface Network Modelling Tools used in Study

This section provides brief explanation of useful simulation tools or software as applied in petroleum industry. Detailed explanations can be found in the user manual of the respective software.

2.10.1 Reservoir Tools

MBAL, a *petroleum experts*' software, the package has various tools designed to help petroleum engineer to have better understanding of reservoir behaviour and performing prediction run (Petroleum Experts, 2005). The prediction run is used to forecast the reservoir performance. The tools incorporated in MBAL are listed below

- Material Balance
- Reservoir Allocation
- Monte Carlo Volumetric
- Decline Curve Analysis
- 1-D Model (Buckley-Leverette) and
- Multi-Layer

2.10.2 Well Tools

PROSPER, a *petroleum experts*' software for the single well model used for generation of well performance and lift curves for simulation. The software assists the production or reservoir engineer to predict tubing and pipeline hydraulics and temperature (Petroleum Experts, 2003).

2.10.3 Surface Network Tools

GAP, *petroleum experts*' software, this tool is powerful and is able to achieve the followings according to (Petroleum Experts, 2003)

- Complete surface production/ injection well modelling
- Optimisation of naturally flowing oil or gas wells, gas lifted wells and ESP operated wells as well as condensate or gas producers, water producers, and water and gas injector
- Allocation of production
- Predictions to forecast production

GAP may also be used as integration tool to integrate the entire production system from the reservoir to production systems. In order to do this, GAP is linked with MBAL and PROSPER.

Simulation in GAP can be performed by either network solving or performing prediction run. During network solving, GAP solves the surface network system for pressure and rates at various nodes of the defined system. Prediction in GAP calculates optimised production rates over specified time steps. GAP uses pressure and saturations from a reservoir model to calculate the well IPR together with relative permeability curves and PVT properties (Petroleum Experts, 2003).

2.10.4 Flow Assurance Tools

HYSYS software is used in simulation of oil and gas, refining and engineering processes. In this study, HYSYS was specifically used to be used to address engineering challenges in multiphase flow for Block 2 field.

2.11 Economic Analysis in Petroleum Industry

The economic evaluation of the fields is usually done from the pre development stages all the way to the abandonment stage.

Economic analysis determines the value of hydrocarbon investments. Investment decision is always driven with project profitability. Economic evaluations are described with cash flow models which show the relationship between the net cash flow, and the revenues obtained from produced natural gas. The cash flow versus time for hydrocarbon field is illustrated in Figure 37.

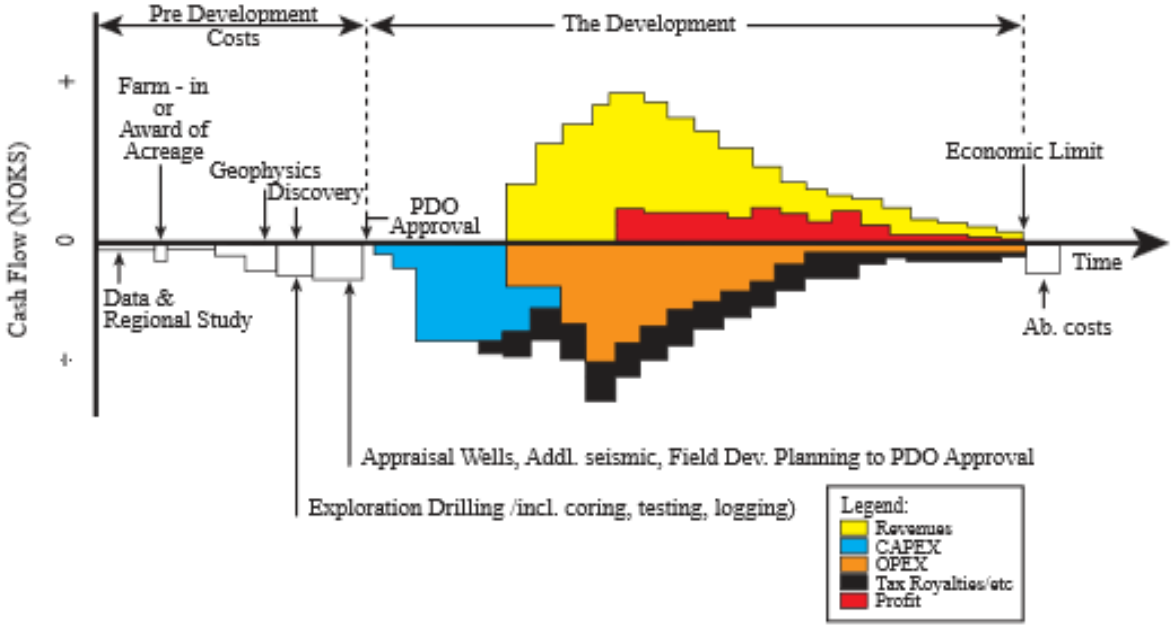

Figure 37-Cash flow versus time during field development (Svalheim, 2005)

The cash flow model includes expenditures, general administration expenses, taxes and royalties which are paid to the producing country and revenues. Several indices may be used to carry out the economic analysis of the field. The following sections highlight some of the normally used indices.

2.11.1 Payback Period

Payback period refers to the length of time required to recover the initial invested cost. This method does not consider time value of money, and an exclusive criterion of decision for this method is to select the project with the shortest time of period in recovering the invested money (OH, 2004).

2.11.2 Net Present Value (NPV)

NPV refers to the sum of all project cash flows discounted back to a common point in time (Adamu, et al., 2013). When making decision with *NPV*, the project with the biggest *NPV* is selected.

Mathematically

$$NPV = \sum_{n=1}^{n} \frac{NCF_n}{(1+r)^n} \quad 2.93$$

NCF can be expressed as

$$NCF = (Gas\ price * Produced\ Gas) - (OPEX + CAPEX + Taxes\ and\ Royalties)$$

Where r=discount rate, n =number of years and NCF_n =net cash flow, OPEX= Operating costs, CAPEX= Capital expenditures.

2.11.3 Internal Rate of Return (IRR)

IRR refers to the discount rate that makes the NPV equals to zero(Eq. 2. 94. IRR method does not incorporate environmental factors, such as interest rate and inflation. The biggest the IRR the best is the project.

$$NPV = \sum_{n=1}^{n} \frac{NCF_n}{(1+IRR)^n} = 0 \quad 2.94$$

When deciding on the best development scheme, sensitivity analyses are performed to examine different development alternatives. The sensitivity analysis is performed by changing potential key factors.

Chapter 3: Calculations and Correlations to Estimate Block 2 Field Parameters

This chapter gives discussion on how different parameters for the Block 2 field were estimated and calculated. Different correlations, good engineering judgements and reasonable assumptions are presented concerning the subject matter. All estimated parameters are found in Appendix 1.

3.1 Reservoir Rock Properties

The reservoir properties discussed in this section are porosity and permeability. Referring to the literature, discovered reservoirs in Block 2 are sandstones. Therefore, the models used to estimate porosity and permeability considered the appropriate lithology.

3.1.1 Porosity

Based on idealized model of packed spheres, it was assumed that the Block 2 field follows the regular rhombohedral –packed spheres which estimates porosity equals to 26%. This porosity value was taken as reference to assume porosity values for the Block 2 reservoirs in the range of $\pm$ 5% depending on reservoir depth.

3.1.2 Permeability

Formation permeability was correlated from logarithmic-linear permeability-porosity relationship for sandstone formations. The correlation is given in Eq. 3. 1.

$$\log_{10} k = C \log_{10} \phi_e + D \qquad 3.1$$

Where C and D are factors which are approximated and equal to 7, based on core data analysis (PetroWiki, 2015).

k=permeability in millidarcies and ϕ_e is the effective porosity

3.1.4 Net-pay Thickness

A simplified correlation was made based on the reported net pay thickness of Zafarani and Lavani main. The model was made by creating a liner relationship between IGIP and Net-pay thickness as shown in Eq. 3. 2

.

$$IGIP = 0.0366(Net - pay\ thickness) - 8.4 \qquad 3.2$$

3.2 Reservoir Fluid Properties

The reservoir fluid properties discussed in this section includes fluid saturation, gas specific gravity, gas viscosity and Z- factor.

3.2.1 Fluid Saturations

The initial water saturation can be obtained from the linearized Buckles correlation for connate water saturation and porosity (Eq. 3. 3). The constant value for sandstone reservoir was taken as 0.06. This is the average of constant value from the given range (0.02-0.1)

$$\log_{10}\ Irreducible\ water\ saturation = \log_{10} Constant - \log_{10} Porosity \qquad 3.3$$

After the irreducible water is obtained, the gas saturation for gas reservoirs can be easily computed using Eq. 3. 4.

$$S_g = 1 - S_w \qquad 3.4$$

3.2.2 Gas Specific Gravity

There was no gas compositions data published for the reservoir fluids of Block 2 offshore Tanzania, and (Holm, 2015) reported that; the reservoir fluids are very dry. Therefore, the dry gas compositions from Songo-Songo onshore gas reservoir were taken as the base for analysis. The average value composition from five wells (Appendix 2) was used for Block 2 field analysis under the assumption that; gas compositions do not vary significantly across the field.

The gas specific gravity was then calculated from the ratio of gas mixture molecular weight to that of air as the reference, the gas mixture molecular weight was obtained from Kay's mixture rule as shown on .

Table 3. The specific gravity of 0.575 obtained and the same value was used for all reservoirs in the field.

Table 3-Gas specific gravity calculation

Components	M_i	**mol%**	y_i	$M_i y_i$
N2	28.01	0.72	0.0072	0.20
CO2	44.01	0.33	0.0033	0.15
C1	16.04	97.35	0.9735	15.61
C3	30.07	1.05	0.0105	0.32
C4	44.10	0.30	0.0030	0.13
i-C4	58.12	0.07	0.0007	0.04
n-C4	58.12	0.09	0.0009	0.05
i-C5	72.15	0.03	0.0003	0.02
n-C5	72.15	0.02	0.0002	0.01
C6	86.18	0.01	0.0001	0.01
C7+	330.00	0.03	0.0003	0.11
Total		100.00	1.0000	16.65
M_{air}	28.97			
S.G	0.575			

3.2.3 Gas Viscosity and Z-factor

VBA in Excel was used to define the functions of gas viscosity and Z-factor. The correlation used to obtain gas viscosity was the Lee Gonzalez and for Z-factor, the standing correlation was used. In commercial software for example in PROSPER, the correlations are built in and merely activated when needed. The same Lee Gonzalez correlation for gas viscosity was used.

3.3 Reservoir Conditions

There are two reservoir conditions which are pressure and temperature. These conditions are highly related to the reservoir burial depths. These parameters were linearly correlated with burial depths.

3.3.1 Reservoir Pressure

For the back pressure equation the pseudo pressure function were used instead of the pressure squared function since all Block 2 reservoirs have pressure greater than 2 500 psia. It was necessary to obtain a model which relates the normal pressures to the pseudo pressure for convenient calculations. The model was numerically generated by creating PVT tables based on gas specific gravity, and then obtaining a plot of pseudo pressure function against normal pressure. The plots gave a linear relationship at pressure above 2 500 psia. These linear models are shown in Table 4; Appendix 3 shows the generated PVT tables and plot.

Table 4-Pseudo pressure-real pressure models

Reservoir	**M(p)-p Model**
[-]	**[psia2/cp]**
Zafarani	$m(p) = 357366p - 5E + 08$
Lavani Main	$m(p) = 360889p - 5E + 08$
Lavani Deep	$m(p) = 357007p - 5E + 08$
Tangawizi	$m(p) = 363604p - 5E + 08$

3.3.2 Reservoir Temperature

With the known water surface (20 to 30 degrees) and the deep sea temperature (+3 to +4 ℃) or (497.07 to 498.87 $°R$), the reservoirs temperature were estimated by extrapolation technique with respect to the burial depth. The geothermal gradient was assumed to be linear. Linear extrapolation technique is shown in Appendix 4.

3.4 Estimation of C_R

The value of C_R was calculated in two ways, (1) by using analytical approach (Eq.3. 5) and (2) estimated by performing equilibrium analysis. The analytical value was set to be standard for verifying the estimated value. Detailed calculations are shown in Appendix 5.

3.4.1 Analytical C_R

The analytical was calculated using Eq.2. 56 which was reduced to Eq.3. 5 when the skin was assumed to be zero.

$$C_R = \frac{0.703kh}{T_R(\ln(\frac{r_e}{r_w}) - \frac{3}{4})} \qquad 3.5$$

C_R =Backpressure coefficient in psia^2/cP/ (Mscf/day).

3.4.2 Estimated C_R

Estimated C_R needs initial reservoir pressure, a well gas rate for the IPR as well as C_T and wellhead pressure for the tubing equation.

For this study, the reservoir pressure was changed to pseudo pressures using reservoir models described in section 3.31, and the initial reservoir pressure was assumed to be close to the average reservoir pressure since the analysis was done at initial reservoir conditions.

With inlet pressure, outlet pressure, inlet temperature, outlet temperature, roughness of the pipe, elevation constant, pipe diameter, gas specific gravity and average gas compressibility Z_{av}, the C_T was obtained using the following formula in Eq.3. 6.

$$C_T = \frac{T_{sc}}{Z_{av}T_{av}p_{sc}}\left(\frac{\pi^2 D^5 g_c}{32 f_f}\right)^{0.5} \frac{e^{s/2}}{(e^s - 1)^{0.5}} \qquad 3.6$$

The following data and assumptions were used

- Outlet pressure= wellhead pressure (assumed)

- Inlet pressure=flowing bottomhole pressure (wellhead pressure =391.6 psia)-fair assumption
- Inlet temperature=Reservoir temperature (Calculated from linear interpolation and extrapolation by assuming linear geothermal gradient)
- Outlet temperature=bottom of the sea temperature (497.07 to 498.87 $°R$) reported value in (Holm, 2015).
- Tubing depth- Reported values TPDC website.
- Tubing diameter- Standard liner casing diameter for deep seal well is 7 inches, the value of 5.64 inches was assumed for internal tubing diameter.
- Friction factor- function of internal diameter (Eq.2. 67)
- Z-factor- from standing correlation.

The gas well rate for C_R estimation, Since the rule of thumb formula estimates the plateau rate (the wells are chocked), in order to obtain some sort of reality on estimating of C_R value, the plateau rate obtained from the rule of thumb formula (Eq. 3. 7) was split into well rates under assumption that all the wells share the same IPR ($\frac{q_{field}}{n_{well}} = q_{well}$) (The number of wells used, were taken from initial number of wells suggested by Statoil (Holm, 2015)). The obtained well rate was multiplied by a factor of 1.3 to obtain unchoked flow rate of the well.

$$Annual\ offtake = 0.04\ x\ R.F\ x\ IGIP \qquad 3.7$$

Where $R.F$ was initially assumed to be equal to 0.7, with factor value of 0.04 being the average between 0.035-0.05 as previously shown in Eq. 2. 83.

The setup for C_R estimation was the single well model (the configuration takes the IPR and tubing equation) as shown in Figure 38.

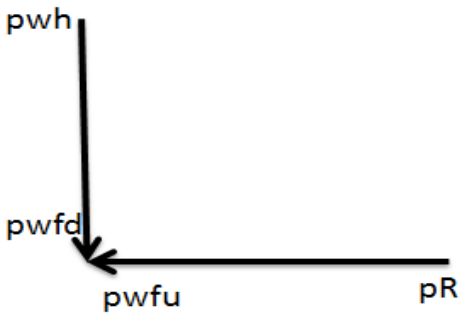

Figure 38-Setup for C_R estimation

Equilibrium analysis (concurrent pressure calculation from reservoir pressure p_R to p_{wfu} and counter current pressure calculation from p_{wh} to p_{wfd}) was done, and then excel solver was used to adjust C_R until $p_{wfd} = p_{wfu}$ with p_{wf} as the reference node. The value obtained was then adjusted to the accuracy of 1-5% difference from the analytical value (section 3.4.1). Lastly, adjustments were done by decreasing and increasing the initial assumed wellhead pressures (p_{wh}) within 1-20% accuracy, until the estimated C_R was more or less equal to the analytical C_R .

The results are illustrated in Table 5 and Table 6. The same estimation approach was used for all reservoirs (Zafarani, Lavani Main, Lavani Deep and Tangawizi) depending on reservoirs configuration, rock and fluid properties.

Table 5-Results for analytical and estimated

CR Estimated based on Rule of Thumb Formula (Mscf/psia^2/D)				
Methods	**Zafarani**	**Lavani Main**	**Lavani Deep**	**Tangawizi**
Estimated	0.0063	0.0119	0.0033	0.0166
Analytical	0.0062	0.0121	0.0034	0.0173
Difference (%)	0.9400	1.8200	1.0900	3.9900

Table 6-Adjustment of assumed p_{wh} to verify estimated C_R

Adjustments of assumed p_{wh} (psia)				
Methods	**Zafarani**	**Lavani Main**	**Lavani Deep**	**Tangawizi**
Estimated	5 293.89	4 739.84	6 671.75	4 523.74
Assumed	5 496.94	4 815.26	6 831.29	3 814.50
Difference (%)	3.69	1.57	2.34	18.59

The Difference (%) in is the percentage error between the assumed or analytical and the respective estimated value.

Chapter 4: Building MBAL, PROSPER AND GAP Models

4.1 GAP Model

The single schematic model for gap was created. The model was made with surface facilities (separator, manifolds, templates, main pipeline, and flowlines), wells and reservoirs (Figure 39). The surface facilities data were directly specified on GAP, but the reservoir model and well information were specified on MBAL and PROSPER as described in section 4.2 and section 4.3 respectively. The PROSPER model and MBAL model were then loaded into GAP.

The wells from one reservoir are grouped together to allow control of all wells from one icon.

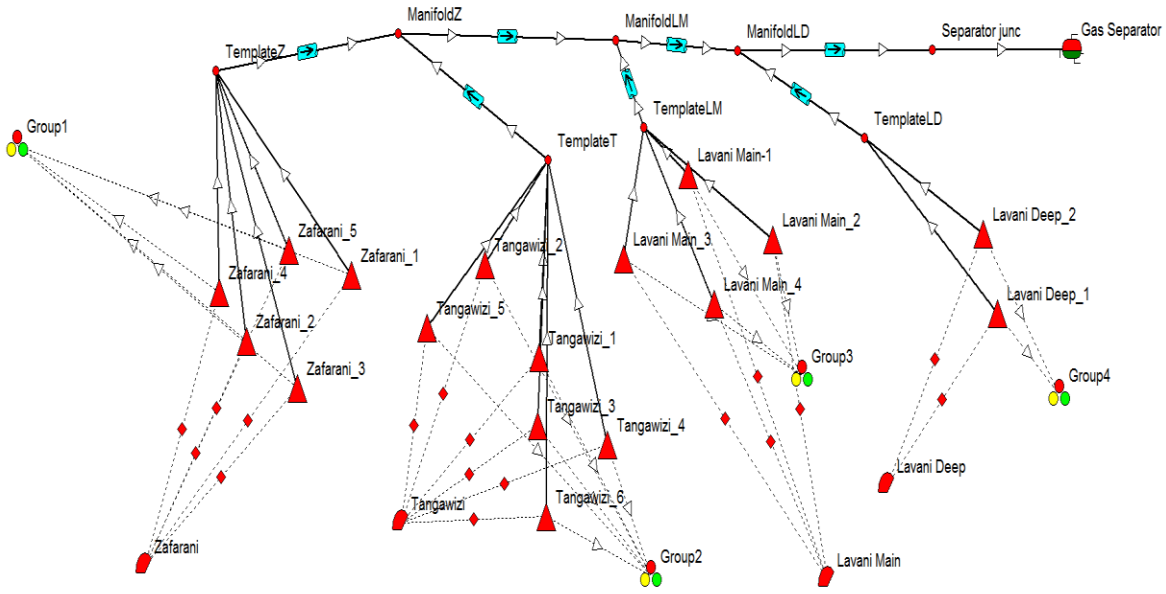

Figure 39: Gap Model

4. 1.1 Surface Network Configuration (Pipe Lengths and Diameters)

Initially, the pipeline and flowlines and lengths and diameters for entire production system were configured as shown inTable 7. The diameters were found in (Holm, 2015), and the lengths were measured from the subsea layout (Figure 17) using thread and given scale.

Table 7-Surface network configurations for Block 2 field

Pipelines		
Segment	**Length**	**Diameter**
[-]	**[km]**	**[inches]**
ManifoldLD to Jsep	90	26
ManifoldLM to ManifoldLD	3	26
ManifoldZ to ManifoldLM	5	26
Flowlines		
Segment	**Length**	**Diameter**
[-]	**[km]**	**[inches]**
TemplateZ to ManifoldZ	11	12
TemplateT to ManifoldZ	5.8	12
TemplateLM to ManifoldLM	4.8	12
TemplateLD to ManifoldLD	5.5	12

4. 1.2 Main Transportation Pipeline Elevations

It was necessary to account for elevations of the main transportation pipeline to account for real topography of the field environments.

The original elevation profile found in (Holm, 2015) (Figure 40) was digitized and segmented to approximate the true vertical depth of pipeline inclination. The digitized elevation profile is shown in Figure 41. Some segments were fairy horizontally approximated. For the case of the flowlines, all flowlines from the wells to the main transportation line were assumed to be fairy horizontal.

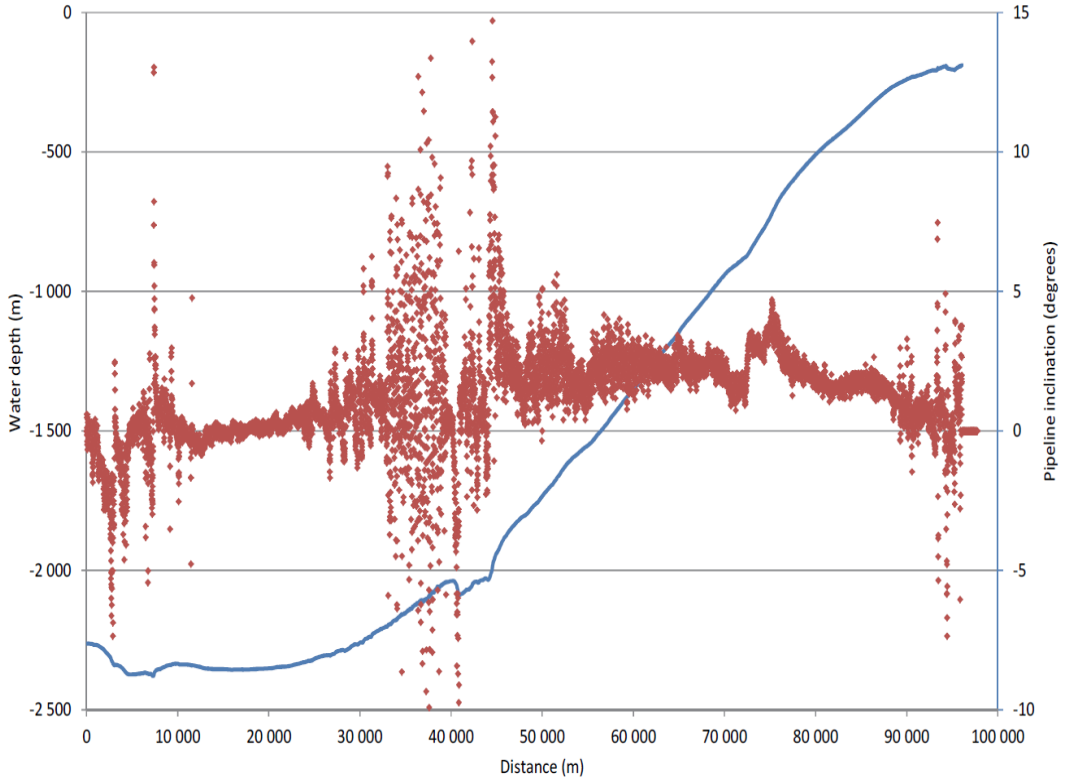

Figure 40: Pipeline elevation profile

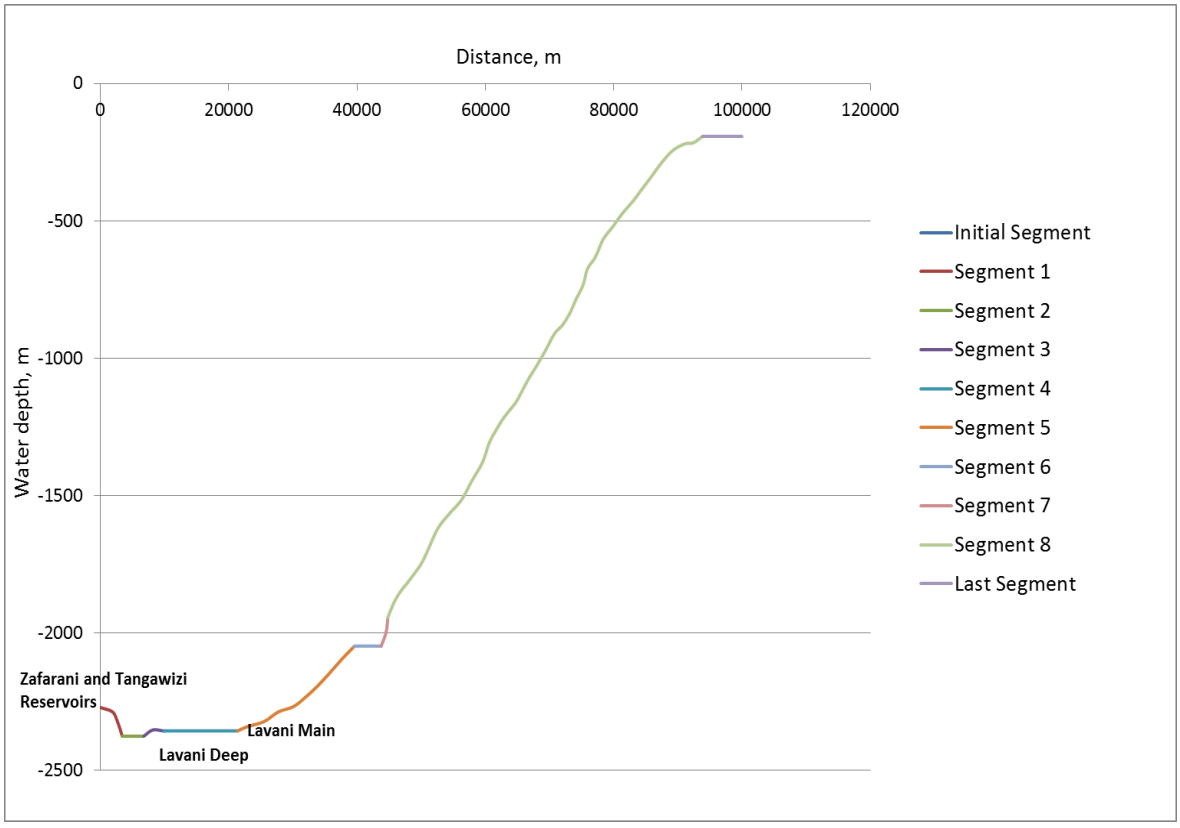

Figure 41- Elevations profile specified in Gap

4.1.3 IPR and VLP Generation with PROSPER

The generation of VLP and IPR for wells were done by batch calls from PROSPER while the user is at GAP interface. The generation was done for all reservoir wells one after another.

On generating VLP, a range of data for gas rates produced, wellhead pressure, water gas ratio and condensate gas ratio needs to be specified. This procedure was automatically populated after specification of minimum and maximum data that covers the possible gas rate production, well head pressures, WGR and CGR.

On generating IPR, GAP opened the PROSPER file, read three points from PROSPER file and then fit those points to the IPR methods (Forchheimer with Pseudo Pressure) used in GAP. IPR were generated by considering a tank as a single layer.

4.2 MBAL Model

The MBAL tool was specified to perform material balance for the reservoirs. Three most steps had to be made to create the MBAL model as described below:

4.2.1 System Setup

System setup was defined; the reservoir fluid was specified to gas reservoir and multiple tank options was selected to allow treatment of more than one tank, with potentially different PVT properties. There was no employment of abnormally pressure method for modelling rock compaction; this allowed the use of normal pressure method from built in correlations. Block 2 field is a new field, consequently, no production history needed for history matching.

4.2.2 Fluid Properties

In this study, fluid was modelled as black oil. Applied PVT model assumed all PVT properties are homogeneous (no variations) in the tank. With dry gas model, it was assumed that; all liquid drop out occurs at the separator. Fluid input parameters including gas specific gravity, separator pressure (to convert amount of condensate to equivalent gas amount), condensate to gas ratio, condensate gravity, water salinity and moles of impurities (H_2O, N_2, CO_2) in the gas stream were also specified. The separation pressure was assumed to be 30 bara (435.113 psia).

The Lee et al correlation was used for viscosity correlation; the model water vapor box was checked to calculate the water vaporized in the gas. The condensate to gas ratio was set to zero since the gas was dry. However, despite that, GAP still required a value for the condensate gravity. It was then set to 50 API.

4.2.3 Tank Data

Tank parameters which are reservoir temperature, porosity, connate water saturation and initial gas in place were specified. The water compressibility was set blank to allow the program to use an internal correlation to evaluate the water compressibility as a function of temperature, pressure and salinity. Zafarani tank input data for MBAL is depicted in Figure 42 as an example.

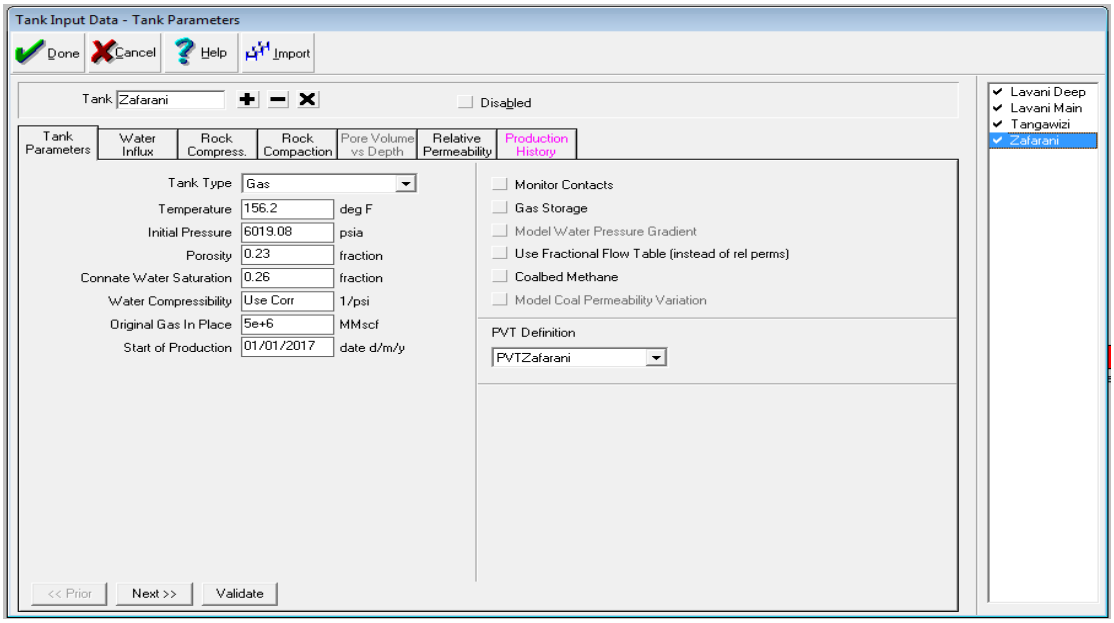

Figure 42-Zafarani tank input data

No aquifer model was included for tank modelling; the rock compressibility was calculated from internal correlations as the function of porosity (Petroleum Experts, 2005). The conditions for use are expressed below:

If porosity > 0.3 then $C_f = 3.2x\ 10^{-6}$

If porosity < 0.3 then $C_f = 3.2x\ 10^{-6} + ((0.3 - porosity)^{2.415})x\ 7.8\ x\ 10^{-05}$

Then the pore volume is calculated using $pV = pV_i(1.0 - C_f(p_i - p))$

Where p_i and V_i are pressure and pore volume at initial conditions.

A rock compaction model was not enabled. Therefore, reversible model option was selected. This option enables the pore volume to increase back to the original volume if the reservoir re-pressurises.

The relative permeability values were defined by using Corey functions. This method for gas systems required defining of residual saturations (the connate saturation for the water phase and critical saturation for gas phase), the end point saturations and Corey exponents.

The end point defines the relative permeability of each phase at their maximum saturation. Therefore, for gas water system $S_g = (1 - S_w)$ expression was used to obtain gas saturations.

The Corey exponents define the shape of the relative permeability curve between zero and the end point. A value of 1.0 gives a straight line. A value less than one gives a shape which curves above the straight line. Then, Corey exponent values ranging from 1.5 to 2 were assumed, so as to have the reasonable curved shape of the relative permeability which is below the straight line (Petroleum Experts, 2005). The relative Corey function method to define the relative permeability for Zafarani tank is shown in Figure 43 as an example.

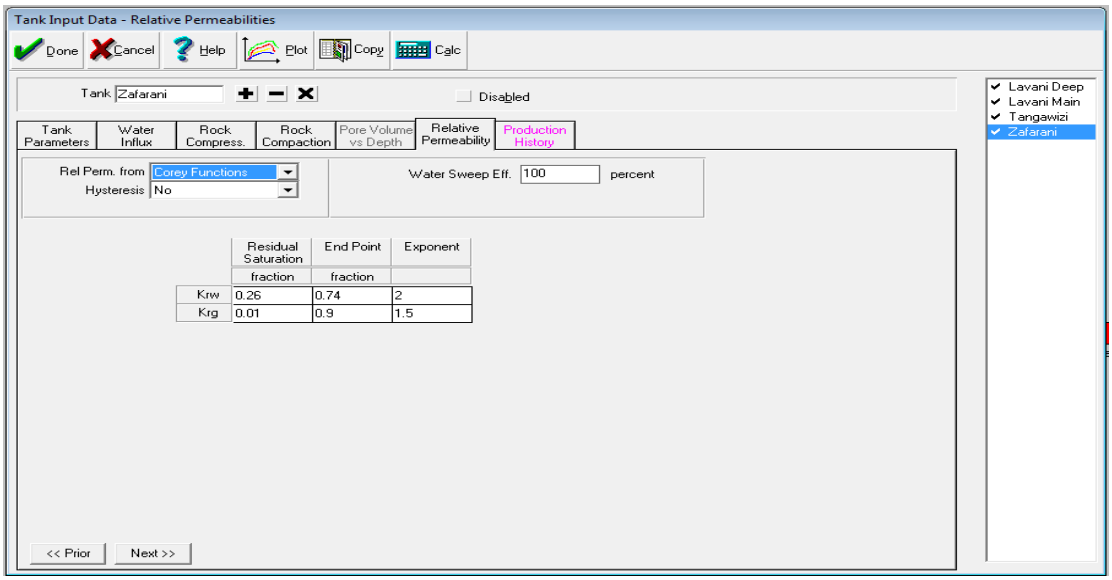

Figure 43-Corey function method to define relative permeabilities of Zafarani tank

4.3 PROSPER Model

PROSPER was specifically used to model the well. The model was made by defining PVT properties, IPR data and Equipment data. The fluid model was then set to Black oil as in MBAL. In every single reservoir, all the wells in that reservoir were assumed the same (they share the same IPR), and different from one reservoir to another because reservoirs PVT properties differ from one another.

The procedures used to model Zafarani, Lavani Main, Lavani Deep and Tangawizi wells were the same. The model from one reservoir to another was distinguished by PVT data and well depths.

4.3.1 PVT Data

The PVT properties for PROSPER are the same to PVT properties specified in MBAL.

4.3.2 Equipment Data

Downhole and survey information such as measured well depth, true vertical depth, tubing and casing measured depths, tubing and casing internal diameters, tubing and casing roughness and the overall heat transfer coefficient were specified. These wells are satellite (their depths are vertical). The well depths are shown in

Table 8.

The following general assumptions were made for all reservoirs:

- The measured depth was assumed to be the same as true vertical depths. Measured depths were referenced from (TPDC, 2014)
- The tubing measured depths were assumed to be 100 ft. less than casing measured depth
- The overall heat transfer efficiency was assumed to be 1.5 W/m^2/K
- The tubing and casing internal diameters are 5.64 and 7 inches respectively for all wells.
- Tubing and casing inside roughness was 0.0006 inches

Table 8: Well depths for different reservoirs

Reservoirs	Total Measured Depth (Includes water depth)	Casing Measured Depth (Excludes water depth)	True Vertical Depth (Excludes water depth)
[-]	[ft.]	[ft.]	[ft.]
Zafarani	16 896.3	8 525.2	8 425.2
Lavani Main	11 604.3	3 830.3	3 730.3
Lavani Deep	17 290.0	8 925.5	8 825.5
Tangawizi	9 940.9	2 495.0	2 395.0

The example of downhole for Zafarani is shown on Figure 44.

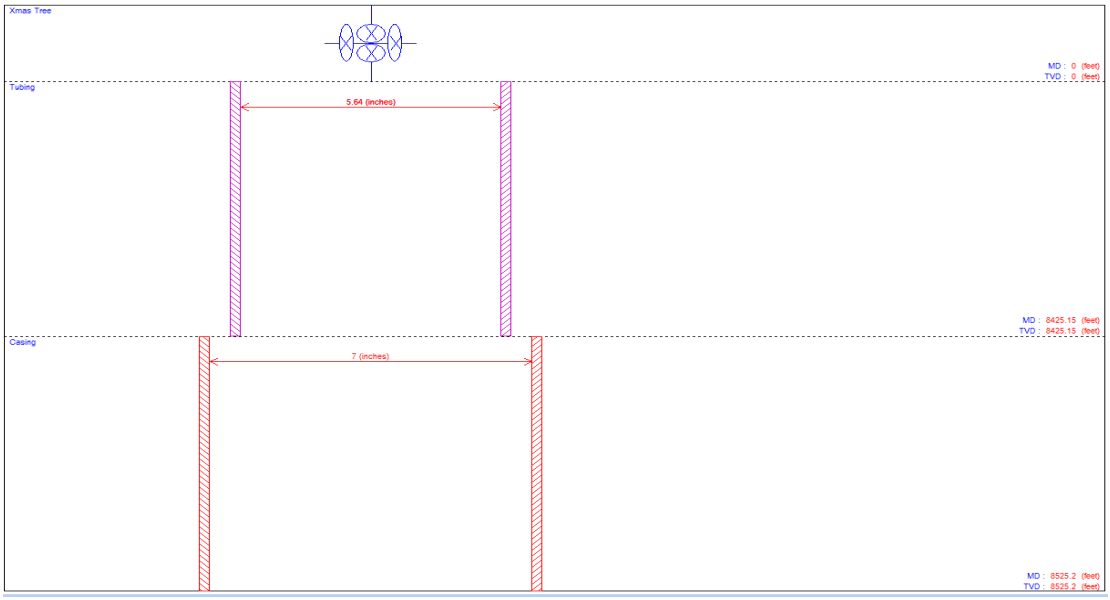

Figure 44: Zafarani well downhole diagram

4.3.3 IPR Model

The Forchheimer with Pseudo Pressure reservoir fluid model was selected since the reservoir pressures for Block 2 are higher than 2 500 psia. The fluid was then assumed linear driving the non-Darcy coefficient to be zero. The Darcy coefficient (A) was taken as the reciprocal of estimated (C_R).

A short background recap on the model,

Forchheimer with Pseudo pressure function (non-linear)

$$Drawdown = Aq + Bq^2 \qquad 4.1$$

Where A = Darcy coefficient, psia^2/cP/ (Mscf/day); B= non-Darcy Coefficient =psia^2/cP/ (Mscf/day) ^2; and q=flow rate, Mscf/day.

Backpressure equation for Pseudo pressure function (linear) when n=1, Laminar flow.

$$Drawdown = q/C_R \qquad 4.2$$

Where C_R= Back pressure coefficient, Mscf/day/ (psia^2/cP) and q=flow rate, Mscf/day.

Now, by assuming Darcy flow, the higher order term in Eq. 4. 1 is neglected and when comparing Eq.4. 1 and Eq.4. 2, the following relationship between A and C_R is obtained (Eq.4. 3).

$$A = 1/C_R \qquad 4.3$$

All the estimated C_R in section 3.4 was converted to Darcy coefficient (A) using equation Eq.4. 3 in order to meet requirements of Forchheimer with Pseudo Pressure reservoir fluid model. The A values are shown in Table 9. Finally, IPR calculations were performed with PROSPER to obtain the AOF of the well.

Table 9- Darcy coefficient valued for Forchheimer with Pseudo Pressure Model

Reservoirs	***A* values**
[-]	**[psia2/cP/ (Mscf/day)]**
Zafarani	159.28
Lavani Main	83.83
Lavani Deep	298.94
Tangawizi	60.35

4.3.4 System IPR and VLP Calculations

IPR and VLP needed specification of top node pressure (well head pressure), as a starting point, the wellhead pressures obtained during estimation of C_R were arbitrary used. On performing IPR and VLP calculations, the VLP and IPR curves did not intersect reflecting that the well is a *non- flowing well*. This was probably due to more accurate correlation used in PROSPER than that used in excel.

To rectify these results, top node pressures were lowered to give intersection of IPR and VLP curves. IPR and VLP calculations was then repeated, and PROSPER calculated a solution node pressure with the respective well gas rate of the system. The results of the system IPR and VLP calculations are given in Table 10.

Table 10-Solution top node pressure and respective well gas rates obtained in PROSPER

Wells	**Gas Rate**	**Lowered Specified Node Pressure**	**Solution Node Pressure**
[-]	**MMscf/day**	**[psia]**	**[psia]**
Zafarani	263.71	4 000	5 919.21
Tangawizi	245.51	3 500	4 023.79
Lavani Main	329.42	4 000	5 139.87
Lavani Deep	274.21	5 300	7 347.04

Chapter 5: Determination of Production Profile

5.1 Estimation of Plateau Rate

For natural gas production, the plateau rate should be determine by sales contract between a buyer and producer (seller) or can be determine from equipment constraints. In this study, there was no open contract which shows the amount of rate to be produced and for how long the production will take place. Therefore, based on the few disclosed information, three approaches were analyzed in order to estimate the production plateau rate. The three approaches are described in the proceeding sections.

5.1.1 Approach One: Sensitivity Analysis on the Layout Suggested by Statoil

In (Holm, 2015) report about Tanzania Gas Project (TPG) it was said that; Statoil has proposed the mode of production as illustrated on Figure 45. The mode presented production strategy of the three reservoirs which are Zafarani, Lavani Main and Lavani Deep. The production scheme was expected to start producing from Zafarani reservoir, and after a quarter of production plateau length, Zafarani plateau rate should be reduced to the fraction of approximately 0.25 of the field production plateau rate. Thereafter, the field plateau rate will be sustained by adding productions from Lavani Deep and Main each with the approximate fraction of 0.375 of the field plateau rate.

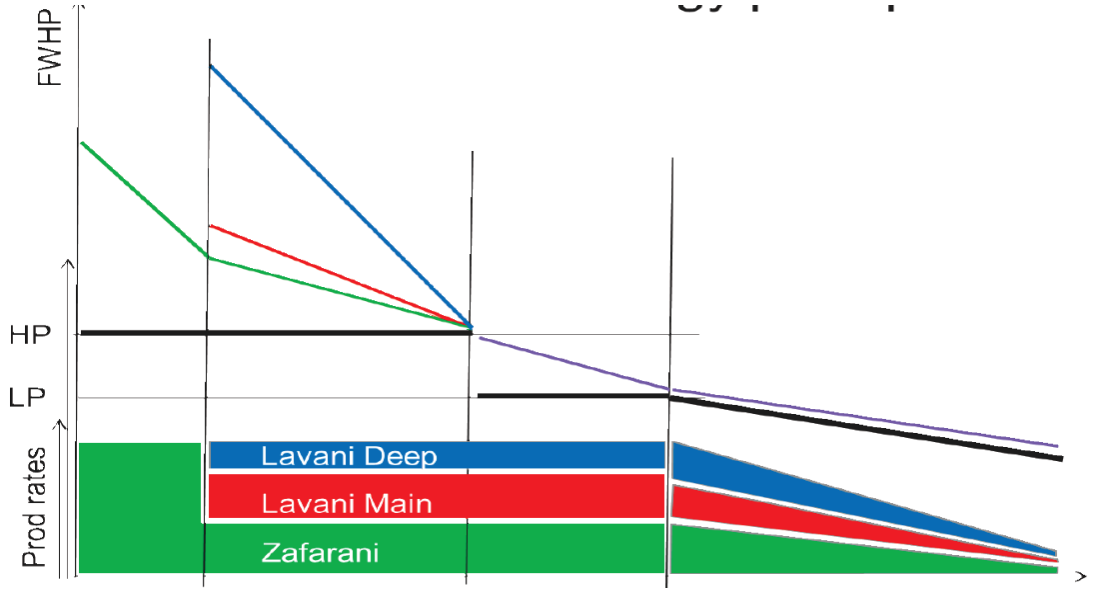

Figure 45: Production strategy proposed by Statoil (Holm, 2015)

In addition, the subsea production layout for the three reservoirs that includes production system dimensions (diameters and lengths of the pipelines and flowlines) was shown Figure 46. This "Daisy Chain" subsea production system was the effort to reduce the CAPEX of the field (Holm, 2015).

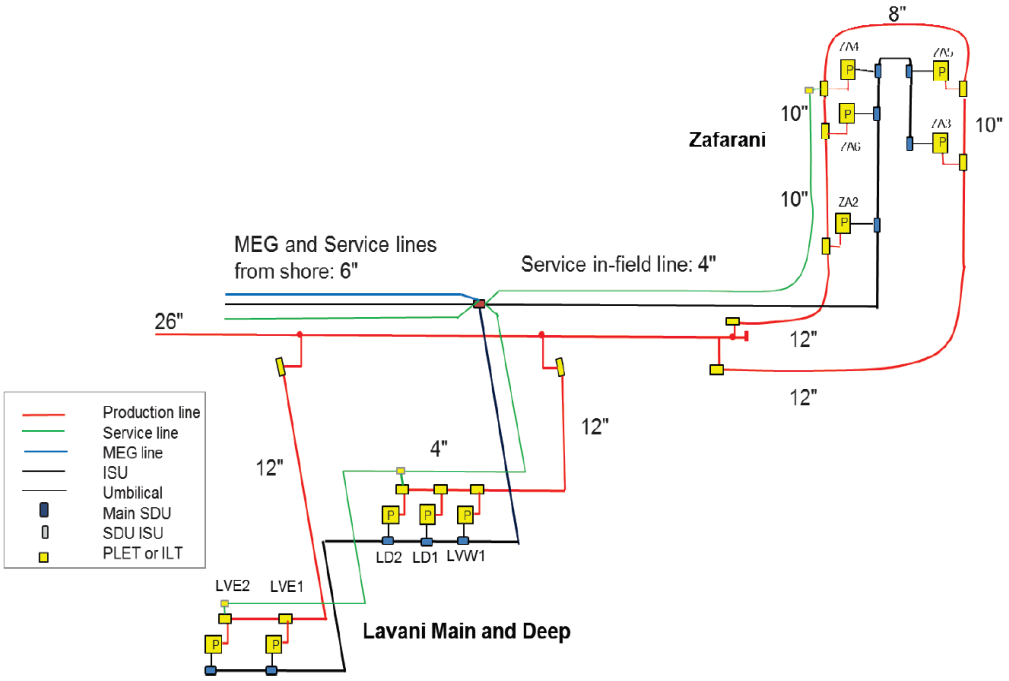

Figure 46: Subsea production layout (Holm, 2015)

Referring to the previous information, the same subsea layout was made in GAP, and then integrated with well models from PROSPER and reservoirs models from MBAL. The wells in a single reservoir shared the same IPR, the IPR of wells are different from one reservoir to another due to the difference of reservoir properties such as permeability, net pay thickness and reservoir conditions, typically pressure and temperature. Figure 47 illustrates the proposed subsea production system made in GAP. Tangawizi reservoir was initially disabled to illustrate the model's correspondence to the subsea layout mentioned in Figure 46.

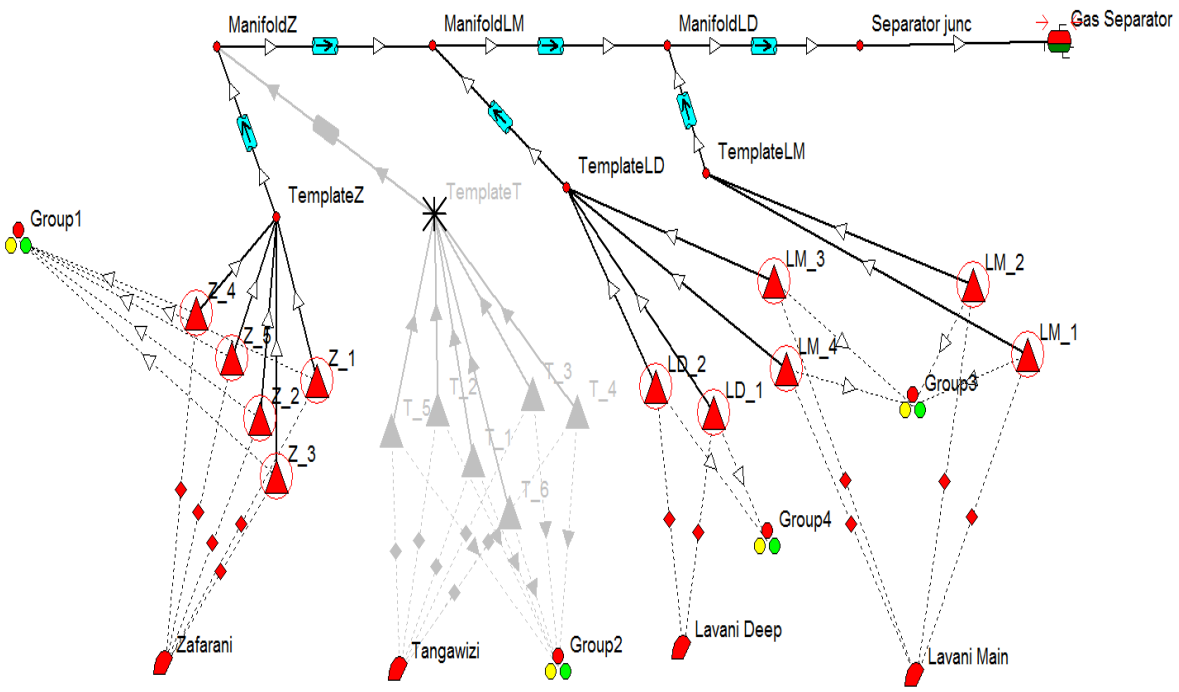

Figure 47: Zafarani, Lavani Main and Lavani deep subsea layout in GAP

In estimating the plateau rate, sensitivity analysis on several plateau rates were done; the base rate of 706.2 MMscf/day was arbitrary chosen based on previous experience from the Snøhvit field in Norway, which have the same development concept (subsea tie back to the onshore LNG plant) as TGP. The base rate was increased and decreased by the percentages of 5%, 10%, 15%, 20% and 25%.

Simulation was then done by network solving and then performing predictions with all wells choked and the maximum gas (plateau rate) specified as the constraint in the system. It was observed that the system (main pipeline) was bottlenecking when simulations with the plateau rates above +5% increments from the base plateau rate were run as shown in Figure 48. This justified that more rate could be produced but with the specified pipe diameter, the pipe limits the flow. Again, for the base plateau rate and rates below in decrement of 5%-25% the system ran efficiently with plateau length increasing with the reduction of plateau rate. Little plateau rate fluctuations happened when the plateau rate was 20 and 25% below the base rate; this was believed to be the results of numerical problems. The results of the runs are shown in Table

11(spotted red colors shows bottlenecked system, and right blue colors shows non-bottlenecking system).

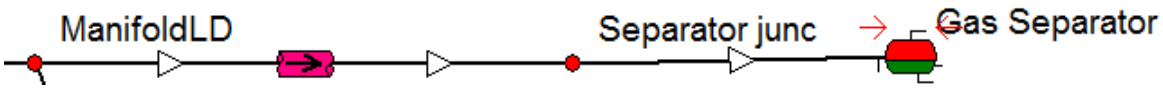

Figure 48-Bottlenecking indicator in the system (red pipe)

Table 11: Plateau rate prediction for Zafarani, Lavani Main and Lavani Deep

Plateau Rate	**Z, LM, LD**
[MMscf/day]	**[Years]**
882.8	18
847.4	19
812.1	20
776.8	22
741.5	22
706.2	24
670.9	27
635.6	30
600.3	31
565.0	34
529.7	37

For the plateau rates which are not bottlenecking the system, the plateau length achieved was between 20-40 years of production. It was then decided to take the average of the plateau rates from the results that are not bottlenecking the system. The average plateau rate achieved was 635.6 MMscf/day.

5.1.2 Approach Two: Extended Sensitivity Analysis on other Suggested Layouts

After the estimation of plateau rate based on three reservoirs as described in section 5.1.1. The study of estimating the production plateau rate was extended to conceptualize estimated plateau rate. At this time, Tangawizi reservoir was included in

the subsea layout (Figure 49), and five cases were made based on reservoirs connectivity to the surface network.

- Case 1- Analysis for Zafarani, Lavani Main, Lavani Deep and Tangawizi
- Case 2- Analysis for Zafarani, Lavani Main and Lavani Deep
- Case 3- Analysis for Zafarani and Tangawizi
- Case 4- Analysis for Tangawizi, Lavani Main and Lavani Deep
- Case 5- Analysis for Tangawizi and Lavani Main

The network solving and production predictions were done in GAP, and the results are shown in Table 12.

The following observations were made after simulation runs:

- In all the cases, the rates above 5% increment (741.5 MMscf/day) of the base plateau rate bottlenecked the system.
- In all the cases, the rate at 5% increment (741.5 MMscf/day) of the base plateau rate and below bottlenecked the system.
- For Case 1 (when four reservoirs are connected), the network solver was ran, and the rates below the base rate showed no flow from any of the reservoir except for the case when the plateau rate was 15% below the base rate.
- For Case 2, 3, 4 and 5, when the network solver was run neither convergence nor bottlenecking problem happened. During production predictions, the plateau rates below the base rate showed reasonable estimation of the plateau rate and length, with small fluctuations in some cases. For example, when predictions were done for Case 3 with the base plateau rate reduced by 20% (529.7 MMscf/day), the plateau rate fluctuated (in year 13 and 14 of production, Zafarani wells closed, Tangawizi went up producing to the maximum of 520.425 MMscf/day below the ultimate production plateau. After that, Zafarani wells opened slowly and Tangawizi wells produced to the rate such that; the field plateau rate was sustained. In year 15 and 35 the ultimate plateau rate went up beyond production plateau rate by producing 532.875 MMscf/day and 550.95 MMscf/day respectively. In year 36, the plateau rate went back to the required ultimate plateau rate, and this was the end of plateau since the ultimate plateau rate could not be delivered (rate decreased continuously)).

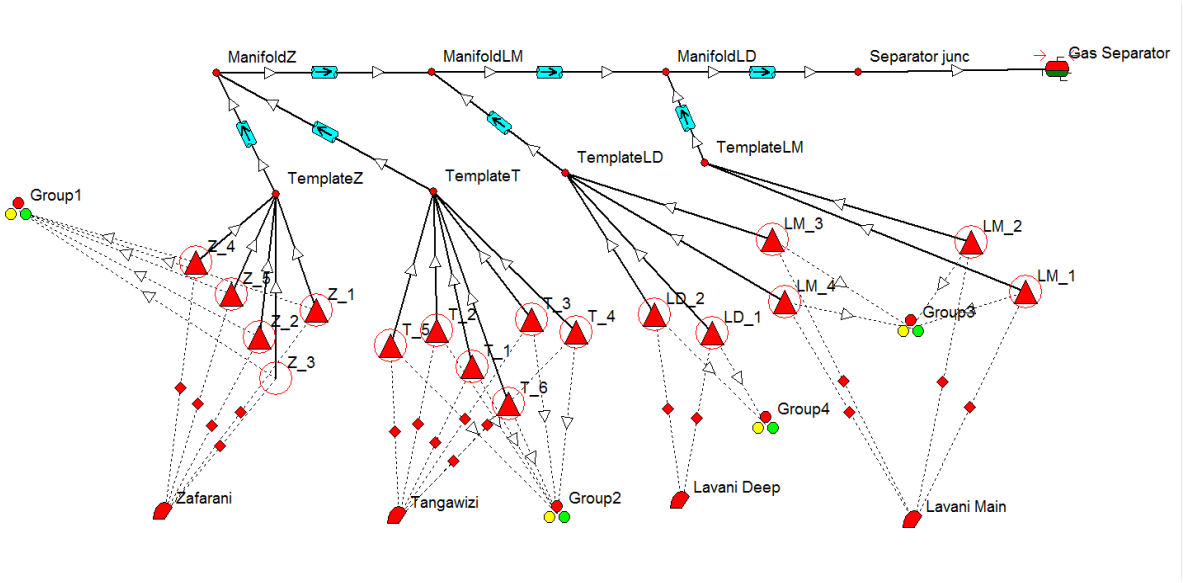

Figure 49: Tangawizi, Zafarani, Lavani Main and Lavani deep subsea layout in GAP

From the above observations, the results indicate that the layout configurations proposed by Statoil cannot produce the field plateau rate above 741.5 MMscf/day. In terms of production plateau length, the simulation provided reasonable results; this boosted the confidence on the estimated plateau (635.6 MMscf/day).

Table 12: More cases ran to conceptualize the plateau rate estimation

Plateau Rate [MMscf/day]	Case 1 [Years]	Case 2 [Years]	Case 3 [Years]	Case 4 [Years]	Case 5 [Years]	Sensitivity Percentages
882.8	30	18	16	19	8	25
847.4	32	19	18	21	9	20
812.1	34	20	19	22	10	15
776.8	36	22	20	24	10	10
741.5	38	22	21	25	11	5
706.2	40	24	24	27	12	Base
670.9	No flow	27	25	29	13	-5
635.6	No flow	30	27	31	14	-10
600.3	49	31	30	34	15	-15
565.0	No flow	34	33	36	17	-20
529.7	No flow	37	36	39	18	-25

5.1.3 Approach Three: Estimation of Plateau Based on LNG Plant Capacity

According to (Holm, 2015), the production capacity is still being evaluated and will typically be in range of 1-2 trains, depending on the train size.

The theoretical background calculations on LNG are:

1 Cargo of LNG approximated to 140 000 m^3, is capable of 86 Million Sm^3 gas. 65 Cargoes/year of LNG means 1 LNG train producing 5 MTPA (Rwechungura, 2016).

In this thesis the capacity was evaluated on 1 and 2 trains, with relying assumption that 1 LNG train producing 5 MTPA.

Performing calculations to obtain capacity of 1 LNG train on daily basis:

$$1\ Cargo \quad \equiv \quad 86\ Million\ Sm3\ gas$$

$$65\ \frac{Cargoes}{year} \quad \equiv \quad ?\ Million\ Sm3\ gas$$

$$65\ \frac{Cargoes}{year}\ x\ \frac{1\ year}{365\ days}\ x\ \frac{86\ Million\ Sm3\ gas}{1\ Cargo} = 15.32\ \frac{Million\ Sm3\ gas}{day}$$

Therefore, 1 LNG train producing 5 Mtpa is approximately 15.32 $\frac{Million\ Sm3\ gas}{day}$. For 2 LNG trains the capacity doubles to approximately 30.64 $\frac{Million\ Sm3\ gas}{day}$

Consider material balance on the processing facilities prior to LNG under the following assumptions

- The pure methane from outlet stream of the processing facility is distributed into two streams, of which 90% is taken to LNG and 10 % for domestic use.
- Overall mass balance on the processing facility, no upgrade of methane which means that, percentage of methane going in the processing facility equals the percentage of methane coming out of the processing facility.

Schematically, the process was presented as illustrated in Figure 50.

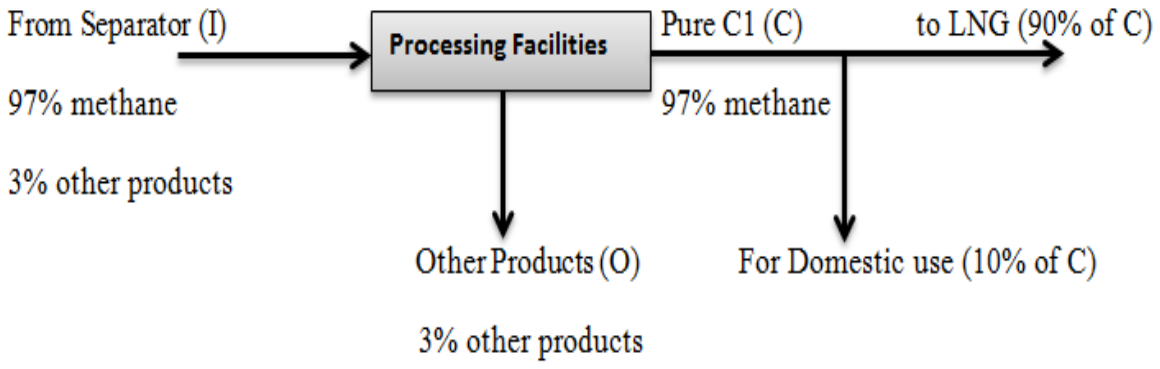

Figure 50-Schematic process for material balance calculations

a) For 1 LNG train (15.32 $\frac{Million\ Sm3\ gas}{day}$)

From Figure 50, the LNG stream has 15.32 Million Sm3 gas/day equals to 90% of stream C; therefore, stream C contains 17.02 Million Sm3 gas/day.

Overall Mass Balance on the processing facility:

I (separator gas rate) =C (97% methane of I) + O (3 % other products of I)

I=17.02 Million Sm3 gas/day + 0.03 I

I=17.55 Million Sm3 gas/day=619.8 MMscf/day

b) For 2 LNG trains (30.64 $\frac{Million\ Sm3\ gas}{day}$)

From Figure 50, the LNG stream has 30.64 Million Sm3 gas/day equals to 90% of stream C; therefore, stream C contains 34.04 Million Sm3 gas/day.

Overall Mass Balance on the processing facility:

I (separator gas rate) =C (97% methane of I) + O (3 % other products of I)

I=34.04 Million Sm3 gas/day + 0.03 I

I=35.09 Million Sm3 gas/day=1202.1 MMscf/day

It was observed that, when 1 LNG train was to be considered, the separator gas rate (plateau rate) to afford the required capacity should be 619.8 MMscf/day. This plateau was very close (2.5 % difference) to the plateau rate estimated using sensitivity analysis in section 5.1.1. When 2 LNG trains are considered the plateau rate should be doubled to 1202.1 MMscf/day, and during sensitivity analysis following subsea layout configuration suggested in (Holm, 2015), it was observed that, any plateau rate above 741.5 MMscf/day will bottleneck the main transportation pipeline which had a diameter 26 inches. Therefore, for 2 LNG trains the transportation pipeline diameter should be increased or a parallel pipeline should be installed.

5.2 Production Scheduling Analysis (1 LNG train capacity)

In order to determine the production profile of Block 2 field, the field production plateau rate estimated using sensitivity analysis was decided and fixed (635.6 MMscf/day). It should be remembered that, this plateau rate reflects capacity of 1 LNG train. The criteria to choose the value from sensitivity analysis was to regard this plateau rate as design capacity, so that, even when the plateau rate is not achieved in some years, still the production capacity required for 1 LNG train will be attained as it only needs 619.8 MMscf/day.

A total of six (6) case scenarios were simulated, four (4) cases had no subcases and the rest of the two (2) cases had subcases. By including subcases, sum of 35 prediction runs were made. Each case followed one of the following strategies.

- Emulating the Statoil proposed production strategy. This means fixing a constant production rate for each reservoir while keeping the plateau rate constant. Initially, the total field plateau rate was produced from one of the biggest reservoir and later it was overtaken by considering productions from Lavani Main and Deep. Different production shares and variations of this strategy were tested in subcases a, b, c, d and e.
- The field production shared production from each reservoir that changed dynamically in type, while keeping the field plateau rate constant to 635.6 MMscf/day. The reservoirs involved in this strategy produced from the beginning of production.

The second strategy was used for Cases Two, Four, Five, and Six. All reservoirs started producing from the beginning, the field plateau rate was fixed and the production shared from each reservoir was dynamically changed by GAP. Cases One and Three were initially producing the field plateau rate of 635.6 MMscf/day from one of the reservoir with the biggest reserves (Zafarani or Tangawizi), and after some years of initial production the rate was reduced and accompanied with other two reservoirs, typically, Lavani Main and Lavani Deep to sustain the initial field plateau rate.

To decide on the initial plateau rates of production, the two reservoirs with the biggest reserves which are Zafarani and Tangawizi were first ran independently in order to see how long each reservoir would take to produce the field plateau rate. The plateau duration obtained, was 8 years for Zafarani and 11 years for Tangawizi. Additional sensitivity cases were made where Zafarani was producing in plateau mode for 5, 7 and 8 years and Tangawizi was produced in plateau mode for 7, 9 and 11 years.

After the prediction of initial plateau rate from the biggest reservoir for each particular case, the production rate from the biggest reservoir was reduced and the smaller reservoirs were brought into production to sustain the plateau rate. The production rates are fixed. Eventually, the reservoirs were unable to sustain the desired rates any longer and entered into decline. The production rates of each reservoir were adjusted such as the contribution from the reservoirs with longer plateau length are increased gradually until all reservoirs started to decline at the same time (adjustments were grouped as subcases a-e as discussed before). Subsequently, the field plateau length was

increased as long as the field plateau rate is fixed (constant). An overview of all cases is illustrated in Table 13.

The naming of individual cases follows the following format example. $\boldsymbol{Case\ One\ 5(a)}$ **-** This is $Case\ one$ with initial plateau length of 5 with a subcase a. The subcases when Zafarani started the production are not necessarily the same as the subcases when Tangawizi started the production.

Table 13-Run cases to estimate the production profiles

Cases	Producing Reservoirs	Mode of Production	1st Initial Plateau Duration	2nd Initial Plateau Duration	3rd Initial Plateau Duration	Subcases
[-]	[-]	[-]	[Years]	[Years]	[Years]	
One	Zafarani, Lavani Main and Lavani Deep	Statoil Proposal	5	7	8	(a-e) applied to all initial plateau duration
Two	Zafarani, Lavani Main and Lavani Deep	Producing all reservoirs from the beginning	-	-	-	
Three	Tangawizi, Lavani Main and Lavani Deep	Start with Tangawizi only	7	9	11	(a-e) applied to all initial plateau duration
Four	Tangawizi, Lavani Main and Lavani Deep	Producing all reservoirs from the beginning	-	-	-	
Five	Tangawizi and Zafarani	Producing all reservoirs from the beginning	-	-	-	
Six	Lavani Main and Lavani Deep	Producing all reservoirs from the beginning	-	-	-	

5.3 Description of GAP Model for Production Scheduling

The GAP schematic model used for all mentioned cases is depicted in Figure 51.

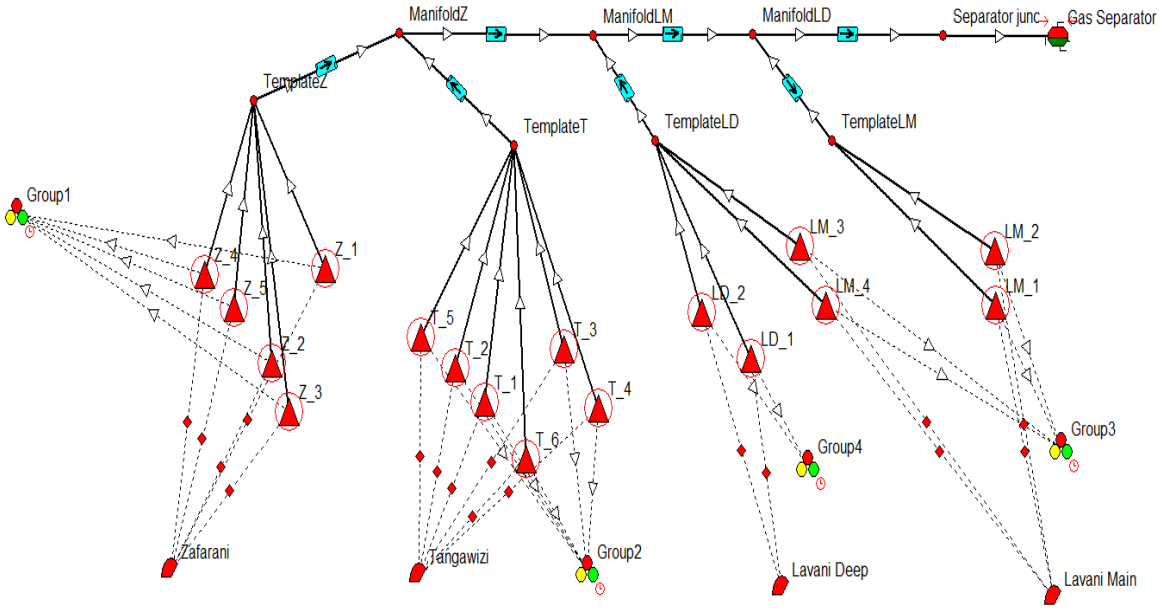

Figure 51-Schematic Gap Model

The wells from each reservoir were assigned into groups, in order to have single control of multiple wells. Zafarani wells were grouped into Group 1, Tangawizi wells grouped to Group 2, Lavani Main wells grouped into Group 3 and Lavani Deep wells grouped into Group 4. All the wells in the production system were potentially choked by activating the dP control to "calculated". The separator constraint was set to produce maximum gas production rate of 635.6 MMscf/day, and the group constraints were set depending on the case under concern. Before any prediction, the solver set up to optimize and honour constraints and see if there was any constraint in the production system. Lastly, the production prediction was assumed to start from 01/01/2025 to 01/01/2073, and was done on yearly basis.

The prediction run was performed by GAP, in each time step the cumulative gas production is calculated, then reservoir pressure, GOR, CGR and WGR are calculated using MBAL, then the MBAL and IPR information are transferred to GAP and then an optimization is run in GAP where the Delta_P of the choke is changed iteratively until the plateau rate specified for the field and all other constraints are honoured.

5.4 Production Profile Analysis

After running all 35 cases, for the most cases, there was no complete flat production plateau achieved(less delivery of plateau rate for some years). This was probably due to the fact that the network did not fully converge in that particular time step (i.e. didn't reach the tolerance of the constraint). To check this, firstly, the setting of the optimizer as shown Figure 52 was changed to tight tolerance (slower) which reduces the "solver-total rate perturbance" and "solver-tolerance F''. Amid the change of the optimizer, some cases showed good improvement in terms of the quality of the plateau (no many fluctuations). Secondly, the timesteps was set to monthly steps, and the results showed no improvement in terms of the quality of the plateau as shown in Figure 53. Therefore it was concluded that this was probably due to numerical problems rather than that, this kind of situations do happen in real life.

The plateau length was then decided on the last year to produce the desired production plateau rate regardless of less production plateau rate delivered in some previous years. Obtained plateau lengths were between 23-31 years of production.

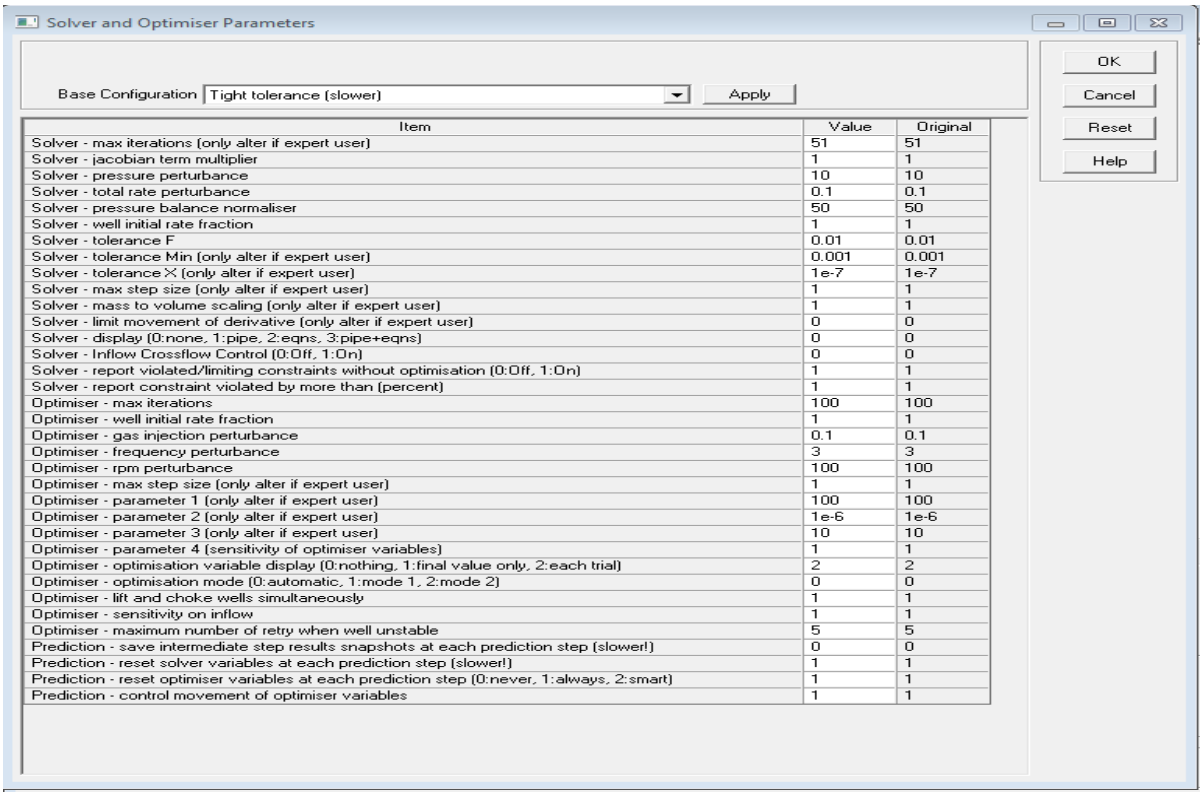

Item	Value	Original
Solver - max iterations (only alter if expert user)	51	51
Solver - jacobian term multiplier	1	1
Solver - pressure perturbance	10	10
Solver - total rate perturbance	0.1	0.1
Solver - pressure balance normaliser	50	50
Solver - well initial rate fraction	1	1
Solver - tolerance F	0.01	0.01
Solver - tolerance Min (only alter if expert user)	0.001	0.001
Solver - tolerance X (only alter if expert user)	1e-7	1e-7
Solver - max step size (only alter if expert user)	1	1
Solver - mass to volume scaling (only alter if expert user)	1	1
Solver - limit movement of derivative (only alter if expert user)	0	0
Solver - display (0:none, 1:pipe, 2:eqns, 3:pipe+eqns)	0	0
Solver - Inflow Crossflow Control (0:Off, 1:On)	0	0
Solver - report violated/limiting constraints without optimisation (0:Off, 1:On)	1	1
Solver - report constraint violated by more than (percent)	1	1
Optimiser - max iterations	100	100
Optimiser - well initial rate fraction	1	1
Optimiser - gas injection perturbance	0.1	0.1
Optimiser - frequency perturbance	3	3
Optimiser - rpm perturbance	100	100
Optimiser - max step size (only alter if expert user)	1	1
Optimiser - parameter 1 (only alter if expert user)	100	100
Optimiser - parameter 2 (only alter if expert user)	1e-6	1e-6
Optimiser - parameter 3 (only alter if expert user)	10	10
Optimiser - parameter 4 (sensitivity of optimiser variables)	1	1
Optimiser - optimisation variable display (0:nothing, 1:final value only, 2:each trial)	2	2
Optimiser - optimisation mode (0:automatic, 1:mode 1, 2:mode 2)	0	0
Optimiser - lift and choke wells simultaneously	1	1
Optimiser - sensitivity on inflow	1	1
Optimiser - maximum number of retry when well unstable	5	5
Prediction - save intermediate step results snapshots at each prediction step (slower!)	0	0
Prediction - reset solver variables at each prediction step (slower!)	1	1
Prediction - reset optimiser variables at each prediction step (0:never, 1:always, 2:smart)	1	1
Prediction - control movement of optimiser variables	1	1

Figure 52-Solver optimizer settings

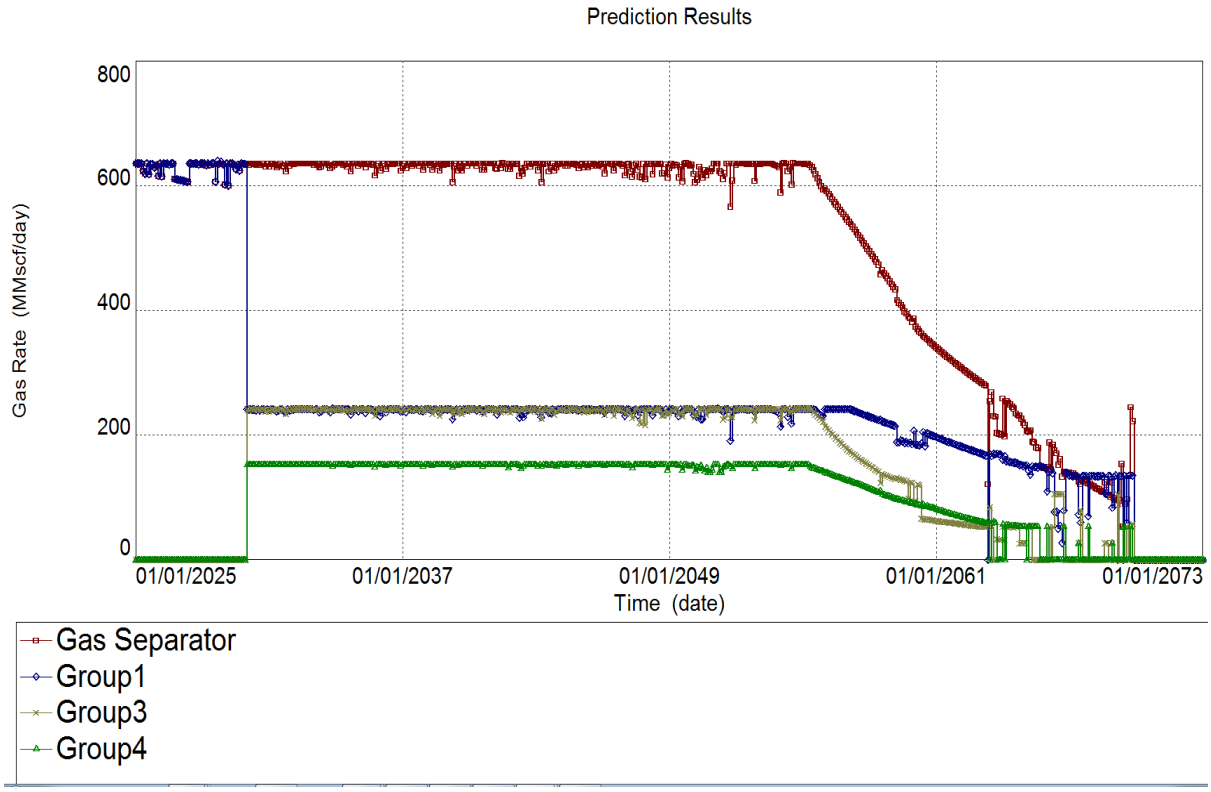

Figure 53-prediction runs in monthly timesteps

After prediction run, two phenomena were observed, some models showed fully convergence by producing plateau rate during the plateau production and other models did not converge. This observation led to splitting of the case scenarios into two parts.

Part I: Models which did not converge

The cases with longest plateau lengths (31 years of production) were selected as most attractive production schedules. These cases are Case One 5(d), Case One, 5(e), Case Three, 7(b), Case Three, 7(c), Case Three, 7(d), Case Three, 9(d) and Case Three, 11(d).

Further analysis was done to screen the seven (7) most attractive production schedules by quantifying them and determine the best solution. The analysis was done quantitatively as well as qualitatively on the field production plateau rate.

One of the indicators used to evaluate the best solution amongst the seven (7) most attractive production schedules, was the deviation between the computed cumulative gas production and the theoretical cumulative gas production. The variable is defined as:

$$\% \, Error \, Qn. = \left| \frac{Cumulative \, Gas \, Production_{Ideal} - Cumulative \, Gas \, Production_{Real}}{Cumulative \, Gas \, Production_{Real}} \right| x100\%$$

The theoretical cumulative gas production is calculated by multiplying the rate times the producing period in consistent units.

Another parameter used to quantify the solution was the relative percentage difference between the actual number of timesteps simulated, where the plateau rate could not be delivered and the total number of timesteps. The variable is defined as:

$$\% \, Error \, Ql. = \left| \frac{Time \, steps(31)_{Ideal} - Time \, steps_{Real}}{Time \, steps(31)_{Ideal}} \right| x100\%$$

The two indicators were averagely weighted with equal weighted fractions (50%) each. The results are presented on Table 14.

$$Percentage \, Weighted \, Average = 0.5 \, x \, \% \, Error \, Qn. + 0.5 \, x \, \% \, Error \, Ql.$$

Table 14-Weighted average to analyse the production plateau length

Cases	**%Error Quantitatively**	**%Error Qualitatively**	**Weighted Average**
[-]	**[%]**	**[%]**	**[%]**
Case One 5(d)	0.2	19.4	9.8
Case One 5(e)	0.8	48.4	24.6
Case Three 7(b)	0.4	32.3	16.3
Case Three 7(c)	0.9	54.8	27.9
Case Three 7(d)	1.3	41.9	21.6
Case Three 9(d)	1.0	41.9	21.5
Case Three 11(d)	1.5	45.2	23.3

Based on the percentage weighted average results the following statement holds to select the best case, “The lower the percentage weighted average error, the bests the solution”. Therefore, Case One 5(d) may be chosen as the best production profile for the Block 2 field.

The production strategy summary for Case One 5(d) is depicted in Table 15(a) and (b). These results confirm relevance to the Statoil proposed strategy. However, the initial production plateau and the production plateau lengths are not the same. Case One 5(d) had initial plateau length of 5 years with 31 years of plateau production (Figure 54), while the Statoil proposed strategy had initial plateau length of approximately 7 years of production with 29 years of plateau production (Figure 55).

Table 15-Production strategy summary for Case One 5(d)

Producing Reservoirs	**Production Strategy**	**Initial Production from Zafarani**	**Ultimate Plateau Rate**
[-]	**[-]**	**[Years]**	**[MMscf/day]**
Zafarani, Lavani Main and Lavani Deep	Begin with Zafarani, Later Connect Lavani Main and Deep	5	635.6

(a)

Producing Reservoirs	**Percentages of Contribution to the Field Plateau**	**Individual Plateau Rate**
[-]	**[%]**	**[MMscf/day]**
Zafarani	0.38	241.5
Lavani Main	0.38	241.5
Lavani Deep	0.24	152.5

(b)

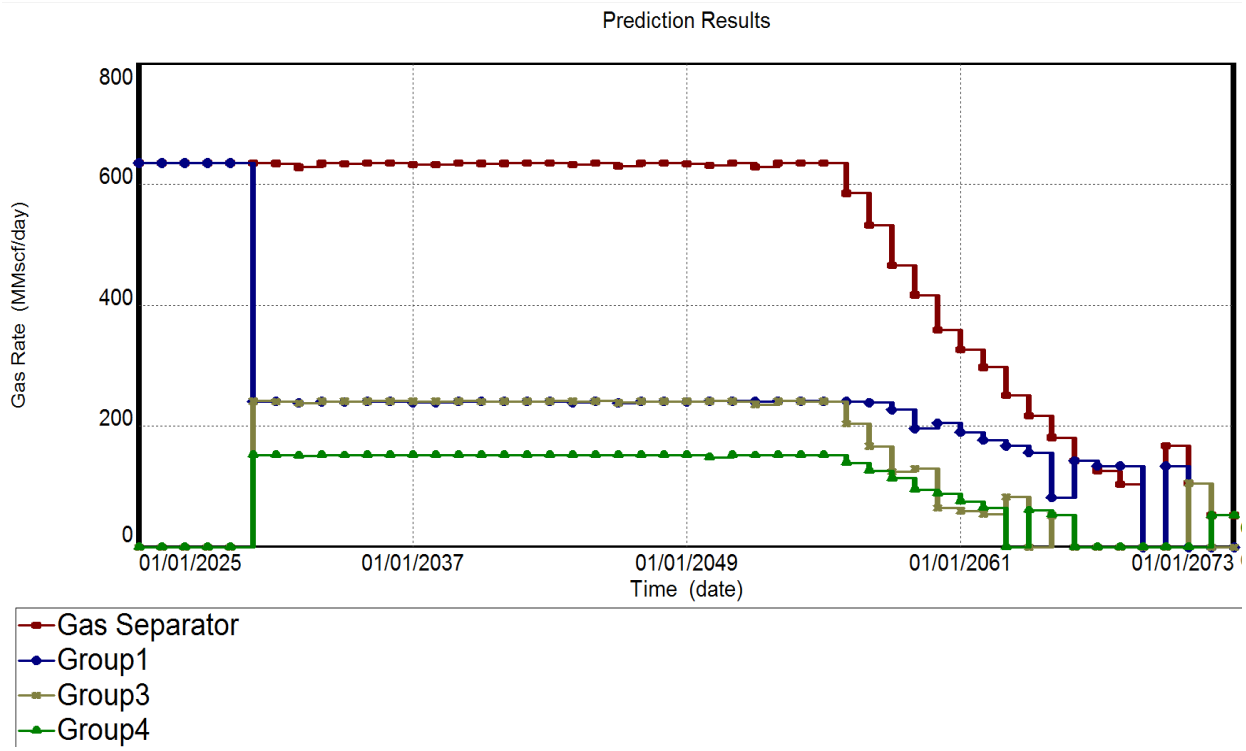

Figure 54-Production plateau profile for Case One 5(d)

Group 1-Zafarani; Group 2-Tangawizi; Group 3- Lavani Main and Group 4-Lavani Deep

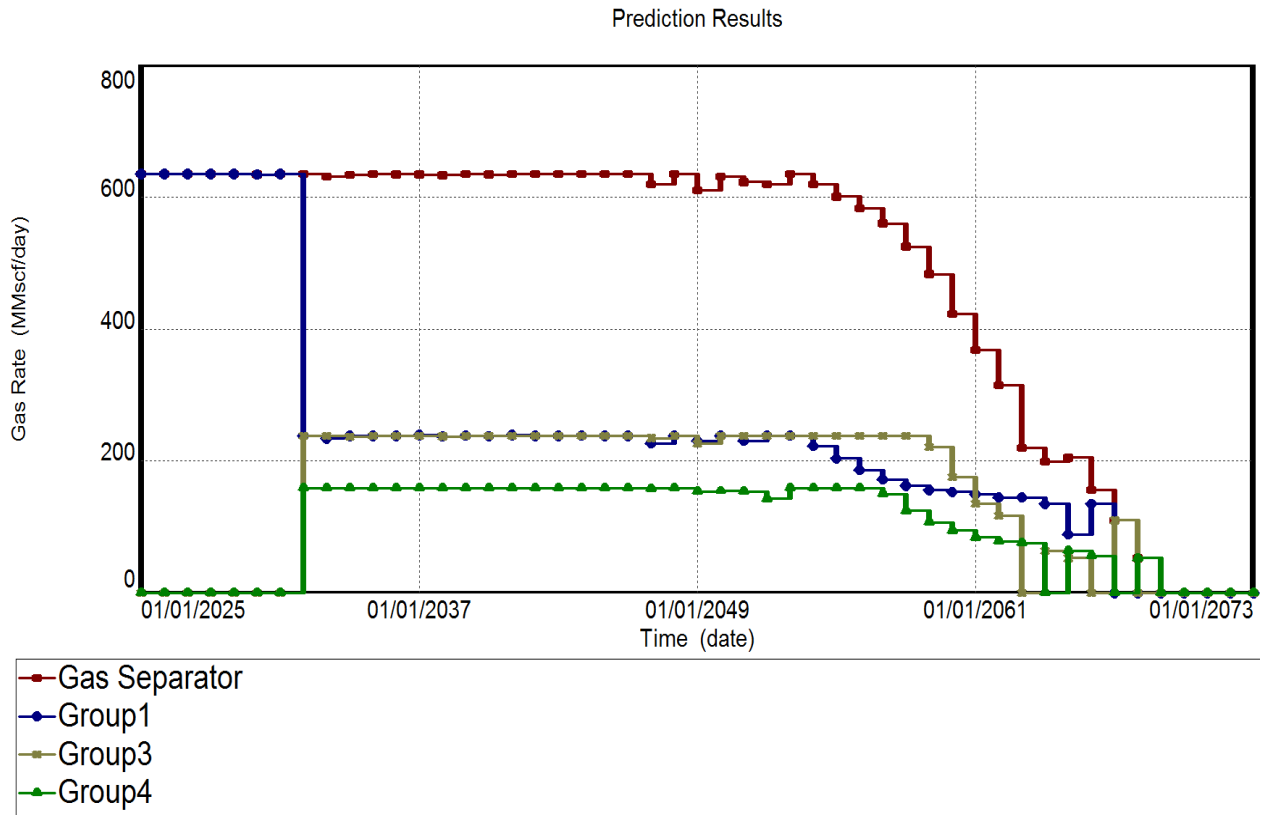

Figure 55- Production plateau profile for the Statoil proposed strategy

Part II: Converged Models

It should be remembered that, the first selection criteria for the plateau rate production cases was mainly based on the longest plateau length of 31 years where seven cases were selected and further screened by quantitative indicators to obtain the best solution. These models did not fully converge (i.e. were unable to produce the plateau rate in some timestep). More investigation was then done to other cases, and it was found that all the cases with the strategy of producing all the connected reservoirs from scratch produced flat plateau production profile; this meant that the model converged. Therefore, amongst these cases, Case Four provided the longest plateau of 30 years.

If it was assumed that the inability to produce at plateau rate was just due to numerical problems (the simulation doesn't converge), therefore, it was fair to say that Case Four is another best optional strategy to start production from Block 2 field Tanzania. The production profile for case for is shown in Figure 56.

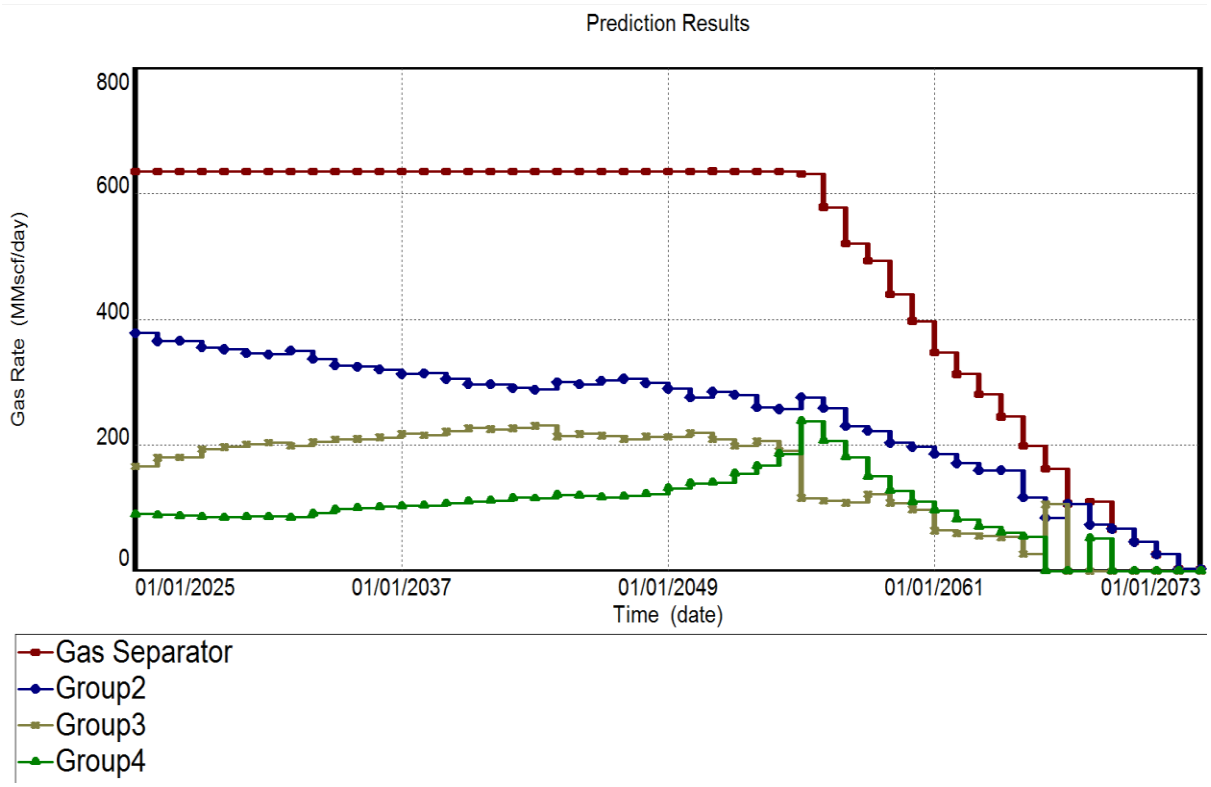

Figure 56- Production plateaus for *Case Four*

When comparing Case One 5(d) and Case Four, The Case One 5(d) gave 31 years of production plateau with few time steps not converging while Case Four gave 30 years of

production with all timesteps converging. The cumulative gas rate for the Case One 5(d) was obtained 591.47 MMscf/day more than that of Case Four; of course this is obvious as the former case produced for 31 years while the latter case produced for 30 years.

For conveniences, let call Case One 5(d) as Optional Strategy One and Case Four as Optional Strategy Two.

5.5 Prolonging the plateau

To extent the plateau after the natural plateau production, three modifications options to the entire production system were made. The modifications were applied to both Optional Strategy One and Optional Strategy Two, "these three options are named as first approach, second approach and third approach".

The results were evaluated with simple economic calculations. In order to evaluate best case among all the cases, The NPV of each case was computed for the period after the natural plateau and compared against the base case.

5.5.1 Economical Model

The model used is given as:

$$NPV = \sum_{n=1}^{n} \frac{CF_n}{(1+r)^n}$$

Where, r is the discount rate, n is the number of years and CF_n Stands for the cash flow

Assumptions made on the economic analysis were:

- Only CAPEX and OPEX were used for analysis, thus the model didn't include taxes and royalties
- The CAPEX accounted for the expenditures of the additional wells and additional pipelines to the base case, as well as compressor costs for the cases when compressor was applied.
- The Drillex for offshore wells range from US$ 80 to 120 million per well (Rwechungura, 2016), the average value which is US$ 100 million per well was used. The OPEX value was set to US$ 200 million/ year (Stanko, 2016). According to (Chandra, 2016), the cost of offshore line is estimated to around

$25 000 to $40 000/in.-km, therefore the average value which is $32 500/in.-km was used in this context. The estimated costs of the offshore lines for Block 2 are shown in Appendix 7.

- Compressors and associated equipment (drivers, coolers, and ancillaries) are priced at US$ 1 500 per demand horsepower which is equivalent to US$ 2 million per demand Megawatts (Chandra, 2016).
- Gas price was assumed to be $2.78/ Mscf as of June 22, 2016 (U.S. Energy Information Administration, 2016).
- The 3% and 1% annual increase was assumed for CAPEX and OPEX respectively
- The discount rate was assumed to be 8%.

Note: The natural gas price was assumed constant for all production years for this analysis, later the sensitivity on the price was done to assess the impact on this factor on the NPV. The higher price levels will improve the economics for increasing production. When detailed economic analysis is considered, in reality there will be a difference that can be significant. However, the presented results are adequate to present the best solutions.

5.5.2 First Approach to Extend the Plateau

This approach was based on increasing number of wells after the natural plateau production of the field. The wells were increased to about 50% of the initial wells present in the field. The new wells were assigned to new groups. The cases to increase wells for the Case One 5(d)) and Case Four are shown on Table 16, and the layout is shown on Figure 57.

Table 16-Wells added to prolong the plateau

Optional Strategy One (Case One 5(d))				
Cases	**Added wells**			
[-]	**Zafarani**	**Lavani Deep**	**Lavani Main**	**Total Wells**
Base Case	0	0	0	0
Case A	1	1	1	3
Case B	2	1	1	4
Case C	2	2	1	5
Case D	1	2	2	5
Case E	2	2	2	6
Optional Strategy Two (Case Four)				
Cases	**Added wells**			
[-]	**Tangawizi**	**Lavani Deep**	**Lavani Main**	**Total Wells**
Base Case	0	0	0	0
Case F	1	0	0	1
Case G	1	1	0	2
Case H	1	1	1	3
Case I	2	2	1	5
Case J	2	2	2	6

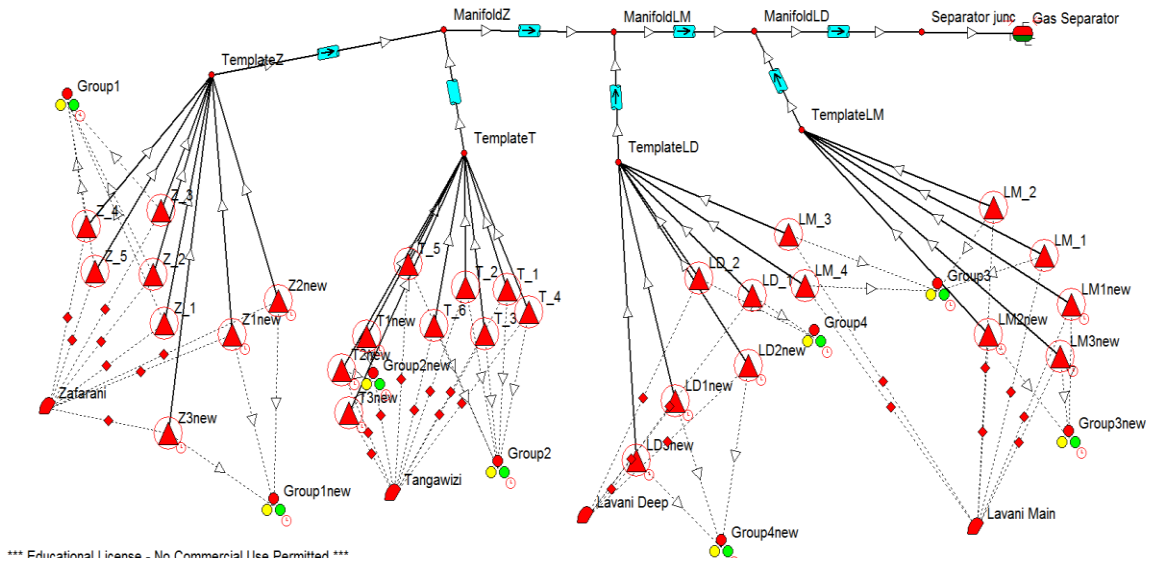

Figure 57- GAP layout for added wells

5.5.3 Results First Approach: Increasing Number of Wells

Table 17 and Table 18 shows the simulation results after increasing number of wells to the production system for the Case One 5(d) and Case Four respectively.

Table 17- Results for Case One 5(d) after increasing number of wells

Optional Strategy One Increasing Number of Wells								
Cases	**Added wells**				**Extension**	**Cum.NPV**	**% Diff.**	**R.F**
[-]	**Zafarani**	**Lavani Main**	**Lavani Deep**	**Total**	**[Years]**	**[USD, Million]**	**[%]**	**[-]**
Base	0	0	0	0	0	3 399	-	0.72
Case A	1	1	1	3	0	3 330	-2.03	0.72
Case B	2	1	1	4	0	3 307	-2.71	0.72
Case C	2	2	1	5	0	3 284	-3.38	0.72
Case D	1	2	2	5	1	3 316	-2.46	0.74
Case E	2	2	2	6	1	3 293	-3.13	0.74

The % Diff. in the table is defined as

$$\%\ Diff. = \frac{NPV_{new} - NPV_{base\ case}}{NPV_{base\ case}}$$

Table 18- Results for Case Four after increasing number of wells

Optional Strategy Two Increasing Number of Wells								
Cases	**Added wells**				**Extension**	**Cum.NPV**	**% Diff.**	**R.F**
[-]	**Tangawizi**	**Lavani Main**	**Lavani Deep**	**Total**	**[Years]**	**[USD, Million]**	**[%]**	**[-]**
Base	0	0	0	0	0	3 271	-	0.70
Case F	1	0	0	1	1	3 281	0.31	0.72
Case G	1	1	0	2	2	3 288	0.53	0.74
Case H	1	1	1	3	2	3 264	-0.20	0.74
Case I	2	2	1	5	2	3 216	-1.68	0.74
Case J	2	2	2	6	3	3 220	-1.53	0.77

In terms of plateau extension, the results showed that adding more wells was more effective for Case Four than Case One 5(d). Case Four was able to extend the plateau length with 3 years more while) could extend the plateau length by maximum of 1 year.

For the Case One 5(d), the results indicated no plateau extension when the number wells added to the system was less than 5. This statement seems to contradict when Case C and Case D were compared, both cases had total of 5 wells added to the production system, the Case D extended the plateau length by 1 year more while Case C did not extend the plateau length. This could be explained by two reasons: (1) the 5 wells in Cases C and D are added in different places thus the locations used in D are more convenient than the locations used in C. The Case C had two added wells from each Zafarani and Lavani Main and only one added well from Lavani deep while the Case D had two added wells from each Lavani Main and Lavani Deep and only one added well from Zafarani. (2) There was very little difference in the plateau extension between the two cases (e.g. 0.9 years and 1.1 years), but the timestep used for the simulation (1 year) was too coarse to show it.

In terms of Cumulative NPV, all the modified cases were compared with the Base case of natural plateau production. The difference of cumulative NPV of natural production plateau and that of when wells were added to the system (% Diff.) were all negative for

Case One 5(d) indicating that the added well expenditures are higher; hence, no profit will be gained after adding the wells. For the Case Four, simulation results depicted that when the number of wells added to the system was above 2, the added wells expenditures become higher than the added profit. Adding two wells to the production system (Case G) provides the best solution by increasing the cumulative NPV by 0.53% with production of 2 years more and the recovery factor of 0.74.

5.5.4 Second Approach to Extend the Plateau Length

In this approach, the unproduced reservoir was brought into production as the satellite reservoir after the end of natural plateau production. After the natural plateau production in Case One 5(d), Tangawizi was brought into production as the satellite reservoir to prolong the plateau, and after the natural plateau production in Case Four, Zafarani was brought into production as the satellite reservoir to prolong the plateau.

5.5.5 Results Second Approach: Producing with unproduced reservoirs

The results for second approach of prolonging the plateau are shown in Table 19 and Table 20. Solver results indicated convergence for Case K, and when solving Case L the last segment of the transportation pipeline (ManifoldLD to Jsep) bottlenecked the system. Modifications were made for Case L by increasing the transportation pipeline segment diameter from 26 inches to 28 inches to allow more flow of production. For consistency and reality as the pipeline installation should be done once prior to production, the calculations and simulations for Case Four were repeated with this new diameter configuration of 28 inches.

Table 19- Results for Case One 5(d) when Tangawizi was connected as satellite reservoir

Produce Tangawizi as Satellite Reservoir						
Cases	**Add Tangawizi**		**Extension**	**Cum.NPV**	**% Diff.**	**R.F**
[-]	**ManifoldLD to Jsep**	**Wells in the Field**	**[Years]**	**[USD, Million]**	**[%]**	**[-]**
Base Case		11	-	3,399	-	0.72
Case K	26'' pipeline	17	14	3 529	3.81	0.69

Table 20- Results for Case Four when Zafarani was connected as satellite reservoir

Produce Tangawizi as Satellite Reservoir						
Cases	**Add Tangawizi**		**Extension**	**Cum.NPV**	**% Diff.**	**R.F**
[-]	**ManifoldLD to Jsep**	**Wells in the Field**	**[Years]**	**[USD, Million]**	**[%]**	**[-]**
Base Case		12	-	3 271	-	0.70
Case L	28'' pipeline	17	15	3 458	5.55	0.70

The prediction results show that, the plateau length could be extended by 14 and 15 years for the Case K and Case L respectively. Economically, Case L would be more attractive compared to Case K. The Case L gave 5.5% added cumulative NPV, the value higher than the 3.81% added cumulative NPV of Case K. Moreover, the recovery factor for Case L would be 0.01 more than Case K.

5.5.6 Third Approach to Extend the Plateau

The third approach was to install subsea compressor to provide additional energy to the fluid and prolong the plateau. This is a preliminary study; no particular compressor model has been proposed or selected yet for the field. A simplified approach was chosen consisting on providing a fixed Delta_P for scooping study. The polytropic efficiency was assumed to be 80%, and the cases were made by performing sensitivity on Delta_P values as shown in Table 21 , whereby the maximum compression deltap was set to be 507.6 psia. The compression schematic model is as depicted in Figure 58. Due to limitations in the commercial software employed, it was not possible to vary the deltap of the compressor with each year.

Table 21-Sensitivity cases on compressor Delta_P

Compression (Poly. Efficiency=80%)	
Cases	**Delta_P**
[-]	**[psia]**
Case i	72.1
Case ii	159.5
Case iii	261.1
Case iv	377.1
Case v	507.6

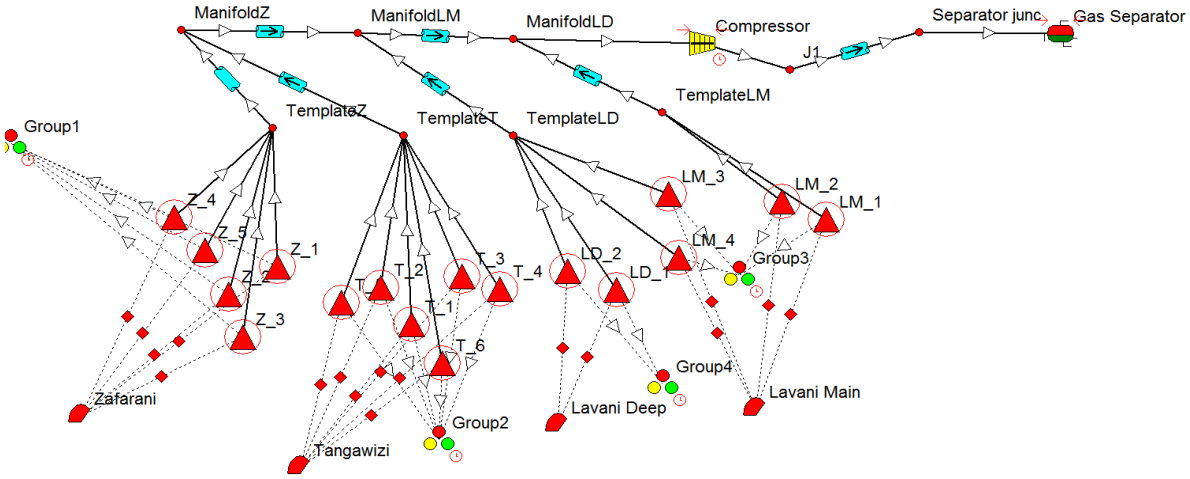

Figure 58-GAP layout with single compressor

Initially, simulation was done with single compressor and no cooling, thereafter, the results were observed to investigate if there was any need of cooling or adding another compressor. The criteria for cooling of the gas and adding compressor are (i) cooling should be necessary if the compressor discharge temperature would be $\geq 450\ K$, this is a maximum allowable temperature of the pipes, of the compressor seals and the hydrate inhibitor, the value was assumed based on the TPG4230 course at NTNU taught by (Stanko & De Andrade, 2015) and (ii) the subsea compression power was limited to$<$ 15 Megawatts, and maximum of three(3) compressors are allowed for subsea, thus

the maximum power required for a single compressor should roughly be 5 Megawatts. (Statoil, 2015). In Åsgard field (relatively dry gas); two compressors each with 10 Megawatts are used. In Gullfalks field; two wet gas compressors with 5 Megawatts each are used (Statoil, 2015).

5.5.7 Results Third Approach: Subsea Compression

After the natural production plateau, a single compressor was installed in the system as presented in Figure 58. The prediction was done and the results are as shown in Table 22 and Table 23 for Case One 5(d) and Case Four respectively.

When the Delta_P compressor was set to 507.6 psia, solver results showed bottleneck on the flowline segment "TemplateZ to ManifoldZ" for Case One 5(d) and "TemplateT to ManifoldZ" for Case Four. Therefore, flowline segment diameters were changed from 12 inches to 13 inches in order to remove bottlenecking problem in the system. These changes were valid for Delta_P compressor of 507.6 psia only.

Usually, when Delta_P of the compressor is fixed, initially the rate is higher than the plateau rate and then starts to decline until it reaches the plateau rate and continues to go down. But in this analysis optimization was run modifying the choke setting of the wells to get exactly the plateau rate.

Technically, boosting of the flow using subsea compression technique to Case Four was feasible compared to when compression was applied to Case One 5(d). The compression boosting for Case Four was capable of extending the plateau to the maximum of four (4) years. This was different for Case One 5(d) when the maximum of one (1) year was extended using the same deltap as in Case Four. For both cases, the cases with Delta_P of 507.6 psia (Case v) required a maximum compression power of approximately 20 Megawatts which exceeded the maximum power limit for subsea compression (15Megawatts).

Economically, for Case One 5(d) and Case Four, the compression with Delta_P of 261.1 psia (case iii) appeared economically viable amongst the others. The added profit of 0.56% and 2.95% were obtained for Case One 5(d) and Case Four respectively with compression Delta_P of 261.1 psia. These are the best solutions for particular case. However, when the Case One 5(d) and Case Four were compared, the case with

compression Delta_P of 159.5 psia for Case Four (case ii) provided better solution than the case with compression Delta_P of 261.1 psia. The overall comparison shows the best compression was attained with compression Delta_P of 261.1, when producing with Case Four strategy. This compression will be able to extend the plateau length with 3 years more, with the highest recovery factor of 0.77 compared to the rest cases which are technically feasible.

Table 22- Compression results for Case One 5(d)

Optional Strategy One (Case One 5(d)) Compression (Poly. Efficiency=80%)							
Cases	**Delta_P**	**Extension**	**Cum.NPV**	**% Diff.**	**Max. Power**	**Max. T discharge**	**R.F**
[-]	**[psia]**	**[Years]**	**[USD, Million]**	**[%]**	**[MW]**	**[K]**	**[-]**
Case i	72.1	0	3 385	-0.41	1.8	317.5	0.72
Case ii	159.5	1	3 416	0.49	4.2	327.8	0.74
Case iii	261.1	1	3 418	0.56	7.6	341.3	0.74
Case iv	377.1	1	3 412	0.37	12.5	360.8	0.74
Case v	507.6	1	3 412	0.39	19.7	389.5	0.74

Table 23- Compression results for Case Four

Optional Strategy Two(Case Four) Compression (Poly. Efficiency=80%)							
Cases	**Delta_P**	**Extension**	**Cum.NPV**	**% Diff.**	**Max. Power**	**Max. T discharge**	**R.F**
[-]	**[psia]**	**[Years]**	**[USD, Million]**	**[%]**	**[MW]**	**[K]**	**[-]**
Case i	72.1	0	3 276	0.14	1.8	321.1	0.70
Case ii	159.5	1	3 309	1.15	4.3	331.4	0.72
Case iii	261.1	3	3 367	2.95	7.7	345.3	0.77
Case iv	377.1	3	3 365	2.88	12.6	313.9	0.77
Case v	507.6	4	3 388	3.58	19.9	393.0	0.79

More investigation on the results showed that all compression cases had compressor discharge temperatures below 450 K; therefore no cooling was required prior to compression. As regards to compression power required, all the uneconomical results are of no interest, only the best case which was Case iii on Case Four was considered.

The maximum compression power required for Case iii of Case Four was 7.7 Megawatts, and based on the 5 Megawatts subsea compressor limit, a single compressor didn't have any problem delivering the used Delta_P. The problem was most likely being the rate, that it was too high. Therefore, using two compressors in parallel was the best option. By implementing two compressors in parallel each with the Delta_P equal to 261.1 psia (Figure 59), the prediction results indicated the maximum power required for compressor 1 and compressor 2 should be 3.9 Megawatts each. This reveals the optimal solution for subsea compression.

However, the current technology indicates that higher capacity compressors (11 Megawatts) have been installed in offshore fields (Forster, et al., 2015), so there should be no problem to have a single compressor to deliver 7.7 Megawatts.

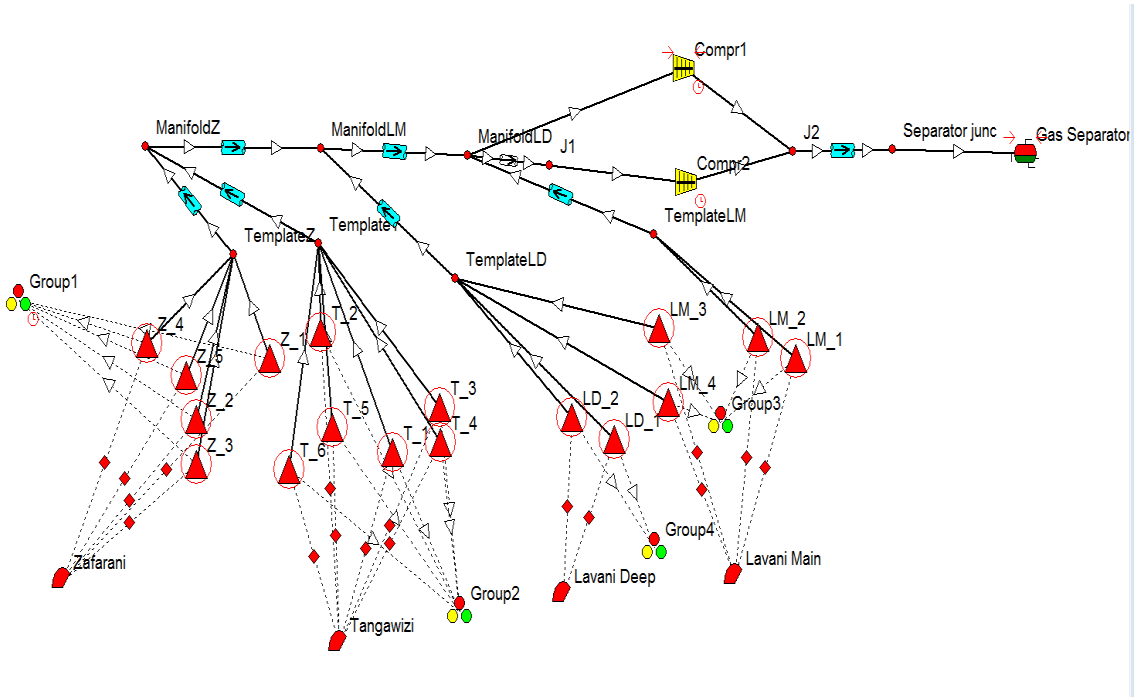

Figure 59- GAP layout with two compressors in parallel

5.6 Production Scheduling Analysis Considering 2 LNG trains

Determination of production plateau profile for 2 LNG trains was initially done for Case One 5(d) and Case Four; the production plateau rate of 1201.1 MMscf/day was used.

5.6.1 Production with higher production rate (2 LNG Trains capacity) for Case One 5(d)

For Case One 5(d), the production strategy required to determine the initial production plateau length from Zafarani. Determination of the initial production plateau length was done by simulation of Zafarani only. Solver results showed bottleneck on flowline "TemplateZ to ManifoldZ" and the trunkline segment "ManifoldLD to Jsep". To remove bottleneck in the system, the diameter of flowline segment "TemplateZ to ManifoldZ" was increased from 12 inches to the minimum of 16 inches, and the diameter of trunkline "ManifoldLD to Jsep" required the diameter to be increased to 31 inches. According to (PetroWiki, 2015), pipelines up to 28 inches diameter are now being installed in the deepwater applications up to 7,000 ft. of water. Therefore, the 31 inches diameter is impractical; the best solution was to put two pipes in pipeline. Two pipelines on segment "ManifoldLD to Jsep" with minimum diameter of 24 inches were parallel installed to give optimal solver solution without bottlenecking the system

(Figure 60). The prediction results were made and with the plateau rate of 1201.1 MMscf/day, maximum 3 years of production plateau was obtained (Figure 61), the prediction was run with Zafarani as the only producing reservoirs, other reservoirs were disabled.

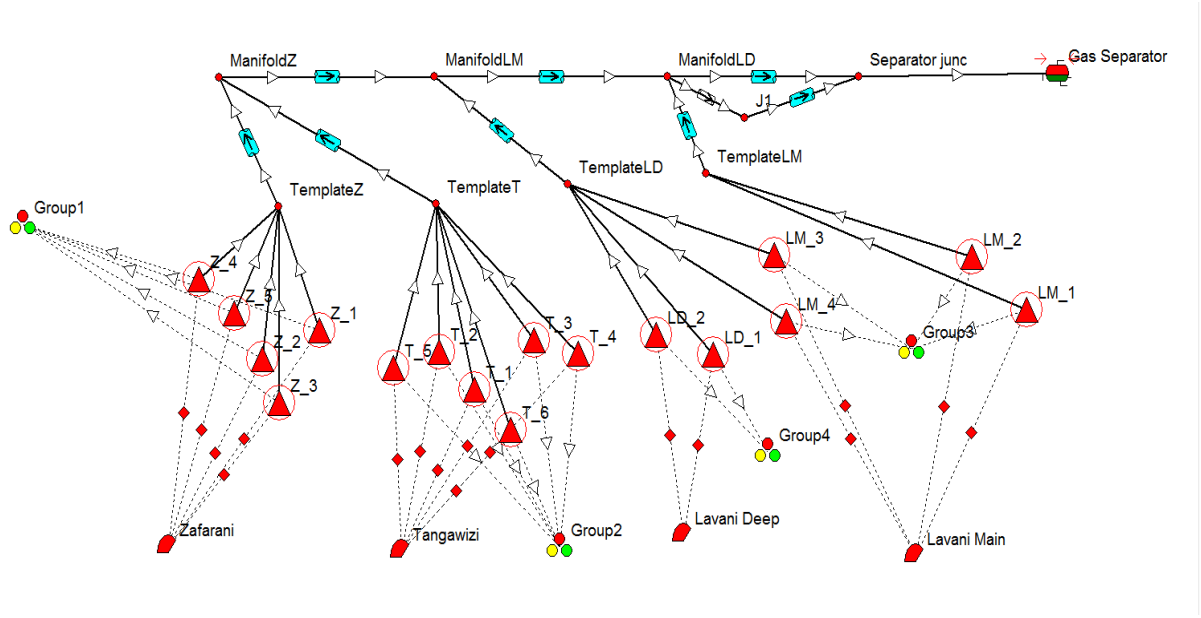

Figure 60-Two parallel lines for optimal solver solution without bottlenecking the system for 2 LNG Capacity

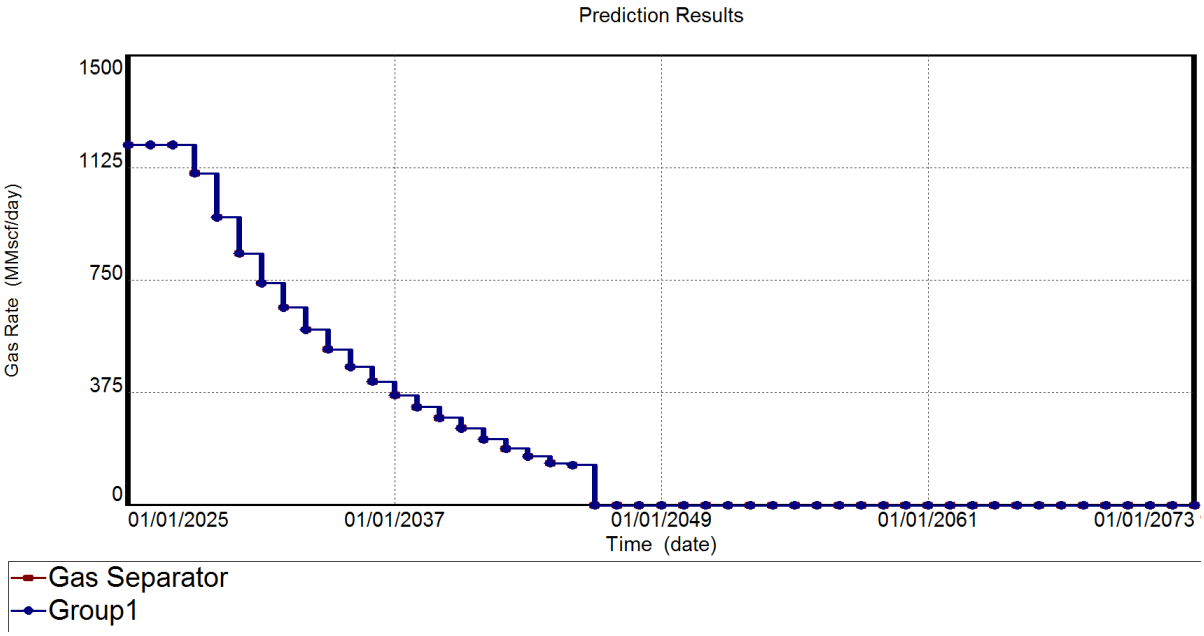

Figure 61-Initial production from Zafarani reservoir with production rate of 1201.1 MMscf/day

After the modifications and determination of the initial plateau length from Zafarani, The prediction run was done with the Case One 5(d) production strategy for 2 LNG trains capacity. Prediction was done to determine the production plateau. The prediction results indicated production plateau length of 14 years. The numerical problem appears to persist when this strategy was used; this led to production of the plateau profile which was not flat. The biggest difference of 1.8% from the desired plateau rate (1201.01 MMscf/day) was recognized in year 2023.

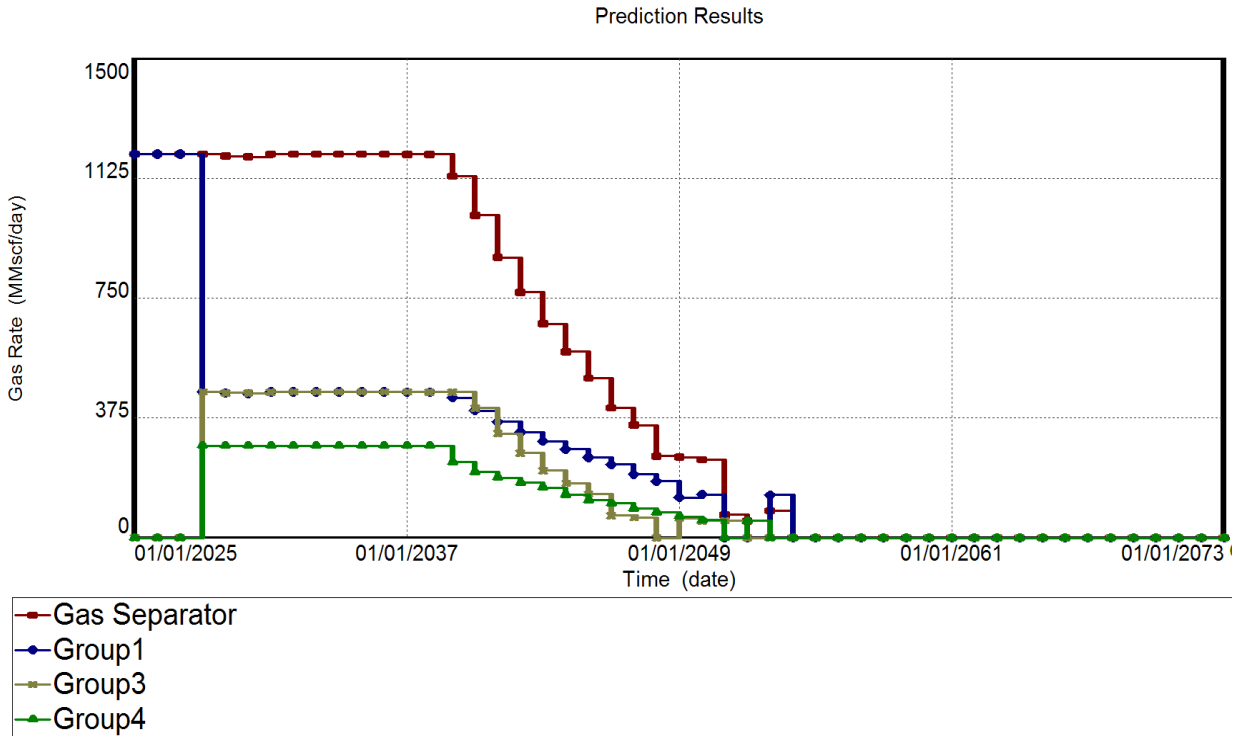

Figure 62- Prediction results for 2 LNG trains, Case One, 5 (a)

5.6.2 Production with 2 LNG Trains capacity for Case Four

For Case Four, all the reservoirs produce from beginning of production. The solver optimal results showed no problem on flowlines, the only modification required installation of two parallel pipes at trunkline segment “ManifoldLD to Jsep”. Each pipe should have a minimum diameter of 24 inches. The plateau length of 13 years was achieved with production of 2 LNG trains capacity using the Case Four (Figure 63). The production plateau was flat, indicating no numerical problems when this approach was applied.

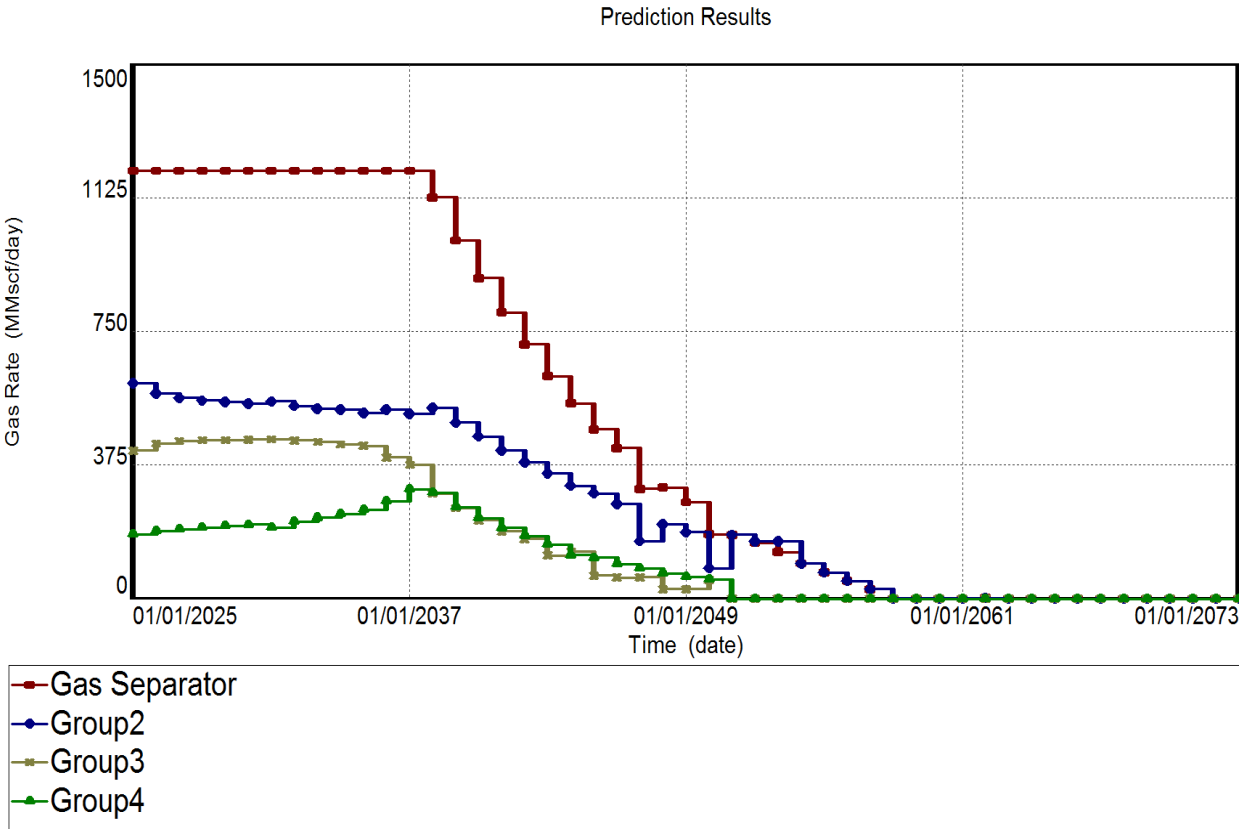

Figure 63- Prediction results for 2 LNG trains, Case Four

5.6.3 Production with higher rate (2 LNG Trains Capacity), production from four reservoirs

The two previous productions involved only three reservoirs, and their results showed the plateau lengths of less than 20 years, for LNG plant this was not practical. It was then decide to produce from four reservoirs (Zafarani, Tangawizi, Lavani Main and Lavani Deep). The four reservoirs were set to produce from the beginning of production. The configuration diameters for this production strategy are the same as that of 2 LNG trains capacity for Case One 5(d) and Case Four when combined together Figure 60. The production plateau length of 21 years was achieved after prediction run (Figure 64).

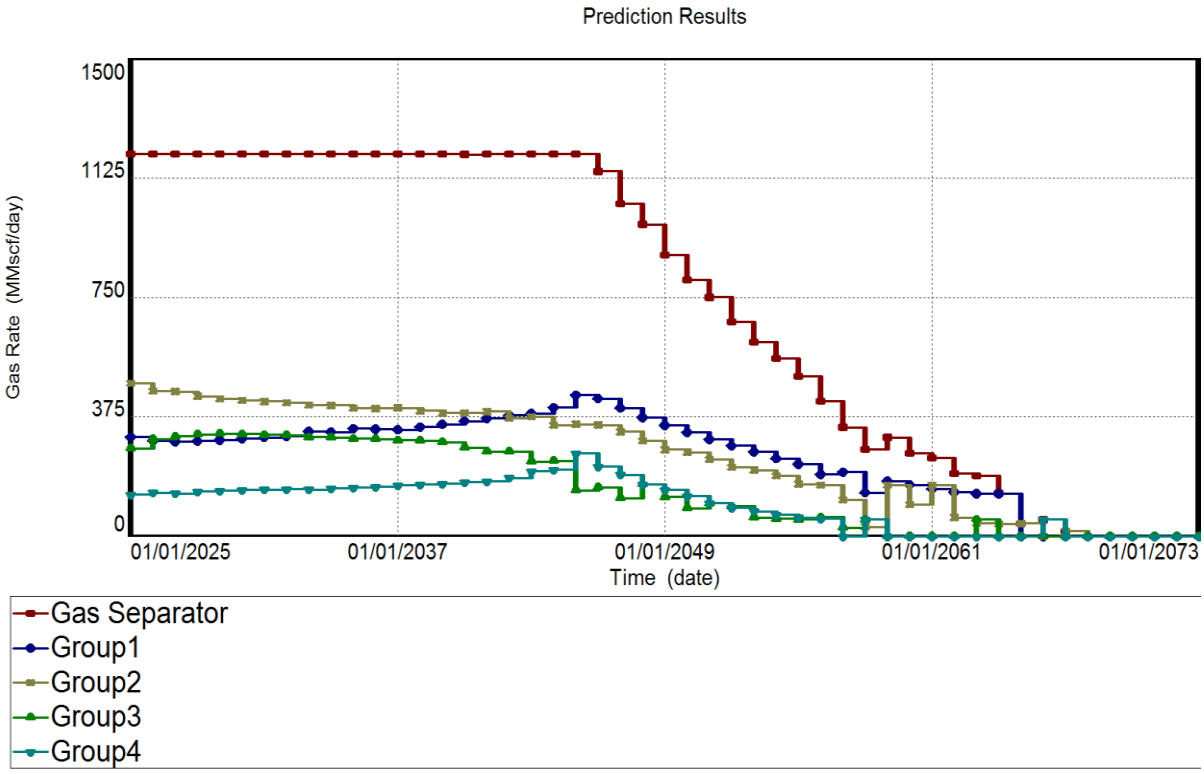

Figure 64- Prediction results for 2 LNG Trains capacity, production from four reservoirs

5.7 Economical Evaluation of the Block 2 Field

Unlike other commodities, the gas price cannot be set by seller. Therefore, economic evaluation of such natural resource is far more dependent on assets and liabilities of the company. In order to explore valuation of Block 2 field in Tanzania, few economical investigations were made based on the estimated physical quantity of plateau rate production. The economic model assumptions are the same to that applied during for prolonging of the plateau length. Two economic analysis indicators which are NPV and IRR were considered for this economic evaluation.

5.7.1 NPV as Indicator for Economic Evaluation

The estimation of present value is sensitive to the estimated gas rate and the future price of extracting gas; therefore three scenarios to perform sensitivity analysis on gas price were made. These scenarios were created with 10%, 20% and 30% higher than the initial assumed gas price ($2.78/ Mscf) for plateau extension model.

The possible outcomes on gas price sensitivity analysis for all the cases (base cases and the modified cases after natural production of plateau) are shown in Appendix 8. At this

juncture, only the best cases (Case G, Case K, Case L and Case iii of Case Four) are presented.

Table 24 illustrates the best results for the project when the field has to be modified by adding number of wells after naturel plateau production. Table 25 illustrates the economic results when the field has to be modified by adding production of either Tangawizi or Zafarani, after the natural production of plateau

Table 24-Economic results for Case G

Optional Strategy Two Increasing Number of Wells						
	10% More		**20% More**		**30% More**	
Cases	**Cum.NPV**	**% Diff.**	**Cum.NPV**	**% Diff.**	**Cum.NPV**	**% Diff.**
[-]	**[USD, Million]**	**[%]**	**[USD, Million]**	**[%]**	**[USD, Million]**	**[%]**
Base	4 002	-	4 735	0	5 439	0
Case G	4 031	0.72	4 774	0.85	5 490	0.95

Table 25-Economic results for Case K and Case L

Produce Tangawizi as Satellite Reservoir								
			10% More		20% More		30% More	
Cases	**Add Tangawizi**		**Cum.NPV**	**% Diff.**	**Cum.NPV**	**% Diff.**	**Cum.NPV**	**% Diff.**
[-]	**ManifoldLD to Jsep**	**Wells**	**[USD, Million]**	**[%]**	**[USD, Million]**	**[%]**	**[USD, Million]**	**[%]**
Case K	26''	6	4 314	4.32	5 100	4.68	5 857	4.93
Produce Zafarani as Satellite Reservoir								
			10% More		**20% More**		**30% More**	
Cases	**Add Zafarani**		**Cum.NPV**	**% Diff.**	**Cum.NPV**	**% Diff.**	**Cum.NPV**	**% Diff.**
[-]	**ManifoldLD to Jsep**	**Wells**	**[USD, Million]**	**[%]**	**[USD, Million]**	**[%]**	**[USD, Million]**	**[%]**
Case L	28''	5	4 245	6.06	5 031	6.29	5 790	6.46

Table 26 indicates the best results when the field has to be modified with subsea compression technique after the natural production of plateau.

Table 26-Economic results for Case iii of Case Four

Optional Strategy Two							
Compression							
		10% More		**20% More**		**30% More**	
Cases	**Delta_P**	**Cum.NPV**	**% Diff.**	**Cum.NPV**	**% Diff.**	**Cum.NPV**	**% Diff.**
[-]	**[psia]**	**[USD, Million]**	**[%]**	**[USD, Million]**	**[%]**	**[USD, Million]**	**[%]**
Case iii	261.1	4 115	2.82	4 863	2.74	5 584	2.68

The NPV evaluations shows that the higher the gas price the higher the NPV, and when comparing all the selected best solutions , the viable project in terms of NPV should be Case L.

5.7.2 IRR as Indicator for Economic Evaluation

The IRR was also made for the best cases (Case G, Case K, Case L and Case iii of Case Four) to evaluate yearly gain on each invested dollar. The results of IRR evaluation approach are shown in Table 27. The highest yearly earning on each invested dollar was obtained on Case K, presenting the best project to start with.

Table 27-IRR economic evaluation results

Cases	**IRR**
[-]	**[-]**
Case G	0.29
Case K	0.31
Case L	0.29
Case iii of Case Four	0.29

CHAPTER 6: Flow Assurance Evaluation

6.1 Estimation of the Maximum Flowrate due to Erosion using Prosper

The study was limited to assessing tubing erosion relatively to the producing well rate. The results from all wells (Zafarani, Tangawizi, Lavani Main and Deep wells) showed that for any well producing a gas rate above 422.295 MMscf/day, erosion will occurs in the tubing. This can clearly be illustrated using in the IPR versus VLP plot for Lavani Deep wells (Figure 65). When comparing this rate with the rates that has been produced in Case One 5(d) and Case Four (Table 28), the well gas rate of 422.295 MMscf/day is extremely higher and unlikely to occur.

Table 28-Maximum gas rate production from producing wells for Case One 5(d) and Case Four

Case One 5(d)		**Case Four**	
Wells	**Maximum Flowrate**	**Wells**	**Maximum Flowrate**
[-]	**MMscf/day**	**[-]**	**MMscf/day**
Z_1	169.81	T_1	63.69
Z_2	133.65	T_2	63.69
Z_3	144.92	T_3	63.69
Z_4	131.02	T_4	63.69
Z_5	194.70	T_5	63.69
LM_1	154.05	T_6	63.69
LM_2	242.55	LM_1	57.14
LM_3	241.70	LM_2	57.14
LM_4	199.78	LM_3	55.00
LD_1	152.36	LM_4	55.00
LD_2	152.36	LD_1	114.68
-	-	LD_2	114.68

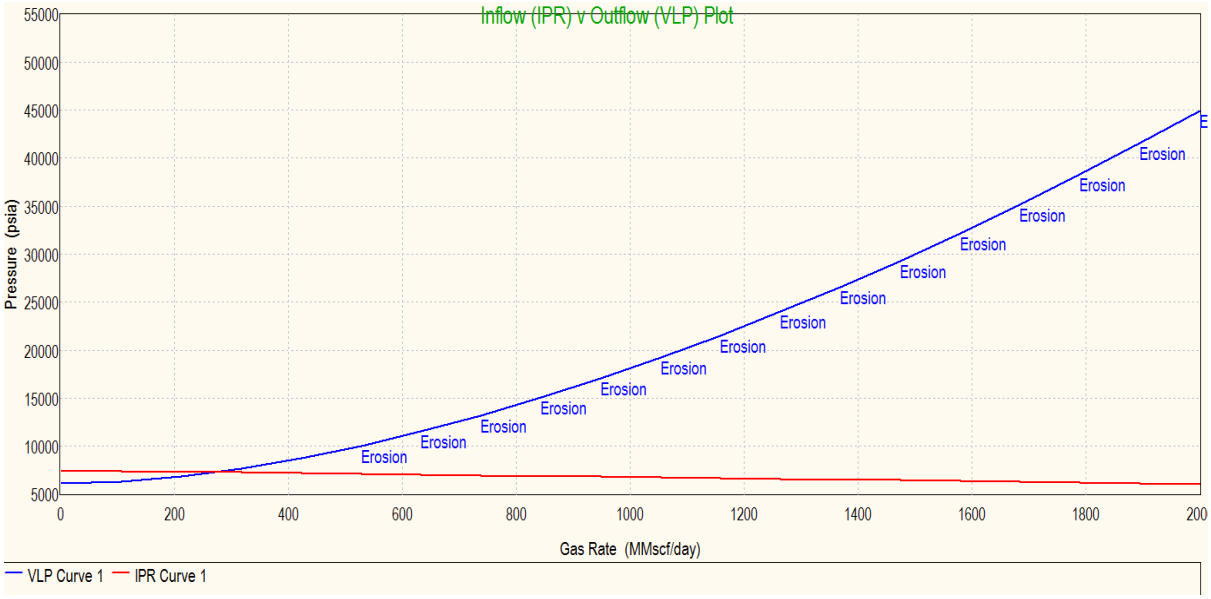

Figure 65-IPR versus VLP curves for Lavani Deep wells depicting erosion status of the well

6.2 Study on Temperature, Pressure, Flow Pattern and Simplified Hydrate Formation Analysis in the Main transportation pipeline to Shore using HYSYS

The aim of HYSYS was to evaluate details of multiphase flow in the main transportation pipeline such as: temperature, pressure, liquid holdup, and flow pattern distribution and also to assess hydrate formation from the results obtained in GAP.

Cases considered for the evaluation were Optional Strategy One and Optional Strategy Two when producing with the field plateau rate designed for 1 LNG train capacity.

The HYSYS setup model (Figure 66) was single pipeline connected to the separator; together with single pressure adjust to change inlet pressure of the pipeline to obtain the separator pressure equal to 30 bara (435.1 psia) after imposing the molar flow. The molar flow was obtained by converting the field plateau rate of 635.6 MMscf/day (18E+6 Sm3/day).

Conversion from Sm3/day to Kg-mole /hr can be expressed as

$$\dot{n}_g = \frac{\dot{q}_g}{24RT_{sc}p_{sc}}$$

Where $\dot{n}_g$=molar flow, Kg-mole/hr; $\dot{q}_g$ =volume flow (plateau rate), Sm3/day; R=universal gas constant, m^3 bara/K kg-mole; T_{sc}= absolute temperature at standard conditions, K; p_{sc}=pressure at standard conditions, bara.

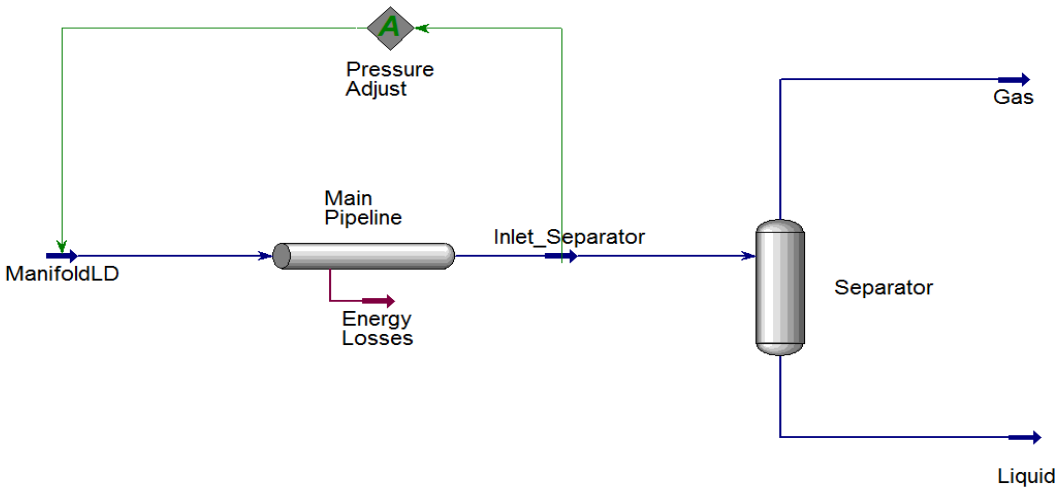

Figure 66-HYSYS model for flow assurance analysis

HYSYS model required specification of inlet conditions (temperature and pressure), gas compositions, pipeline parameters (elevations, lengths and diameters) and molar flow. All the input data used for HYSYS model were the same to the corresponding data used in GAP simulations. Detailed information for HYSYS input data is given in Appendix 10. The following assumptions were made for HYSYS model

- The gas compositions for Songo Songo were used (Appendix 2).
- The pipeline outer diameter was assumed to be 3.3 inches more than inner diameter
- The pipeline length was approximately 90.1 Km (from ManifoldLD to the Separator)
- The overall heat transfer coefficient was assumed to be 1.5 W/m^2/°C
- The predictive model used Peng Robinson(PR) property method
- The horizontal pipeline flow correlation used Beggs and Brill (1973)

6.2.1 Inlet conditions specifications

In realistic, these specifications should be treated in yearly basis. But, for simplicity and based on the results from GAP simulations. The following methods and assumptions were used to find the approximate conditions.

a) Optional Strategy One (Case One 5(d))

Figure 67 depicts the temperature and pressure results at ManifoldLD when Optional Strategy One was used. This data was taken from the previous section (GAP simulations). Pressure values at the junction were almost the same for all plateau production years. The temperature showed the same values of 29.18 ℃, during initial plateau production from Zafarani reservoir only. When production of three reservoirs began the temperature rose to the average value 37.71 ℃ with the small change happening in the 20 year of production, this small change was assumed to be noisy data and it was ignored by user.

Therefore, the pressure values were averaged and fixed to 60.45 bara, and two cases depending on the temperature values were made for flow assurance evaluation ((1) temperature=29.18 ℃, and (2) temperature=37.71℃).

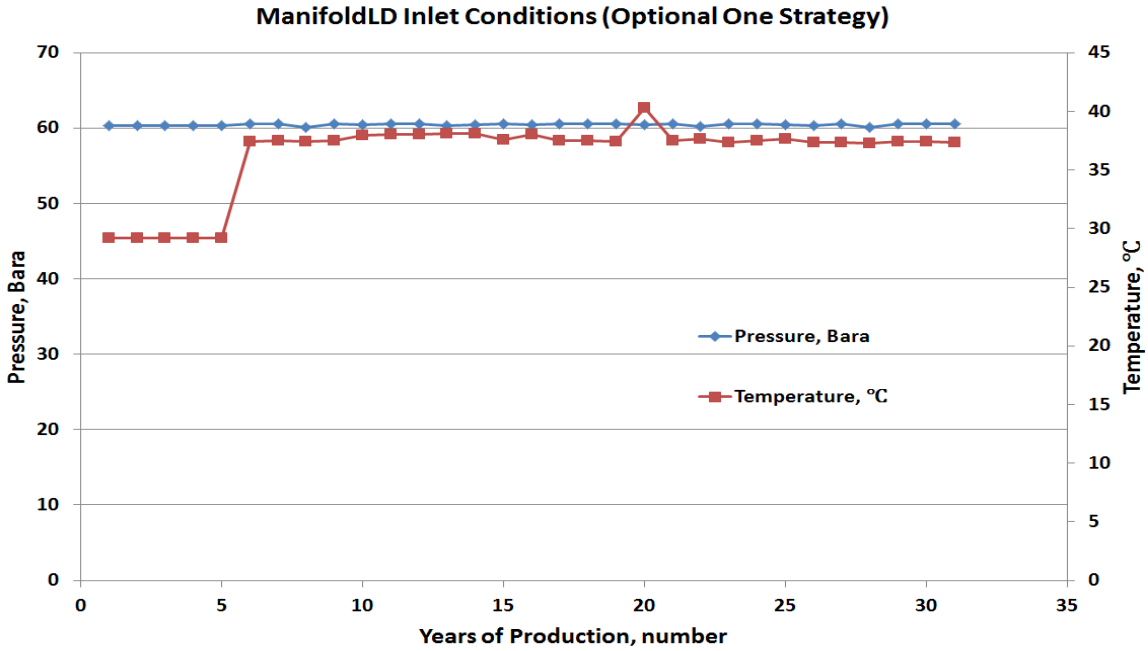

Figure 67- Temperature and pressure at ManifoldLD for Optional Case One Strategy

b) Optional Strategy Two (Case Four)

As illustrated in Figure 68, the pressure at the junction was nearly the same for all production years, and the temperature values appeared to increase gradually with the increase in production years.

Again, two cases were made for flow assurance evaluation of Optional Strategy Two, whereby the pressure values were averaged and fixed to 60.60 bara for all cases while the temperature value (38.7 ℃) for the first year of production and the temperature value (41.01 ℃) for the last year of production were selected for analysis. The summary of all cases created for flow assurance evaluation were given in Table 29.

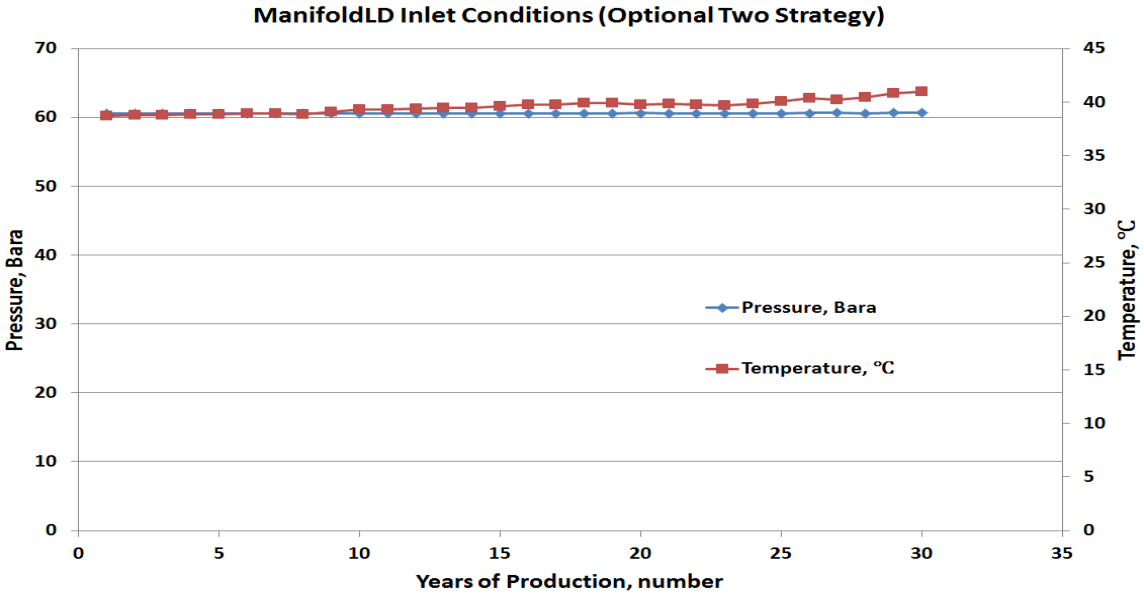

Figure 68- Temperature and pressure at junction ManifoldLD for Optional Case Two Strategy

Table 29- Summary of the HYSYS simulation Cases

Cases	**Production Strategy**	**Inlet Pressure**	**Inlet Temperature**
[-]	**[-]**	**[bara]**	**[℃]**
First Case	Optional Strategy One	60.45	29.18
Second Case	Optional Strategy One	60.45	37.71
Third Case	Optional Strategy Two	60.60	38.70
Fourth Case	Optional Strategy Two	60.60	41.01

6.2.2 Analysis of the HYSYS Results

6.2.2.1 Inlet Conditions

For all cases, the initial inlet junction pressures from GAP results did not show convergence to the pipeline system due to negative pressure calculated in pipe segment of the main pipeline, as the result of inaccuracy of Beggs and Brill Acceleration Pressure Drop model under the given conditions. In order to fix this, a bit high pressure of around 75 bara had to be used.

This could be because the pressure drop correlation employed in HYSYS (Beggs and Brill) was different than the one employed in GAP (Mukherjee Brill). This can be also taken as the comparison point, since no method exists for performing these calculations accurately for all conditions. However, Beggs and Brill method appear to be the best with the lowest error of 14% according to (Behnia, 1991).

6.2.2.2 Pressure Drop in the Main Pipeline

During simulation runs, the inlet pressure was adjusted while constraining the separator pressure equal to 30 bara. The pressure drops and the adjusted inlet pressure of main pipeline are depicted in Table 30.

The main transportation pipeline pressure drops for all cases showed a slightly difference. But, HYSYS pressure drops were higher than the pressure drops obtained using GAP.

Table 30-Pressure Drops Comparison

Cases	**Production Strategy**	**Inlet Pressure**	**Pressure Drops (HYSYS)**	**Pressure Drops (GAP)**
[-]	**[-]**	**[bara]**	**[bara]**	**[bara]**
First Case	Optional Strategy One	72.56	42.52	30.45
Second Case	Optional Strategy One	72.83	42.75	30.45
Third Case	Optional Strategy Two	72.86	42.81	30.61
Fourth Case	Optional Strategy Two	73.21	43.11	30.61

6.2.3 Discussions of the Observations for all Cases

The following general observations were made in all cases.

6.2.3.1 Pressure Profiles

As illustrated in Figure 69, pressure decreased with distance along the main transportation pipeline. This phenomenon was probably associated with friction inside the pipe and gravitational acceleration as the consequence of pipeline elevations. For different inlet temperatures, the pressure profile showed slight differences, suggesting that the inlet temperature does not significantly affect the pressure drop along the pipeline.

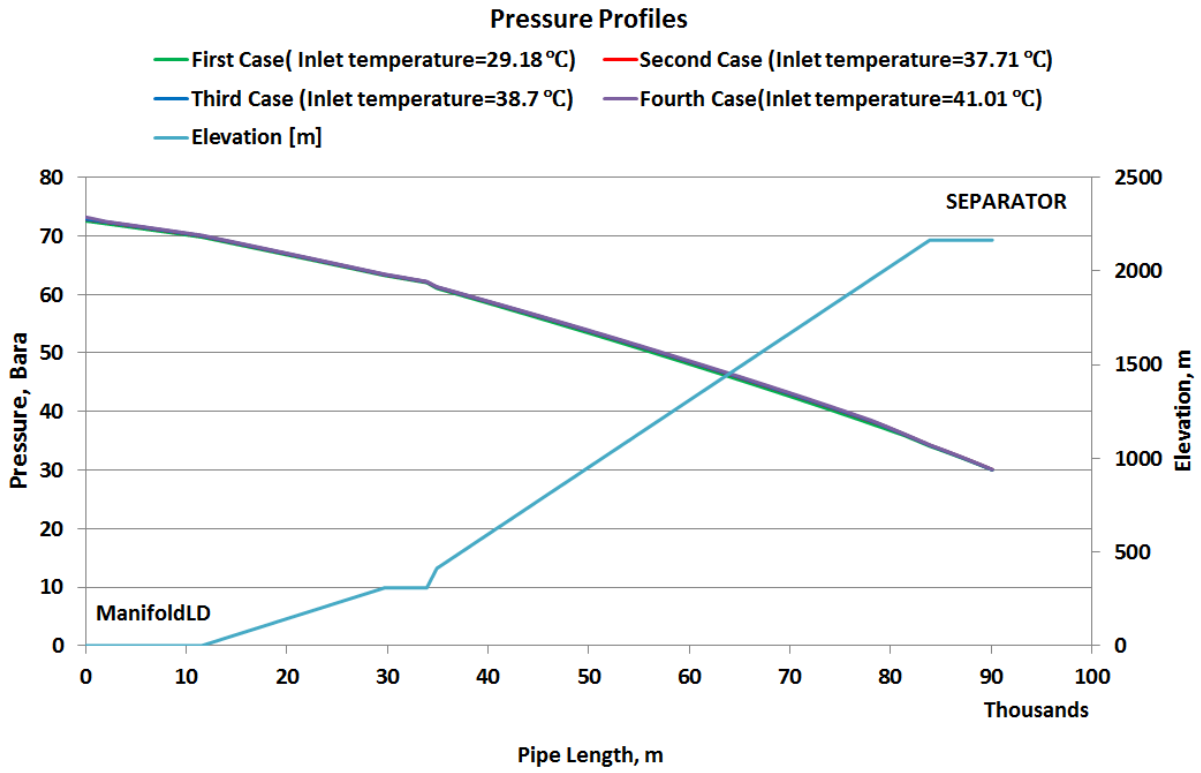

Figure 69-Pressure profile along the main pipeline

6.2.3.2 Temperature Profiles

As shown in Figure 70, temperature dropped with the distance due to heat exchange of the environment (sea) and pipe, and the drops became even quicker with sharp elevations. The strong temperature drop was recognized at the end part of the pipeline, where the temperature drop went below the temperature of the surroundings as the

consequence of Joule-Thompson effect. It could also be suggested that, the Joule-Thompson effect could be eliminated by increasing temperature of the pipeline. This can be easily seen when the inlet temperature was higher the Joule Thompson effect was delayed.

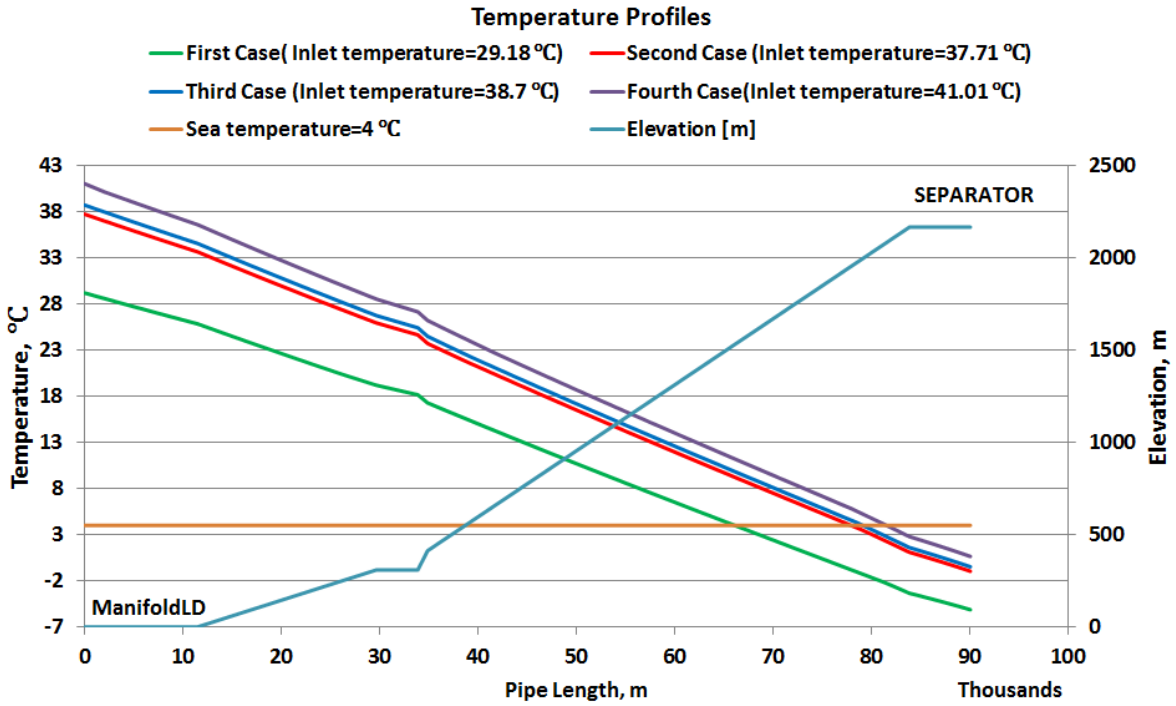

Figure 70-Temperature profiles along the main pipeline

6.2.3.3 Pressure, Temperature and Liquid Holdup

Figure 71 illustrates how the liquid holdup increased with temperature and pressure drops along the main transportation pipelines. This was influenced by mass transfer between the moving fluids, as the liquid drops out from gas phase when the temperature and pressure dropped below the hydrocarbon (gas) dew point.

Figure 71 shows the results for the first case when the temperature at the inlet pipeline junction was 29.18 °C. The figures for the rest cases were appended in Appendix 10. The nature of the plots was the same and the above descriptions apply for all cases.

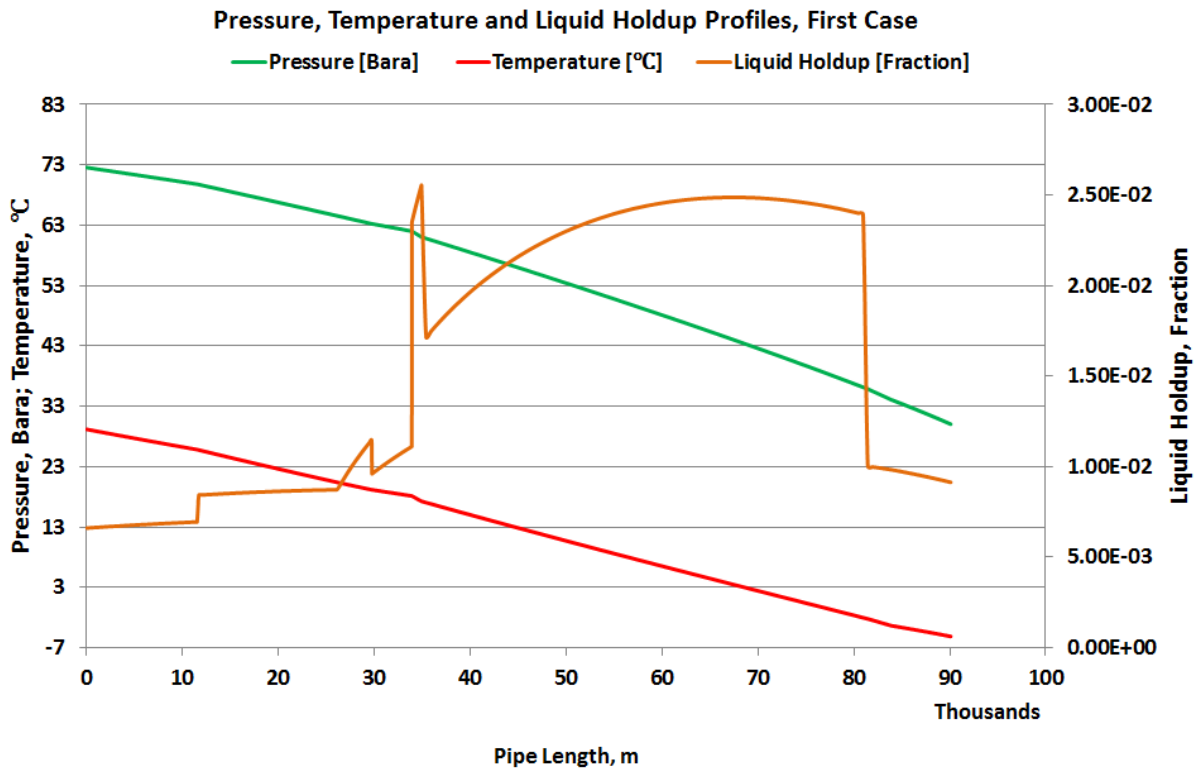

Figure 71-Pressure and temperature effects on liquid holdup

6.2.3.4 Liquid Holdup Profiles

The pipeline flow was characterized with low liquid loading to the maximum of 0.0256 fraction of liquid holdup as illustrated in Figure 72. For horizontal pipeline section, the liquid holdup increased with the distance, this was because of the flow dynamics of the phases as the gas moved faster than liquids. For uphill sections, it should be expected that the liquid holdup would be less since the liquid is denser than gas and should have been held back, but the abnormal situations were probably due to heat transfer mechanism between phases being dominant than the flow dynamics of the phase. However, normal situation can be depicted at the pipeline segment between approximately 37E+3 to 84E+3 metres. At this segment, the liquid holdup decreases with the long elevated distance indicating that the liquid was held back.

Furthermore, the liquid holdups become less with increase of temperatures; this suggested less gas condensation occurred with temperature increase.

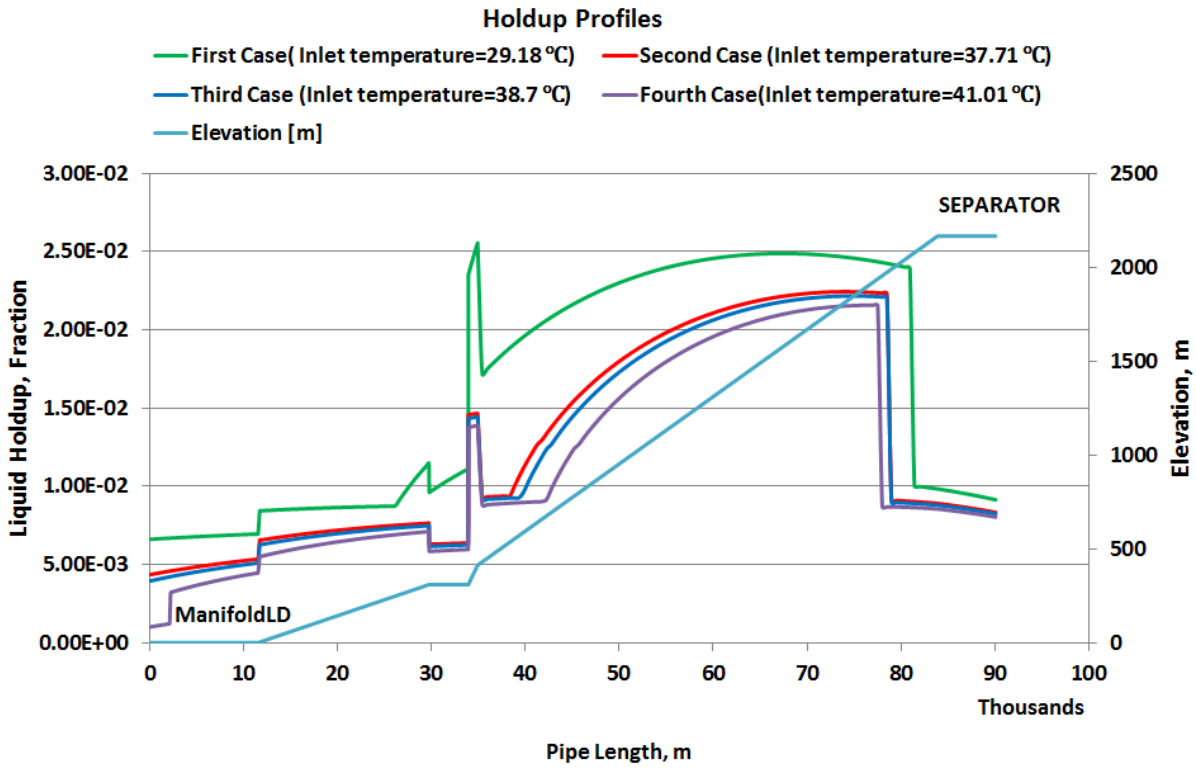

Figure 72-Elevation effect on liquid holdup

6.2.3.5 Hydrate Formation

The main transportation pipeline indicated presence of Type II hydrate formation for all cases. The formation conditions (pressures and temperatures) are shown in Table 31; these conditions are the conditions above which the hydrate Will NOT Form. Hydrate formation was delayed when pressure in the pipeline was higher. Additionally, the hydrate formation was severe for low temperatures cases (first, second and third cases) which indicated formation of solid particles ice pellets.

Table 31-Hydrate formation pressure and temperature with respective pipeline lengths

Cases	Inlet Temperature	Distance	Hydrate Formation Pressure	Hydrate Formation Temperature
[-]	[℃]	[m]	[bara]	[℃]
First Case	29.18	5 0580	53.11	10.46
Second Case	37.71	6 6750	44.83	8.95
Third Case	38.70	6 8220	44.05	8.90
Fourth Case	41.01	7 2140	41.97	8.47

Graphically, hydrate formation conditions are depicted in Figure 73 and Figure 74 for the first case when the temperature at the inlet pipeline junction was 29.18 °C. The Type II hydrate formation is indicated after line intersections, where the temperature was lower than the hydrate formation temperature. The figures for the rest cases were appended in Appendix 10. The nature of the plots was same for all cases.

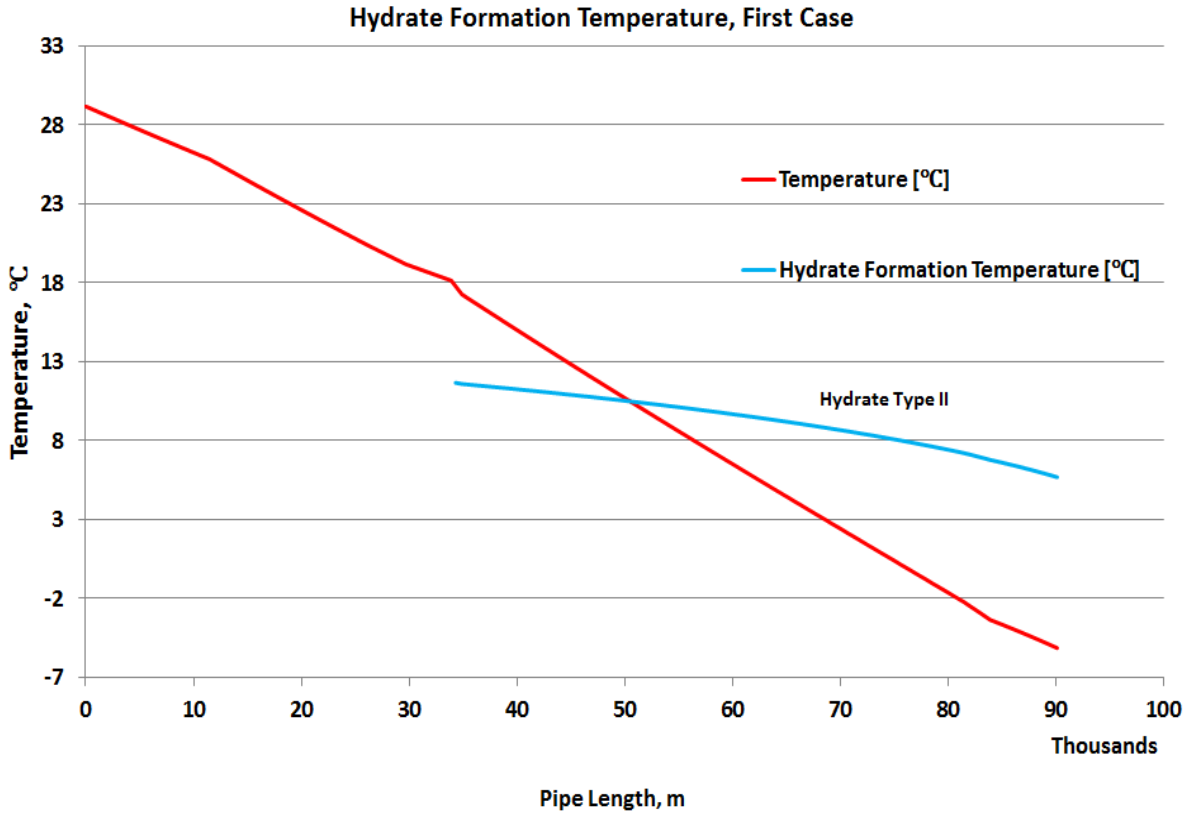

Figure 73-Hydrate formation temperature in the main transportation pipeline (inlet temperature=29.18°C)

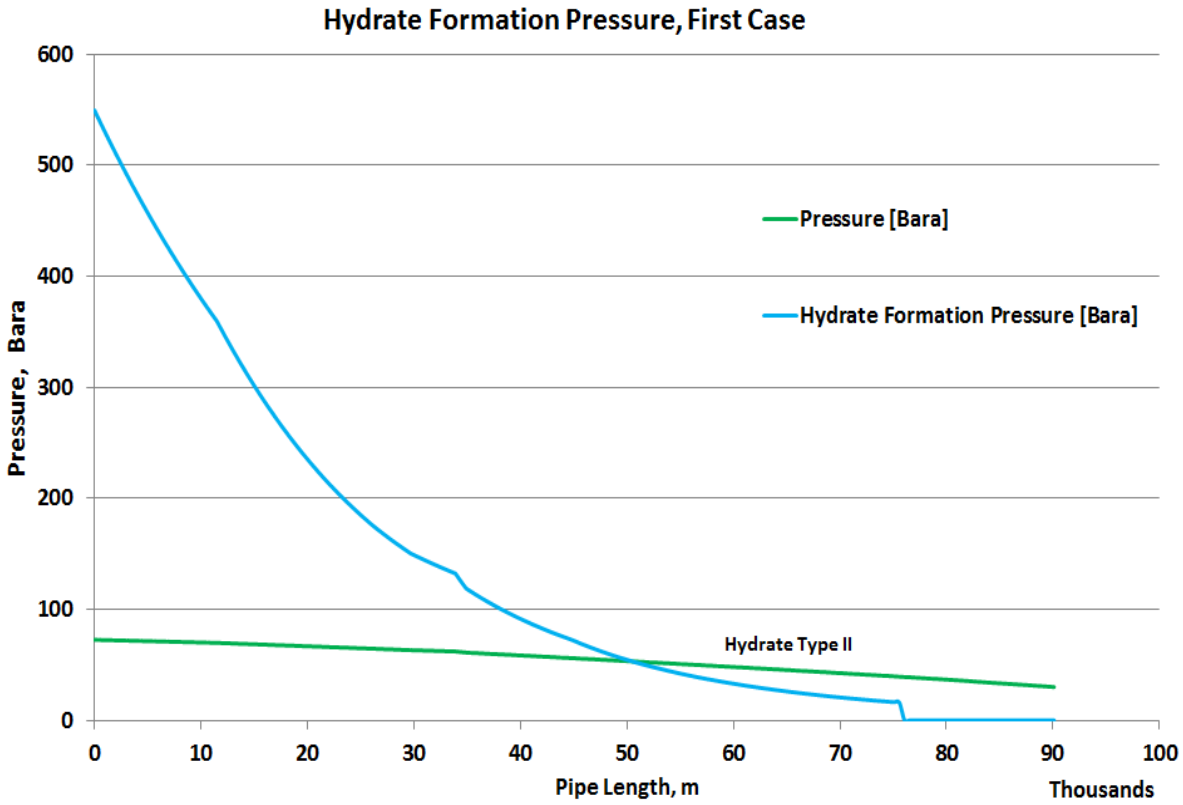

Figure 74- Hydrate formation pressure in the main transportation pipeline (inlet temperature=29.18°C)

6.2.3.6 Flow Pattern

The flow pattern chances from segregated to distributed flow along the pipeline.

6.2.4 Inhibition of Hydrate Formation

There number of available options to avoid formation of hydrates. For example, the operating conditions can be set to be outside the predicted equilibrium curves for hydrate, or injection inhibitor such as glycols or alcohols to suppress hydrate formation. In this analysis, chemical inhibition was suggested. Two different chemical inhibitors which are methanol (MeOH), Triethylene glycol (TEG) were assessed.

The HYSYS model in Figure 66 was modified to included inhibitor solvent stream and the mixer to combine the inhibitor solvent stream and Process (hydrocarbon) stream as presented in Figure 75. For fast simulation time, another pressure adjust (pressure adjust-2) was included to adjust the inhibitor injection stream while honouring separator pressure equal to 30 bara.

Inhibitor injection stream conditions were sufficiently defined. The temperature and pressure were same as that of hydrocarbon stream. The inhibitor stream was assumed to contain inhibitors mass fraction of one (1).

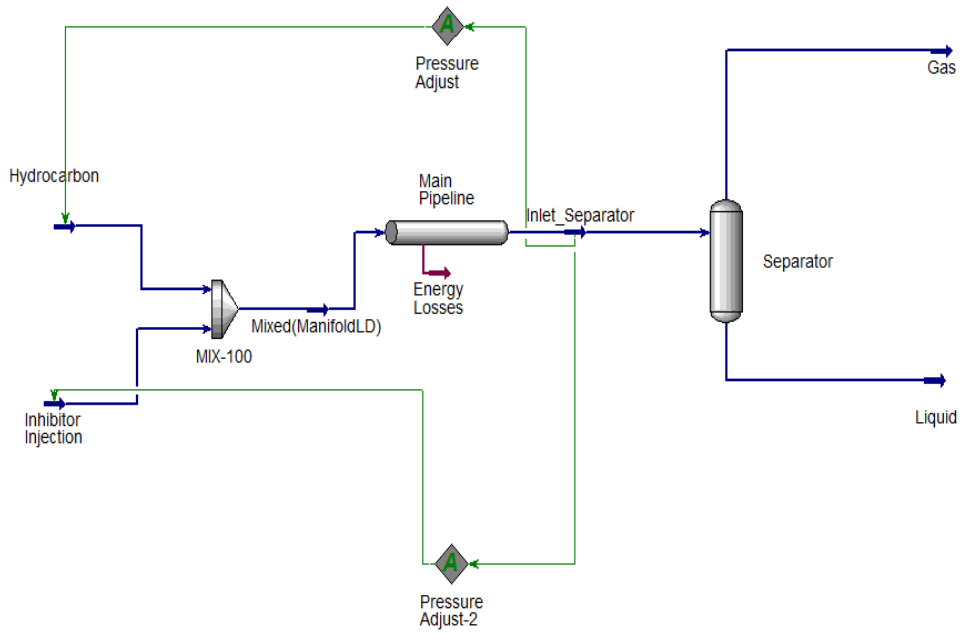

Figure 75- Aspen HYSYS V8.3 flow assurance model including inhibitor injection stream

Since Aspen HYSYS V8.3 was used for analysis, in order to obtain the minimum inhibitor required to suppress hydrate from forming at the specified conditions, guess-estimating of the mass flowrate to the inhibitor was done while observing the yielded results. With Aspen HYSYS V8.8, the minimum inhibitor required to suppress hydrate from forming can be easily done, since it contains "Hydrate Suppression" group which allows selection of the inhibitor used, and gives the recommended amount of hydrate inhibitor required to suppress formation of hydrates.

The obtained minimum amount of inhibitors required to suppress hydrate formation are presented in Table 32. The extent of suppression for the case with first case (inlet temperature=29.18) are presented in Figure 76 & Figure 77 for MeOH injection, and Figure 78 & Figure 79 after TEG injection. The figures of the rest cases can be viewed in Appendix 10.

Table 32-Minimum inhibitor required to suppress hydrate formation in the main pipeline

Cases	Methanol	TEG
[-]	[kg/s]	[kg/s]
First Case	0.226	1.704
Second Case	0.364	1.704
Third case	0.360	1.720
Fourth Case	0.076	1.784

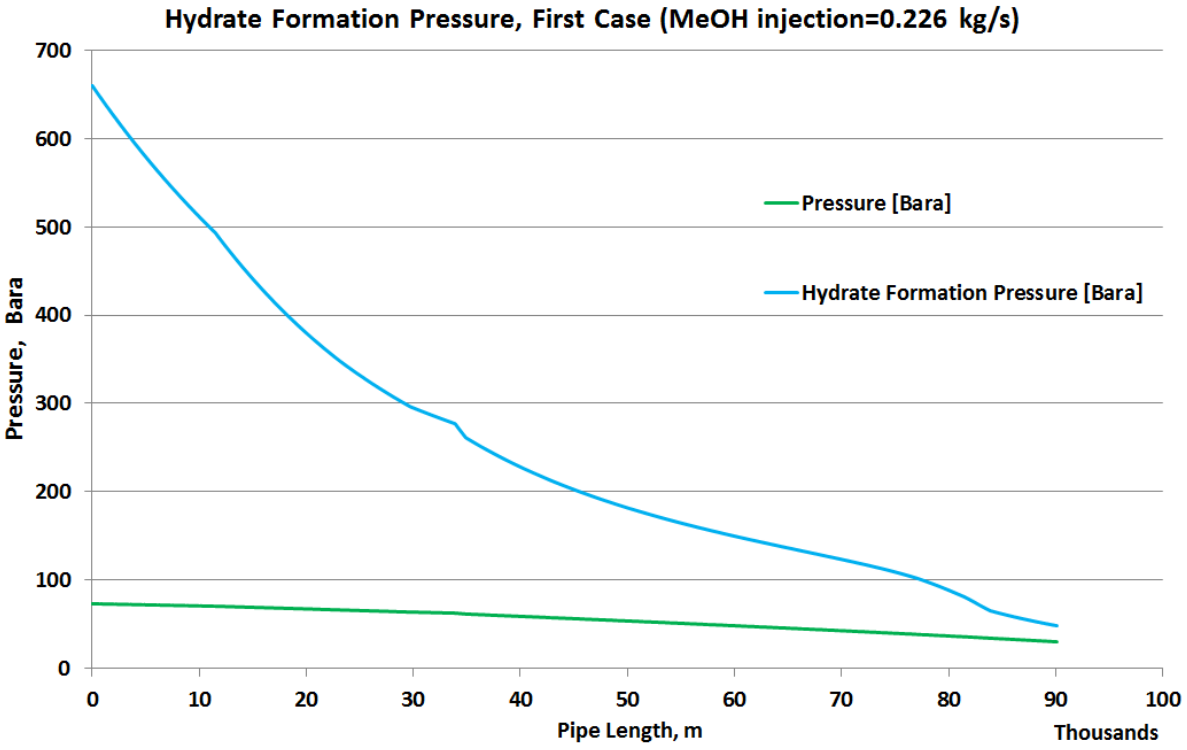

Figure 76-Hydrate formation pressure after MeOH injection at 0.226 kg/s

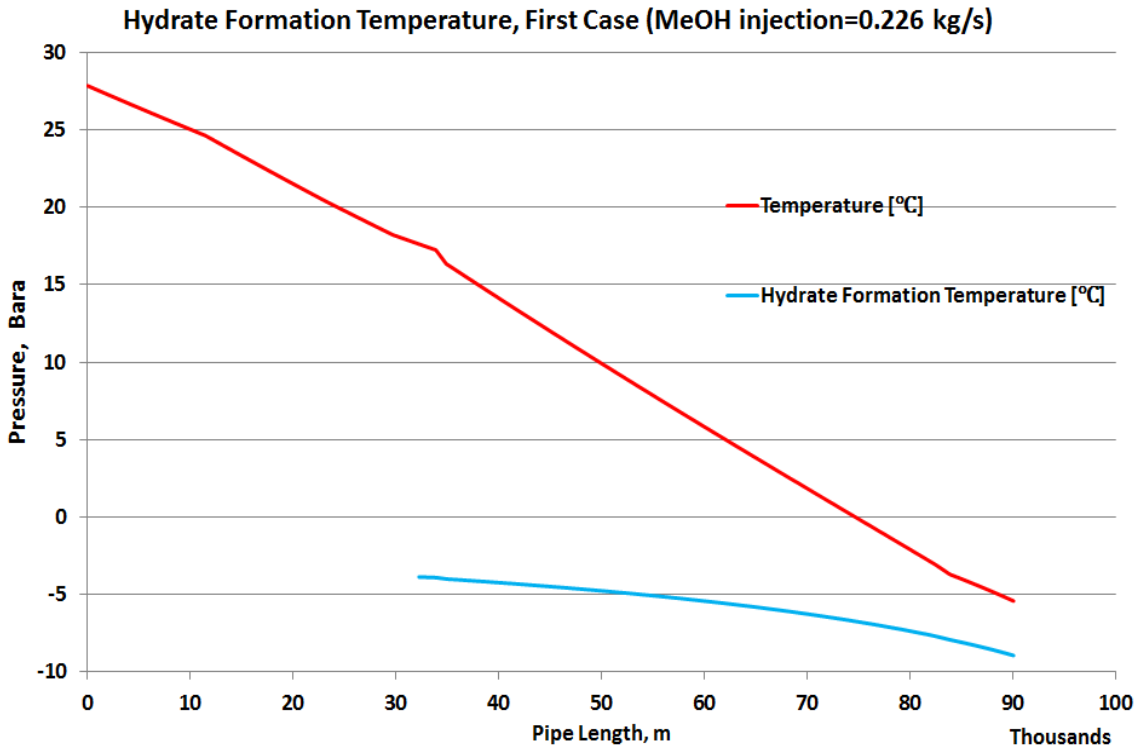

Figure 77- Hydrate formation temperature after MeOH injection at 0.226 kg/s

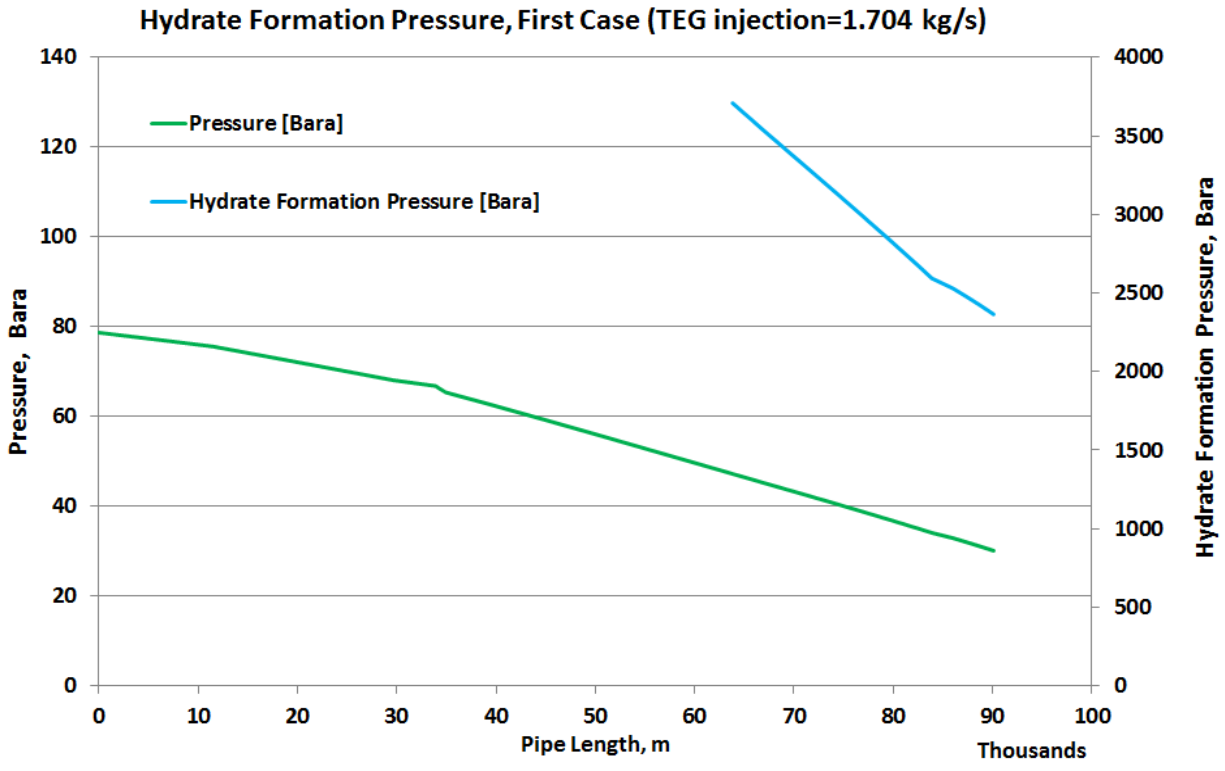

Figure 78- Hydrate formation pressure after TEG injection at 1.704 kg/s

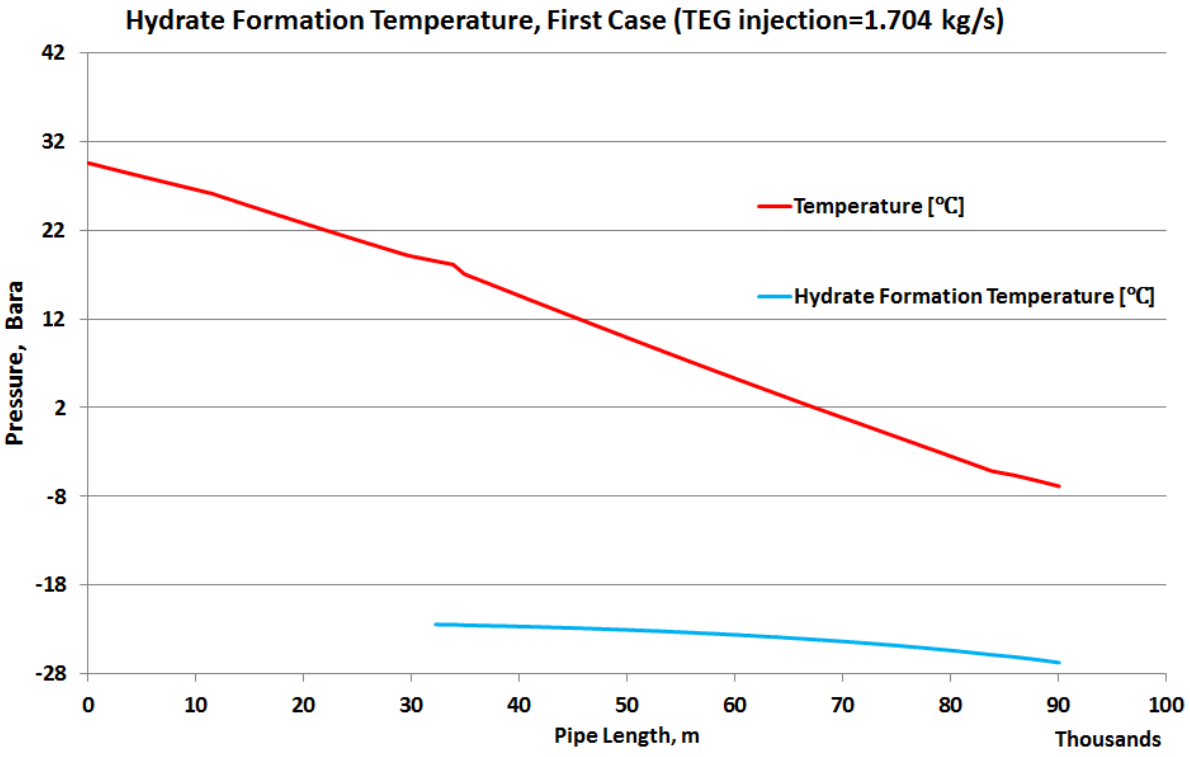

Figure 79- Hydrate formation temperature after TEG injection at 1.704 kg/s

Chapter 6: Conclusion and Recommendation

6.1 Conclusion

The objective of this study was to perform field development studies on an offshore Tanzania gas asset using reservoir and surface network simulations. The specific objectives and their results are explained below.

6.1.1 Numerical Models using Data available in Public Domain

Reasonable assumptions were used, and then numbers of sensitivity analyses were made to develop the reservoir and production system models. After implementation of these models, one of the attractive production strategies (Case One 5(d)) approximately resembled to Statoil production strategy proposed in (Holm, 2015) with only significant difference of 2 years of initial production from Zafarani reservoir. This model might be applied in different cases due to its reasonable results.

6.1.2 Plateau Production Profile

Plateau production profile represented the period of gas production with relatively flat gas production rate. In this study, the plateau production profile was determined using MBAL, PROSPER and GAP software. The conclusion of the results is presented below

a. Two most attractive production plateau profiles were obtained which are Optional Strategy One and Optional Strategy Two. Optional Strategy Two provided converged model by producing a flat field production plateau while Optional Strategy One provided the model which did not fully converge, for example, the field rates in some timesteps was lower than the desired target rate. However, the results obtained were reasonable and presentable.
b. With 1 LNG train Capacity, the production plateau length of Optional Strategy One yielded 31 years of field production plateau rate of 635.6 MMscf/day, and its initial production plateau length from Zafarani reservoir was 5 years. Optional Strategy Two yielded 30 years with the same field production plateau rate with all reservoirs producing from the beginning of production.
c. With 2 LNG trains Capacity, some modifications on the pipelined configurations were made. 2 LNG capacity required installation of two parallel pipelines each with 24 inches diameter. Also, when producing with Optional Strategy One, the

diameter of flowline from Zafarani wells to the trunkline should be 16 inches instead of 12 inches. In terms of plateau length, Optional Strategy One produced the field plateau length of 14 years with the initial plateau from Zafarani reservoir being 3 years. Optional Strategy Two produced the field plateau length of 13 years with all reservoirs producing from the beginning of production.

d. When all four reservoirs (Tangawizi, Zafarani, Lavani Main and Lavani Deep) were considered for the production with 2 LNG trains capacity; 21 years of natural production plateau length was achieved.

6.1.3 Prolonging the Production Plateau

Prolonging the production plateau ensures additional recovery from gas reservoirs after natural depletion of the reservoir. Conclusion of investigated techniques to prolong the plateau are presented below

a. When investigating the well addition techniques to prolong the plateau, the well expenditures were higher than profit for the Optional Strategy One. For the Optional Strategy Two, maximum of two wells could be added to the production system to provide additional cumulative NPV of 0.53% with the ultimate recovery factor of 0.74.
b. By using fixed Delta _P compression method, Optional Strategy Two revealed optimal subsea compression technique to prolong the plateau, which required installation of two parallel subsea compressors each having the Delta_P of 261.1 psia and compression power of 3.9 Megawatts. This strategy also provided the ultimate recover factor 0.77. However, with the developing technology it is possible to use a single compressor with compression power of 7.7 Megawatts (which approximately doubles the power of two suggested parallel compressors).
c. The overall best option to prolong production plateau was obtained when producing with Zafarani as a satellite reservoir after natural plateau production from Optional Strategy Two. The added cumulative NPV of 5.55% and ultimate recovery factor of 0.7 were achieved.

6.1.4 Flow Assurance Analysis

Flow assurance will ensure economical and technical feasible way of producing multiphase flow from the reservoir to the separator. The following conclusion was made on flow assurance analysis

a. Using PROSPER, it was observed that erosion will occur when the well production rate is above 422.295 MMscf/day. This well rate was extremely higher compared to the well production rates of Case One 5(d) and Case Four. This signified that, tubing erosion will not occur during production life of the reservoir unless sand production occurs
b. HYSYS simulation results indicated low liquid loading to the maximum of 0.0256 fraction of the liquid holdup. Type II hydrates were also detected, and inhibition was done by injecting MeOH and TEG.

Generally, each production strategy conducted in this study has its own advantage and disadvantages either economically or technically. Optional Strategy One provided a longest production plateau length but it is not economical in prolonging plateau using addition of wells technique. Optional Strategy Two gave better results in prolonging the production plateau using the techniques applied in this study. However, the overall best option to prolong production plateau was obtained when producing with Zafarani as a satellite reservoir after natural plateau production from Optional Strategy Two.

6.3 Recommendations

a. It is recommended that, more studies should be done in the reservoirs using simulator which includes spatial variations and anisotropy, for example Eclipse.
b. Real data should be used rather than calculations and assumptions to compare the results. However, the approach used and results obtained in this context might be significant in academic use and industry.
c. It is recommended that more studies to assess if the produced rate does not cause sand production or damage to the formation.
d. Field development studies assumed steady state production system. This is not always the case since unsteady state conditions might happen in the production system. Therefore, more studies should be performed using the transient flow dynamics software, for example, studies of “Large Scale Low Liquid Loading

Two-phase Flow Tests (SINTEF)" and "Tanzania Core Model Evaluation and Flow Assurance Risk Study" (Schlumberger SPTC) presented in (Holm, 2015).

Appendices

Appendix 1- Estimated parameters for Block 2 Field

a. Table of parameters

			Zafarani	Lavani Main	Lavani Deep	Tangawizi	Mronge	Mdalasini	Piri	Girigiliani	Total Block 2
Reservoir	Reservoir Fluid Type	Units	Dry Gas	Dry Gas	Dry Gas	Dry Gas	Dry Gas	Dry Gas	Dry Gas	Dry Gas	Dry Gas
	IGIP	Tcf	6.00	3.00	2.00	4.00	2.00	1.80	2.00	1.20	22.00
	Reservoir Pressure	psi	6019.08	5206.86	7541.98	4061.06			7687.01		
	Reservoir Pressure	bar	415.00	359.00	520.00	280.00			530.00		
	m(p)	bara2/cp	9.09E+06	7.60E+06	1.19E+07	5.48E+06			1.22E+07		
	m(p)	psi2/cp	1.91E+09	1.60E+09	2.50E+09	1.15E+09			2.56E+09		
	Reservoir Temperature	˚F	156.20	140.00	157.84	127.30			163.63		
		R	616.87	600.67	618.51	587.97	460.67	460.67	624.30		
	Measured Depth	ft	16896.33	11604.33	17290.03	9940.94			18684.38		
	Water Depth	ft	8471.13	7874.02	8464.57	7545.93			7742.78		
	Gas Gravity	[-]	0.57	0.57	0.57	0.57			0.57		
	Porosity	[-]	0.23	0.26	0.22	0.28			0.20		
	Permeability	mD	100-200	500-1000	100-150	1000-1200			85-120		
	Net pay zone	ft	393.70	311.68	0.00	120.00			95.00		
	Water saturation	[-]	0.26	0.23	0.27	0.21			0.30		
	Gas saturation	[-]	0.74	0.77	0.73	0.79			0.70		
	Z	[-]	1.14	1.11	1.20	1.07			1.20		
	Bgi	cu ft/scf	0.00329	0.00361	0.00277	0.00437			0.00276		
	Drainage Area	sq. ft	295275524.54	173663563.05	#VALUE!	661992511.15			415163249.53		

	Input
	Calculated
	Input Converted(linear correlation with depth)
	Assumed
	Calculated linear interpolation

b. Net –pay model

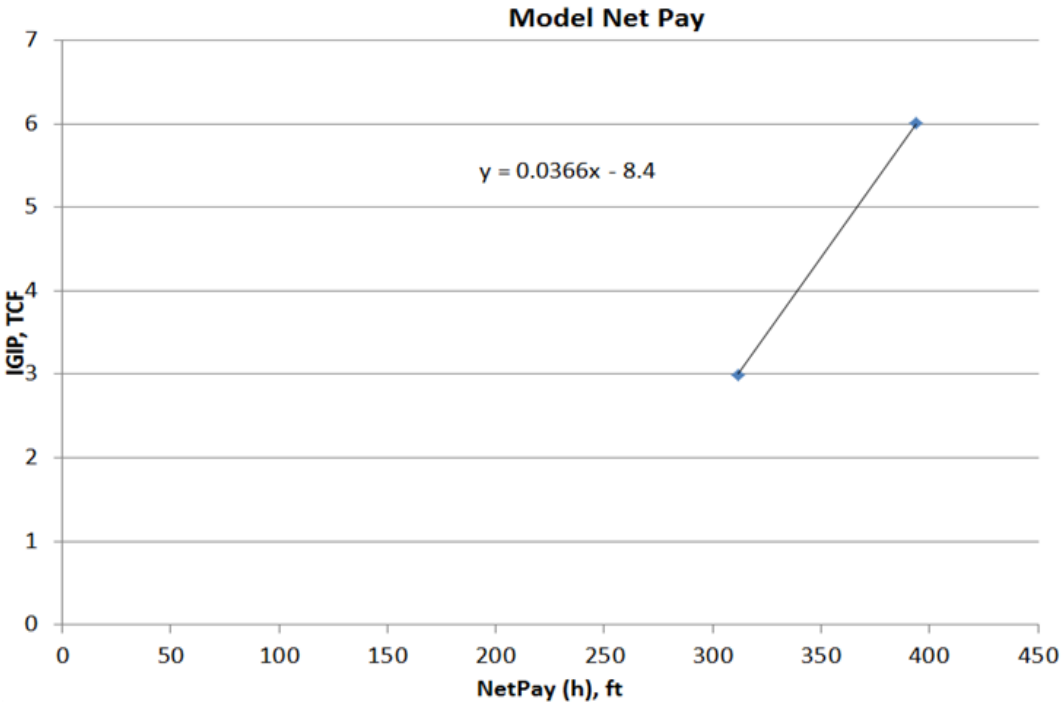

Appendix 2-Songo Songo gas compositions used for Block 2 studies (Bujulu, 2013)

Date of Sampling	**26/07/1997**	**13/03/2003**	**02/07/1997**	**26/05/1997**	**31/08/1987**	
Well	**SS-9**	**SS-3**	**SS-7**	**SS-5**	**SS-4**	**Average**
Component	**mole%**	**mole%**	**mole%**	**mole%**	**mole%**	**mole%**
N2	0.72	0.72	0.85	0.79	0.53	0.72
CO2	0.46	0.00	0.40	0.56	0.23	0.33
C1	97.34	97.74	97.16	97.14	97.35	97.35
C3	0.98	0.99	1.08	1.05	1.14	1.05
C4	0.28	0.29	0.30	0.29	0.33	0.30
i-C4	0.07	0.06	0.08	0.06	0.08	0.07
n-C4	0.09	0.08	0.07	0.08	0.11	0.09
i-C5	0.03	0.03	0.03	0.02	0.04	0.03
n-C5	0.01	0.02	0.03	0.00	0.04	0.02
C6	0.01	0.02	0.00	0.00	0.04	0.01
C7+	0.01	0.04	0.00	0.00	0.11	0.03
Total	100.0	100.0	100.0	100.0	100.0	100.0

Songosongo compositions used in HYSYS model (water fraction was assumed to be 0.0015) (Andalu, 2013)

Component	**Percentage (%)**	**Fractions**
Nitrogen	0.71	0.0071
CO2	0.37	0.0037
Methane	97	0.97
Ethane	1.03	0.0103
Propane	0.31	0.0031
i-Butane	0.07	0.0007
n-Butane	0.09	0.0009
i-Pentane	0.03	0.0003
n-Pentane	0.03	0.0003
n-Hexane	0.03	0.0003
n-Heptane	0.11	0.0011
n-Octane	0.05	0.0005
n-Nonane	0.02	0.0002
H2O	0.15	0.0015
Summation	100	1

Appendix 3-Numerical calculation of Pseudopressure functions

a. Generated PVT table for Zafarani Reservoir

							Constants	
R	83.143	cm^3bar/mol-K					A1	130.16
Mg	16	g/mol					A2	5.21
T	342.15	K	616.87	degR	69	degC	A3	1.29
S.G	0.57	-						

						a	b			
p	p	ρ	μ	Z	2p/μZ	2p/μZav	delta P	a*b	m(p)	m(p)
[bara]	[psia]	[g/cm3]	[cp]	[-]	[bara/cp]	[bara/cp]	[bara]	[bara2/cp]	[bara2/cp]	[psia2/cp]
0	0	0	0	0	0	0	0	0.00E+00	0.00E+00	0.00E+00
50	725.19	0.0281	1.37E-02	1.0	7266.77	3633.38	50	1.82E+05	1.82E+05	3.82E+07
100	1450.38	0.0562	1.48E-02	1.0	13377.11	10321.94	50	5.16E+05	6.98E+05	1.47E+08
150	2175.57	0.0844	1.61E-02	1.0	18173.22	15775.17	50	7.89E+05	1.49E+06	3.13E+08
200	2900.76	0.1125	1.78E-02	1.0	21672.45	19922.84	50	9.96E+05	2.48E+06	5.22E+08
250	3625.95	0.1406	1.97E-02	1.1	23982.76	22827.61	50	1.14E+06	3.62E+06	7.62E+08
300	4351.14	0.1687	2.20E-02	1.1	25260.54	24621.65	50	1.23E+06	4.86E+06	1.02E+09
350	5076.33	0.1969	2.47E-02	1.1	25681.46	25471.00	50	1.27E+06	6.13E+06	1.29E+09
400	5801.52	0.2250	2.79E-02	1.1	25420.47	25550.96	50	1.28E+06	7.41E+06	1.56E+09
450	6526.71	0.2531	3.16E-02	1.2	24639.50	25029.98	50	1.25E+06	8.66E+06	1.82E+09
500	7251.9	0.2812	3.59E-02	1.2	23480.97	24060.23	50	1.20E+06	9.86E+06	2.07E+09
550	7977.09	0.3093	4.10E-02	1.2	22065.43	22773.20	50	1.14E+06	1.10E+07	2.31E+09

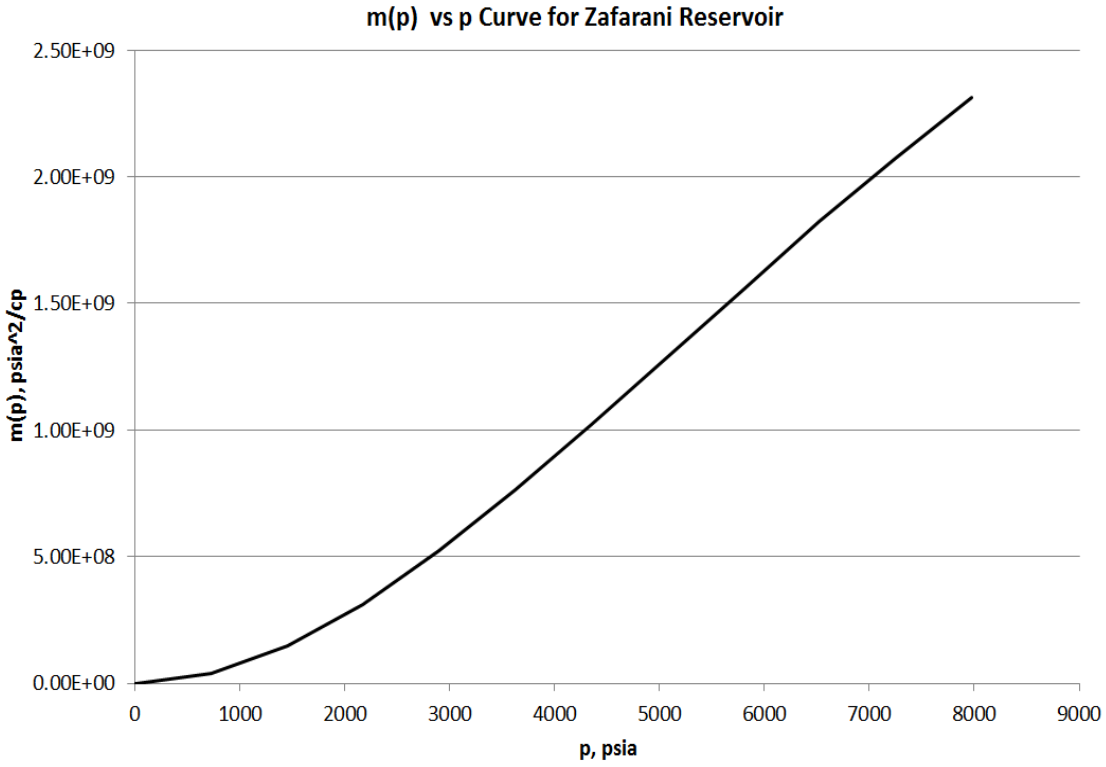

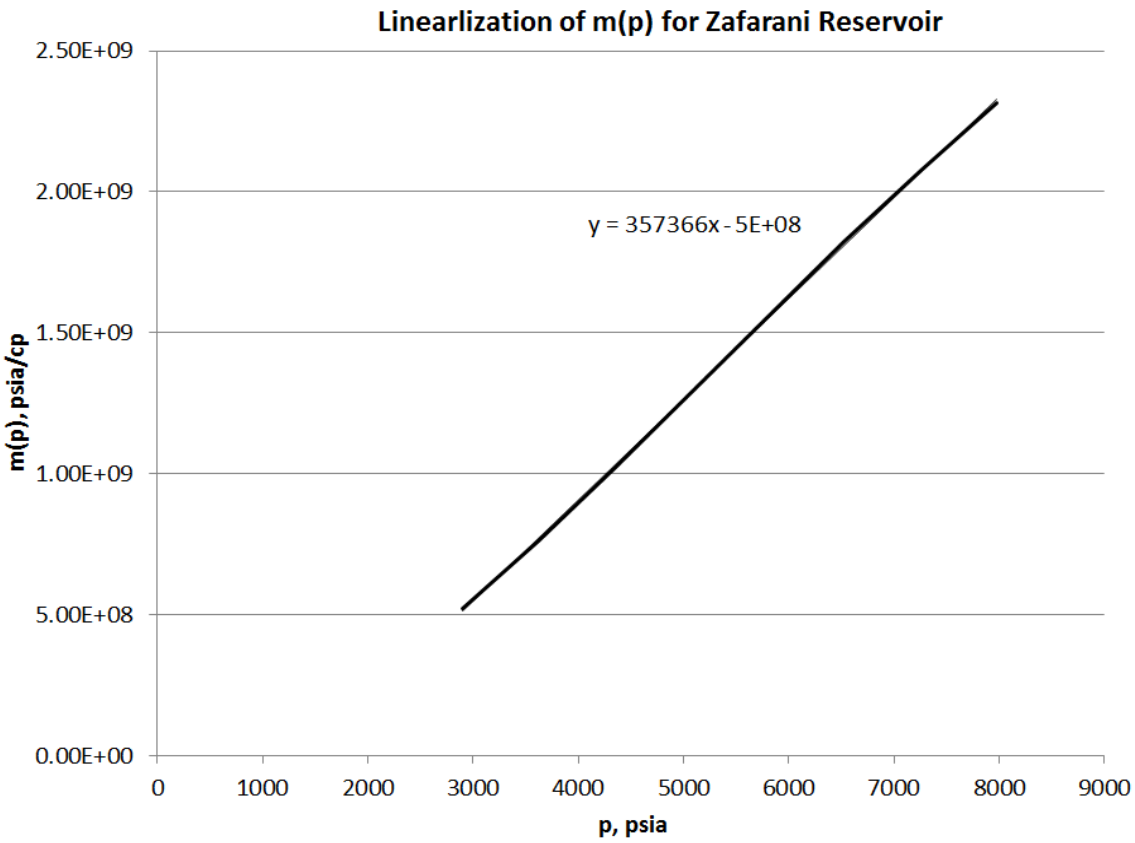

b. Generated PVT table for Lavani Main Reservoir

							Constants	
R	83.143	cm^3bar/mol-K					A1	126.88
Mg	16	g/mol					A2	5.25
T	342.15	K	600.67	degR	60	degC	A3	1.28
S.G	0.57	-						

						a	b			
p	p	ρ	μ	Z	2p/μZ	2p/μZav	delta P	a*b	m(p)	m(p)
[bara]	[psia]	[g/cm3]	[cp]	[-]	[bara/cp]	[bara/cp]	[bara]	[bara2/cp]	[bara2/cp]	[psia2/cp]
0	0	0.0000	0	0	0	0	0	0.00E+00	0.00E+00	0.00E+00
50	725.19	0.0281	1.34E-02	1.0	7441.69	3720.84	50	1.86E+05	1.86E+05	3.91E+07
100	1450.38	0.0562	1.45E-02	1.0	13671.84	10556.76	50	5.28E+05	7.14E+05	1.50E+08
150	2175.57	0.0844	1.58E-02	1.0	18534.91	16103.37	50	8.05E+05	1.52E+06	3.20E+08
200	2900.76	0.1125	1.75E-02	1.0	22056.07	20295.49	50	1.01E+06	2.53E+06	5.33E+08
250	3625.95	0.1406	1.94E-02	1.1	24353.24	23204.65	50	1.16E+06	3.69E+06	7.77E+08
300	4351.14	0.1687	2.18E-02	1.1	25593.26	24973.25	50	1.25E+06	4.94E+06	1.04E+09
350	5076.33	0.1969	2.45E-02	1.1	25961.37	25777.32	50	1.29E+06	6.23E+06	1.31E+09
400	5801.52	0.2250	2.77E-02	1.1	25640.54	25800.95	50	1.29E+06	7.52E+06	1.58E+09
450	6526.71	0.2531	3.14E-02	1.2	24798.79	25219.66	50	1.26E+06	8.78E+06	1.85E+09
500	7251.9	0.2812	3.58E-02	1.2	23582.82	24190.81	50	1.21E+06	9.99E+06	2.10E+09
550	7977.09	0.3093	4.09E-02	1.2	22115.86	22849.34	50	1.14E+06	1.11E+07	2.34E+09

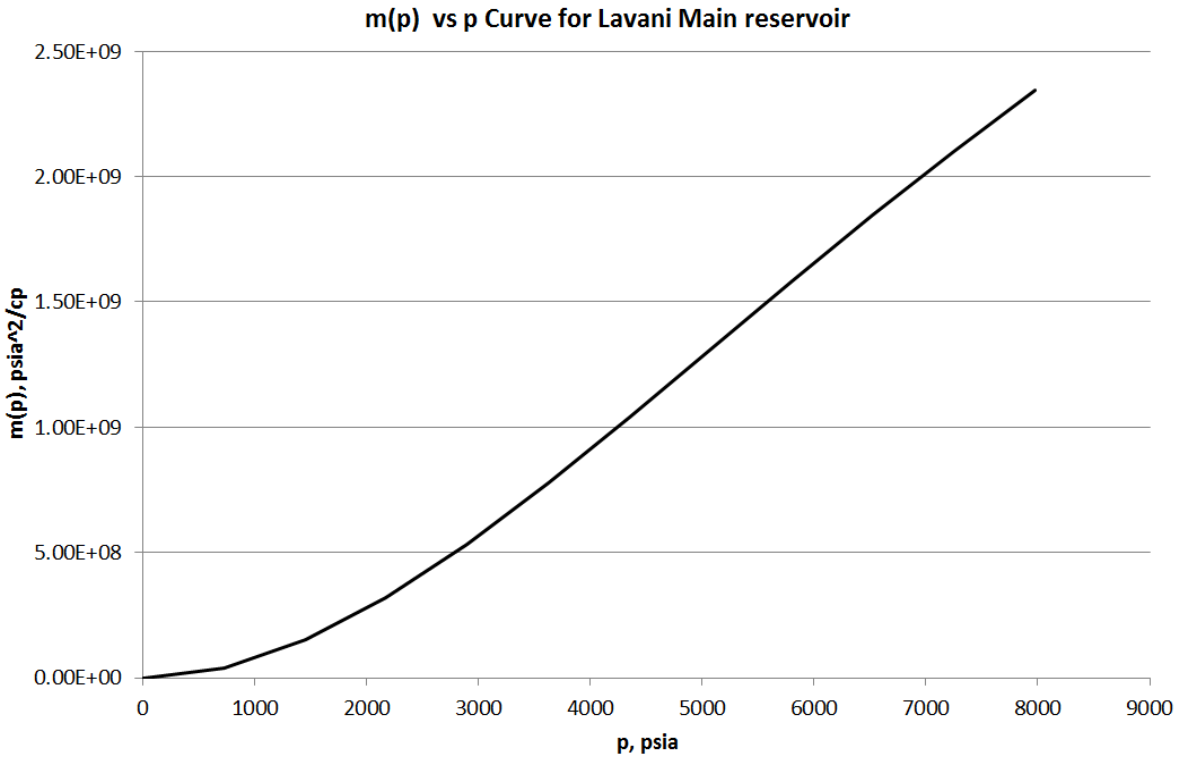
m(p) vs p Curve for Lavani Main reservoir
2.50E+09
2.00E+09
1.50E+09
1.00E+09
5.00E+08
0.00E+00
m(p), psia^2/cp
0
1000
2000
3000
4000
5000
6000
7000
8000
9000
p, psia

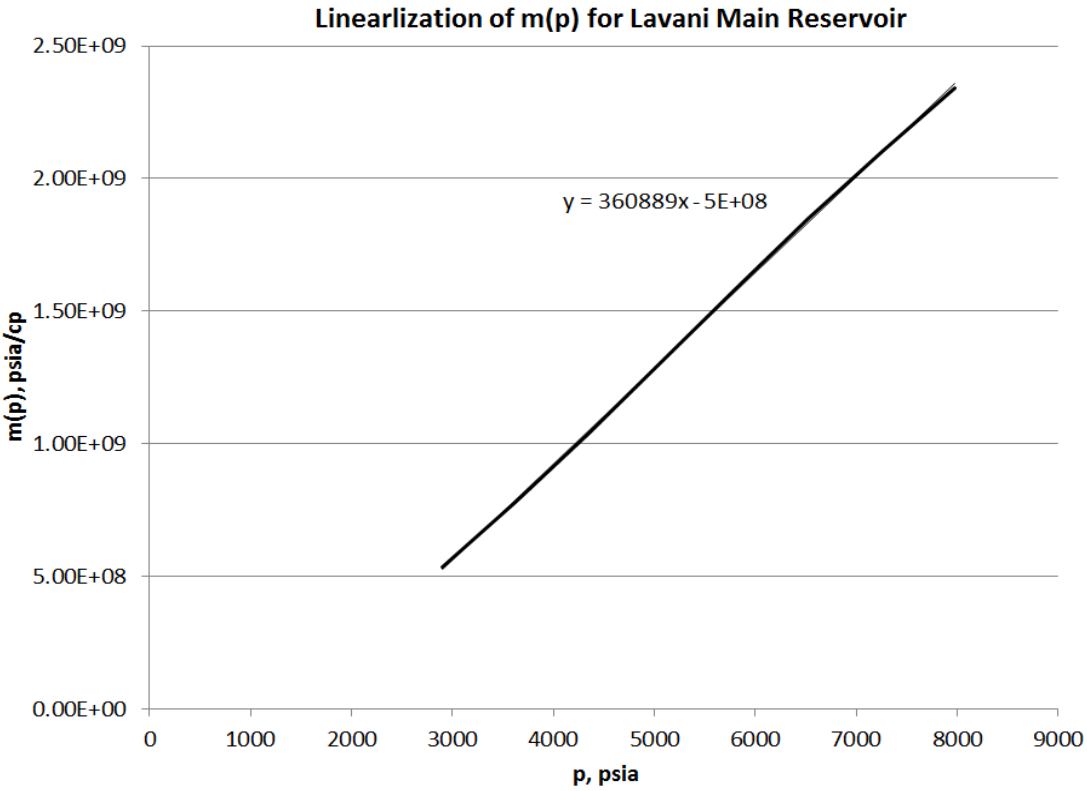
Linearlization of m(p) for Lavani Main Reservoir
y = 360889x - 5E+08
2.50E+09
2.00E+09
1.50E+09
1.00E+09
5.00E+08
0.00E+00
m(p), psia/cp
0
1000
2000
3000
4000
5000
6000
7000
8000
9000
p, psia

c. Generated PVT table for Lavani Deep Reservoir

							Constants	
R	83.143	cm^3bar/mol-K					A1	130.49
Mg	16	g/mol					A2	5.20
T	342.15	K	618.51	degR	69.91	degC	A3	1.29
S.G	0.57	-						

						a	b			
p	p	ρ	μ	Z	2p/μZ	2p/μZav	delta P	a*b	m(p)	m(p)
[bara]	[psia]	[g/cm3]	[cp]	[-]	[bara/cp]	[bara/cp]	[bara]	[bara2/cp]	[bara2/cp]	[psia2/cp]
0	0	0	0	0	0	0	0	0.00E+00	0.00E+00	0.00E+00
50	725.19	0.0281	1.37E-02	1.0	7249.56	3624.78	50	1.81E+05	1.81E+05	3.81E+07
100	1450.38	0.0562	1.48E-02	1.0	13348.02	10298.79	50	5.15E+05	6.96E+05	1.46E+08
150	2175.57	0.0844	1.62E-02	1.0	18137.38	15742.70	50	7.87E+05	1.48E+06	3.12E+08
200	2900.76	0.1125	1.78E-02	1.0	21634.27	19885.82	50	9.94E+05	2.48E+06	5.21E+08
250	3625.95	0.1406	1.98E-02	1.1	23945.68	22789.98	50	1.14E+06	3.62E+06	7.61E+08
300	4351.14	0.1687	2.20E-02	1.1	25227.03	24586.36	50	1.23E+06	4.85E+06	1.02E+09
350	5076.33	0.1969	2.47E-02	1.1	25653.02	25440.02	50	1.27E+06	6.12E+06	1.29E+09
400	5801.52	0.2250	2.79E-02	1.1	25397.84	25525.43	50	1.28E+06	7.39E+06	1.56E+09
450	6526.71	0.2531	3.16E-02	1.2	24622.82	25010.33	50	1.25E+06	8.65E+06	1.82E+09
500	7251.9	0.2812	3.60E-02	1.2	23469.96	24046.39	50	1.20E+06	9.85E+06	2.07E+09
550	7977.09	0.3093	4.11E-02	1.2	22059.51	22764.74	50	1.14E+06	1.10E+07	2.31E+09

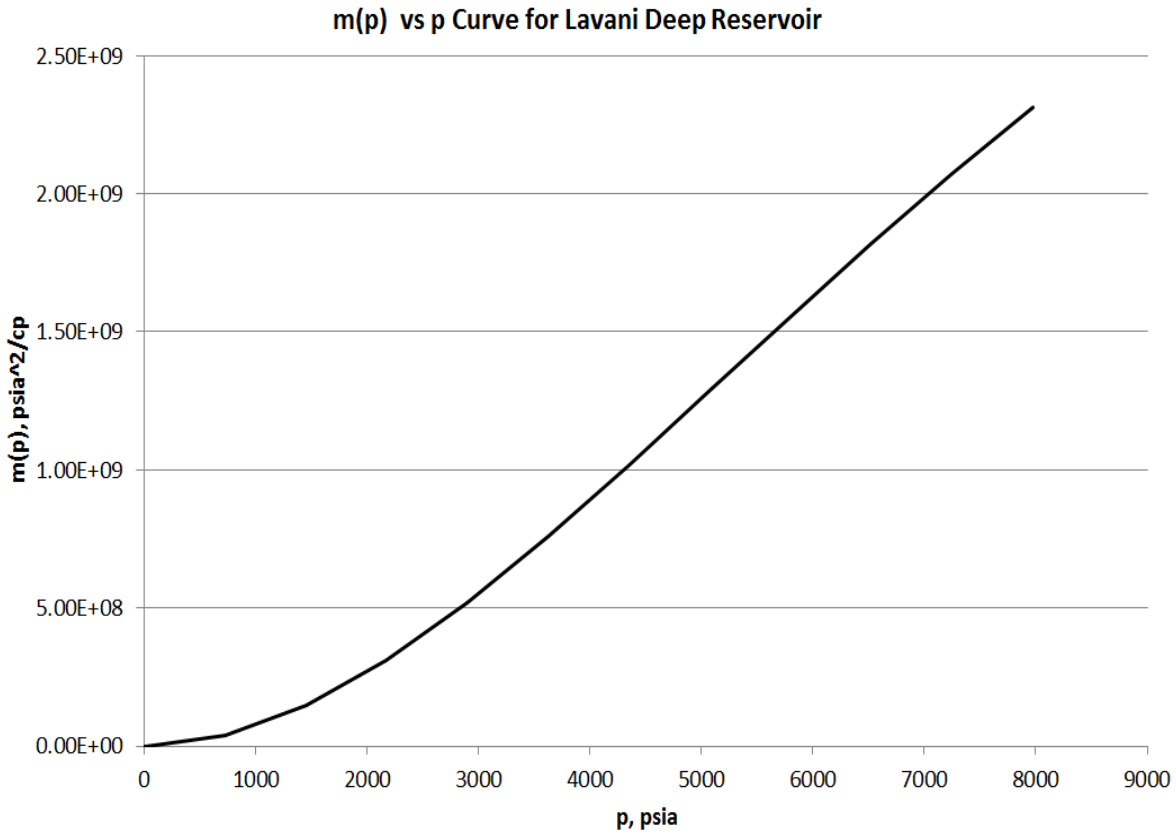

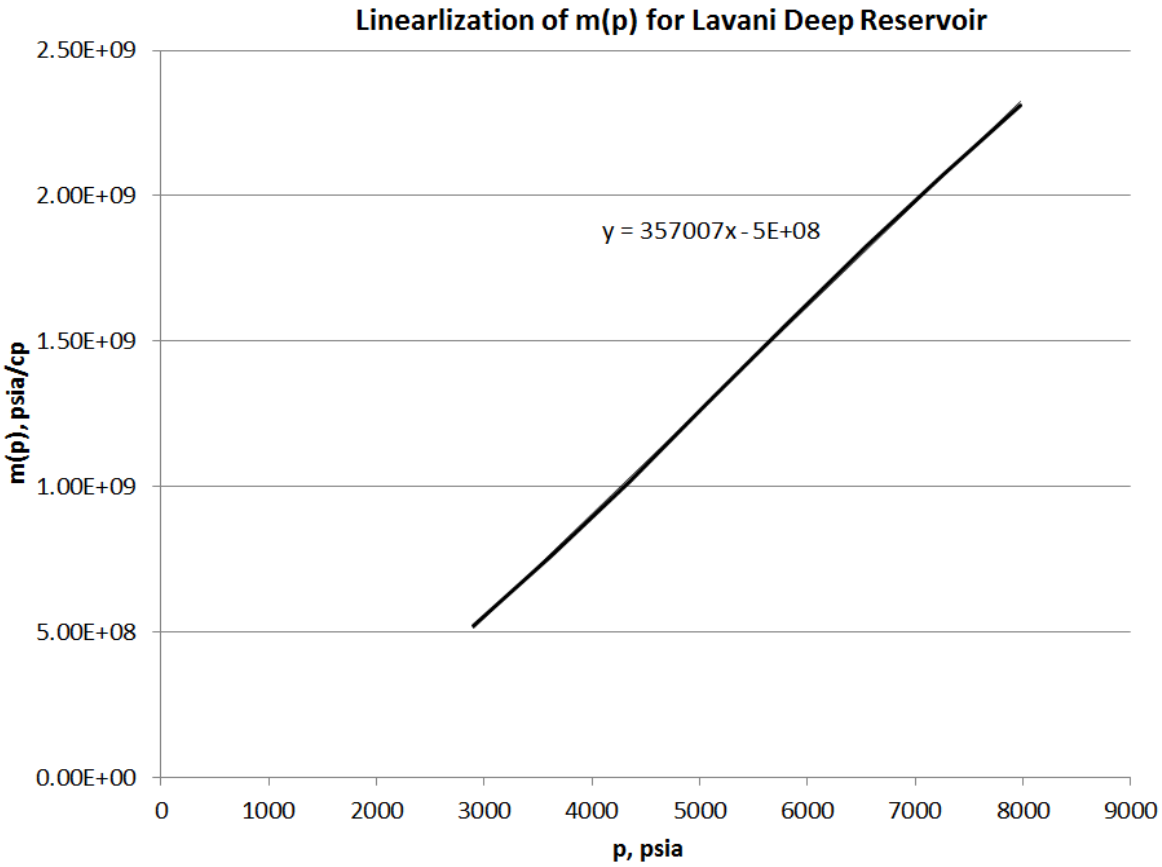

d. Generated PVT table for Tangawizi Reservoir

							Constants	
R	83.143	cm^3bar/mol-K					A1	124.29
Mg	16	g/mol					A2	5.29
T	342.15	K	587.97	degR	52.94	degC	A3	1.27
S.G	0.57	-						

						a	b			
p	p	ρ	μ	Z	2p/μZ	2p/μZav	delta P	a*b	m(p)	m(p)
[bara]	[bara]	[g/cm3]	[cp]	[-]	[bara/cp]	[bara/cp]	[bara]	[bara2/cp]	[bara2/cp]	[psia2/cp]
0	0	0	0	0	0	0	0	0.00E+00	0.00E+00	0.00E+00
50	725.19	0.0281	1.32E-02	1.0	7585.42	3792.71	50	1.90E+05	1.90E+05	3.99E+07
100	1450.38	0.0562	1.42E-02	1.0	13912.50	10748.96	50	5.37E+05	7.27E+05	1.53E+08
150	2175.57	0.0844	1.56E-02	1.0	18828.24	16370.37	50	8.19E+05	1.55E+06	3.25E+08
200	2900.76	0.1125	1.73E-02	1.0	22364.78	20596.51	50	1.03E+06	2.58E+06	5.42E+08
250	3625.95	0.1406	1.92E-02	1.1	24648.64	23506.71	50	1.18E+06	3.75E+06	7.89E+08
300	4351.14	0.1687	2.16E-02	1.1	25855.50	25252.07	50	1.26E+06	5.01E+06	1.05E+09
350	5076.33	0.1969	2.43E-02	1.1	26178.66	26017.08	50	1.30E+06	6.31E+06	1.33E+09
400	5801.52	0.2250	2.75E-02	1.1	25807.71	25993.18	50	1.30E+06	7.61E+06	1.60E+09
450	6526.71	0.2531	3.12E-02	1.2	24915.68	25361.70	50	1.27E+06	8.88E+06	1.87E+09
500	7251.9	0.2812	3.57E-02	1.2	23652.70	24284.19	50	1.21E+06	1.01E+07	2.12E+09
550	7977.09	0.3093	4.08E-02	1.2	22144.08	22898.39	50	1.14E+06	1.12E+07	2.36E+09

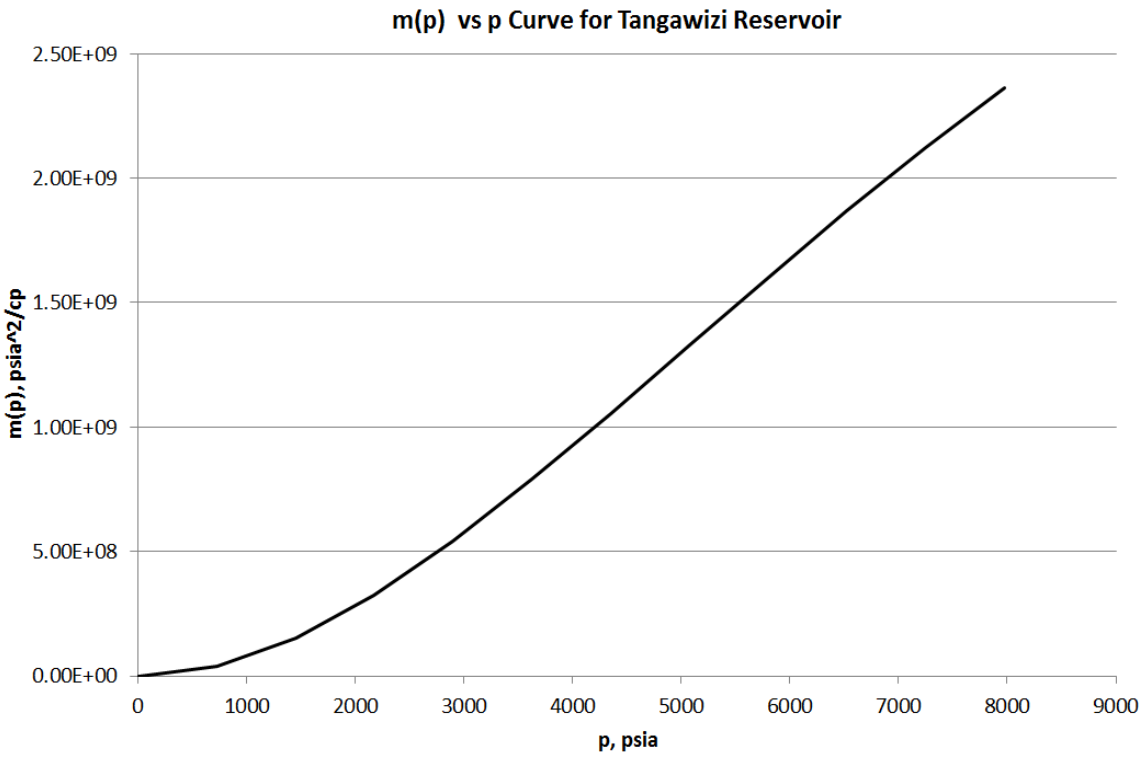
m(p) vs p Curve for Tangawizi Reservoir
2.50E+09
2.00E+09
1.50E+09
1.00E+09
5.00E+08
0.00E+00
m(p), psia^2/cp
0
1000
2000
3000
4000
5000
6000
7000
8000
9000
p, psia

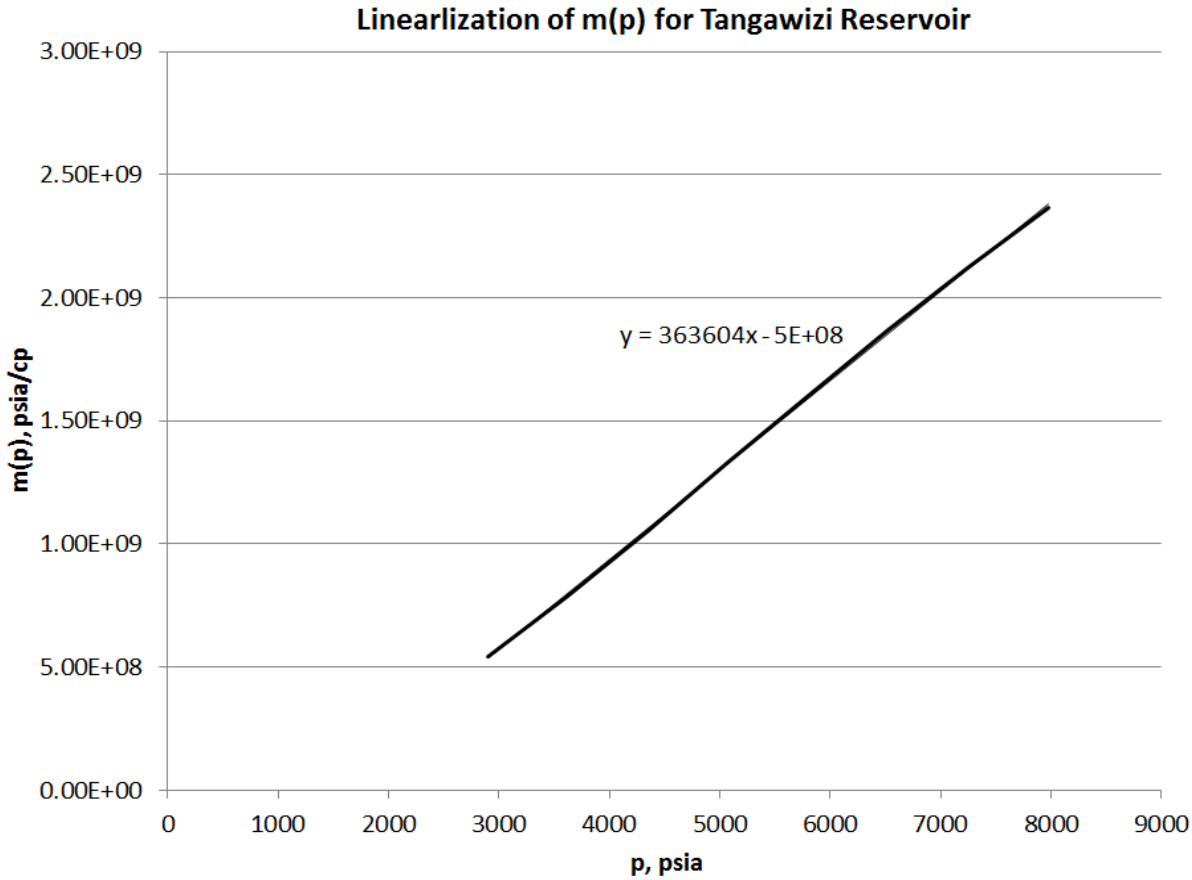
Linearlization of m(p) for Tangawizi Reservoir
3.00E+09
2.50E+09
2.00E+09
1.50E+09
1.00E+09
5.00E+08
0.00E+00
m(p), psia/cp
y = 363604x - 5E+08
0
1000
2000
3000
4000
5000
6000
7000
8000
9000
p, psia

Appendix 4-Linear interpolation and extrapolation

Having seven values of, x_1, x_2, x_3, y_1, y_2 *or* y_3

The value of interest can be solved by using the general formula:

$$\frac{(x_1 - x_2)}{(x_1 - x_3)} = \frac{(y_1 - y_2)}{(y_1 - y_3)}$$

Appendix 5- Calculations on how to estimate CR values

Bottomhole network solving for Zafarani Reservoir							
PR	**qwell**	**Pwfu**	**Pwfd**	**Pwh**	**CR**	**(pwfu-pwfd)**	**Analytical_CR**
[psia]	**[ft3/D]**	**[psia]**	**[psia]**	**[psia]**	**scf/psia^2**	**[psia]**	**Mscf/D/psia^2/cP**
6019.08	1.25E+08	5963.52	5963.52	5293.89	6.2784	0.00	0.0062
					0.0063	Mscf/D/psia^2/cP	

Bottomhole network solving for Lavani Main Reservoir							
PR	**qwell**	**Pwfu**	**Pwfd**	**Pwh**	**CR**	**(pwfu-pwfd)**	**Analytical_CR**
[psia]	**[ft3/D]**	**[psia]**	**[psia]**	**[psia]**	**scf/psia^2**	**[psia]**	**Mscf/D/psia^2/cP**
5206.86	9.35E+07	5185.15	5185.15	4739.84	11.9287	0.00	0.0121
					0.0119	Mscf/D/psia^2/cP	

Bottomhole network solving for Lavani Deep							
PR	**qwell**	**Pwfu**	**Pwfd**	**Pwh**	**CR**	**(pwfu-pwfd)**	**Analytical_CR**
[psia]	**[ft3/D]**	**[psia]**	**[psia]**	**[psia]**	**scf/psia^2**	**[psia]**	**Mscf/D/psia^2/cP**
7541.98	1.25E+08	7437.59	7437.59	6671.75	3.3451	0.00	0.0034
					0.0033	Mscf/D/psia^2/cP	

Bottomhole network solving for Tangawizi Reservoir							
PR	**qwell**	**Pwfu**	**Pwfd**	**Pwh**	**CR**	**(pwfu-pwfd)**	**Analytical_CR**
[psia]	**[ft3/D]**	**[psia]**	**[psia]**	**[psia]**	**scf/psia^2**	**[psia]**	**Mscf/D/psia^2/cP**
4952.87	1.04E+08	4935.63	4935.63	4523.74	16.5704	0.00	0.0173
					0.0166	Mscf/D/psia^2/cP	

Appendix 6-Cases to estimate the production profile

Case One, 5	Producing Reservoirs Production Strategy Max. Production Plateau from Zafarani Ultimate Plateau Rate	Zafarani, Lavani Main and Lavani Deep Statoil Proposed Strategy 5 years 635.6 [MMscf/day]		
	% Plateau Rate Production [-]	**Z-Plateau Rate [MMscf/day]**	**LM-Plateau Rate [MMscf/day]**	**LM-Plateau Rate [MMscf/day]**
a	Z (0.375), LM (0.375), LD (0.25)	238.4	238.4	158.9
b	Z (0.4), LM (0.4), LD (0.2)	254.2	254.2	127.1
c	Z (0.42), LM (0.35), LD (0.23)	267.0	222.5	146.2
d	Z (0.38), LM (0.38), LD (0.24)	241.5	241.5	152.5
e	Z (0.39), LM (0.37), LD (0.24)	247.9	235.2	152.5

Case One, 7	Producing Reservoirs Production Strategy Maximum Production Plateau from Zafarani Ultimate Plateau rate	Zafarani, Lavani Main and Lavani Deep Statoil Proposed Strategy 7 years 635.6 [MMscf/day]		
	% Plateau Rate Production [-]	**Z-Plateau Rate [MMscf/day]**	**LM-Plateau Rate [MMscf/day]**	**LM-Plateau Rate [MMscf/day]**
a	Z (0.375), LM (0.375), LD (0.25)	238.4	238.4	158.9
b	Z (0.36), LM (0.39), LD (0.25)	228.8	247.9	158.9
b*	Z (0.4), LM (0.4), LD (0.2)	254.2	254.2	127.1
c	Z (0.35), LM (0.4), LD (0.25)	222.5	254.2	158.9
d	Z (0.45), LM (0.3), LD (0.25)	286.0	190.7	158.9
e	Z (0.4), LM (0.35), LD (0.25)	254.2	222.5	158.9

Case Two, 8	Producing Reservoirs Production Strategy Max. Production Plateau from Zafarani Ultimate Plateau Rate	Zafarani, Lavani Main and Lavani Deep Statoil Proposed Strategy 8 years 635.6 [MMscf/day]		
	% Plateau Rate Production [-]	**Z-Plateau Rate [MMscf/day]**	**LM-Plateau Rate [MMscf/day]**	**LM-Plateau Rate [MMscf/day]**
a	Z (0.375), LM (0.375), LD (0.25)	238.4	238.4	158.9
b	Z (0.36), LM (0.38), LD (0.26)	228.8	241.5	165.3
c	Z (0.345), LM (0.39), LD (0.265)	219.3	247.9	168.4
d	Z (0.34), LM (0.4), LD (0.26)	216.1	254.2	165.3
e	Z (0.32), LM (0.41), LD (0.27)	203.4	260.6	171.6
e*	Z (0.31), LM (0.42), LD (0.27)	197.0	267.0	171.6

Case Two, 7	Producing Reservoirs Production Strategy Max. Production Plateau from Tangawizi Ultimate Plateau Rate	Tangawizi, Lavani Main and Lavani Deep Statoil Proposed Strategy 7 years 635.6 [MMscf/day]		
	% Plateau Rate Production [-]	**T-Plateau Rate [MMscf/day]**	**LM-Plateau Rate [MMscf/day]**	**LM-Plateau Rate [MMscf/day]**
a	T (0.375), LM (0.375), LD (0.25)	238.4	238.4	158.9
b	T (0.36), LM (0.385), LD (0.255)	228.8	244.7	162.1
c	T (0.35), LM (0.395), LD (0.255)	222.5	251.1	162.1
d	T (0.34), LM (0.405), LD (0.255)	216.1	257.4	162.1

Case Two, 9	Producing Reservoirs Production Strategy Max. Production Plateau from Tangawizi Ultimate Plateau Rate	Tangawizi, Lavani Main and Lavani Deep Statoil Proposed Strategy 9 years 635.6 [MMscf/day]		
	% Plateau Rate Production [-]	**T-Plateau Rate [MMscf/day]**	**LM-Plateau Rate [MMscf/day]**	**LM-Plateau Rate [MMscf/day]**
a	T (0.375), LM (0.375), LD (0.25)	238.4	238.4	158.9
b	T (0.365), LM (0.385), LD (0.25)	232.0	244.7	158.9
c	T (0.345), LM (0.4), LD (0.255)	219.3	254.2	162.1
d	T (0.315), LM (0.42), LD (0.265)	200.2	267.0	168.4
e	T (0.34), LM (0.405), LD (0.255)	206.6	267.0	162.1

Case Two, 11	Producing Reservoirs Production Strategy Max. Production Plateau from Tangawizi Ultimate Plateau Rate	Tangawizi, Lavani Main and Lavani Deep Statoil Proposed Strategy 11 years 635.6 [MMscf/day]		
	% Plateau Rate Production [-]	**T-Plateau Rate [MMscf/day]**	**LM-Plateau Rate [MMscf/day]**	**LM-Plateau Rate [MMscf/day]**
a	T (0.375), LM (0.375), LD (0.25)	238.4	238.4	158.9
b	T (0.33), LM (0.4), LD (0.27)	209.7	254.2	171.6
c	T (0.2), LM (0.5), LD (0.3)	127.1	317.8	190.7
d	T (0.25), LM (0.45), LD (0.3)	158.9	286.0	190.7
e	T (0.23), LM (0.47), LD (0.3)	146.2	298.7	190.7

Appendix 7-Pipelines Costs

Optional Strategy One				
Gas Transmission Line Pipeline Costs				
	Length	**Diameter**	**Unit**	**Cost**
	[km]	**[Inches]**	**[Inch.-km]**	**[USD]**
Pipeline				
ManifoldLD to Jsep=85 km	85	26	2 210	7 182 5000
ManifoldLM to ManifoldLD=3 km	3	26	78	2 535 000
ManifoldZ to ManifoldLM= 5 km	5	26	130	4 225 000
Pipeline diameter= 26 in			**Subtotal**	**78 585 000.00**
Flowlines				
TemplateZ to ManifoldZ= 11 km	11	12	132	4 290 000
TemplateLM to ManifoldLM= 4.8 km	4.8	12	57.6	1 872 000
TemplateLD to ManifoldLD= 5.5 km	5.5	12	66	2 145 000
Flowlines diameter= 12 in			**Subtotal**	**8 307 000.00**
			Total	**86 892 000.00**

Optional Strategy Two				
Gas Transmission Line Pipeline Costs				
	Length	**Diameter**	**Unit**	**Cost**
	[km]	**[Inches]**	**[Inch.-km]**	**[USD]**
Pipeline				
ManifoldLD to Jsep=85 km	85	26	2 210	71 825 000
ManifoldLM to ManifoldLD=3 km	3	26	78	2 535 000
ManifoldZ to ManifoldLM= 5 km	5	26	130	4 225 000
Pipeline diameter= 26 in			**Subtotal**	**78 585 000.00**
Flowlines				
TemplateT to ManifoldZ= 5.8 km	5.8	12	69.6	2 262 000
TemplateLM to ManifoldLM= 4.8 km	4.8	12	57.6	1 872 000
TemplateLD to ManifoldLD= 5.5 km	5.5	12	66	2 145 000
Flowlines diameter= 12 in			**Subtotal**	**6 279 000.00**
			Total	**84 864 000.00**

Main Case				
Gas Transmission Line Pipeline Costs				
	Length	**Diameter**	**Unit**	**Cost**
	[km]	**[Inches]**	**[Inch.-km]**	**[USD]**
Pipeline				
ManifoldLD to Jsep=85 km	85	28	2380	77 350 000
ManifoldLM to ManifoldLD=3 km	3	26	78	2 535 000
ManifoldZ to ManifoldLM= 5 km	5	26	130	4 225 000
Pipeline diameter= 26 in			**Subtotal**	**84 110 000.00**
Flowlines				
TemplateT to ManifoldZ= 5.8 km	5.8	12	69.6	2 262 000
TemplateLM to ManifoldLM= 4.8 km	4.8	12	57.6	1 872 000
TemplateLD to ManifoldLD= 5.5 km	5.5	12	66	2 145 000
Flowlines diameter= 12 in			**Subtotal**	**6 279 000.00**
			Total	**90 389 000.00**

Optional Strategy One				
Gas Transmission Line Pipeline Costs				
	Length	**Diameter**	**Unit**	**Cost**
	[km]	**[Inches]**	**[Inch.-km]**	**[USD]**
Pipeline				
ManifoldLD to Jsep=85 km	85	26	2210	71 825 000
ManifoldLM to ManifoldLD=3 km	3	26	78	2 535 000
ManifoldZ to ManifoldLM= 5 km	5	26	130	4 225 000
Pipeline diameter= 26 in			**Subtotal**	**78 585 000.00**
Flowlines				
TemplateZ to ManifoldZ= 11 km	11	13	143	4 647 500
TemplateLM to ManifoldLM= 4.8 km	4.8	12	57.6	1 872 000
TemplateLD to ManifoldLD= 5.5 km	5.5	12	66	2 145 000
Flowlines diameter= 12 in			**Subtotal**	**8 664 500.00**
			Total	**87 249 500.00**

Optional Strategy Two				
Gas Transmission Line Pipeline Costs				
	Length	**Diameter**	**Unit**	**Cost**
	[km]	**[Inches]**	**[Inch.-km]**	**[USD]**
Pipeline				
ManifoldLD to Jsep=85 km	85	26	2210	71 825 000
ManifoldLM to ManifoldLD=3 km	3	26	78	2 535 000
ManifoldZ to ManifoldLM= 5 km	5	26	130	4 225 000
Pipeline diameter= 26 in			**Subtotal**	**78 585 000.00**
Flowlines				
TemplateT to ManifoldZ= 5.8 km	5.8	13	75.4	2 450 500
TemplateLM to ManifoldLM= 4.8 km	4.8	12	57.6	1 872 000
TemplateLD to ManifoldLD= 5.5 km	5.5	12	66	2 145 000
Flowlines diameter= 12 in			**Subtotal**	**6 467 500.00**
			Total	**85 052 500.00**

Appendix 8- Economic evaluation results for the Block 2 Field

Optional Strategy One Increasing Number of Wells						
	10% More		20% More		30% More	
Cases	**Cum.NPV**	**% Diff.**	**Cum.NPV**	**% Diff.**	**Cum.NPV**	**% Diff.**
[-]	**[USD, Million]**	**[%]**	**[USD, Million]**	**[%]**	**[USD, Million]**	**[%]**
Base	4 135	-	4 877	0.00	5 582	0.00
Case A	4 066	-1.67	4 807	-1.42	5 513	-1.24
Case B	4 043	-2.23	4 780	-1.89	5 490	-1.65
Case C	4 020	-2.78	4 757	-2.36	5 467	-2.06
Case D	4 058	-1.89	4 799	-1.49	5 515	-1.20
Case E	4 035	-2.44	4 776	-1.96	5 492	-1.61
Optional Strategy Two **Increasing Number of Wells**						
	10% More		**20% More**		**30% More**	
Cases	**Cum.NPV**	**% Diff.**	**Cum.NPV**	**% Diff.**	**Cum.NPV**	**% Diff.**
[-]	**[USD, Million]**	**[%]**	**[USD, Million]**	**[%]**	**[USD, Million]**	**[%]**
Base	4 002	-	4 735	0.00	5 439	0.00
Case F	4 018	0.40	4 756	0.46	5 467	0.51
Case G	4 031	0.72	4 774	0.85	5 490	0.95
Case H	4 007	0.12	4 750	0.34	5 466	0.50
Case I	3 959	-1.08	4 702	-0.67	5 418	-0.38
Case J	3 969	-0.84	4 717	-0.36	5 438	-0.02

Produce Tangawizi as Satellite Reservoir								
			10% More		20% More		30% More	
Cases	**Add Tangawizi**		**Cum.NPV**	**% Diff.**	**Cum.NPV**	**% Diff.**	**Cum.NPV**	**% Diff.**
[-]	Flowline	Wells	**[USD, Million]**	**[%]**	**[USD, Million]**	**[%]**	**[USD, Million]**	**[%]**
Case K	26''	6	4 314	4.32	5 100	4.68	5 857	4.93
Produce Zafarani as Satellite Reservoir								
			10% More		**20% More**		**30% More**	
Cases	**Add Zafarani**		**Cum.NPV**	**% Diff.**	**Cum.NPV**	**% Diff.**	**Cum.NPV**	**% Diff.**
[-]	Flowline	Wells	**[USD, Million]**	**[%]**	**[USD, Million]**	**[%]**	**[USD, Million]**	**[%]**
Case L	28''	5	4 245	6.06	5 031	6.29	5 790	6.46

Optional Strategy One Compression							
		10% More		20% More		30% More	
Cases	**Delta_P**	**Cum.NPV**	**% Diff.**	**Cum.NPV**	**% Diff.**	**Cum.NPV**	**% Diff.**
[-]	**[psia]**	**[USD, Million]**	**[%]**	**[USD, Million]**	**[%]**	**[USD, Million]**	**[%]**
Case i	72.10	4,120	-0.37	4,855	-0.34	5,569	-0.32
Case ii	159.5	4,156	0.50	4,897	0.51	5,617	0.52
Case iii	261.1	4,159	0.57	4,900	0.58	5,615	0.59
Case iv	377.1	4,152	0.41	4,892	0.43	5,607	0.45
Case v	507.6	4,153	0.43	4,894	0.46	5,609	0.48
Optional Strategy Two Compression							
		10% More		**20% More**		**30% More**	
Cases	**Delta_P**	**Cum.NPV**	**% Diff.**	**Cum.NPV**	**% Diff.**	**Cum.NPV**	**% Diff.**
[-]	**[psia]**	**[USD, Million]**	**[%]**	**[USD, Million]**	**[%]**	**[USD, Million]**	**[%]**
Case i	72.10	4 007	0.11	4 738	0.09	5 443	0.08
Case ii	159.5	4 046	1.09	4 783	1.05	5 494	1.02
Case iii	261.1	4 115	2.82	4 863	2.74	5 584	2.68
Case iv	377.1	4 113	2.77	4 861	2.69	5 582	2.64
Case v	507.6	4 140	3.46	4 894	3.38	5 619	3.32

Appendix 9-HYSYS Input Data

Inputs		
Outlet pressure (separator pressure)	30	bara
Inlet temperature Zafarani as only producing reservoir	29.18	℃
Inlet temperature for Zafarani, Lavani Main and Deep	37.71	℃
Inlet temperature for Tangawizi, Lavani Main and Deep (first year)	38.7	℃
Inlet temperature for Tangawizi, Lavani Main and Deep (last year)	41.01	℃
Flowrate (plateau rate)	1.36E+07	Sm^3/D
Temperature of the sea	4	℃
Pipe ID	26	Inches
Pipe OD (including insulation)	29.3	Inches
Pipe length all cases	90.1	Km
Inclination	4-5	degrees
Pin for Zafarani	0.00	bara
Pin for Zafarani, Lavani Main and Deep		bara
Pin for Tangawizi, Lavani Main and Deep	48.29	bara
Overall Heat Transfer (HTC or U)	1.5	W/(m^2 C)

Conversion of Std. Volumetric flow to Molar Flow		
$\dot{q}_g$	1.80E+07	Sm3/day
RTsc/Psc	23.689	Sm3/kgmol
$\dot{n}_g$	7.60E+05	kg-mole/day
$\dot{n}_g$	3.17E+04	kg-mole/hr

Appendix 10-HYSYS simulation results

a. Pressure, Temperature and Liquid Holdup in the Main Pipeline

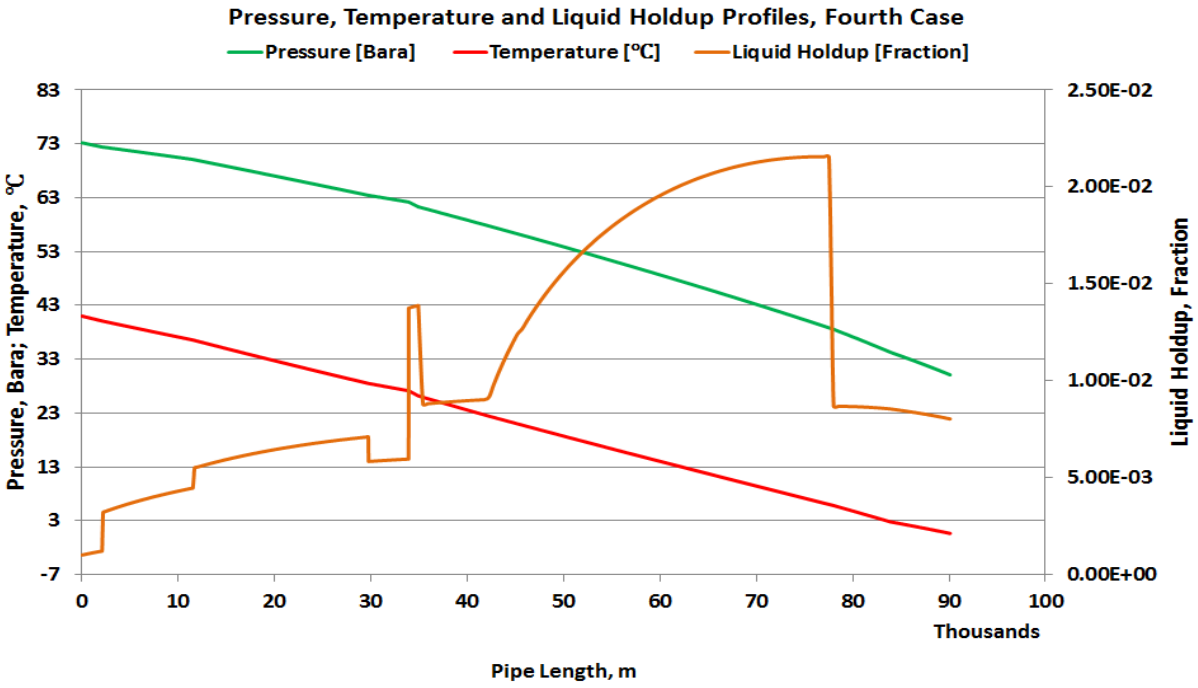

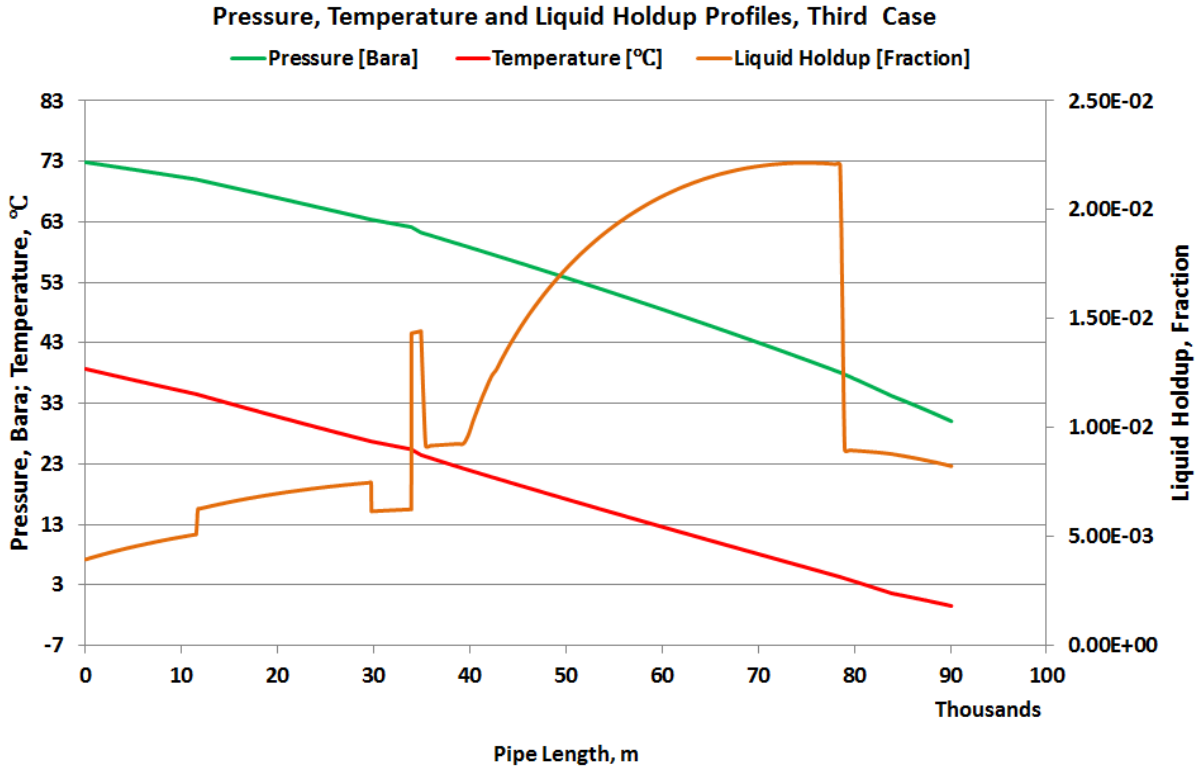

b. Hydrate Formation Temperature for Second, Third and Fourth Cases

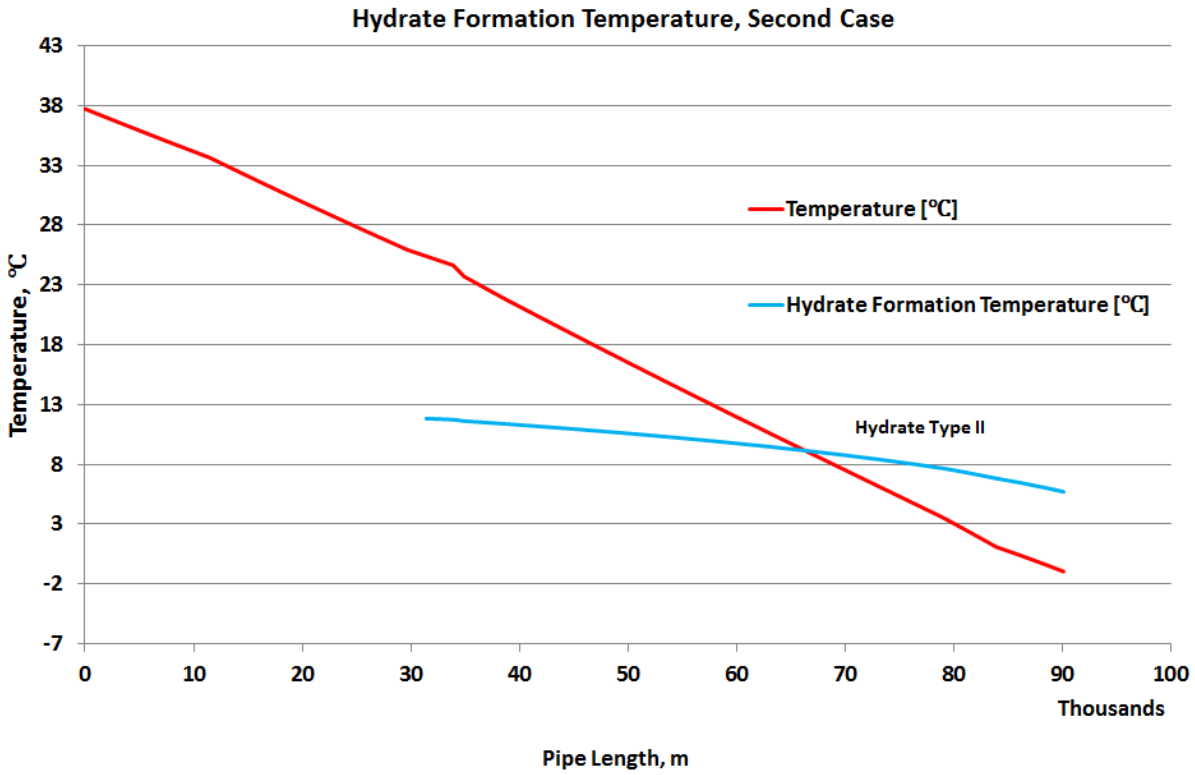

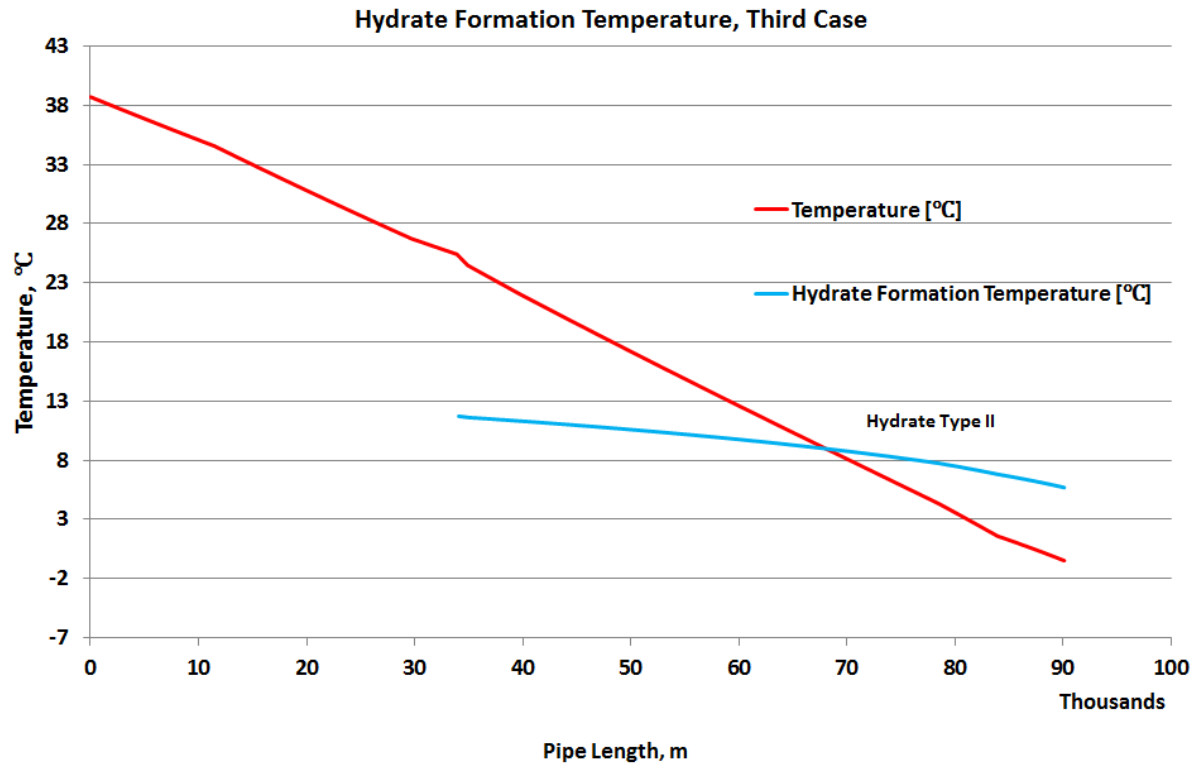

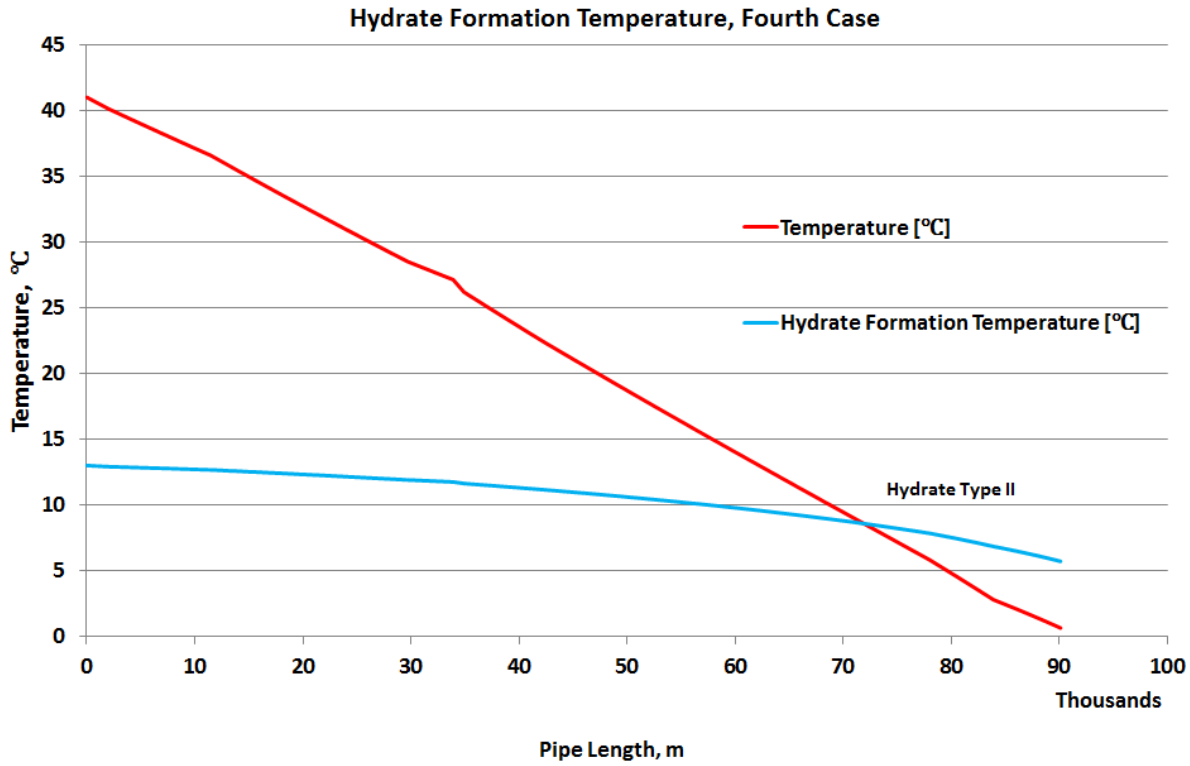

c. Hydrate Formation Pressure for Second, Third and Fourth Cases

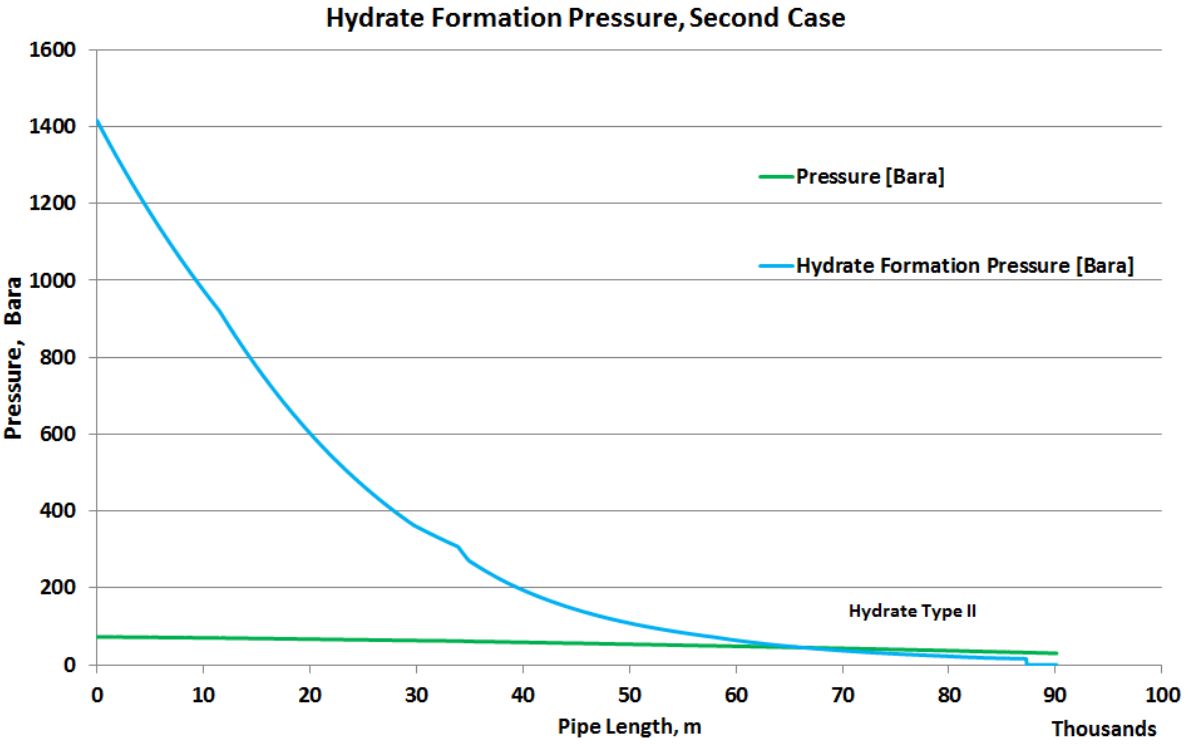

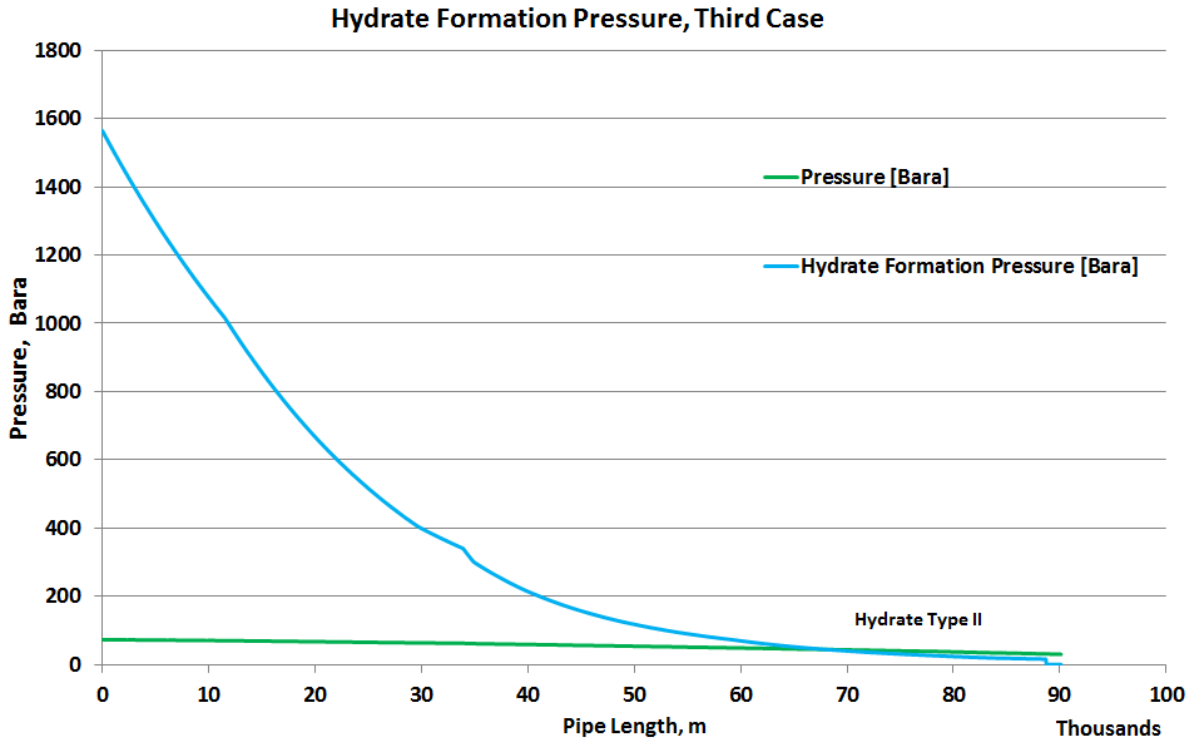
Hydrate Formation Pressure, Third Case
1800
1600
1400
1200
1000
800
600
400
200
0
Pressure, Bara
Pressure [Bara]
Hydrate Formation Pressure [Bara]
Hydrate Type II
0
10
20
30
40
50
60
70
80
90
100
Pipe Length, m
Thousands

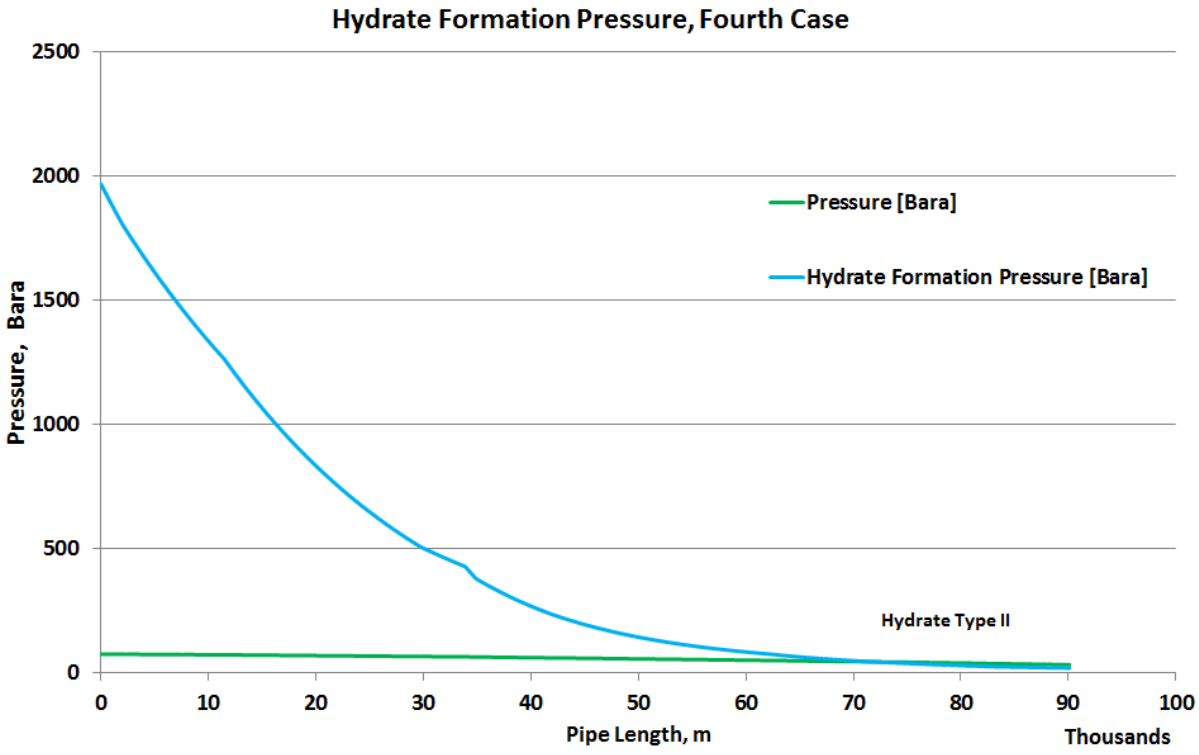
Hydrate Formation Pressure, Fourth Case
2500
2000
1500
1000
500
0
Pressure, Bara
Pressure [Bara]
Hydrate Formation Pressure [Bara]
Hydrate Type II
0
10
20
30
40
50
60
70
80
90
100
Pipe Length, m
Thousands

d. Hydrate formation pressure and temperature after injection of MeOH for the Second, Third and Fourth Case

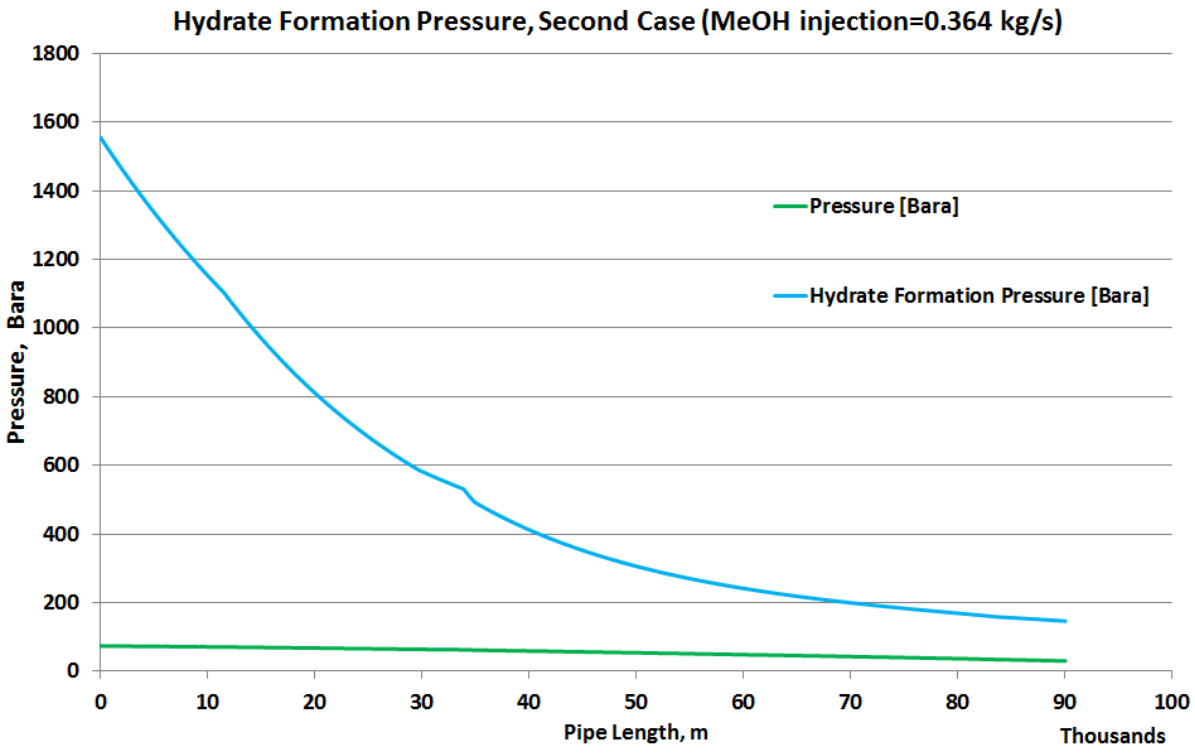

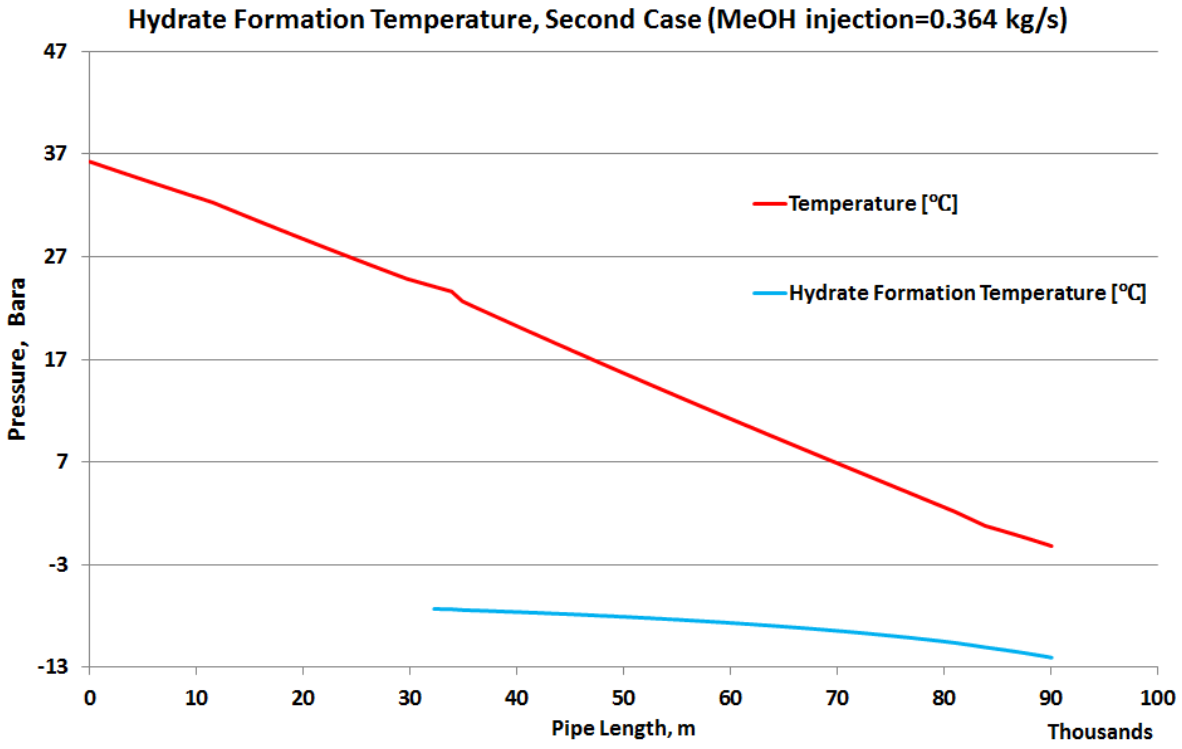

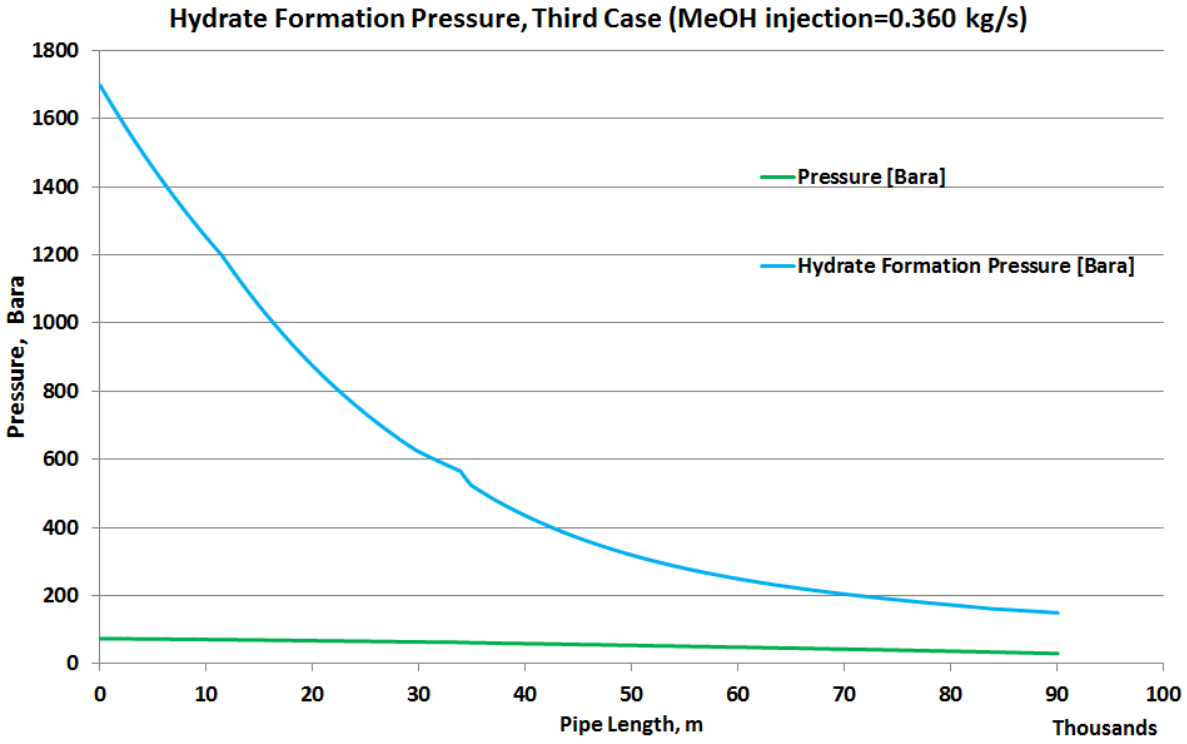
Hydrate Formation Pressure, Third Case (MeOH injection=0.360 kg/s)
1800
1600
1400
1200
1000
800
600
400
200
0
Pressure, Bara
Pressure [Bara]
Hydrate Formation Pressure [Bara]
0
10
20
30
40
50
60
70
80
90
100
Thousands
Pipe Length, m

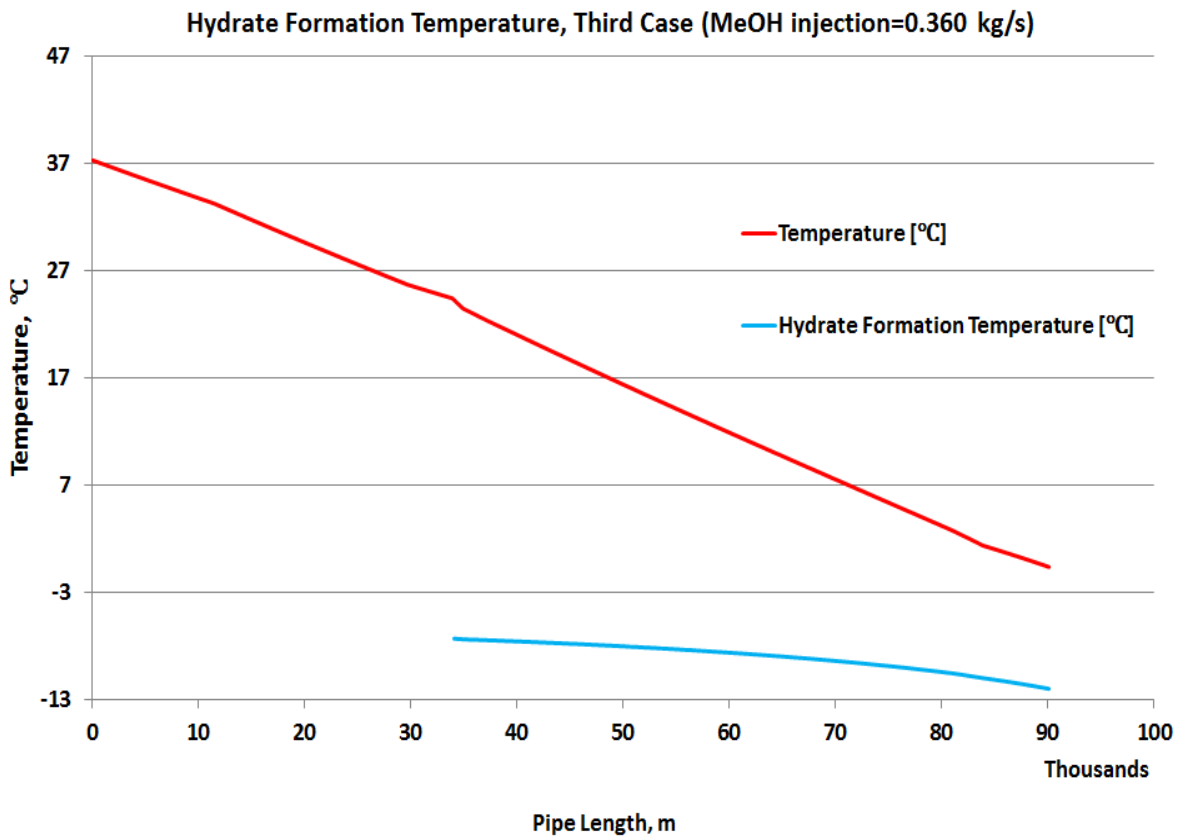
Hydrate Formation Temperature, Third Case (MeOH injection=0.360 kg/s)
47
37
27
17
7
-3
-13
Temperature, ℃
Temperature [℃]
Hydrate Formation Temperature [℃]
0
10
20
30
40
50
60
70
80
90
100
Thousands
Pipe Length, m

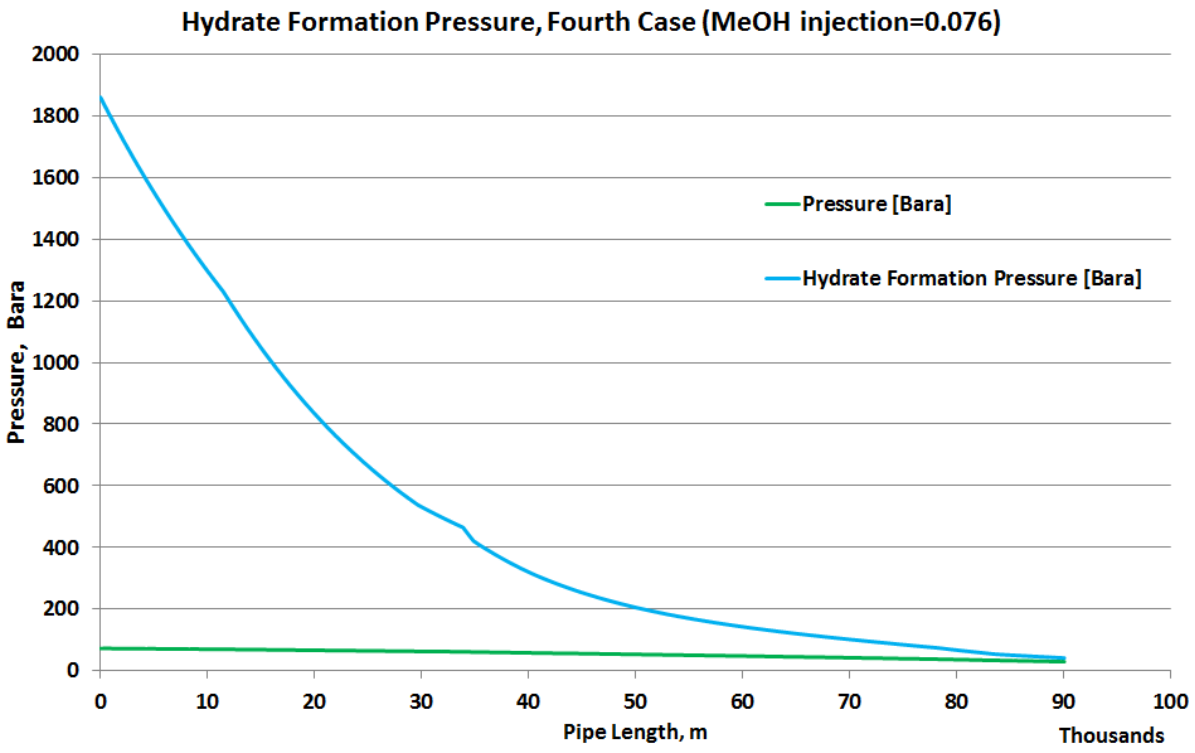
Hydrate Formation Pressure, Fourth Case (MeOH injection=0.076)
Pressure [Bara]
Hydrate Formation Pressure [Bara]
Pressure, Bara
2000
1800
1600
1400
1200
1000
800
600
400
200
0
0
10
20
30
40
50
60
70
80
90
100
Thousands
Pipe Length, m

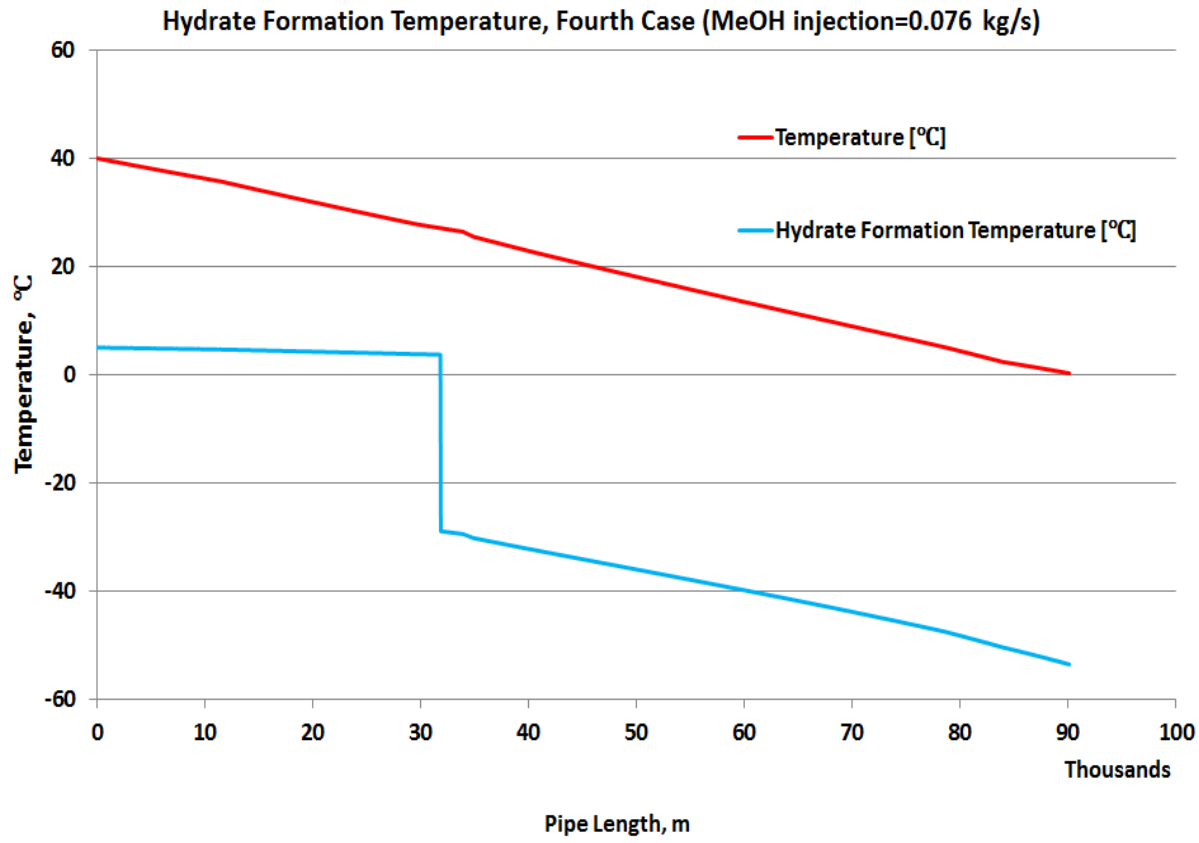
Hydrate Formation Temperature, Fourth Case (MeOH injection=0.076 kg/s)
Temperature [°C]
Hydrate Formation Temperature [°C]
Temperature, °C
60
40
20
0
-20
-40
-60
0
10
20
30
40
50
60
70
80
90
100
Thousands
Pipe Length, m

e. Hydrate formation pressure and temperature after injection of TEG for the Second, Third and Fourth Case

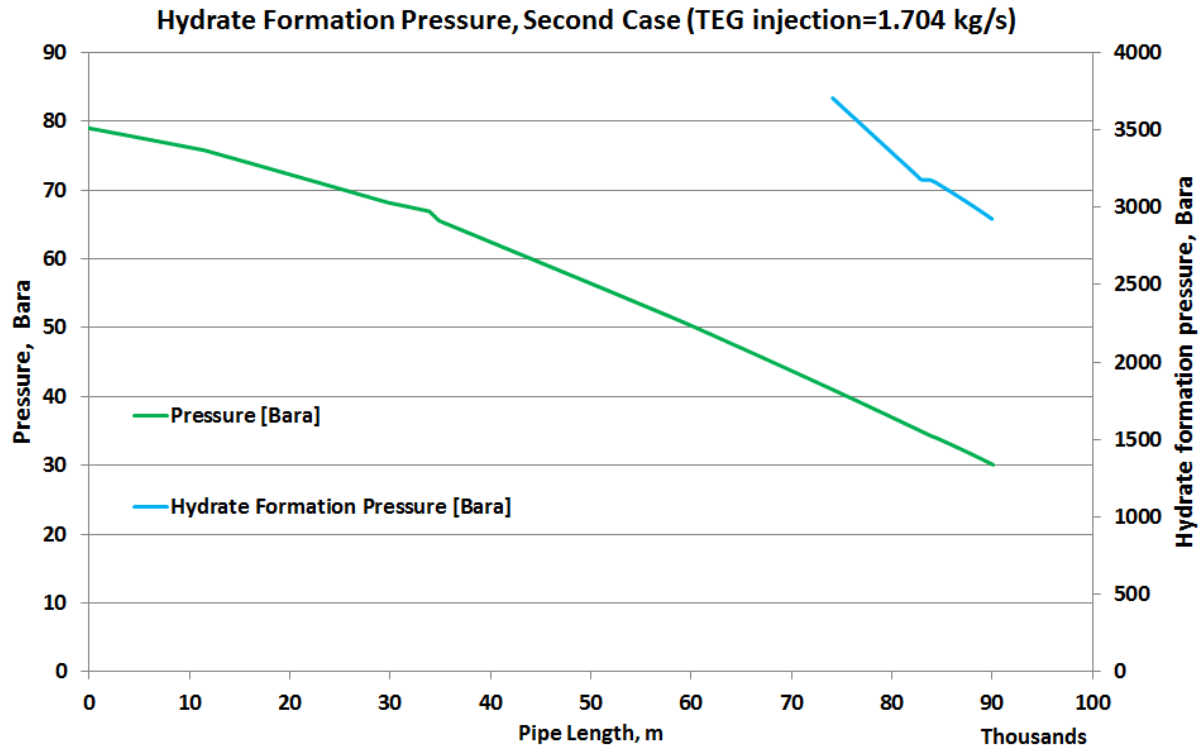

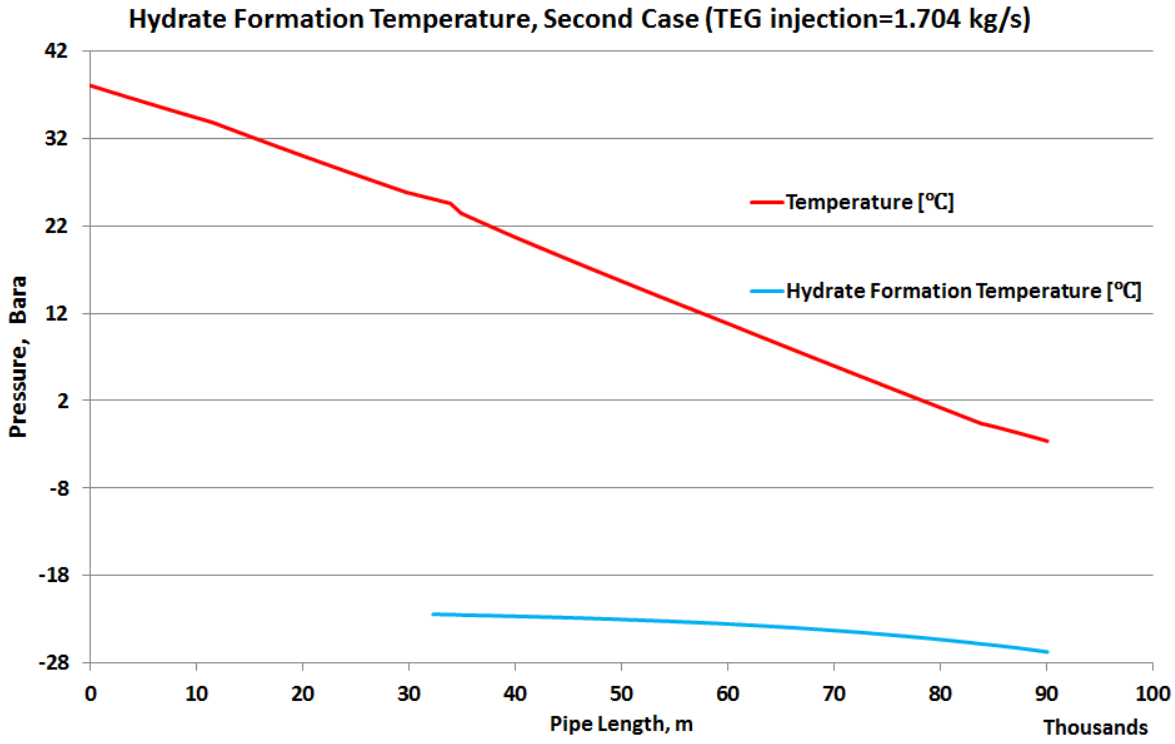

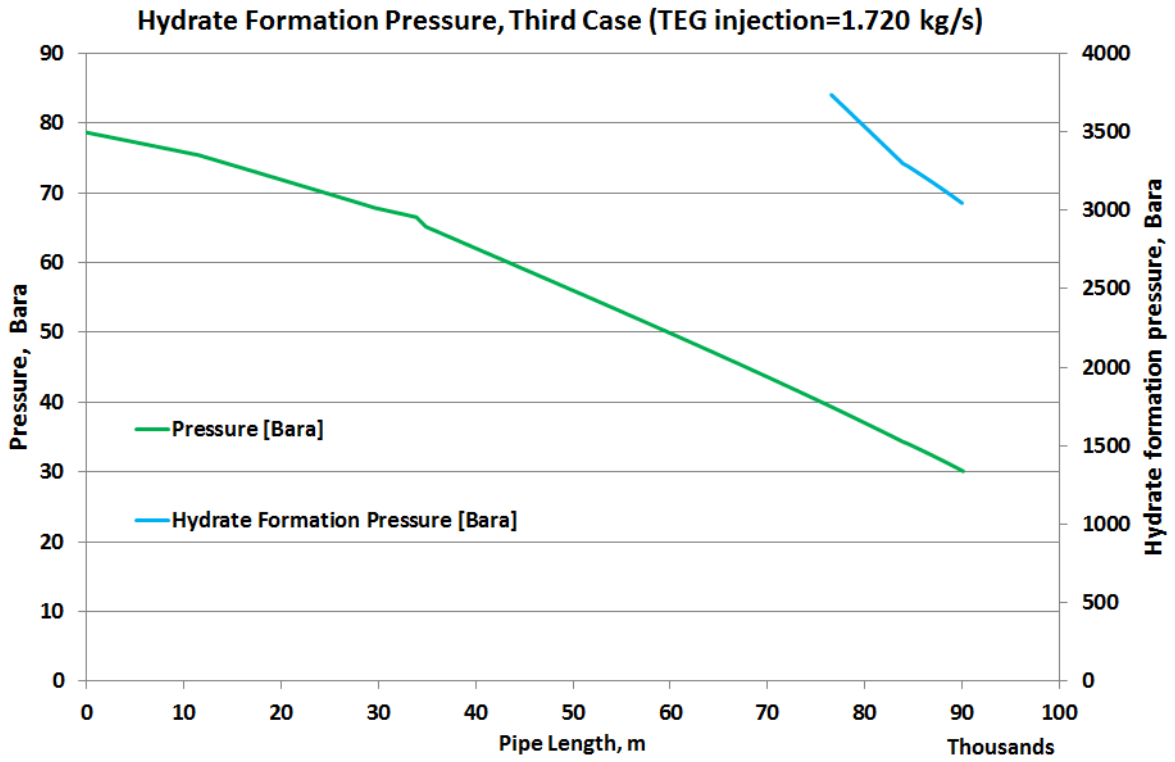
Hydrate Formation Pressure, Third Case (TEG injection=1.720 kg/s)
Pressure, Bara
Hydrate formation pressure, Bara
Pressure [Bara]
Hydrate Formation Pressure [Bara]
Pipe Length, m
Thousands
0
10
20
30
40
50
60
70
80
90
100
500
1000
1500
2000
2500
3000
3500
4000

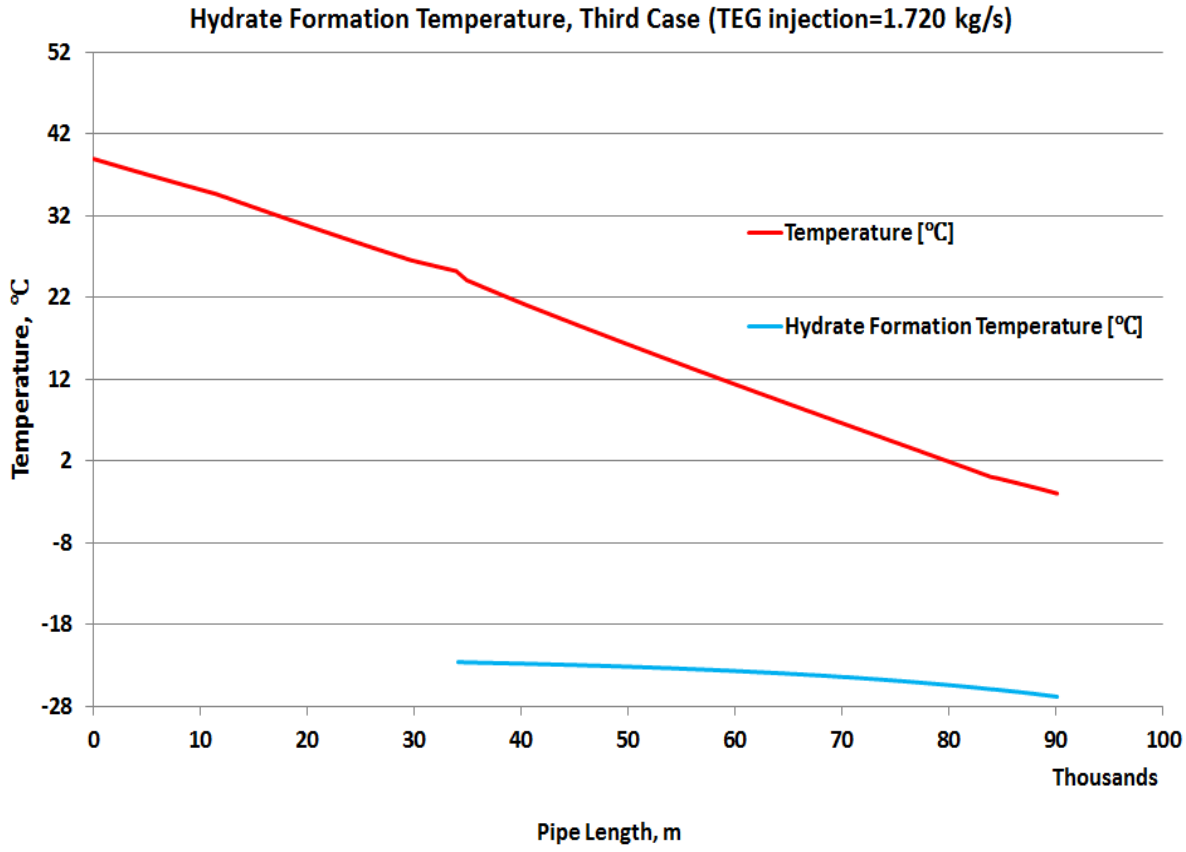
Hydrate Formation Temperature, Third Case (TEG injection=1.720 kg/s)
Temperature, ℃
Temperature [℃]
Hydrate Formation Temperature [℃]
Pipe Length, m
Thousands
52
42
32
22
12
2
-8
-18
-28
0
10
20
30
40
50
60
70
80
90
100

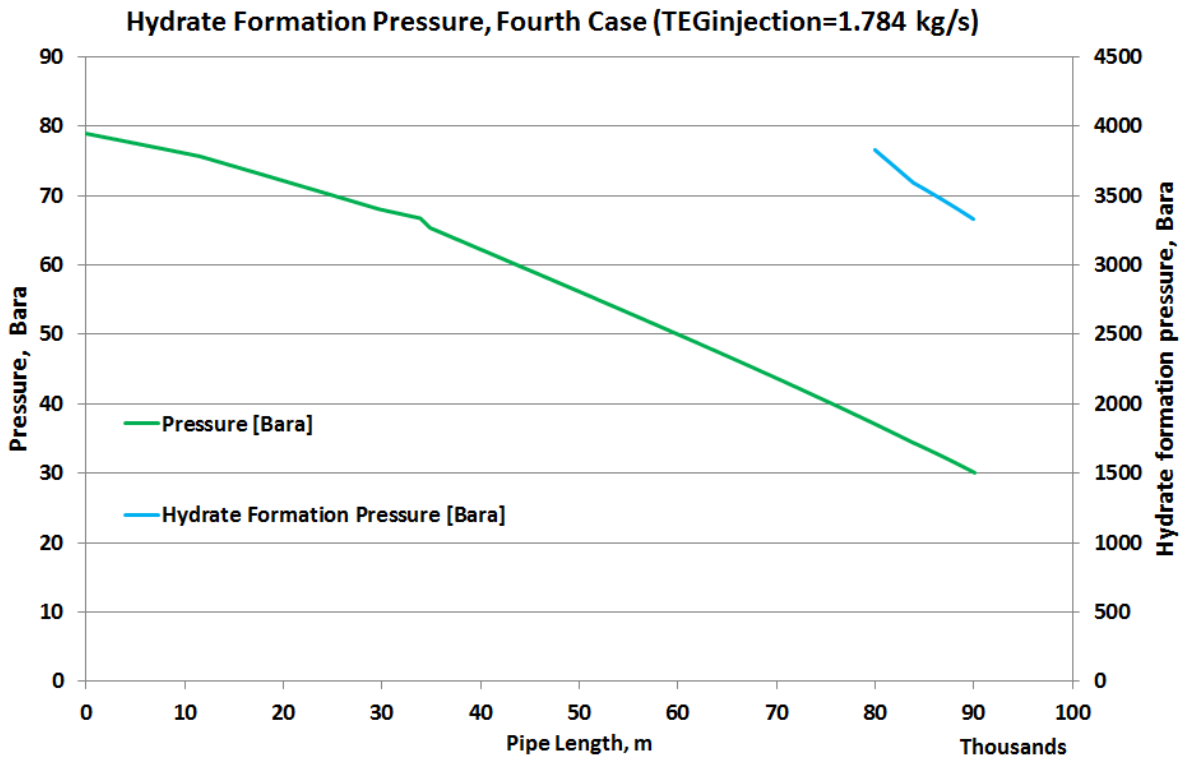
Hydrate Formation Pressure, Fourth Case (TEGinjection=1.784 kg/s)
Pressure, Bara
Hydrate formation pressure, Bara
Pressure [Bara]
Hydrate Formation Pressure [Bara]
Pipe Length, m
Thousands
0
10
20
30
40
50
60
70
80
90
100
500
1000
1500
2000
2500
3000
3500
4000
4500

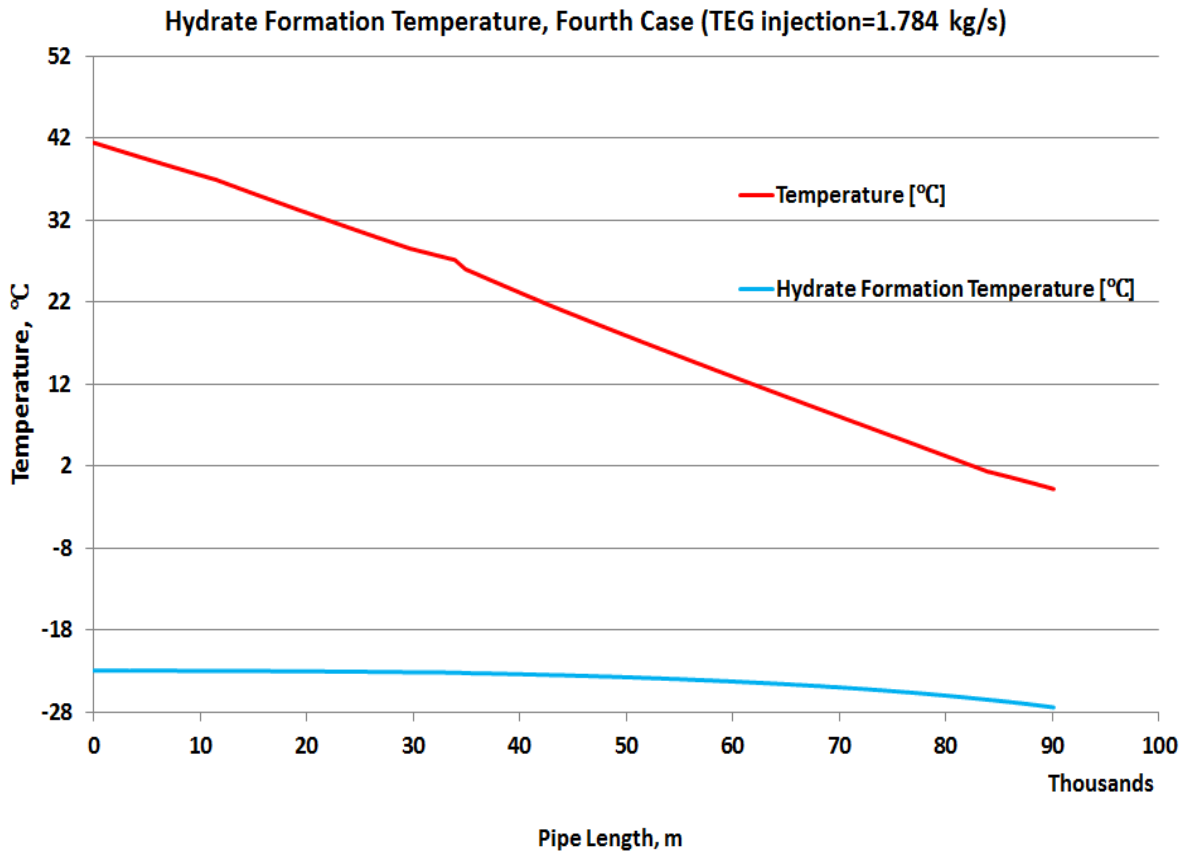
Hydrate Formation Temperature, Fourth Case (TEG injection=1.784 kg/s)
Temperature, ℃
Temperature [℃]
Hydrate Formation Temperature [℃]
Pipe Length, m
Thousands
52
42
32
22
12
2
-8
-18
-28
0
10
20
30
40
50
60
70
80
90
100

Reference

A. Muggeridge, A. K. W. T. P., 2013. *Recovery rates, enhanced oil recovery and technological limits.* [Online] Available at: http://rsta.royalsocietypublishing.org/content/372/2006/20120320 [Accessed 6 November 2015].

A. Rojey, C. J. S. G. B. S. M., 1997. *NATURAL GAS PRODUCTION PROCESSING TRANSPORT.* Paris: Editions Technip.

Abbott, P., D'Souza, R., Solberg, I. & Eriksen, K., 1995. Evaluating Deepwater Development Concepts. *Journal of Petroleum Technology,* 47(04), pp. 314-321.

Adamu, M. A., Anjieka, J. A. & Ikiensikimama, S. S., 2013. Economics Analysis on the Development of Nigerian Offshore Marginal Fields Using Probabilistic Approach. *Advance in Petroleum Exploration and Development,* 6(01), pp. 11-21.

Adewumi, M. A., 1997. Natural gas transportation issues. *Journal of petroleum technology,* 49(02), pp. 139-143.

Ahmed, T. & Mckinney, P. D., 2005. *Advanced Reservoir Engineering.* Oxford: Gulf Professional Publishing .

Amyx, J. W., Bass, D. M. J. & Whiting, R. L., 1960. *Petroleum reservoir engineering: physical properties.* Vol. 1 ed. Texas: McGraw Hill-College .

Andalu, F. W., 2013. *NATURAL GAS RESERVOIR AND WELLBORE PERFORMANCE. Semester project at NTNU,* Trondheim: NTNU.

ARPS, J. J., 1944. *Analysis Of Decline Curves,* Houston: A.I.M.E.

Aziz, K. & Govier, G. W., 1972. Pressure drop in wells producing oil and gas. *Journal of Canadian Petroleum Technology,* 11(03).

Bai, Y. & Qiang, B., 2005. *Subsea Pipelines and Risers.* s.l.:Elsevier .

Baker Hughes, 2010. *Reservoir Performance Analysis and Prediction,* Houston: Baker Hughes incorporated.

Barnea, D., 1987. A Unified Model for Predicting Flow-Pattern Transitions for the Whole Range of Pipe Inclinations. *International Journal of Multiphase Flow,* 13(1), pp. 1-12.

Beggs, H. & Brills, J., 1973. A Study of Two-Phase in Inclined Pipes. *Journal of Petroleum Technology,* 25(05), pp. 607-617.

Behnia, M., 1991. Most accurate two-phase pressure drop correlation identified. *Oil and Gas Journal,* 89(37).

Bikoro, F., 2005. *Production Performance Optimisation.* s.l., s.n.

Bokin, E., Febrianti, F., Khabibullin, E. & Perez, C. E. S., 2010. *Flow assuarance and Sour Gas in Natural Gas Production,* Trondheim: NTNU.

Brown, K. E. & Lea, J. F., 1985. Nodal Systems Analysis of Oil and Gas Wells. *Journal of petroleum technology,* 37(10), pp. 1-751.

Buckles, R. S., 1965. Correlating and Averaging Conate water Saturation Data.. *Journal of Cannadian Petroleum Technology ,* 4(01), pp. 42-52.

Bujulu, E. G. N., 2013. *The Successful Development & Management of Songo Songo and Mnazi Bay Gas Fields against Imposing Reservoir, Market and Location Challenges paper at The 2nd Tanzanian Oil and Gas Conference and Exhibitions (TOGaGE-2013), 176p..* Dar es Salaam, University of Dar es Salaam.

Chandra, V., 2016. *natgas.info.* [Online] Available at: http://natgas.info/gas-information/what-is-natural-gas/gas-pipelines [Accessed 21 June 2016].

Chawarwan Khana, R. A. G. M., 2013. Carbon dioxide injection for enhanced gas recovery and storage (reservoir simulation). *Egyptian Journal of Petroleum,* 22(2), pp. 225-240.

Coats, K. H., 1980. An Equation of State Compositional Model. *Society of Petroleum Engineers Journal,* 20(05), pp. 363-376.

Costa, A., 2006. Permeability-porosity relationship: A reexamination of the Kozeny-Carman equation based on a fractal pore-space geometry assumption. *Geophisical research letters,* 33(2).

Covington, K. C., III, J. T. C. & D., S. D. B., 1999. *Selection of Hydrate Suppression Methods for Gas Streams. in Proceedings of the Seventy-Eight GPA Annual Convention, Nashvile, TN: Gas processors Association, pp.46-52..* Texas, Bryan Research and Engineering, Inc..

Craft, B., Hawkins, M. & Terry, R. E., 1991. *Applied Petroleum Reservoir Engineering.* 2nd ed. Provo: Englewood, NJ 07632, Prentice-Hall.

Curtis H. Whiston, M. R. B., 2000. *Phase Behaviour.* Texas: Society of Petroleum Engineers.

Dake, L., 1983. *Fundamentals of reservoir engineering.* 1st ed. Amsterdam: Elsevier .

Dale, E. K., 2013. *Design of Gas Transport Systems.* Trondheim, NTNU.

Davalath, J., Patni, S., Bryson, B. & Chen, T., 2004. Bijupira Salema: Flow Assurance Analysis to Support Operating Strategy. *Offshore Technology Conference.*

Demirbas, A., 2010. *Natural Gas,* s.l.: Springer 2010.

Devold, H., 2013. *Oil and gas production handbook: an introduction to oil and gas production transport, refining and petrochemical industry.* Aberdeen : Lulu.com.

Diego Vannucci, R., 2011. *Platform Technologies for Offshore Renewable Energy Conversion.* Milan, IWES.

Duns, H. & Ros, N., 1963. *Vertical flow of gas and liquid mixtures in wells. In 6th World Petroleum Congress.* Tokyo, World Petroleum Congress.

Economides, M. J., Hill, A. D. & Ehlig-Economides, C., 1994. *Petroleum Production Systems.* United States of America: Prentice Hall.

Ehizoyanyan, O., Appah, D. & Sylvester, O., 2015. Estimation of Pressure Drop, Liquid Holdup and Flow Pattern in a Two Phase Vertical Flow. *International Journal of Engineering and Technology ,* V(4), pp. 241-253.

Fetkovich, M. J., 1975. *Multipoint Testing of Gas Wells. SPE Mid-Continent Section Continuing Education Course.* Tulsa, OK, s.n.

Fetkovich, M. J., Reese, D. E. & Whiston, C., 1998. Application of a General Material Balance for High Pressure Gas Reservoir (includes associated paper 51360). *SPE journal,* III(1), pp. 3-13.

Forster, L. et al., 2015. *2015 WORLDWIDE SURVEY OF SUBSEA PROCESSING: SEPARATION, COMPRESSION,PUMPING SYSTEMS.* Houston, TX, INTECSEA WorleyParsons and Offshore Magazine .

Gentry, R. W., 1972. Decline-Curve Analysis. *Journal of Petroleum Technology ,* I(24), pp. 38-41.

Golan, M. & Stanko, M., 2015. *TPG 4230 Spring 2015, Field Development course at NTNU.* [Online]
Available at: http://folk.ntnu.no/stanko/Courses/TPG4230/2015/Notes/TPG4230_Notes_2015.pdf TPG4230
[Accessed 6 February 2016].

Golan, M. & Whitson, C. H., 1991. *Well Performance.* 2nd ed. Trondheim: Prentice Hall.

Guðmundsson, J. S., 2011. *TPG 4140 - NATURAL GAS at NTNU.* [Online] Available at: http://www.ipt.ntnu.no/~jsg/undervisning/naturgass/lysark/LysarkGudmundssonFlowAssurance2011.pdf
[Accessed 7 May 2016].

Guðmundsson, J. S., 2011. *TPG 4140 - NATURAL GAS at NTNU.* [Online] Available at:

http://www.ipt.ntnu.no/~jsg/undervisning/naturgass/lysark/LysarkGudmundssonFlowAssurance2011.pdf
[Accessed 7 November 2015].

Guo, B., Duan, S. & Ghalambor, A., 2006. A simple model for predicting heat loss and temperature profiles in insulated pipelines. *SPE Production & Operations,* 21(01), pp. 107-113.

Hagedorn, A. K. & Brown, K. E., 1965. Experimental study of pressure gradients occurring during continuous two-phase flow in small-diameter vertical conduits. *Journal of Petroleum Technology,* 17(04), pp. 475-484.

Hallset, J. O., 2009. *Subsea Field Development and Production Enhancement (IOR). Presented at Offshore Europe.* Aberdeen, Poseidon Group.

Hein, M. A., 1987. *Nodal Analysis as Applied to Pipelines and Risers. In PSIG Annual Meeting.* Tulsa, Oklahoma, Pipeline Simulation Interest Group .

Holm, H., 2015. *Tanzania gas development – flow assurance challenges. In 17th International Conference on Multiphase Production Technology,* Stavanger: BHR Group.

Holm, H., 2015. *Tanzania gas development – flow assurance challenges. In the 17th International Conference on Multiphase Production Technology,* Stavanger: BHR Group.

Hossain, M. S., 2008. *Production Optimization and Forecasting.* Dhaka, BUET.

Ikoku, C. U., 1984. *Natural Gas Reservoir Engineering.* 1st ed. Pennsylvania: Krieger Publishing Company.

Irmann-Jacobsen, T. B., 2012. *Flow Assuarance- a system perspective. MEK4450 Offshore Technology Course.* Oslo, Universitet i Oslo, Matematisk Institutt.

Javanmardi, J., Nasrifar, K., Moshfeghian, M. & Najibi, H., 2007. Natural Gas Transportation, NGH or LNG. *World review of science, Technology and Sustainable Development,* 4((2-3)), pp. 258-267.

John, L. & Wattenbarger, R. A., 1996. *Gas Reservoir Engineering.* Texas: s.n.

Johnston, J., Lee, W. & Blasingame, T., 1991. *Estimating the Stabilized Deliverability of a Gas Well Using the Rawlins and Schellhardt Method: Analytical Approach. Paper SPE 23440 presented at Eastern Regional Meeting held in Lexington, Kentucky.* Texas, Society of Petroleu Engineers.

Jr., D. H. & Ros, N., 1963. *Vertical flow of gas and liquid mixtures in wells. In 6th World Petroleum Congress.* Tokyo, World Petroleum Congress.

Kiyuga, N. B., 2016. *Field Development Studies of an Offshore Gas Asset in Tanzania, Case Study: Block 2 Tanzania,* Trondheim: NTNU.

Maden, N., 2015. *Statoil Official Website.* [Online] Available at: http://www.statoil.com/en/NewsAndMedia/News/2015/Pages/30Mar_Tanzania.aspx [Accessed 24 January 2016].

Maden, N., 2015. *Statoil Official Website.* [Online] Available at: http://www.statoil.com/en/NewsAndMedia/News/2015/Pages/30Mar_Tanzania.aspx [Accessed 4 December 2015].

Michael J. Economides, A. D. H. C. E.-E., 1994. *Petroleum Production Systems.* United States of America: Prentice Hall.

Michael, H., Holmes, A. & Holmes, D., June 7-10 2006. *Relationship between Porosity and Water Saturation: Methodology to Distinguish Mobile from Capillary Bound Water. In AAPG Annual Convention.* Denver, AAPG.

Michelsen, O., 2014. *Statoil Official Website.* [Online] Available at: http://www.statoil.com/en/NewsAndMedia/News/2014/Pages/03Mar_Tazania.aspx [Accessed 17 March 2016].

Modisette, J. L., 2000. *Equation of State Tutorial. In PSIG Annual Meeting..* Houston-TX, Pipeline Simulation Interest Group.

Muhongo, P. S., 2016. *More gas seen on Ruvu Basin. News from newspaper..* Dar es Salaam : Daily News Tanzania.

Mukherjee, H. & Brill, J. P., 1985. Pressure Drop Correlations for Inclined Two-phase Flow. *Journal of energy resources technology,* 107(4), pp. 549-554.

Multiphase Technology, Inc, 2015. *Introduction on Multiphase Flow.* [Online] Available at: http://www.cortest.com/multiphase.htm [Accessed 15 December 2015].

National Petroleum Council (America), 2011. *SUBSEA DRILLING, WELL OPERATIONS AND COMPLETIONS. Working Document of the NPC North American Resource Development Study. Prepared bythe Offshore Operations Subgroup of the Operations & Environment Task Group.* Washington, D.C, NPC.

Nelson, P. H., 1994. Permeability-porosity relationship of sedimenatry rocks. *The log analyst,* 35(3).

OH, S. H., 2004. *Petroleum Economic Evaluation,* Ulsan: Korea Nationa Oil Company.

Padget, R. R. & Tuer, D., 1980. Gas Field Deliverability Forecasting and Facility Scheduling. *Journal of canadian Petroleum Technology,* 19(4), pp. 51-56.

Petroleum Experts, 2003. *GAP, General Allocation Program Version 5.00,* Edinburgh: Petroleum Experts.

Petroleum Experts, 2003. *PROSPER, Single Well System Analysis Version 8,* Edinburgh: Petroleum Experts.

Petroleum Experts, 2005. *MBAL, Reservoir Engineering Toolkit,* Edinburgh: Petroleum Experts.

PetroWiki, 2015. *PetroWiki.* [Online] Available at: http://petrowiki.org/Permeability determination [Accessed 1 April 2016].

PetroWiki, 2015. *PetroWiki.* [Online] Available at: http://petrowiki.org/Pipelines [Accessed 5 July 2016].

Renpu, W., 2011. Selection and determination of tubing and production casing sizes . In: *Advanced well completion engineering.* Houston, TX : Gulf Professional Publishing, pp. 117-170 .

Rodriguez-Sanchez*, et al., 2012. *Concept Selection for Hydrocarbon Field Development Planning,* Mexico: Scientific Research.

Rodriguez-Sanchez*, J. E., Godoy-Alcantar, J. M. & Ramirez-Antonio, I., 2012. *Concept Selection for Hydrocarbon Field Development Planning,* Mexico: Scientific Research.

Rwechungura, R., 2016. *LNG Calculations* [Interview] (28 May 2016).

Schulumberger , 2010. *Developments in Gas Hydrates,* Paris: Schulumberger .

Smith, C. H. & Lyinda, Z., 2015. *Woodford Completions: Ensuring the Most Efficient Completions. In SPE Production and Operations Symposium.* Oklahoma , Society of Petroleum Engineers.

Stanko, M., 2016. *Class 2 - Part 1, Youtube channel by Milan Stanko at NTNU. https://www.google.no/?gfe_rd=cr&ei=Bt5nV6WyFo-r8wfzy4GoCg&gws_rd=ssl#q=milan+edvard+wolf+stanko.* Trondheim: Youtube Channel.

Stanko, M., 2016. *Offshore Expenditures* [Interview] (27 June 2016).

Stanko, M. & De Andrade, J., 2015. *TPG 4230 Spring 2015, Field Development course at NTNU.* [Online] Available at: http://folk.ntnu.no/stanko/Courses/TPG4230/2015/Notes/TPG4230_Notes_2015.pdf TPG4230
[Accessed 15 May 2016].

Stanko, M. & Golan, M., 2015. *TPG 4230-Field Development course at NTNU.* [Online] Available at: http://folk.ntnu.no/stanko/Courses/TPG4230/2015/Notes/TPG4230_Notes_2015.pdf TPG4230
[Accessed 8 March 2016].

Statoil , 2014. *Statoil Official Website.* [Online] Available at: http://www.statoil.com/en/NewsAndMedia/News/2014/Pages/18Jun_Tanzania.aspx
[Accessed 18 March 2016].

Statoil, 2012. *Statoil Official Website.* [Online] Available at: http://www.statoil.com/en/NewsAndMedia/News/2012/Pages/14June_Tanzania.aspx
[Accessed 20 March 2016].

Statoil, 2013. *Presentation about Flow Assurance- Why oil companies focus on multiphase transport.* Trondheim, NTNU.

Statoil, 2013. *Statoil Offical Website.* [Online] Available at: http://www.statoil.com/en/NewsAndMedia/News/2013/Pages/06Dec_Mronge.aspx
[Accessed 18 March 2016].

Statoil, 2013. *Statoil Official Website.* [Online] Available at: http://www.statoil.com/en/NewsAndMedia/News/2012/Pages/20Dec_Lavani2.aspx
[Accessed 20 March 2016].

Statoil, 2013. *Statoil Official Website.* [Online] Available at: http://www.statoil.com/en/NewsAndMedia/News/2013/Pages/18Mar_Tanzania.aspx
[Accessed 10 March 2016].

Statoil, 2013. *Statoil Official Website.* [Online] Available at: http://www.statoil.com/en/NewsAndMedia/News/2012/Pages/24Feb_Tanzania.aspx
[Accessed 16 March 2016].

Statoil, 2014. *Statoil Official Website.* [Online] Available at: http://www.statoil.com/en/NewsAndMedia/News/2014/Pages/14Oct_Tanzania.aspx
[Accessed 13 June 2016].

Statoil, 2015. *Statoil Official Website.* [Online] Available at:

http://www.statoil.com/en/technologyinnovation/fielddevelopment/aboutsubsea/Pages/GullfaksVaatgasskompresjon.aspx
[Accessed 13 July 2016].

Statoil, 2015. *Statoil Official Website.* [Online] Available at: http://www.statoil.com/en/technologyinnovation/fielddevelopment/aboutsubsea/Pages/The%C3%85sgardComplex.aspx
[Accessed 13 July 2016].

Statoil, 2016. *Statoil Tanzania Website.* [Online] Available at: http://www.statoil.com/en/about/worldwide/tanzania/pages/default.aspx?gclid=CjwKEAjw-e7BRDs97mdpJzXwh0SJABSdUH0vixhfw21rK7Bkf4gWaKJ_u5lSRvOKFDFado4daZEexoC5dzw_wcB
[Accessed 2 March 2016].

Stopford, P., 2011. *Flow Assurance and Separation for the Oil & Gas Industry.* Pennsylvania, ANSYS, Inc.

Svalheim, M. S., 2005. *Petroleum Economics.* Stavanger, Norwegian Petroleum Directorate.

Szilas, A., 1975. *Production and Transport of Oil and Gas.* Amsterdam : Elsevier.

Thome, J. R., 2004. *Engineering data book III.* Lausanne: Wolverine Tube Inc, 2010.

TPDC website, 2015. *Information center.* [Online] Available at: http://www.tpdc-tz.com/deepwells.php
[Accessed 14 April 2016].

TPDC, 2014. *Status of Deep Wells.* [Online] Available at: http://www.tpdc-tz.com/deepwells.php
[Accessed 01 April 2016].

TPDC, 2014. *TPDC-Website.* [Online] Available at: http://www.tpdc-tz.com/upstream.php
[Accessed 12 February 2016].

U.S. Energy Information Administration, 2016. *eia.gov.* [Online] Available at: http://www.eia.gov/naturalgas/weekly/
[Accessed 24 June 2016].

Whiston, C. H. & Brule, M. R., 2000. *Phase Behaviour.* Texas: Society of Petroleum Engineers.

Whiston, C. W., 2002. *Advanced PVT and EOS Fluid Characterization.* Vienna: HOT Engineering GmbH.

Zolotukhin, A. B. & Ursin, J.-R., 2000. *Introduction to petroleum reservoir engineering.* Kristiansand, Norwegien Academic Press (HóyskoleForlaget),.